Adaptation strategies of mutualistic rhizobacteria on Arabidopsis roots

张浩

Hao Zhang

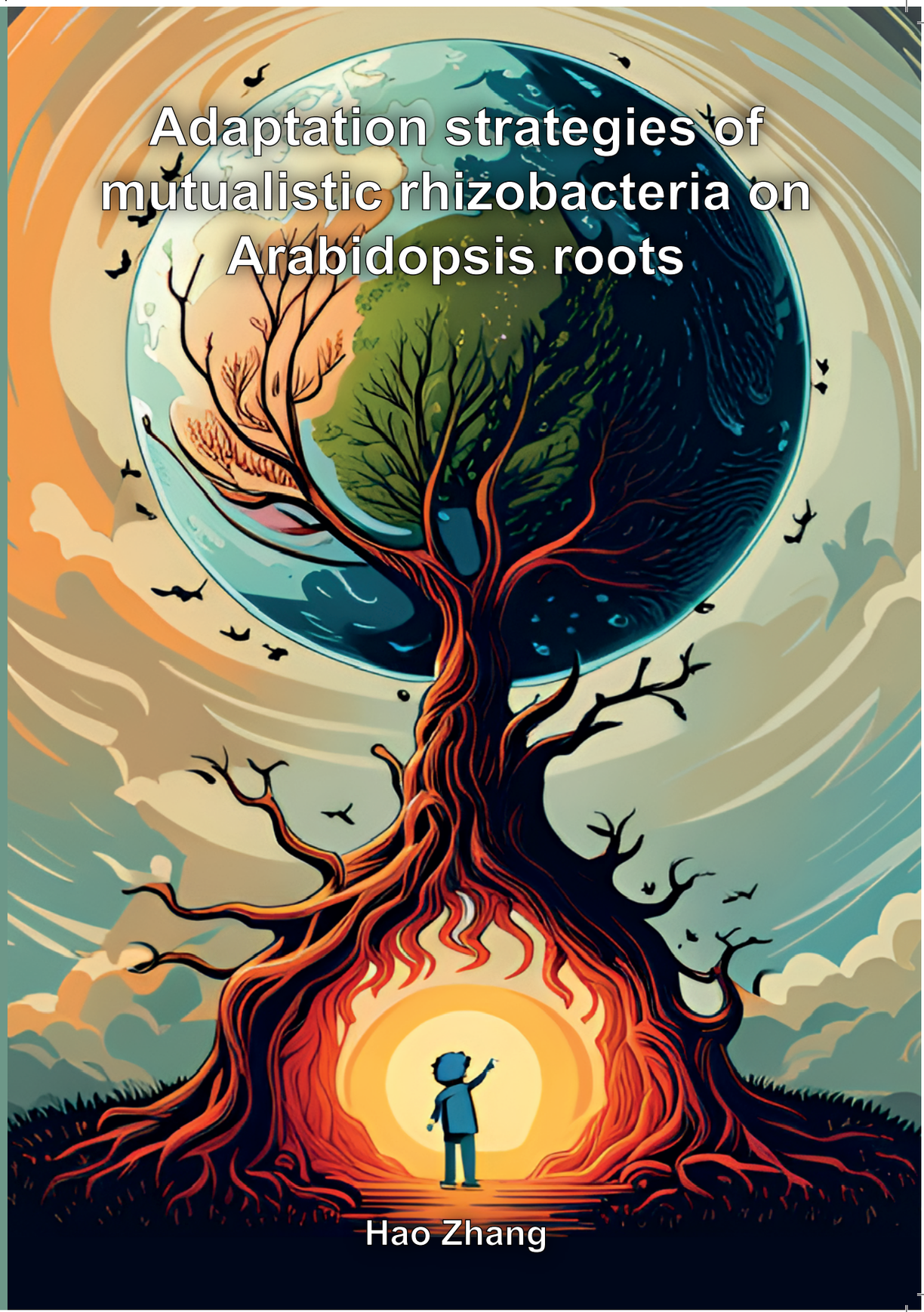

Adaptation strategies of mutualistic rhizobacteria on Arabidopsis roots

Adaptatiestrategieën van mutualistische rhizobacteriën op Arabidopsis wortels

Hao Zhang

PhD thesis:
Adaptation strategies of mutualistic rhizobacteria on Arabidopsis roots
Hao Zhang
Plant-Microbe Interactions | Utrecht University | 2023

ISBN: 978-94-6469-416-1

Cover: Hao Zhang | Staybility.AI | beta.dreamstudio.ai
The cover design is inspired by the 'Hercules statue created by William Brodie around 1863 (Portmeirion, Wales)'.
Layout: ProefschriftMaken.nl
Printing: ProefschriftMaken.nl

Adaptation strategies of mutualistic rhizobacteria on Arabidopsis roots

Adaptatiestrategieën van mutualistische rhizobacteriën op Arabidopsis wortels
(met een samenvatting in het Nederlands)

互利共生根际菌在拟南芥根上的适应策略
（内附中文摘要）

Proefschrift

ter verkrijging van de graad van doctor aan de
Universiteit Utrecht
op gezag van de
rector magnificus, prof.dr. H.R.B.M. Kummeling,
ingevolge het besluit van het college voor promoties
in het openbaar te verdedigen op

maandag 3 juli 2023 des ochtends te 10.15 uur

door

Hao Zhang
geboren op 4 november 1988
te Lingbao, China

Promotor:

Prof. dr. C.M.J. Pieterse

Copromotor:

Dr. R. de Jonge

Beoordelingscommissie:

Prof. dr. A.T. Kovács
Prof. dr. E.E. Kuramae
Prof. dr. M. Suárez-Diez
Prof. dr. B.P.H.J. Thomma
Prof. dr. J.P.M. Tommassen
Prof. dr. A. de Visser

This thesis was partly accomplished with financial support from China Scholarship Council (No. 201406300090).

To my friends and family,

Three passions, simple but overwhelmingly strong, have governed my life:
the longing for love,
the search for knowledge,
and the pity for the suffering of mankind.

- Bertrand Russell
(1872-1970)

Contents

1

CHAPTER 1

General introduction

Hao Zhang[1], Corné M.J. Pieterse[1] and Ronnie de Jonge[1]

[1]Plant-Microbe Interactions, Department of Biology, Science4Life,
Utrecht University, Utrecht, the Netherlands.

Adapted from:
Stringlis IA, Zhang H, Pieterse CMJ, Bolton MD, De Jonge R.
Microbial small molecules-weapons of plant subversion.
Natural Product Reports 35: 410–433 (2018)

Abstract

Plants live in close association with a myriad of microbes that are generally harmless. However, the minority of microbes that are pathogens can severely impact crop quality and yield, thereby endangering food security. By contrast, beneficial microbes provide plants with important services, such as enhanced nutrient uptake and protection against pests and diseases. Like pathogens, beneficial microbes can modulate host immunity to efficiently colonize the nutrient-rich niches within and around the roots and aerial tissues of a plant, a phenomenon mirroring the establishment of commensal microbes in the human gut. Numerous ingenious mechanisms have been described by which pathogenic and beneficial microbes in the plant microbiome communicate with their host, including the delivery of immune-suppressive effector proteins, the production of phytohormones, toxins and other bioactive molecules, and the decoration of microbial cell surface components. Plants signal to their associated microbes via exudation of photosynthetically fixed carbon sources, quorum-sensing mimicry molecules and selective secondary metabolites such as strigolactones and flavonoids. Molecular communication thus forms an integral part of the establishment of both beneficial and pathogenic plant-microbe relations. Here, we review the current knowledge on microbe-derived small molecules that aid plant colonization by microbes, that can act as signaling compounds to stimulate plant growth and health by beneficial microbes, but that could also be used as weapons for plant invasion by pathogens. As an exemplary case, we used comparative genomics to assess the small molecule biosynthetic capabilities of the *Pseudomonas* genus, a genus rich in both plant pathogenic and beneficial microbes. We highlight the biosynthetic potential of individual microbial genomes and the population at large, providing evidence for the hypothesis that the distinction between detrimental and beneficial microbes is increasingly fading. Knowledge on the biosynthesis and molecular activity of microbial small molecules will aid in the development of successful biological agents boosting crop resiliency in a sustainable manner and could also provide scientific routes to pathogen inhibition or eradication.

Author contributions:

H.Z. played an important role in designing and writing of the original manuscript as well as creating the illustrations. H.Z. was responsible for restructuring the published manuscript into its current form as general introduction. All authors participated in the content discussions and made contributions to the final published version.

The role of plant-associated microbiota in plant health

Plants, unlike animals and insects, are rooted in their environment, and are consequently unable to flee from stressful situations. Therefore, plants employ a variety of mechanisms to tolerate or mitigate stress factors. It is becoming clear that plant-associated microbiota play an important role in plants' ability to avert the negative effects of stress (Bakker *et al.*, 2018). Through exudation of sugars, amino acids and organic acids, plants invest a significant proportion (up to 20 percent) (Bais *et al.*, 2006a; Philippot *et al.*, 2013) of their photosynthetically-fixed carbon towards the maintenance of their rhizosphere- and phyllosphere-associated microbiota (Berendsen *et al.*, 2012; Bulgarelli *et al.*, 2013; Pieterse *et al.*, 2016; Zhalnina *et al.*, 2018). In return, beneficial microbiota, commonly referred to as the plant growth-promoting rhizobacteria (PGPR) and fungi (PGPF) provide plants with important benefits including enhanced mineral uptake, nitrogen fixation and biocontrol (Bais *et al.*, 2006a; Philippot *et al.*, 2013), which makes them essential for plant growth and health. Establishment of intimate beneficial plant-microbe interactions requires exchange of signaling molecules to tune immunity and promote colonization. A well-studied example is nodule formation that occurs as a symbiosis between nitrogen-fixing bacteria from the order Rhizobiales and Leguminosae plants. Nodule formation requires the coordinated development of bacterial infection and root nodule organogenesis (Oldroyd *et al.*, 2011), and is initiated by the biosynthesis of rhizobial nodulation factors upon perception of plant flavonoids. Nodulation factors are recognized by plant receptors and trigger transcriptional and physiological changes that lead to root hair curling and bacteria entrapment, creating a suitable environment for nitrogen fixation and bacterial proliferation.

In addition to such symbiotic relationships, many other naturally free-living microbes can boost plant growth. When associating with their plant host, such microbes can facilitate nutrient uptake, stimulate changes in root architecture (Zamioudis *et al.*, 2014, 2015) or promote plant health. For example, plant health may benefit from selected microbes that suppress pathogens through antibiosis or competition for limited nutrients, or trigger a host immune response called induced systemic resistance (ISR) (Lugtenberg & Kamilova, 2009; Pieterse *et al.*, 2014, 2016; Venturi & Keel, 2016). PGPR and PGPF are increasingly used as biocontrol agents and biostimulants to improve crop health in a sustainable way, therewith reducing the input of fertilizers and pesticides. However, unlike well-studied symbioses involving nitrogen-fixing bacteria, relatively little is known about the molecular signals and mechanisms that govern the interaction between PGPR and PGPF with the plant.

PGPR promote plant growth and health by interfering with root development. For example, selected pseudomonads induce root architecture modifications by activation of developmental programs that inhibit primary root elongation, while promoting lateral root formation and root hair growth (Zamioudis *et al.*, 2013). Such modifications facilitate plant establishment and increase the root's exploratory capacity for water and nutrients. Root attachment is a critical initial step of successful plant colonization, and involves extracellular structures such as flagella and/or pili for root surface adhesion as well as a variety of species-specific polysaccharides such as exopolysaccharides and lipopolysaccharide (Rodríguez-Navarro *et al.*, 2007; Berne *et al.*, 2015; Wheatley & Poole, 2018). Microbe-induced developmental changes, however, can also be observed without direct contact of the PGPR, demonstrating that microbially produced volatile organic compounds (VOCs) are potent inducers of plant growth (Ryu *et al.*, 2003; Blom *et al.*, 2011) and are drivers of root architecture changes (Zamioudis *et al.*, 2013). VOCs have long been known to play essential roles in the communication with other organisms (Dicke & Sabelis, 1988), including those between plants and their root-associated microbiota (Bitas *et al.*, 2013; Schmidt *et al.*, 2015; van Dam *et al.*, 2016). Recent work further suggest that VOCs from both plant pathogenic and plant beneficial microbes have profound effects on plant host transcription and development (Cordovez *et al.*, 2015, 2017; Park *et al.*, 2015; Cheng *et al.*, 2016; Martínez-Medina *et al.*, 2017). Intriguingly, production of VOCs by the fungal root pathogen *Rhizoctonia solani* also enhances growth and accelerates development of *Arabidopsis thaliana* (hereafter Arabidopsis) similar to VOCs from known beneficial microbes (Cordovez *et al.*, 2017). Future studies should reveal whether these physiological changes in the plant are part of an integrated plant defense strategy. For example, enhanced root growth may be the plants attempt to "outrun" disease. Alternatively, it may be a pathogen's strategy to increase root surface and biomass to boost the chance of successful infection.

Production of VOCs by plant-associated microbes and their subsequent perception by plants is one of the many forms of plant-microbe interactions that could ultimately result in the microbial establishment on and/or within nutrient-rich plant tissue. Successful establishment further depends on the microbes' ability to subvert plant immunity. Immune-suppressive effector proteins that are part of the microbial weaponry are best known for their role at this stage (Göhre & Robatzek, 2008), but also small molecules, also known as natural products or secondary metabolites, contribute to microbial establishment. For example, microbe-derived phytohormones such as auxin, gibberellin and cytokinins can influence plant physiology in a plant-like manner, toxic compounds can disrupt cellular physiology or inhibit plant growth in general, and microbial molecules such as siderophores, lipopeptides, exopolysaccharides, and lipopolysaccharide assist in colonization but can also help the plant in

nutrient uptake or stimulate plant immunity. Intriguingly, biosynthesis of these plant immunity-subverting molecules contributes to the plant-associated lifestyles of both pathogenic and beneficial microbes. Here, we summarize recent scientific literature, on microbial metabolites that play a role in plant-microbe interactions. We highlight commonalities and particularities among plant pathogenic and beneficial microbes in a context- and host-dependent manner with an emphasis on small, natural molecules of non-proteinaceous origin. We further explore the biosynthetic potential within the genome sequences of the well-studied, plant-, and animal-associated microbial genus *Pseudomonas* emphasizing on traits that are associated with plant-microbe interactions. Lastly, we highlight several microbial polysaccharides, i.e., exopolysaccharides and lipopolysaccharides that are important for plant root colonization and that play a central role in this thesis.

Characterized chemical compounds with roles in plant-microbe interactions

Many microbial molecules have been identified to date that play a role in the establishment of intricate plant-microbe interactions. We broadly classify these molecules in three groups, namely microbe-derived plant hormones (microbial phytohormones), toxins, and stimulatory compounds (Stringlis *et al.*, 2018c). Microbial phytohormones are microbial molecules that mimic or influence endogenous plant hormones or their activities, and microbial enzymes that modify plant hormone abundance and/or distribution. Microbes, both pathogenic and beneficial, produce a variety of phytohormones such as auxin, cytokinins and gibberellins, or influence their concentration by interfering with host transcription and/or enzymatic pathways (Bastián *et al.*, 1998; Duca *et al.*, 2014; Glick, 2014; Kang *et al.*, 2014; Ludwig-Müller, 2015; Venturi & Keel, 2016). The production of these microbial phytohormones by microbes is not considered to play a direct role in microbial development but rather contribute to their interaction with the environment, particularly with plants, and are classified as secondary metabolites. Microbial toxins have a high biochemical complexity and diversity, but secondary metabolites all arise from a limited number of precursors from primary metabolism. Consequently, fungal secondary metabolites are generally classified into four canonical chemical categories based on the enzyme class involved in the biosynthesis of the first intermediate. These include the polyketides (e.g., aflatoxin, T-toxin, and perylenequinone toxins), non-ribosomal peptides (NRPs, e.g., HC-toxin and sirodesmin siderophores such as ferricrocin), terpenes (e.g., T-2 toxin and gibberellins), and indole alkaloids (e.g., ergotamine, paxilline and lolitrems). Biosynthesis in each secondary metabolite category is governed by the core enzymes polyketide synthases, non-ribosomal peptide synthetases (NRPSs), terpene synthases/cyclases, and dimethylallyl tryptophan synthases (DMATSs), respectively. Microbial stimulatory

compounds are a broad group of microbial molecules that benefit microbial spread and persistence, and/or act as activators of plant immunity or alteration-factors of plant physiology. Some of these well-known stimulatory compounds are elucidated in the following sections.

Stimulatory compounds

PGPR and PGPF promote plant growth and health in various ways, with microbial production of phytohormones being one of them. Some PGPR boost plant immunity by inducing systemic defense priming known as ISR (Pieterse *et al.*, 2014). A multitude of determinants have been identified as elicitors of ISR, including cell envelope components such as lipopolysaccharides (LPS) and extracellular polysaccharides (EPS) that mediate microbial interactions and surface adhesion, and secreted compounds like siderophores, (cyclic) lipopeptides, volatiles, antibiotics such as 2,4-diacetylphloroglucinol (DAPG) and the phenazine pyocyanin, quorum sensing molecules such as the N-acyl homoserine lactones, as well as flagella (reviewed by De Vleesschauwer and Höfte (De Vleesschauwer & Höfte, 2009)). Application of multiple purified bacterial determinants could reproduce ISR in the absence of the bacteria. Nevertheless, individual knockout mutants that no longer produce the respective determinants were not impaired in their ability to elicit ISR, suggesting that bacterial determinants may act redundantly in the elicitation of ISR (Van Wees *et al.*, 1997; Meziane *et al.*, 2005; Berendsen *et al.*, 2015). Different plant-beneficial *Pseudomonas* strains trigger ISR on a partially overlapping set of plants (Meziane *et al.*, 2005; Berendsen *et al.*, 2015). Comparative genome analyses of three pseudomonads, i.e., *Pseudomonas simiae* strain WCS417, *Pseudomonas capeferrum* strain WCS358 and *Pseudomonas defensor* strain WCS374, with differential capacities to trigger ISR on various plants, revealed multiple compounds that could act as determinants of ISR. These include their respective siderophores and a cyclic lipopeptide (CLP) in WCS358 (Berendsen *et al.*, 2015). Siderophores and lipopeptides play important roles in the natural life of the bacteria that produce them.

Siderophores

Siderophores are low molecular weight compounds that sequester ferric ions (Fe^{3+}) in the environment and are typically produced by microbes under conditions of low iron availability. In most natural soils, iron availability is low, as poorly soluble ferric hydroxides dominate the pool of iron. Through their iron-sequestering activities, the producing microbes can compete with their neighbors including soil-borne pathogens, an important trait for biological control strains (Bakker *et al.*, 1990). In the case of *Pseudomonas protegens* strain Pf-5 it was demonstrated that its siderophores contribute to resistance towards the mycotoxin fusaric acid produced by several soil-borne pathogens of the genus *Fusarium*, through their iron sequestration activities

(Ruiz *et al.*, 2015). Competition for iron is important for the lifestyles of both plant and microbial pathogens, and consequently perturbation of iron homeostasis is a key interaction platform between plants and pathogens (Aznar *et al.*, 2015; Aznar & Dellagi, 2015; Trapet *et al.*, 2016; Verbon *et al.*, 2017). Plants on the one hand can use iron-withholding tactics to reduce pathogen virulence or to locally increase iron levels to activate a toxic oxidative burst. Pathogens counteract such measures by producing siderophores that can acquire iron from the host and thereby act as virulence factors (Aznar & Dellagi, 2015; Verbon *et al.*, 2017). *Pseudomonas aeruginosa*, the causal agent of severe lung disease infections, relies on the production of the siderophores pyoverdine and pyochelin to infect mice (Cornelis & Dingemans, 2013). However, the animal model species *Caenorhabditis elegans*, recognizes *P. aeruginosa* pyochelin through chemosensory detection by GPCRs (G protein-coupled receptors) resulting in pathogen avoidance and host survival (Meisel *et al.*, 2014). Noteworthy, many plant pathogens (Scharf *et al.*, 2014), and insect pathogens (Dieppois *et al.*, 2015; Li *et al.*, 2016) rely on the production of siderophores to cause full disease in their hosts. In agreement with their ability to modulate behavior in *C. elegans*, siderophores not only act as virulence factors, they can also be perceived by the host triggering a variety of responses in an iron-dependent and -independent manner (Verbon *et al.*, 2017).

Two major pathways exist for siderophore biosynthesis. One depends on NRPSs and the other involves siderophore synthetases that are part of the IucA/IucC family of proteins (de Lorenzo & Neilands, 1986). A classic example of the former are the fluorescent pigments in the large and diverse pyoverdine class, involved with the characteristic appearance of the fluorescent pseudomonads (Visca *et al.*, 2007). Pyoverdines are produced by many *Pseudomonas* spp., and biosynthesis within one strain involves as many as seven genomically dispersed biosynthetic gene clusters (BGCs) (Loper *et al.*, 2012). Siderophores produced through the second pathway, also known as the NRPS-independent pathway or NIS pathway, are less frequently observed and studied to a lesser extent (reviewed by Challis, 2005) (Challis, 2005). Nevertheless, since the initial discovery of the involvement of the IucA and IucC siderophore synthetases in the biosynthesis of aerobactin in *Escherichia coli*, various other siderophores, including rhizobactin, achromobactin, desferrioxamines and vibrioferrin, were linked to biosynthetic pathways incorporating *IucC*/*IucA* homologs. Some pyoverdines can alleviate symptoms associated with iron deprivation in Arabidopsis, possibly by boosting the expression of genes involved in iron uptake such as *IRT1* and *FRO2* (Trapet *et al.*, 2016; Verbon *et al.*, 2017). Also, siderophores from diverse pseudomonads can trigger ISR in a plant-specific manner (De Vleesschauwer & Höfte, 2009; Berendsen *et al.*, 2015).

Lipopeptides

Lipopeptides are composed of a lipid tail linked to short linear or cyclic oligopeptide (CLPs). They act as microbial surfactants (biosurfactants), which function to lower surface or interfacial tension (Raaijmakers *et al.*, 2010). Biosurfactants are produced by many organisms, including bacteria and fungi, and through their activity they can affect cell differentiation, signaling, biofilm formation and motility. In plant-related environments they have been associated with so-called wettability, or the ability to reduce surface tension to water. Wetting of plant leaves is thought to promote microbial cell motility on them, and might also provide a stage for exchange of signals and nutrients, and consequently it contributes to pathogen virulence (Xin *et al.*, 2016). Besides their role as biosurfactants, lipopeptides are also well known for their broad-spectrum antimicrobial activity, particularly as an important defense mechanism against protozoa (Raaijmakers *et al.*, 2010). The proposed primary mode of action is pore formation in membranes, leading to imbalance in transmembrane ion fluxes and cell death. Lipopeptides, and in particular CLPs, differ greatly in their structural appearance resulting from variability in the length and composition of the lipid moiety and the type, number and configuration of the amino acids in the peptide chain (Raaijmakers *et al.*, 2010; Loper *et al.*, 2012). Like many siderophores, CLPs are synthesized via large multidomain NRPSs that are part of even larger BGCs incorporating various additional proteins related to transcriptional and post-transcriptional regulation as well as transport. Through their biosurfactant activities, lipopeptides enhance beneficial as well as detrimental microbes with regards to their potential to colonize their respective hosts.

The plant biological control bacterium *P. protegens* strain CHA0 produces the CLP orfamide A, through the *orfamide* BGC *Ofa*, which aids in its swarming motility. Orfamides play an important role in biocontrol activities through their antimicrobial activities (Ma *et al.*, 2016a). Intriguingly, orfamides also possess dose-dependent insecticidal activities, and consequently orfamide-producing strains can be used as biocontrol measures against insect pests on crops (Flury *et al.*, 2016, 2017; Ma *et al.*, 2016a). Orfamide A belongs to the larger orfamide family, also encompassing the poaeamides (Zachow *et al.*, 2015) and the bananamides, e.g., bananamide A (Nguyen *et al.*, 2016). Poaeamide A produced by the endophyte *Pseudomonas poae* contributes to plant rhizosphere colonization as well as suppression of soil-borne plant pathogens (Zachow *et al.*, 2015). Remarkably, poaeamide-deficient mutants accumulate at higher density than the respective wildtype on the roots of *R. solani* tolerant sugar beet plants. Also, D'aes *et al.* showed that the interplay between two different classes of CLPs produced by *Pseudomonas* sp. CMR12a determine its ability to form biofilms and achieve settlement on plant root surfaces (D'aes *et al.*, 2014). Localized cell density can greatly affect the exerting lifestyle through quorum sensing (QS), and

thus differences in the spatial distribution and root surface adherence may contribute to the overall higher colony numbers for the CLP mutants (Zachow *et al.*, 2015).

A variety of CLPs, like siderophores, affect host immunity. In this regard, they resemble MAMPs (microbe-associated molecular patterns) that are recognized by host cell surface receptors, representing the first surveillance system of the host for non-self-perception (Dodds & Rathjen, 2010). A multitude of both recent and past research has shown that purified CLPs from *Pseudomonas*, *Bacillus* and *Streptomyces* spp. can stimulate host immune responses and trigger ISR (Raaijmakers *et al.*, 2010; Falardeau *et al.*, 2013). Tran *et al.* and Ongena *et al.* were among the first to report CLP-mediated stimulation of ISR in tomato by massetolide A from *Pseudomonas fluorescens*, and in tomato and bean by fengycins and surfactins from *Bacillus subtilis* respectively (Ongena *et al.*, 2007; Tran *et al.*, 2007). More recently, Farace *et al.* showed that three CLPs produced by *B. subtilis*, surfactin, mycosubtilin and plipastatin, are each independently perceived by grapevine cells, and activate partially overlapping signaling pathways and defense responses (Farace *et al.*, 2015). Importantly, application of each of these CLPs can protect grapevine leaves against the necrotrophic pathogen *Botrytis cinerea*. Similarly, *Pseudomonas* sp. CMR12a produces two classes of CLPs, namely orfamides and sessilins, that stimulate defense responses in rice and consequently activate ISR against diverse plant pathogens such as *Magnaporthe oryzae* and *Cochliobolus miyabeanus* in a differential, concentration-dependent manner (Ma *et al.*, 2016b, 2017). The lipopeptides produced by members of the *Pseudomonas* and *Bacillus* genera are structurally and functionally highly diverse (Raaijmakers *et al.*, 2010), further corroborated by the extensive genomic variability at the relevant BGCs (Nguyen *et al.*, 2016; Tracanna *et al.*, 2017).

Polysaccharides

Polysaccharides are a type of long-chain polymeric carbohydrates composed of monosaccharide units. Depending on their localization, microbial polysaccharides can be broadly divided into three groups, namely intracellular microbial polysaccharides, cell wall polysaccharides, and extracellular polysaccharides (Khan *et al.*, 2022). Intracellular microbial polysaccharides, such as glycogen, are produced and accumulated inside the cell, and serve as energy and carbon reserve. Cell wall polysaccharides, such as chitin, heteropolysaccharide peptidoglycan and LPS form structural parts of the cell wall. EPS, on the other hand, are secreted by cells, and can be found as capsules associated with cell surfaces, or as slime, loosely bound to cell surface. Microbial EPS has received considerable attention due to their commercial values, such as xanthan (*Xanthomonas campestris*), gellan (*Sphingomonas paucimobilis* and *Pseudomonas elodea*), cellulose and xylinan (*Acetobacter xylinum*) and succinoglycan (*Rhizobium* sp.) (Morris & Harding, 2009; Ahmad *et al.*, 2015).

The microbial surface is decorated with striking variations of polysaccharides, including numerous EPS varieties, various structures of peptidoglycan on gram-positive bacteria (Vollmer *et al.*, 2008; Vollmer & Seligman, 2010), and high variations of O-antigen, an important constituent of gram-negative bacterial LPS (Lerouge & Vanderleyden, 2001; Wang *et al.*, 2010; Lam *et al.*, 2011). Cell-surface-decorating polysaccharides play important roles in bacterial processes such as biofilm formation, as well as in host-microbe interactions by serving as a virulence determinant (Raetz & Whitfield, 2002; Huszczynski *et al.*, 2020) or by promoting host cell adhesion (Rodríguez-Navarro *et al.*, 2007; Berne *et al.*, 2015; Wheatley & Poole, 2018). LPS is also recognized as a MAMP. During plant-microbe interactions, plants are able to sense all three major constituents of LPS, namely lipid A, core oligosaccharide, and the aforementioned O-antigen. Purified LPS as well as lipid A from several bacterial sources can induce nitric oxide production in Arabidopsis, a hallmark of plant immunity (Zeidler *et al.*, 2004). The lipid A moiety and the core oligosaccharide are recognized by plant cells, and trigger a localized immune response including expression of the defense-related genes, *PR1* and *PR2*, in Arabidopsis (Silipo *et al.*, 2005). In addition, Bedini *et al.* and Madala *et al.* highlighted how several known plant stress and defense response-related genes can be induced by application of synthetic O-antigen or purified bacterial O-antigen (Bedini *et al.*, 2005; Madala *et al.*, 2012).

The mechanism of LPS perception by plants and the cognate signal transduction pathway was first reported by Ranf *et al.* in 2015 (Ranf *et al.*, 2015). LPS, in particular the lipid A moiety, could be detected by the bulb-type lectin S-domain-1-receptor-like kinase LORE (lipooligosaccharide-specific reduced elicitation) of Arabidopsis (Ranf *et al.*, 2015). However, LPS preparations from *Salmonella enterica*, *E. coli* or *Burkholderia* spp., unlike that from *Pseudomonas* spp. and *X. campestris*, could not activate plant immune responses through LORE (Kutschera *et al.*, 2019). These bacterial lipid A or LPS fractions, which are comprised of medium-chain 3-hydroxy fatty acid (mc-3-OH-FA) building locks, appeared devoid of free mc-3-OH-FAs (Kutschera *et al.*, 2019). Together with evidence showing that synthetic mc-3-OH-FAs could elicit LORE-dependent immunity (Kutschera *et al.*, 2019), these results suggested that the previously identified LPS receptor, LORE, rather than being a receptor for LPS, represents a receptor for bacterial mc-3-OF-FA. Interestingly, 3-OH-FA might be one of the weakest elicitors of MAMP-triggered immunity (MTI) among MAMPs. Bjornson *et al.* performed a detailed transcriptomic analysis of immune-related genes in Arabidopsis (Bjornson *et al.*, 2021). Among seven tested MAMPs, 3-OH-FA was the weakest elicitor, determined by the lowest number of differentially expressed genes (DEGs). It induced about one fifth of the flg22 (another common bacterial elicitor of MTI)-induced DEGs. These discoveries led to the suggestion that plants possess only low affinity for LPS, which was already proposed in another study much

earlier (Zeidler *et al.*, 2004). Most of the experiments, which study LPS triggered plant immune response, were conducted with a synthetic LPS moiety, or by using a LPS preparation from *in vitro*-cultured bacteria. Bacteria in nature might contain even lower concentrations of LPS when in the host environment, which might not even achieve the required minimum dose to elicit most of the effects described above. On the contrary, long chain O-antigen of X*ylella fastidiosa* LPS delayed rather than stimulated plant initial recognition, thus facilitating plant colonization (Rapicavoli *et al.*, 2018).

In silico and *in vivo* mining for functional biosynthetic pathways of novel small natural compounds

Comparative genome analyses-driven pathway identification

Comparative genome analyses, or comparative genomics, is a field of biological research in which genomic features encoded by different organisms or strains are compared. It involves DNA and/or protein sequence alignment, and can incorporate phylogenetic interference with hundreds to thousands of gene families, commonly referred to as phylogenomics (Eisen, 1998). Comparison of individual gene trees with the accepted taxonomy further allows for the identification of lateral or horizontal gene or gene cluster transfer events, as these typically behave differently from what is expected based on that same taxonomy. Comparative analyses of ten *P. fluorescens* genomes revealed multiple pathways for the biosynthesis of the siderophores achromobactin and pseudomonine and the antibiotic 2-hexyl-5-propyl-alkylresorcinol (Loper *et al.*, 2012). Moreover, core and pangenome analysis of these ten genomes demonstrated that only 45 to 52% of the predicted coding genes is shared between all genomes, highlighting an enormous genetic heterogeneity (Loper *et al.*, 2012). Likewise, previously Flury *et al.* examined the phylogenetic distribution of the *fit* toxin gene across the *P. fluorescens* group (Flury *et al.*, 2016). The Fit toxin is the best studied bacterial virulence factor against insects and it contributes to biocontrol activity of various pseudomonads, such as *P. protegens* strain CHA0. By comparing the phylogenetic distribution of *fit* with insecticidal activity assays it was demonstrated that the presence of this gene is a determining factor in the biocontrol potential of pseudomonads (Flury *et al.*, 2016).

Case study: The *Pseudomonas* genus

To further highlight the enormous genetic diversity and capacity across a single plant-associated bacterial genus and simultaneously demonstrate the power of comparative genomics we here survey a custom set of 168 *Pseudomonas* genomes for their potential to synthesize natural products that can affect microbial interaction with plants. The 168 genomes are selected from public databases to represent the breadth of genetic diversity across the genus and incorporate most plant-associated pseudomonads based

on their annotation in NCBI GenBank (Fig. 1). Many plant-associated pseudomonads, both of pathogenic and beneficial nature, encode the capacity to synthesize the auxin indole-3-acetic acid or IAA via the IAM and IPA pathways in their genome sequences. Here, we detected 118 and 29 homologues for *iaaM* and *iaaH* respectively, involved with IAA biosynthesis via the IAM pathway, but only three *ipdC* genes, involved with IAA biosynthesis via the IPA pathway (Fig. 1). All 168 genomes except one, contain a *miaA* ortholog. *MiaA* encodes a tRNA modification enzyme that was previously reported to be an important determinant for microbial biosynthesis of the cytokinins. In the beneficial *P. fluorescens* strain G20-18, miaA contributes to biocontrol activity against *Pseudomonas syringae* on Arabidopsis. Curiously, the universal distribution we observe here supports a role for *miaA* in primary metabolism instead, which was also reported previously in *P. chlororaphis* strain 30-84 (Yu *et al.*, 2017). Nevertheless, *miaA* mutants in G20-18 accumulate to similar density *in planta* and therefore differences in bacterial growth cannot fully explain the lack of biocontrol in the *miaA* mutant (Großkinsky *et al.*, 2016). We also identified 16 candidate *acdS* genes, across 16 genomes, which included pathogenic and beneficial species (Fig. 1). *AcdS*, regulated by *acdR*, encodes the ACC deaminase which can break down the precursor for the phytohormone ethylene, ACC, and can thus affect ethylene levels in the plant. In conclusion, both pathogenic and beneficial pseudomonads can use similar mechanisms to modulate plant hormone levels.

Another feature commonly associated with plant-beneficial microbes is their capacity to control fungal diseases via competition for iron using high affinity siderophores. Moreover, there is extensive literature on the stimulation of ISR by beneficial microbes that suggest an important role for siderophores (Pieterse *et al.*, 2014). Siderophore biosynthesis typically proceeds via a NRPS-dependent or NRPS-independent (NIS) fashion. Scanning of the 168 *Pseudomonas* genome sequences for BGCs associated with siderophore biosynthesis via the NIS pathway by antiSMASH 183 revealed 46 such BGCs (Fig. 1). Examination of the predicted NRPS BGCs by cross-comparisons with known BGCs for siderophore production (C. Hider & Kong, 2010; Loper *et al.*, 2012; Berendsen *et al.*, 2015; Medema *et al.*, 2015) as well as the siderophores pseudomonine (Mercado-Blanco *et al.*, 2001), ferroverdin (Neilands, 1966), paenibactin (Wen *et al.*, 2011), xanthoferrin (Pandey & Sonti, 2010) and turnerbactin (Han *et al.*, 2013) yielded an additional set of 253 NRPS-dependent BGCs for the biosynthesis of siderophores. Overall, we identified 292 BGCs associated with siderophore biosynthesis, and each genome encodes between 0 and 4 BGCs related to siderophore production (Fig. 1). From the distribution, it becomes apparent that the biosynthetic potential for (diverse) siderophore production coincides with a plant-associated lifestyle, be it pathogenic or beneficial, as well as animal/human pathology (particularly *P. aeruginosa* strains).

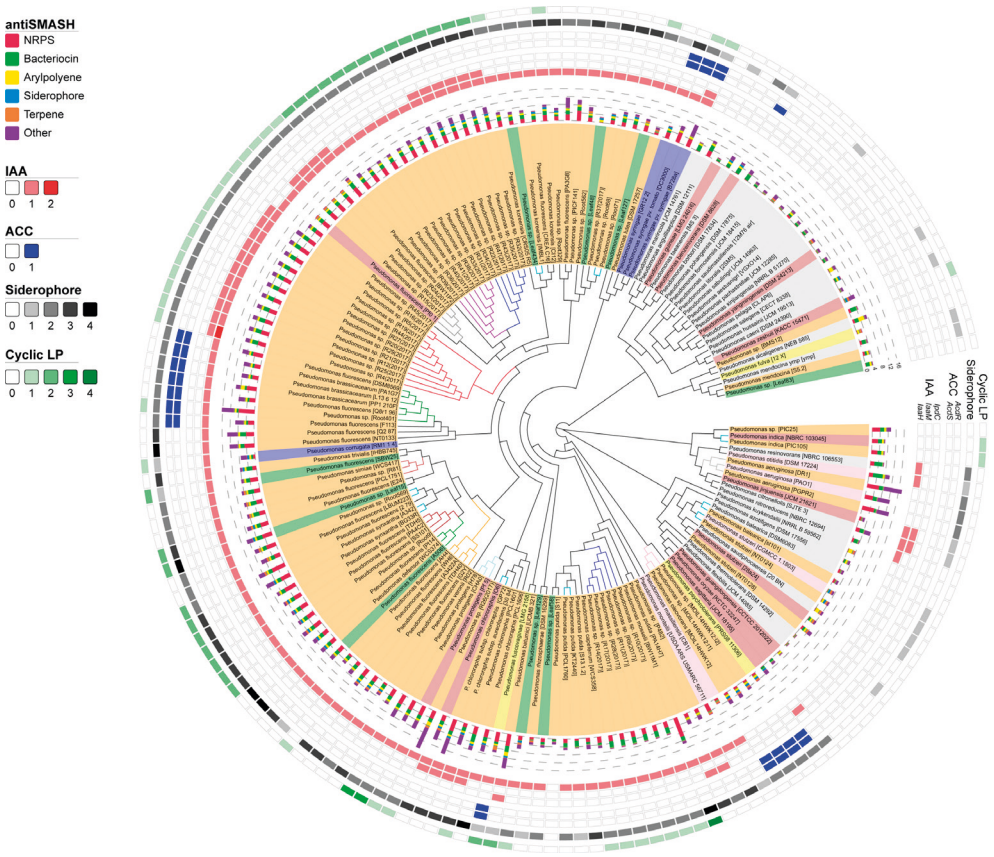

Figure 1 Whole-genome phylogeny of the *Pseudomonas* genus.
The phylogenetic tree, represented by the circular cladogram, is built by Phylip from 28,224 (168 times 168) Mash-derived genome-to-genome pair-wise distances. Genomes with distances below 0.05, equivalent to an average nucleotide identity of 95% or larger, are considered as the same species and are depicted with same-colored branches. *Pseudomonas* genomes were selected from the NCBI database based on three criteria: 1) when depicted as 'representative genomes', 2) when obtained from the phyllosphere or rhizosphere and 3) based on reports in the literature. Colored shades highlight the source of collection and/or pathogenic status and refer to (agricultural) soil (brown), rhizosphere (orange), phyllosphere (green), other plant-associated niches (seeds, rice paddies; yellow), plant pathogen (blue), human and/or animal pathogen (pink) or from a variety of other niches such as oil brines, sludge and contaminated soils (grey). The last category consequently reflects a generally non-plant associated lifestyle. The stacked bar chart reflects the number of predicted BGCs by antiSMASH. The outer rings display the frequency of genes or gene clusters involved with IAA biosynthesis, ACC deaminase activity, and siderophores and cyclic lipopeptides.

In addition to siderophores, NRPSs are also key to biosynthesis of lipopeptides and other natural products. To obtain a more broad understanding of the capacity to synthetize lipopeptides and other NRPs and/or derivates, we calculated NRPS-BGC cluster-to-cluster pairwise distances via mash sketch (Ondov *et al.*, 2016) analysis on amino acid level (k-mer = 9) using the coding sequences from antiSMASH predicted BGCs as input. Pairwise distances were transformed into an all-versus-all distance

matrix and used to generate a neighbor joining tree with Phylip (Fig. 2). The NRPS-BGC phylogeny reflects known literature and highlights the astonishing diversity of BGCs across this selected set of 168 *Pseudomonas* genomes. BGCs for siderophores and CLPs are mostly distinct, with multiple exceptions. For example, it appears that at least one (of two) BGCs involved with viscosin biosynthesis clusters alongside a large clade of BGCs associated with biosynthesis of the siderophore pyoverdine. The BGCs for COR and syringafactin cluster alongside the large clade of CLPs, but are markedly different and support the current hypothesis that they are synthesized only by pathogenic *P. syringae* strains (Medema *et al.*, 2015; Blin *et al.*, 2017). Based on BLAST analysis, only *Pseudomonas corrugata* RM-1-1-4 of the 168 *Pseudomonas* genomes encodes the *crpDE* pathway (Strano *et al.*, 2015) for corpeptin biosynthesis. Nonetheless, the phylogenetic analysis presented here suggest that evolutionary conserved BGCs critical for biosynthesis of the related peptin-like CLPs fuscopeptin and syringopeptin (*syp*) (Scholz-Schroeder *et al.*, 2001) can be found in various other pseudomonads, including the plant pathogenic bacteria *P. syringae* pv. *syringae* strain B278a and *Pseudomonas fuscovaginae* strain LMG 2158, and several others (Fig. 2).

Microbiome-level comparisons

In contrast to the individual genome comparisons, sequencing-based profiling of entire microbial communities, or microbiomes, combined with comparative sequence analyses has gained increasing attention recently. This methodology, in which the abundance and activity of all microbial members of a community is determined via high-throughput DNA (or RNA) sequencing is coined metagenomics/metatranscriptomics (Shafquat *et al.*, 2015). Consequently, research into microbial community ecology has expanded dramatically in the last decade. The microbial communities associated with plant roots (the root microbiome) and leaves (the phyllosphere microbiome), much like those that colonize the human gut, play an important role in plant functioning as they influence plant physiology and development (Bakker *et al.*, 2018). A more comprehensive understanding of these microbiomes will greatly benefit future endeavors to manipulate crop plants to protect them from biotic and abiotic stressors and boost yield (Mendes *et al.*, 2013; Mendes & Raaijmakers, 2015; Bakker *et al.*, 2018; Berendsen *et al.*, 2018). Chapelle *et al.* used metagenome and metatranscriptome sequencing to determine the composition and activity of the rhizosphere microbiome of sugar beet plants grown in soils that are naturally suppressive against the soil-borne fungal pathogen *R. solani* (Chapelle *et al.*, 2016). Comparative metagenome/transcriptome analyses of the rhizosphere microbiome community identified members of the Oxalobacteraceae, Burkholderiaceae, Sphingobacteriaceae and Sphingomonadaceae bacterial families to be enriched in the rhizosphere upon fungal invasion. Moreover, bacterial stress-related genes for the stringent response (*ppGpp* metabolism) and oxidative stress were upregulated within these families. The direct

biological triggers of these changes are yet to be identified, but it is hypothesized that oxidative stress or acidic stress incurred by oxalic acid or phenylacetic acid production by *R. solani* plays an important role (Chapelle *et al.*, 2016). Within our laboratory we are currently investigating the impact of genotype- and environment-driven plant root exudation on microbial activity in the rhizosphere, related to iron-deprivation and ISR (Bakker *et al.*, 2018; Berendsen *et al.*, 2018; Stringlis *et al.*, 2018b). By combining metagenome sequence assembly, computational BGC identification and transcriptional activity profiling via metatranscriptome sequencing, we aim to identify exudate-responsive microbial BGCs that interact with host plant physiology and development under the tested conditions.

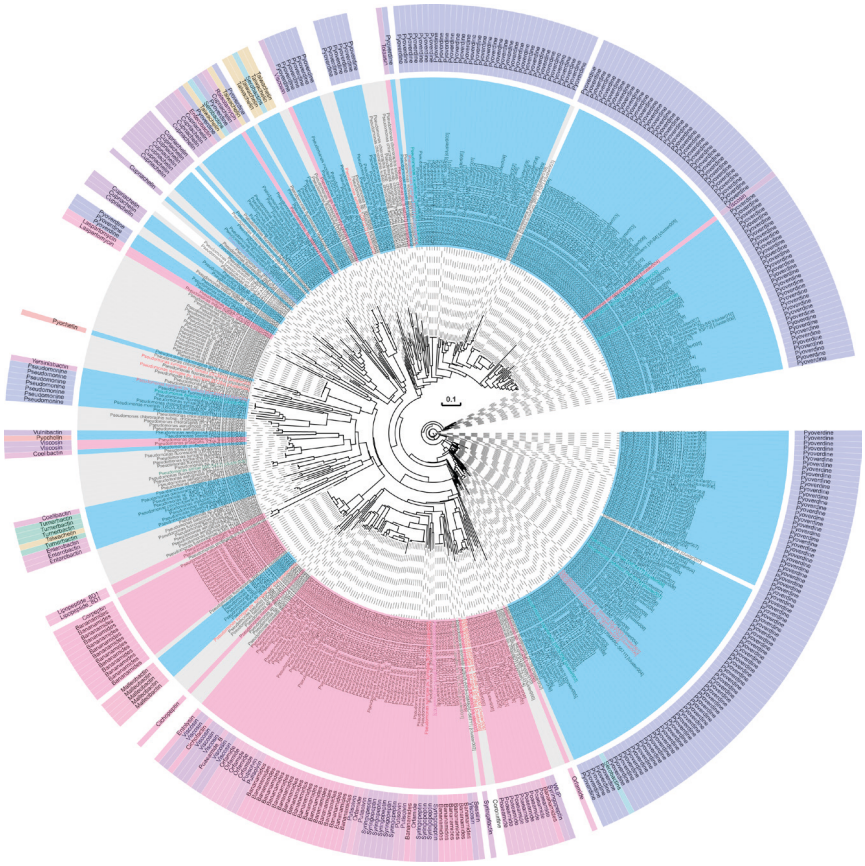

Figure 2 Phylogeny of 449 NRPS biosynthetic gene clusters from 168 *Pseudomonas* genomes.
The phylogenetic tree, represented by the circular phylogram in which branch length depicts distance, is built from 201,601 (449 times 449) Mash-derived BGC pair-wise distances. Colored shades distinguish BGCs predicted for siderophore biosynthesis (blue), cyclic lipopeptides (pink) or a group of other products, oftentimes antibiotics (grey). The leaf names of few BGCs are colored based on their origin, i.e., those from Berendsen *et al.* (WCS strains) are in green, and plant pathogenic strains are in purple. As predicted from the clusterBLAST analyses, syringopeptin-like BGCs appear in various other pseudomonads.

Identification of microbial compounds of plant-microbe interactions through functional genomics screens

In addition to sequence-derived identification of genes, pathways and putative compounds with roles in plant-microbe interactions, various research teams are undertaking high-throughput functional genomics screening. High-throughput screens can involve targeted disruption of all bacterial genes within a certain species or strain followed by individual or combinatorial assessment of their fitness (van Opijnen & Camilli, 2013), but also expression of DNA fragments of selected species or strains, and/or metagenomic fragments in a heterologous host (Cecchini *et al.*, 2013; Lam *et al.*, 2015). Genome-wide identification of bacterial colonization genes in *P. simiae* strain WCS417 by Cole *et al.* via barcoded transposon mutagenesis sequencing (TnSeq) led to the identification of 115 genes that are required for maximal competitive colonization of the Arabidopsis rhizosphere (Cole *et al.*, 2017). A number of these genes could be readily linked to established rhizosphere competence traits such as motility and carbon metabolism (Lugtenberg *et al.*, 2001a), whereas for others no previous implication in rhizosphere competence was observed. All but one of these genes are non-unique and can be found in other *Pseudomonas* genomes based on our orthogroup assignment here. The frequency of orthologs range from 3 till 448, and we anticipate that sensible integration of this resource and others helps to predict universal mechanisms of plant-microbe interactions.

Concluding remarks

Biological roles of microbe-derived natural products on microbial associations with plants, we mentioned in this review, display interesting parallels between microbes that are detrimental and those that are beneficial for the plant. Both groups of microbes use analogous strategies to colonize their host, and thus this division, to some extent, is context dependent. Even more so, certain pathogenic microbes might cause severe disease on one plant but are endophytic on others. It is uncertain whether the molecular mechanisms employed by these microbes are different on the different hosts. In the case of Fusarium head blight, caused by *Fusarium graminearum*, it was shown that symptomatic infections on cultivated wheat and barley differ from asymptomatic infections on alternative native grasses (Lofgren *et al.*, 2018). On the former, significant accumulation of trichothecene mycotoxins is observed, whereas those are absent from the latter. This is congruent with previous work suggesting that mycotoxin production by *F. graminearum* is required for full disease symptom development on cultivated wheat (Goswami & Kistler, 2005). An open question is whether *F. graminearum* does not produce these mycotoxins whilst infecting native grasses, or whether these grasses have evolved mechanisms to metabolize or detoxify them. It is not unlikely that other agriculturally eminent plant pathogens can also

resort in wild relatives of their cognate crops or in other uncultivated plants. A classic example of such is black stem rust on wheat caused by *Puccinia graminis* f. sp. *tritici*. To complete its sexual lifecycle, *Puccinia* depends on an alternative host, the barberry (*Berberis vulgaris*). It should be noted that *Puccinia* does cause disease on this alternative host. The interaction between the model plant Arabidopsis and the endophytic fungus *Colletotrichum tofieldiae* represents another attractive example of the dynamic nature of plant-microbe interactions. *C. tofieldiae* was originally isolated from asymptomatic Arabidopsis plants, and re-inoculations on germ-free Arabidopsis confirmed its ability to colonize the root interior without causing discernible disease symptoms (García *et al.*, 2013; Hiruma *et al.*, 2016). Thus, under these conditions *C. tofieldiae* behaves as a true endophyte, distinct from other *Colletotrichum* species that are notorious agents of anthracnose disease on a multitude of host plants. Moreover, when plants were grown under phosphate-starvation conditions, *C. tofieldiae* promotes plant growth by active translocation of phosphate into the plant (Hiruma *et al.*, 2016). Intriguingly, plant growth promotion by *C. tofieldiae* depends on functional tryptophan-derived indole glucosinolate metabolism; and the absence thereof flips the interaction from beneficial to detrimental (Hacquard *et al.*, 2016; Hiruma *et al.*, 2016). Noteworthy, we have recently shown that *C. tofieldiae*, unlike related *Colletotrichum* species, lacks the entire cercosporin toxin biosynthetic gene cluster and we postulate that loss of this pathway might be associated with its endophytic lifestyle (De Jonge *et al.*, 2018).

As we have highlighted, natural products play an important role in the communication between microbes and plants. Through the production and/or modulation of phytohormones, microbes subvert plant physiology and immunity to maximize microbial proliferation. Whereas in some cases this results in a mutualistic association in which microbial expansion goes hand in hand with growth promotion, in other cases plants succumb to pathogenic microbes resulting in disease development, and in the case of agriculture, diminished yields. Toxins, on the other hand, are not only of concern because they contribute to disease development in the case of many plant pathogens, but they also may cause severe problems if consumed by animals, including us humans. Aflatoxin and aflatoxin-like compounds produced by *Aspergillus* species cause frequent problems for human consumption as they are important risk factors for the development of (liver) cancer in humans. Due to its status as mycotoxin, contaminated foods, and feeds, cannot be sold and thus in addition to its health effects it also has severe economic consequences. Thus, knowledge on natural product biosynthesis is not only important in the context of food security, but it also has significant impact on food safety.

Understanding the why, how, when and where of microbial natural product biosynthesis in relation to plant growth and health will be vital to provide maximal benefits

of beneficial microbes and limit the impact of pathogenic ones. We envisage that in the future, microbial bioinoculants could be supplemented with natural products that stimulate microbial establishment on the plant and promote plant health and growth. Also, better understanding of toxin biosynthesis might aid in the development of detoxifying microbial inoculants, much alike the principles of contaminated soil phytoremediation.

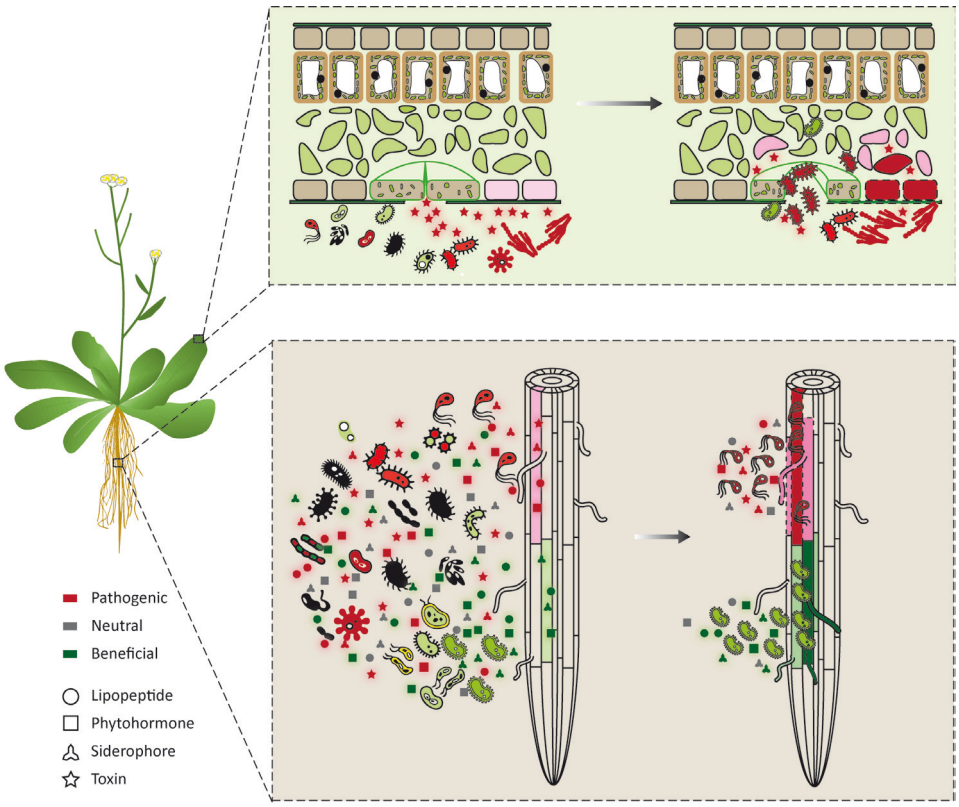

Figure 3 Microbial small molecules subvert plant immunity, and alter plant physiology and development.
Plants both above-ground and below-ground interact with a myriad of microbes that can be pathogenic (red), neutral (black) or beneficial (green). To become established in the plant, these microbes resort to various, overlapping strategies to subvert plant immunity and maximize colonization. Production of toxins facilitates pathogen entry or can induce cellular damage (red zones) whereas lipopeptides with biosurfactant properties enable microbial movement towards and along the plant. Microbe-derived phytohormones on the other hand affect general plant development and physiology, by altering root architecture or inducing cellular proliferation, boosting plant growth by beneficial microbes (green zones) or facilitating disease development by pathogens (red zones).

The computational case study presented here across the well-studied genus *Pseudomonas*, which incorporated plant beneficial, detrimental and human pathogenic strains and species, has revealed the tremendous diversity across this genus and should help to direct research towards understanding the role of pseudomonads in the environment. This data appears to support a picture in which pathogenic, commensal and beneficial microbes are more similar than previously anticipated and consequently the strict lifestyle boundaries as defined in older literature are fading (Fig. 3). Considering the dynamic nature of these genomes, such information also greatly affects the way by which we assess the pathogenic or beneficial potential of a certain sample or strain. The rapidly advancing fields of host-microbe interactions, bioinformatics, metabolomics and metagenomics will be highly instrumental in uncovering novel mechanisms and microbial molecules by which pathogens and beneficial microbes interact with their host, and in the development of novel strategies for sustainable crop protection.

Acknowledgments

This work was supported by a China Scholarship Council fellowship (to H.Z.).

Thesis outline

The plant-associated bacterial genus *Pseudomonas* encodes a large genetic diversity and capacity, including the potential to synthesize a variety of natural products while interacting with plants. These natural products support microbial survival in the rhizosphere in manifold ways, including nutrient acquisition, countering competing microbes, and by facilitating plant colonization. The benefits of selected products to microbial hosts appear context dependent as many of these products are observed in both beneficial and pathogenic microbes. So far, it is not clear how and when these products become useful or harmful to the plants, which could be one reason contributing to the inconsistent performance of plant-beneficial microbes in the field. Consequently, while pathogenic microbes might cause severe disease on one plant, they could be endophytic on another. The plasticity of microbial behavior redefines the boundary between plant-beneficial and plant-pathogenic. Li *et al.* conducted a landmark study on the evolution of the root-dwelling *Pseudomonas protegens* CHA0 (CHA0) bacterium in the rhizosphere of Arabidopsis (Li *et al.*, 2021a). The study reveal that CHA0, which initially reduced growth of Arabidopsis, under rapid evolution, leading to the emergence of plant-beneficial isolates that promoted plant growth. The evolved isolates showed improved competitiveness for root exudates and greater tolerance towards the plant-secreted antimicrobial scopoletin, thereby enhancing their fitness in the rhizosphere (Li *et al.*, 2021a).

This thesis describes the continued work on these evolved plant-beneficial CHA0 isolates, focusing on the characterization of a crucial LPS O-antigen biosynthesis gene cluster. This cluster plays a significant role in the adaptation of CHA0 and likely many others.

In **Chapter 2**, we describe the identification of thirty-five mutations distributed over twenty-eight genes in the evolved CHA0 isolates. These mutations are located in global regulators gacS/gacA, and in genes regulating siderophore production, cell surface decoration, attachment, as well as microbial motility. Phenotypic characterization, next, revealed increased swimming motility of mutants derived from independent evolutionary lines, thus providing evidence for parallelism in the experimental evolution. We conclude that the followed methodology of simplified and repeated experimental evolution can be a useful tool to understand bacterial adaption.

Among the thirty-five mutations, four mutations in three *OBC3* (O-antigen polysaccharide biosynthesis cluster 3) genes were identified. In **Chapter 3**, we describe the characterization of these three O-antigen decoration genes, i.e., *oafA*, *galE*, and *RS09880*. We focus, specifically, on *oafA*, which was mutated in two independently

evolved CHA0 lines. Protein sequence analysis predicted that *oafA* encodes a candidate O-antigen acetyltransferase. This class of proteins is involved in the acetylation of the O-antigen portion of bacterial LPS. We compared the metabolic versatility of one of the *oafA* mutants with the ancestral CHA0 isolate and show that enhanced fitness of this mutant is plant host dependent. *In vitro* experiments further show that enhanced root competence is due to increased root attachment.

As O-antigen modification is also known as a mechanism of gram-negative bacteria to defend against bacteriophage attack, in **Chapter 4**, we assessed phage sensitivity of the *OBC3* mutants. To corroborate the experimental work, we quantified the presence of phages in the evolutionary experiment and performed a computational analysis to identify prophages in the genome of CHA0. Prophages are inactive phages integrated in the host genome that could become active when bacteria experience particular stresses. Although we identified four such prophages in CHA0, the experimental analysis revealed neither phage activation *in vitro* nor presence of phages in the evolutionary experiment. Unlike *galE* and *RS09880* mutants, the *oafA* mutant demonstrated unaltered phage sensitivity compared to CHA0, leading us to believe that phages likely didn't play a role during selection of these mutants. Lastly, we characterize the distribution and structure of the *OBC3* gene cluster among environmental *P. protegens* strains. Several *oafA* mutations were found among these environmental strains with markedly similar mutations as the ones we identified in CHA0. Also, it appeared that *OBC3* mutations are common in nature, possibly related to its role in bacteria-phage interactions.

In the closing discussing **Chapter 5**, I revisit all the identified mutants and draw a picture of the potential evolutionary strategies of CHA0 in the rhizosphere. I discuss the selection pressure imposed by plants which might affect bacterial adaptation with particular emphasis on motility and biofilm formation and cell surface decoration. The impact and the limitations of these findings are also discussed.

2

CHAPTER 2

Experimental-evolution-driven identification of Arabidopsis rhizosphere competence genes in *Pseudomonas protegens*

Erqin Li[1,*], Hao Zhang[1,*], Henan Jiang[1], Corné M.J. Pieterse[1], Alexandre Jousset[2], Peter A.H.M. Bakker[1], Ronnie de Jonge[1]

[1]Plant-Microbe Interactions, Department of Biology, Science4Life, Utrecht University, Padualaan 8, 3584 CH, Utrecht, the Netherlands

[2]Ecology and Biodiversity, Department of Biology, Science4Life, Utrecht University, Padualaan 8, 3584 CH, Utrecht, the Netherlands.

*E.L. and H.Z. contributed equally to this article.

Published:
mBio 12: e00927-21 (2021)

Abstract

Beneficial plant root-associated microorganisms carry out a range of functions that are essential for plant performance. Establishment of a bacterium on plant roots, however, requires overcoming several challenges, including competition with neighboring microorganisms and host immunity. Forward and reverse genetics has led to the identification of mechanisms that are used by beneficial microorganisms to overcome these challenges such as the production of iron-chelating compounds, the formation of strong biofilms, or the concealment of characteristic microbial molecular patterns that trigger the host immune system. However, how such mechanisms arose from an evolutionary perspective is much less understood. To study bacterial adaptation in the rhizosphere, we employed experimental evolution to track the physiological and genetic dynamics of root-dwelling *Pseudomonas protegens* in the *Arabidopsis thaliana* rhizosphere under axenic conditions. This simplified binary one plant-one bacterium system allows for the amplification of key adaptive mechanisms for bacterial rhizosphere colonization. We identified 35 mutations, including single-nucleotide polymorphisms, insertions, and deletions, distributed over 28 genes. We found that mutations in genes encoding global regulators, and in genes for siderophore production, cell surface decoration, attachment, and motility accumulated in parallel, underlining that bacterial adaptation to the rhizosphere follows multiple strategies. Notably, we observed that motility increased in parallel across multiple independent evolutionary lines. Altogether these results underscore the strength of experimental evolution to identify key genes, pathways, and processes for bacterial rhizosphere colonization, and a methodology for the development of elite beneficial microorganisms with enhanced root-colonizing capacities that can support sustainable agriculture in the future.

Author contributions:

Both H.Z. and E.L. contributed equally to the experimental design, execution, and the analysis of the resulting data. Additionally, they both played major roles in writing the manuscript. E.L., H.Z., A.J., C.M.J.P., P.A.H.M.B., and R.D.J. designed experiments; E.L., H.Z., and H.J. performed experiments; E.L., H.Z., and R.D.J. analyzed data. All authors participated in content discussions and made contributions to the final published version.

Introduction

Plants are associated with complex microbial communities assembled into a functional microbiome that safeguards optimal plant performance under harsh environmental conditions (Bakker *et al.*, 2020). The rhizosphere is a particularly interesting hotspot of plant-microbe interactions. Plants deposit up to 44% of their photosynthetically fixed carbon into the rhizosphere, fueling a specific microbial community (Bais *et al.*, 2006b). The microbial species pool in the bulk soil is the source from which the root microbiome is recruited, and plant genotype, immune responses, and environmental factors are postulated to affect this process (Philippot *et al.*, 2013; Bakker *et al.*, 2018; Sasse *et al.*, 2018; Stringlis *et al.*, 2018b). The establishment of beneficial microbial associations requires a high degree of coordination of both plant and microbial responses by means of a continuous molecular dialogue (Bais *et al.*, 2004; Zamioudis & Pieterse, 2012). Plant-associated microorganisms can improve plant yield by protecting the plant from abiotic stresses (Yang *et al.*, 2009), improving plant nutrition and growth (Ryu *et al.*, 2003; Lugtenberg & Kamilova, 2009; Browne *et al.*, 2009), antagonizing soil-borne pathogens (Haas & Défago, 2005), or stimulating plant immunity (Pieterse *et al.*, 2014). To exert their beneficial effects on plant performance, bacteria must colonize the roots efficiently and establish significant populations. For example, bacterial population densities above 10^5 cells per gram of root are required for efficient suppression of soil-borne plant pathogens by *Pseudomonas* spp. (Raaijmakers *et al.*, 1995, 1999). Therefore, bacterial adaptation to the plant root environment may be essential for the successful implementation of microbiome services in agriculture in order to support plant health.

Among all root-dwelling organisms, fluorescent *Pseudomonas* spp. are well characterized in terms of the traits required for their growth in the rhizosphere and for the establishment of beneficial plant-microbe interactions (Lugtenberg *et al.*, 2001b; Pieterse *et al.*, 2021). To study bacterial traits involved in efficient root colonization, mutants defective in specific traits suspected to be involved in colonization, are compared to the parental strains for their ability to colonize plant roots. Such studies have highlighted a range of bacterial traits involved in efficient root colonization, including flagella (De Weger *et al.*, 1987), surface lipopolysaccharides (LPS) (De Weger *et al.*, 1989b), and amino acid synthesis (Simons *et al.*, 1997). Using random mutagenesis and by determining the fitness of each mutant in competition with its parental strain in the rhizosphere, many other important traits for rhizosphere competence in *Pseudomonas* were discovered (Lugtenberg *et al.*, 2001b). Recently, random mutagenesis in *Pseudomonas capeferrum* WCS358 led to the identification of two genes that are important for gluconic acid (GA) biosynthesis. GA, in turn, is essential for the suppression of local, flagellin-induced root immune responses (Yu *et al.*, 2019). Such suppression was

shown to be important for rhizosphere competence as GA-deficient mutants maintain reduced populations in the rhizosphere (Yu *et al.*, 2019). In another recent study, genome-wide saturation mutagenesis of *Pseudomonas simiae* WCS417r revealed that 2% of the protein-coding genes are important for successful root colonization (Cole *et al.*, 2017). Mutations that negatively affect rhizosphere competence, and mutations that confer a competitive advantage were identified in this study. The identification of mutations that can lead to increased root colonization (Cole *et al.*, 2017), suggests that there is room for improvement of bacterial fitness in the rhizosphere.

In the present study we used an experimental evolution approach (Kawecki *et al.*, 2012) to study how *Pseudomonas protegens* CHA0 (CHA0) evolves during repeated colonization of the rhizosphere of the model plant *Arabidopsis thaliana* (Arabidopsis). The model biological control agent CHA0 displays broad-spectrum antagonistic activity against several plant pathogenic fungi and bacteria (Lugtenberg & Kamilova, 2009), and its complete genome sequence is available (Jousset *et al.*, 2014). We performed highly controlled experimental evolution in a gnotobiotic and carbon-free sand system in which bacteria depend solely on the plant for supply of carbon. Following inoculation and establishment on the roots, bacterial populations were transferred to new plants, and this cycle was repeated eight times. We hypothesized that the repeated colonization and establishment of the bacterial population on the plant root would create an environment in which selection pressure drives the accumulation of better colonizers. *In vitro* characterization of individual bacterial colonies from these populations combined with sequencing analysis led to the identification of several evolutionary trajectories involving 35 distinct mutations that impact social traits representing inter-population communication and cooperation, carbon source utilization, motility, or biocontrol activity. By combining experimental evolution with whole genome re-sequencing, we created a powerful screen for the identification of adaptive mutations with positive effects on rhizosphere colonization.

Results

Mutational events in independent evolutionary lines

We previously studied five experimental evolutionary populations, referred to as lines, of CHA0 evolving in the rhizosphere of Arabidopsis in a gnotobiotic system. Independent populations were introduced on the roots and after four weeks of plant growth the populations were transferred to new plants. This cycle of transferring was repeated eight times, and we performed extensive characterizations up until cycle six to account for feasibility (Li *et al.*, 2021a). In short, for each line, after every cycle we plated a fraction of the population on culture media and randomly picked 16 colonies for extensive phenotypic assessment of bacterial life history traits (Li *et al.*, 2021a). In order to study adaptation at the genetic level, we selected six colonies from each line at cycles 2, 4, and 6 such that they represented most of the observed phenotypic diversity among the 16 colonies that were initially picked and characterized. These colonies, as well as six colonies from the ancestral population that was initially introduced on the roots, were re-sequenced to an average depth of 25-fold coverage (minimum 10, maximum 70) and used for the identification of single nucleotide polymorphisms (SNPs), as well as small and large insertions or deletions (INDELs). In total we thus set out to acquire genetic data for 96 bacterial colonies (5 lines * 3 cycles * 6 colonies + 6 ancestral colonies). Unfortunately, we were unable to acquire sufficient sequencing data for two colonies from line 4 at cycle 4, yielding a final set of 94 (88 evolved, 6 ancestral) re-sequenced colonies. The six ancestral colonies were all identical, indicating that there was no genetic variation in the starting population and that all observed mutations are *de novo* mutations. In total, one or more mutations were detected in 64 evolved colonies, which collectively represent 73% of the 88 characterized bacterial colonies (Table S1). We identified 5 synonymous substitutions, 20 nonsynonymous substitutions, and 4 deletions ranging in length from 1 base pair (bp) to about 400 bp, distributed over 22 genes, and 6 additional mutational events located in intergenic regions (Table 1). Mutations located in intergenic regions possibly affect transcription of nearby genes via affecting their regulatory proteins binding sites and subsequent changes in their promoter activity (Carroll, 2008; Oren *et al.*, 2014). Several mutations were found to be clustered in select genes and/or regions in the CHA0 genome, e.g., those in the response regulator *gacA* gene (PFLCHA0_RS17965; *NC_021237:4,039,113-4,039,754*) or in the *OBC3* gene cluster involved in LPS biosynthesis (*NC_021237:2,173,707-2,196,028*) (Kupferschmied *et al.*, 2016), but the majority of the mutations were spread across the 6.1 Mbp CHA0 genome (Fig. 1). Functional characterization of the mutated genes by analyzing their Clusters of Orthologous Groups (COGs) annotation revealed that the majority of these genes are involved in transcription (COG term 'K'), signal transduction mechanisms (COG term 'T'), amino acid transport and metabolism (COG term 'E') and cell wall/membrane/envelope biogenesis (COG term 'M') (Fig. 1, Table 1).

Table 1 Mutations that occurred in 28 genes during Arabidopsis rhizosphere adaptation divided over five replicate CHA0 populations (lines)

Locus tag	Gene name	Description	COG[1]	Line	Total number of alleles	Number of mutations in protein-coding genes			Number of intergenic mutations
						Non-synonymous	Synonymous	Deletions	
PFLCHA0_RS02080	*hutI*	Imidazolonepropionase	F	4	1	0	1	0	0
PFLCHA0_RS03400	*accC*	Biotin carboxylase, acetyl-CoA carboxylase subunit	I	2	1	1	0	0	0
PFLCHA0_RS05510	*nudL*	Coenzyme A pyrophosphatase/nudix hydrolase NudL	L	4	1	0	1	0	0
PFLCHA0_RS06125	*rpoS*	RNA polymerase sigma factor RpoS	K	5	1	1	0	0	0
PFLCHA0_RS08340	*fleQ*	Sigma-54-dependent Fis family transcriptional regulator	T	5	1	1	0	0	0
PFLCHA0_RS08490	*flhA*	Flagellar biosynthesis protein FlhA	N	4	1	0	0	1	0
PFLCHA0_RS09880	*RS09880*	Glycosyltransferase (GT)	M	5	1	1	0	0	0
PFLCHA0_RS09890	*oafA*	O-antigen acetylase	I	1, 3	2	1	0	1	0
PFLCHA0_RS09920	*galE*	UDP-glucose 4-epimerase	M	2	1	1	0	0	0
PFLCHA0_RS11785	*RS11785*	LysR family transcriptional regulator	K	4	1	1	0	0	0
PFLCHA0_RS11820	*RS11820*	PaaI family thioesterase	Q	4	1	0	1	0	0
PFLCHA0_RS12070	*RS12070*	2OG-Fe(II) oxygenase superfamily	S	5	1	0	1	0	0
PFLCHA0_RS13000	*yvaQ2*	Methyl-accepting chemotaxis protein	NT	2	1	0	0	0	1

PFLCHA0_RS14960	*tetR*	TetR/AcrR family transcriptional regulator	K	5	1	1	0	0	0
PFLCHA0_RS17350	*RS17350*	Methyltransferase domain-containing protein	H	1	1	0	0	1	0
PFLCHA0_RS17965	*gacA*	UvrY/SirA/GacA family response regulator transcription factor	K	1, 2, 4	6	5	0	0	1
PFLCHA0_RS18525	*RS18525*	ABC transporter substrate-binding protein	E	5	1	1	0	0	0
PFLCHA0_RS21265	*pvdS*	RNA polymerase factor sigma-70	K	1	1	0	0	0	1
PFLCHA0_RS21275	*RS21275*	Transporter substrate-binding domain-containing protein	ET	1	1	1	0	0	0
PFLCHA0_RS21855	*wbpM*	Polysaccharide biosynthesis protein/NDP-sugar epimerase	GM	1	1	1	0	0	0
PFLCHA0_RS22600	*gacS*	Hybrid sensor histidine kinase/response regulator	T	3	1	1	0	0	0
PFLCHA0_RS22950	*argT5*	ABC transporter substrate-binding protein/Lysine-arginine-ornithine-binding periplasmic protein ArgT	ET	4	1	0	0	1	0
PFLCHA0_RS25175	*mraZ*	Division/cell wall cluster transcriptional repressor MraZ	K	2	1	0	0	0	1
PFLCHA0_RS26215	*osmY*	Osmotically-inducible protein OsmY/BON domain-containing protein	S	2	1	0	0	0	1
PFLCHA0_RS27515	*rpsH*	30S ribosomal protein S8	J	4	1	0	0	0	1

Table 1 Mutations that occurred in 28 genes during Arabidopsis rhizosphere adaptation divided over five replicate CHA0 populations (lines)

Locus tag	Gene name	Description	COG[1]	Line	Total number of alleles	Number of mutations in protein-coding genes			Number of intergenic mutations
						Non-synonymous	Synonymous	Deletions	
PFLCHA0_RS30075	*sadB*	Surface attachment defective (SadB) ortholog/HDOD domain-containing protein	T	1	2	2	0	0	0
PFLCHA0_RS30120	*tssM*	Type VI secretion system membrane subunit TssM	S	2	1	0	1	0	0
PFLCHA0_RS31060	*nlpD*	Lipoprotein nlpD/lppB/LysM domain-containing protein	D	3	1	1	0	0	0
Total	28				35	20	5	4	6

[1]Clusters of Orthologous Groups (COGs); https://www.ncbi.nlm.nih.gov/COG/(Galperin *et al.*, 2015)

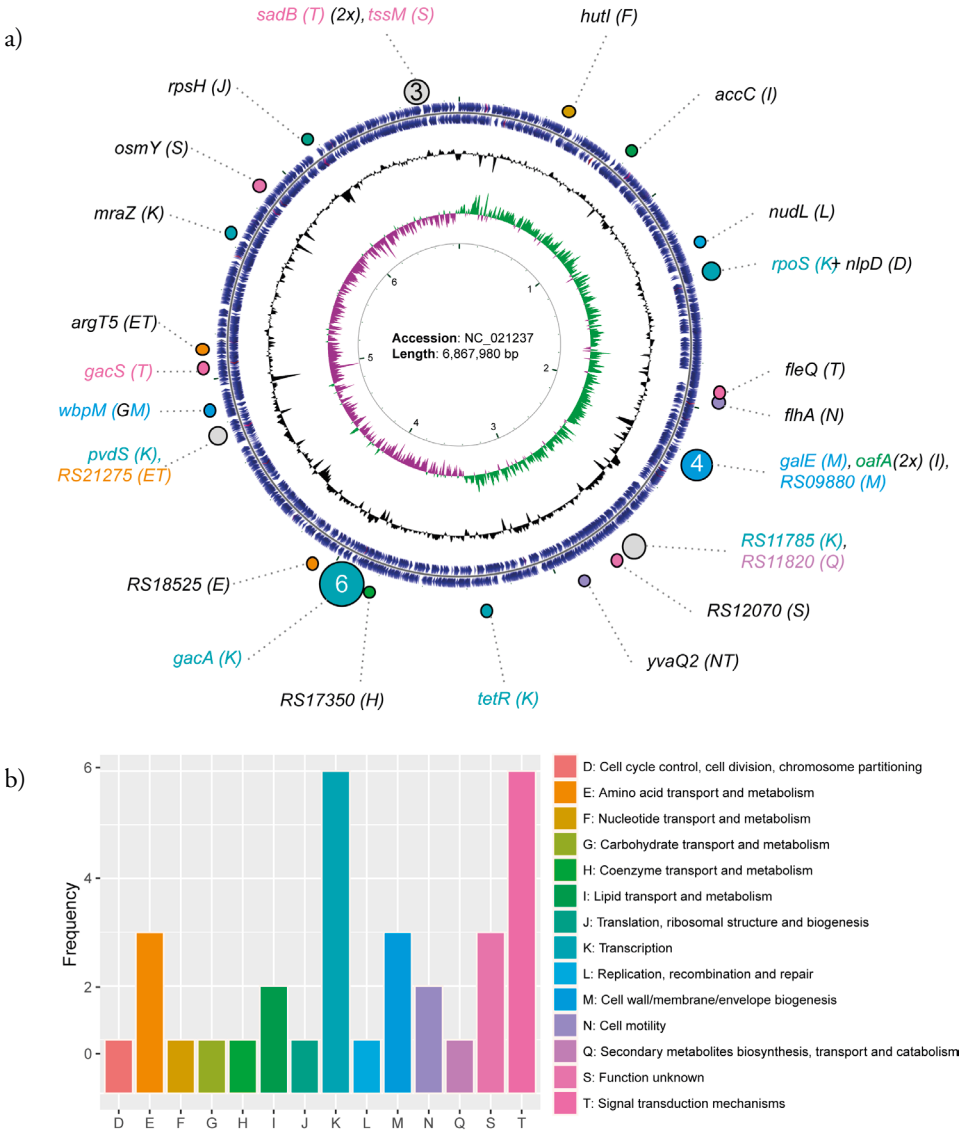

Figure 1 Genomic distribution of *P. protegens* CHA0 evolutionary adaptations.
a) Rings from inside to outside: Ring 1, nucleotide position indicator; Ring 2, green/purple GC-skew (-/+); Ring 3, %GC; Ring 4, protein-coding genes; Ring 5, distribution of identified mutations arisen during the evolutionary experiment. Functional annotations of mutated genes are indicated by color representing Cluster of orthologous groups (COGs); the key of which can be seen in panel B. b) Frequency of mutations per COG class, highlighting enrichment in the classes T (signal transduction), K (transcription), M (cell wall) and E (amino acid transport and metabolism).

Identification of potential root colonization genes

Bacterial genes that are involved in colonization of plant roots can be revealed by identifying beneficial mutations that evolve during adaption of bacteria to the rhizosphere environment and have positive effects on root colonization. Over time, such mutants will outcompete the ancestral strain and become dominant in the bacterial population. The observation that only a limited number of mutations accumulated relative to the total number of genes within the genome across the entire experiment, makes it highly unlikely that the same gene would acquire several changes by chance in independent evolutionary lines. Nevertheless, we observe recurrent mutations in several of the same genes and/or pathways (Table 1), which is a strong indication for adaptive evolution. Genes or pathways that acquired mutations in multiple independent CHA0 populations included *gacA* and *gacS*, the *OBC3* gene cluster (*oafA*; *galE*; *PFLCHA0_RS09880* (Kupferschmied *et al.*, 2016)), and a putative pyoverdine siderophore biosynthesis cluster (*pvdS*; *PFLCHA0_RS21275*). Other genes, like *sadB*, were targeted more than once in the same population. Because these genes were repeatedly identified in the CHA0 evolution experiment, they can be assumed to contribute significantly to bacterial fitness in the rhizosphere (Table 1, Fig. 2). Moreover, it suggests that the independent evolutionary lines converge on similar evolutionary trajectories involving overlapping biological processes and molecular mechanisms.

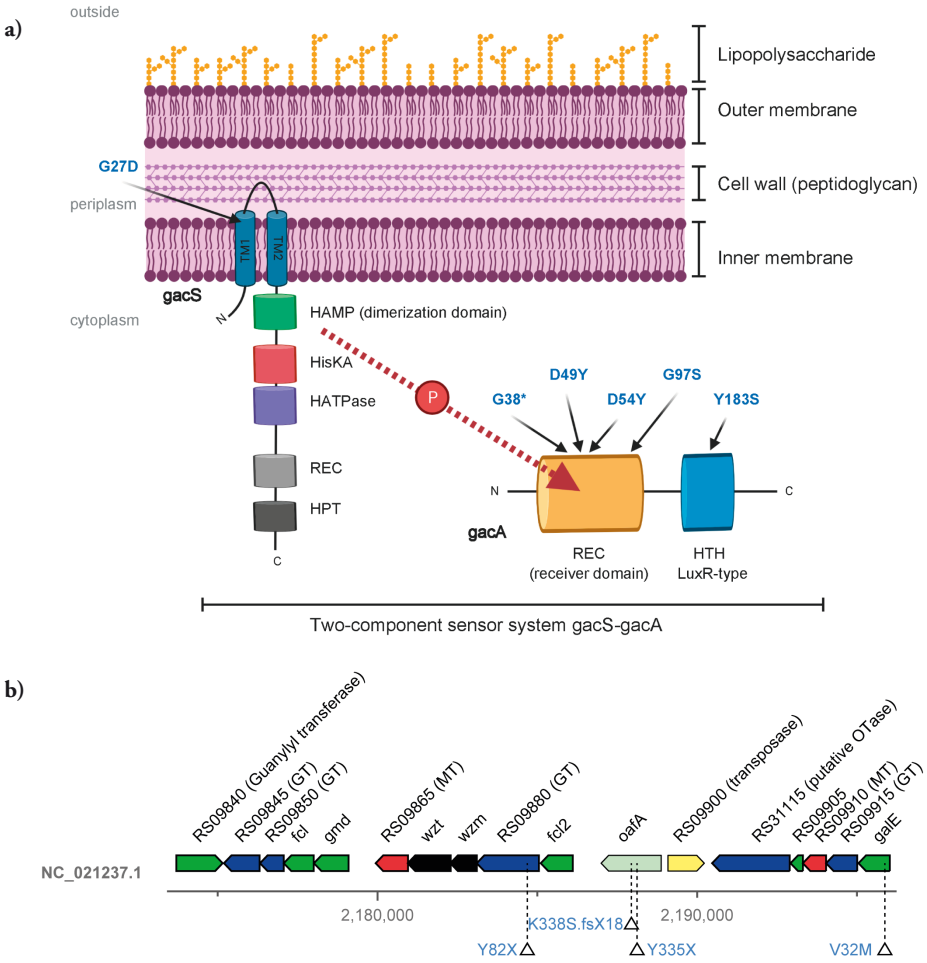

Figure 2 Localization of *gac* and *OBC3* mutations identified in the evolutionary experiment .
a) Schematic view of the cell wall of the gram-negative bacterium *P. protegens* highlighting the presence of the lipopolysaccharide (LPS) on the outside and the presence of the two-component regulator system GacS/GacA on the inner membrane and in the cytoplasm. The arrows indicate the location of the amino acid substitutions that were identified in this study in GacS (G27D) and GacA (G38X, D49Y, D54Y, G97S and Y183S). Note the travel of a phosphate group (P) from GacS to GacA upon signal perception which is accepted by either the Asp49 or Asp54 residue in GacA which are both found mutated in two different mutants. b) Genomic region harboring the *OBC3* gene cluster responsible for the synthesis of long O-polysaccharide (O-PS) on the LPS and indicated mutations that were identified in a glycosyl transferase (*RS09880*; Y82X), the O-antigen acetyltransferase *oafA* (K338S.fsX18 and Y335X) and the UDP-glucose 4-epimerase (*galE*; V32M).

To illustrate the diverse evolutionary trajectories, we constructed phylogenetic trees of each replicate population (line) using all mutations that were detected (Fig. 3). In each line, both the number and depth of branches are very different (Fig. 3, Table 2). In line 1 and 3, the populations were swept early by oafA mutants and later by specific gac mutants, while in line 2 and 4, co-existence of multiple genotypes characterized by gac mutations was observed indicative of clonal interference between lineages (Fig. 3) (Maddamsetti *et al.*, 2015)). Notably, the relative abundance of each genotype in the population is estimated from a small set of sequenced individuals and therefore is expected to lack precision. The evolved isolates contain one to four mutations in general, and in each line, 3 (line 3) to 9 (line 2 and 4) mutations were identified in total. All mutations were unique for each line, as is expected for independently evolving populations.

As the frequency of each mutation (Fig. 3, Table 2) was determined from only six bacterial colonies that were isolated and sequenced from each evolutionary line at cycles 2, 4 and 6, we further investigated and accurately measured the population-level frequency at the end of each experimental cycle. We determined the frequency of three *gac* mutations, i.e., *gacA*^{D49Y}, *gacA*^{D54Y}, and *gacS*^{G27D}, with increased accuracy, i.e., by PCR-based high-resolution melting (HRM) analysis incorporating mutation-specific HRM probes (Table S2), and increased sampling depth, i.e., at the end of experimental cycles 1 to 8. The HRM methodology allows for the accurate quantification of mutant frequency across a wide range for all three mutations ($p < 0.001$; Fig. S1). Using this method, we found that the population-level frequency of these three mutations in the respective evolutionary lines corresponded remarkably well with the frequency previously obtained from the cultured and sequenced isolates (Table 2, Fig. S2). These findings corroborate the culture-based quantification of mutant frequency suggesting they provide a reasonable measure for population-level frequency. Intriguingly, it can be seen that the *gacS*^{G27D} mutation reaches fixation after eight experimental cycles, while the *gacA*^{D49Y} and *gacA*^{D54Y} mutants stabilize at around 50% and 25%, respectively (Fig. S2). Stabilization of mutations is indicative of frequency-dependent (FD) selection putatively reinforced by clonal interference with co-existing lineages carrying beneficial mutations in *sadB* ^{L258Q} and *gacA*^{G97S} (Fig. 3). FD selection describes the phenomenon that the fitness of a particular genotype or phenotype is dependent on its frequency. Such context-dependency has been linked to cheating behavior in which microbial cells that lack or have limited production of certain costly compounds benefit from other cells that do produce these compounds. When a minimal amount of such compound increases genotype or phenotype fitness, FD selection can occur resulting in stabilization of the mutation frequency.

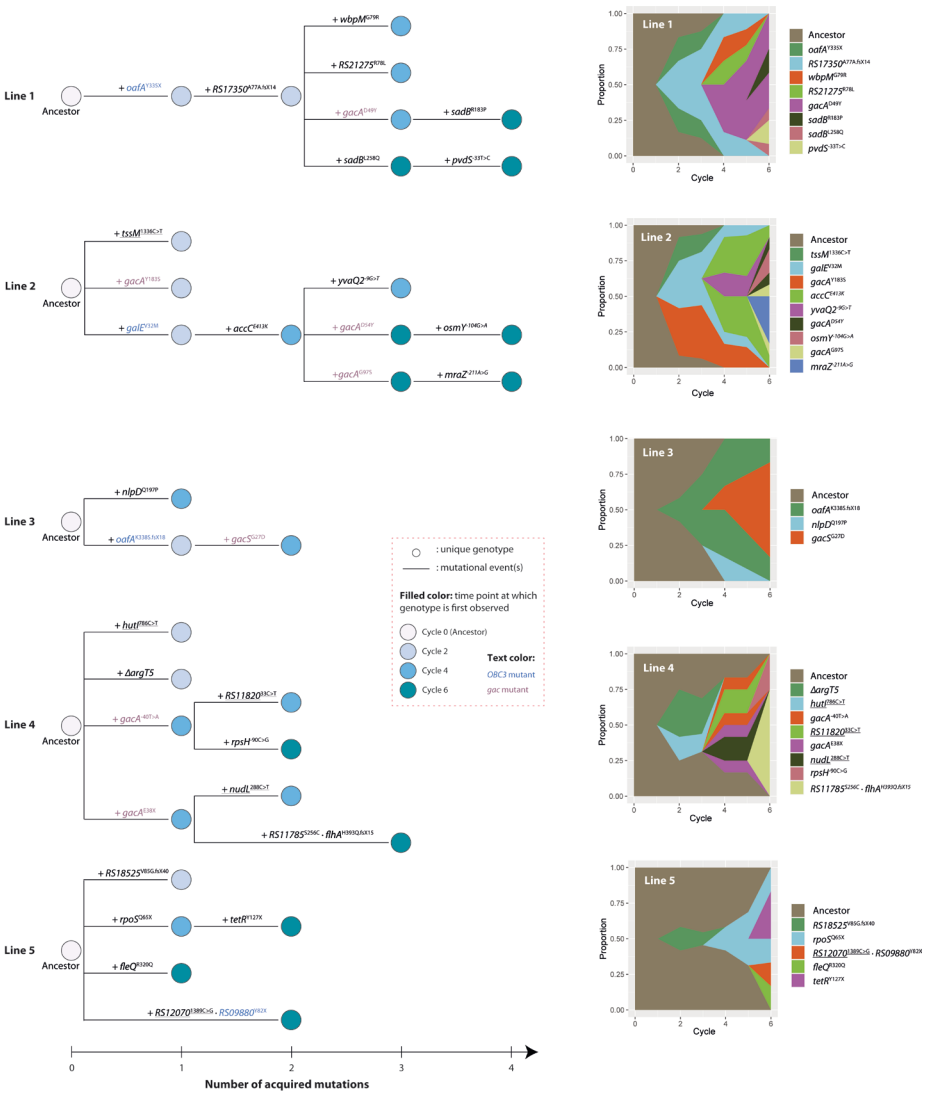

Figure 3 Phylogenetic trees and Muller plots of five independently evolving *P. protegens* CHA0 populations.

Left) Phylogenies for 18 genomes from each population (16 for the population in experimental line 4), based on the sequential appearance of mutations are shown. Synonymous mutations are underlined. Circles represent unique bacterial genotypes. The color of the circle fill represents the time point at which a genotype was firstly detected. *OBC3* and *gac* mutants are highlighted in blue and purple, respectively. Right) Muller plots depicting the dynamics of mutant alleles during the evolutionary experiment. The Muller plots show the estimated frequencies, by their height, of 33 mutations in the respective population over 6 experimental cycles. Descendant genotypes are shown emerging from inside their respective ancestors. The frequency of each mutation in the respective population can also be found in Table 2. Muller plots are prepared using ggmuller in R (Noble, 2019).

Table 2 Nomenclature for CHA0 mutations and variants and their frequency/cycle in each respective population

Line	Locus tag	Gene name	DNA sequence change[1]	Amino acid change (three-letter code)[2]	Standard nomenclature (used in text)	Frequency in the population (x/6)			
						Cycle 2	Cycle 4	Cycle 6	RQ-HRM[3]
1	PFLCHA0_RS09890	*oafA*	c.1005C>A	p.Tyr335X	Y335X	4/6	6/6	6/6	
1	PFLCHA0_RS17350	*RS17350*	c.230delC	p.Ala77Ala.fsX14	A77A.fsX14	2/6	6/6	6/6	
1	PFLCHA0_RS17965	*gacA*	c.145G>T	p.Asp49Tyr	D49Y	-	2/6	4/6	
						9.2%	19.1%	46.7%	x
1	PFLCHA0_RS21855	*wbpM*	c.235G>C	p.Gly79Arg	G79R	-	1/6	-	
1	PFLCHA0_RS21275	*RS21275*	c.233G>T	p.Arg78Leu	R78L	-	1/6	-	
1	PFLCHA0_RS21265	*pvdS*	c.-33T>C	NA	-33T>C	-	-	1/6	
1	PFLCHA0_RS30075	*sadB*	c.548G>C	p.Arg183Pro	R183P	-	-	1/6	
1			c.773T>A	p.Leu258Gln	L258Q	-	-	2/6	
2	PFLCHA0_RS17965	*gacA*	c.548A>C	p.Tyr183Ser	Y183S	2/6	1/6	-	
2	PFLCHA0_RS09920	*galE*	c.94G>A	p.Val32Met	V32M	2/6	5/6	6/6	
2	PFLCHA0_RS30120	*tssM*	c.1336C>T	p.Leu446Leu	1336C>T	1/6	-	-	
2	PFLCHA0_RS03400	*accC*	c.1237G>A	p.Glu413Lys	E413K	-	4/6	6/6	
2	PFLCHA0_RS13000	*yvaQ2*	c.-9G>T	NA	-9G>T	-	1/6	-	
2	PFLCHA0_RS17965	*gacA*	c.160G>T	p.As54Tyr	D54Y	-	-	2/6	
						5.5%	4.5%	15.5%	x
2	PFLCHA0_RS17965	*gacA*	c.289G>A	p.Gly97Ser	G97S	-	-	3/6	
2	PFLCHA0_RS25175	*mraZ*	c.-211A>G	NA	-211A>G	-	-	2/6	
2	PFLCHA0_RS26215	*osmY*	c.-104G>A	NA	-104G>A	-	-	1/6	
3	PFLCHA0_RS09890	*oafA*	c.1013delA	p.Lys338Ser. fsX18	K338S.fsX18	1/6	5/6	6/6	

3	PFLCHA0_RS22600	*gacS*	c.80G>A	p.Gly27Asp	G27D	-	1/6	4/6	
						3.8%	19.9%	75.6%	x
3	PFLCHA0_RS31060	*nlpD*	c.590A>C	p.Gln197Pro	Q197P	-	1/6	-	
4	PFLCHA0_RS22950	*argT5*	c.120-533del	p.Lys40-Leu185del.fsX6	Δ*argT5*	2/6	-	-	
4	PFLCHA0_RS02080	*hutI*	c.786C>T	p.Phe262Phe	786C>T	1/6	-	-	
4	PFLCHA0_RS17965	*gacA*	c.-40T>A	NA	-40T>A	-	2/6	1/4	
4	PFLCHA0_RS17965	*gacA*	c.112G>T	p.E38X	E38X	-	2/6	3/4	
4	PFLCHA0_RS05510	*nudL*	c.288C>T	p.Ser96Ser	288C>T	-	1/6	-	
4	PFLCHA0_RS11820	*RS11820*	c.33C>T	p.Ala11Ala	33C>T	-	1/6	-	
4	PFLCHA0_RS08490	*flhA*	c.1176delT	p.His393Gln.fsX15	H393Q.fsX15	-	-	3/4	
4	PFLCHA0_RS11785	*RS11785*	c.766A>T	p.Ser256Cys	S256C	-	-	3/4	
4	PFLCHA0_RS27515	*rpsH*	c.-90C>G	NA	-90C>G	-	-	1/4	
5	PFLCHA0_RS18525	*RS18525*	c.254delT	p.Val85Gly.fsX40	V85G.fsX40	1/6	-	-	
5	PFLCHA0_RS06125	*rpoS*	c.193C>T	p.Gln65X	Q65X	-	1/6	4/6	
5	PFLCHA0_RS08340	*fleQ*	c.959G>A	p.Arg320Gln	R320Q	-	-	1/6	
5	PFLCHA0_RS14960	*tetR*	c.381C>G	p.Tyr127X	Y127X	-	-	2/6	
5	PFLCHA0_RS09880	*RS09880*	c.246C>A	p.Tyr82X	Y82X	-	-	1/6	
5	PFLCHA0_RS12070	*RS12070*	c.1389C>G	p.Pro463Pro	1389C>G	-	-	1/6	

[1]DNA sequence change positions are relative to the cDNA (c); del represents a deletion
[2]X represents a stop codon (at its relative position in case of a shifted frame); fs represents a frame shift; del represents a deletion
[3]Mutations that are selected for the analysis of their frequency trajectories using RQ-HMR analysis

Early adaptations are driven by cell surface-related genes

In general, mutations that are fixed early on in the rhizosphere adaptation process tend to have a high selective advantage (Barrett *et al.*, 2006). Disruptive mutations in *oafA*, resulting in premature stops halfway the coding region, were detected as the first acquired mutations in two independent evolutionary lines (lines 1 and 3) and appear to have swept the population in the following generations (Table 2). *OafA* is part of the O-polysaccharide (O-PS, O-antigen) biosynthesis cluster 3 (*OBC3*) (Kupferschmied *et al.*, 2016), and encodes an O-acetyltransferase which is postulated to acetylate the O-antigen component of the outer membrane LPS (Allison & Verma, 2000). Another *OBC3* mutation that accumulated early on in the rhizosphere adaptation process, $galE^{c.94G>A}$, leads to an amino acid substitution (V32M) in galE and this mutation swept through the population in evolutionary line 2, reaching fixation in cycle 6 (Table 2; Fig. 3). *GalE* encodes an UDP-glucose 4-epimerase which is involved in O-antigen and LPS core biosynthesis (Samuel & Reeves, 2003; Chang *et al.*, 2008; Liu *et al.*, 2008). One colony with a mutation in a third *OBC3* cluster gene, *RS09880*, encoding a putative glycosyl transferase (GT) was found in cycle 6 of evolutionary line 5. Thus, in four out of the five evolutionary lines mutations that likely affect bacterial LPS structure appeared during rhizosphere adaptation, and these mutations became dominant in three out of four evolutionary lines. These results strongly suggest that modifying bacterial cell surface structure is an important bacterial strategy in early adaptation to the rhizosphere.

Adaption driven by global regulators

In the present study, six mutations were detected in *gacA* in three out of five evolutionary lines, representing approximately 20% of all missense mutations. Notably, in evolutionary lines 2 and 4, multiple *gacA* alleles accumulated, some of which were detected in early experimental cycles (Table 2). Additionally, a *gacS* mutation accumulated in line 3. *GacA* and *gacS* encode the main constituents of the conserved GacA/GacS two-component regulator system, i.e., the hybrid sensor histidine kinase GacS and the cognate response regulator GacA (Fig. 2). In gram-negative bacteria, activation of GacS results in cross-phosphorylation of GacA via phosphotransfer which in turn leads to activation of the expression of the small RNA genes *rsmY* and *rsmZ* via its helix-turn-helix (HTH) domain-binding domain (Brencic *et al.*, 2009). In CHA0, this regulatory pathway is known to control quorum sensing as well as secondary metabolism and stress resistance (Heeb *et al.*, 2002, 2005; Valverde *et al.*, 2003; Brown, 2010). In the closely related strain *P. protegens* Pf-5 this pathway was shown to have a big impact on bacterial genome-wide gene expression, affecting the expression of more than 10% of the annotated genes (Hassan *et al.*, 2010). Similarly, *gacA* mutants that arose on the edge of swarming Pf-5 colonies showed dramatically altered genome-wide gene expression patterns (Song *et al.*, 2016).

Including *gacS* and *gacA*, about half of the mutated genes in this study are global regulators or sigma factors (Table 1, Fig. 1). This high frequency suggests that global regulator-controlled networks are evolvable and play a major role in rapid bacterial adaptation. Pleiotropic adaptive mutations in global regulator genes have been shown to be important for bacterial adaption both in laboratory (Zambrano *et al.*, 1993; Hunter, 2008), and in natural settings (Sumby *et al.*, 2006; Giraud *et al.*, 2008). Remodeling and continuous optimization of existing regulatory networks by single mutations is an important strategy for bacterial adaptation to the host (Damkiaer *et al.*, 2013).

Bacterial motility

Bacterial motility is an important trait for rhizosphere competence, mediating colonization of distal parts of the root system (Sánchez-Contreras *et al.*, 2002), and both LPS and the GacS/GacA two-component regulator system are known to affect this trait. The O-antigen side chain of the LPS was reported to contribute to swimming and swarming motility in the plant pathogenic bacterium *Erwinia amylovora* (Berry *et al.*, 2009; Bowden *et al.*, 2013). The GacS/GacA two-component regulator system controls bacterial motility, for example by affecting transcription of genes related to flagella and biosurfactant biosynthesis (Sánchez-Contreras *et al.*, 2002; Lapouge *et al.*, 2007; Song *et al.*, 2016). We also identified several other mutations across the various evolutionary lines that can be linked to bacterial motility. For instance, a disruptive mutation in the flagellar biosynthesis protein-coding gene *flhA* (H393Q. fsX15) that is involved in the biogenesis of the bacterial flagellum (Table 1) appeared in evolutionary line 4, reaching up to a predicted frequency of 75% (Table 2; Fig. 3). In *P. fluorescens* Pf-5, and in *Pseudomonas aeruginosa* PA01 FlhA is reported to be essential for swimming motility (Hassan *et al.*, 2010).

Furthermore, we identified one amino-acid substitution, R320Q, in FleQ and two in SadB, R183P and L258Q respectively, that based on sequence similarity to well-studied, homologous proteins in other bacteria can be linked to motility in addition to several other bacterial traits. FleQ is a σ^{54}-dependent Fis family transcriptional regulator which regulates flagellar motility, biofilm formation as well as Pel exopolysaccharide (EPS) production in response to cellular c-di-GMP levels in *P. aeruginosa* (Matsuyama *et al.*, 2016). *P. protegens* FleQ shares 84% sequence identity and 98% sequence coverage with *P. aeruginosa* FleQ and like *P. aeruginosa* FleQ it is comprised of the N-terminal flagellar regulatory FleQ domain (PF06490), a central AAA+/ATPase σ^{54}-interaction domain (PF00158), and a C-terminal Fis-type HTH DNA-binding domain (PF02954). The R320Q substitution we identified here is found in the AAA+/ATPase σ^{54}-interacting domain in between the arginine (Arg) finger (amino acid 300-303) and a c-di-GMP-binding motif, ExxxR (amino acid 330-334)

(Matsuyama *et al.*, 2016). The conserved arginine residues in FleQ, including the here mutated Arg^{320}, are thought to be important for protein oligomerization, and substitution of any of these residues abolishes ATPase activity in *Vibrio cholerae* EpsE completely (Patrick *et al.*, 2011). Finally, *sadB*, encodes a HD-related output domain (HDOD)-containing protein (Table 1) that shares 77% sequence identity and 99% sequence coverage with *P. aeruginosa* SadB. In *P. aeruginosa*, SadB stimulates Pel EPS production and the chemotaxis-like cluster CheIV, which in turn affect flagellar motility as well as biofilm formation (Caiazza & O'Toole, 2004). In *Pseudomonas fluorescens* F113, SadB, together with FleQ control flagellar motility, dependent and independent of the GacS/GacA two-component regulator system (Martínez-Granero *et al.*, 2012; Muriel *et al.*, 2019).

Parallelism of targeted mutations on this functional motility pathway impelled us to assess bacterial motility and track its dynamics across all evolutionary lines. We selected all *OBC3* and *gac* mutants as well as mutants in *sadB*, *fleQ* and *flhA*. Additionally, we included two *gacA* mutant progenitors with mutations in *accC* and *RS17350*, encoding a biotin carboxylase and a methyltransferase, respectively, plus two *gacA* mutant descendants with mutations in *osmY* and *mraZ* that encode for an osmotically inducible protein and a transcriptional repressor, respectively (Table 1). Altogether, we assessed swimming and swarming motility of seventeen distinct genotypes (Fig. 4; Fig. S3). We found that *OBC3* mutants, the *gacA* progenitors with mutations in *accC* and *RS17350*, and the *gacA* descendants with mutations in *osmY* and *mraZ* were unaltered compared to their respective ancestors when considering both swimming and swarming motility, with the exception of a small yet significant increase in swarming motility in $oafA^{Y335X}$. However, g*ac* mutants themselves were significantly affected; both in swimming, which is generally enhanced, and in swarming, which is repeatedly decreased (Fig. 4). *SadB* mutants, like *gac* mutants display enhanced swimming and worsened swarming when compared to their respective progenitors. Oddly, both the *fleQ* and the *flhA* mutant displayed severely reduced swimming and swarming motility, thus representing two examples of an alternative evolutionary route towards adaptation in the rhizosphere in which motility is reduced. Loss of motility might coincide with another trait in these cases, such as EPS production and/or biofilm formation, regulated via shared yet oftentimes opposing mechanisms. Also, the frequency of the *fleQ* mutant is low, i.e., only one out of six isolates from cycle 6 of experimental line 5 carried this mutation and therefore whether this mutant is truly beneficial is unclear. On the other hand, the *flhA* mutant was found in three out of the four cultured and sequenced isolates from cycle 6 of line 4 and therefore could represent a significant proportion of the total population.

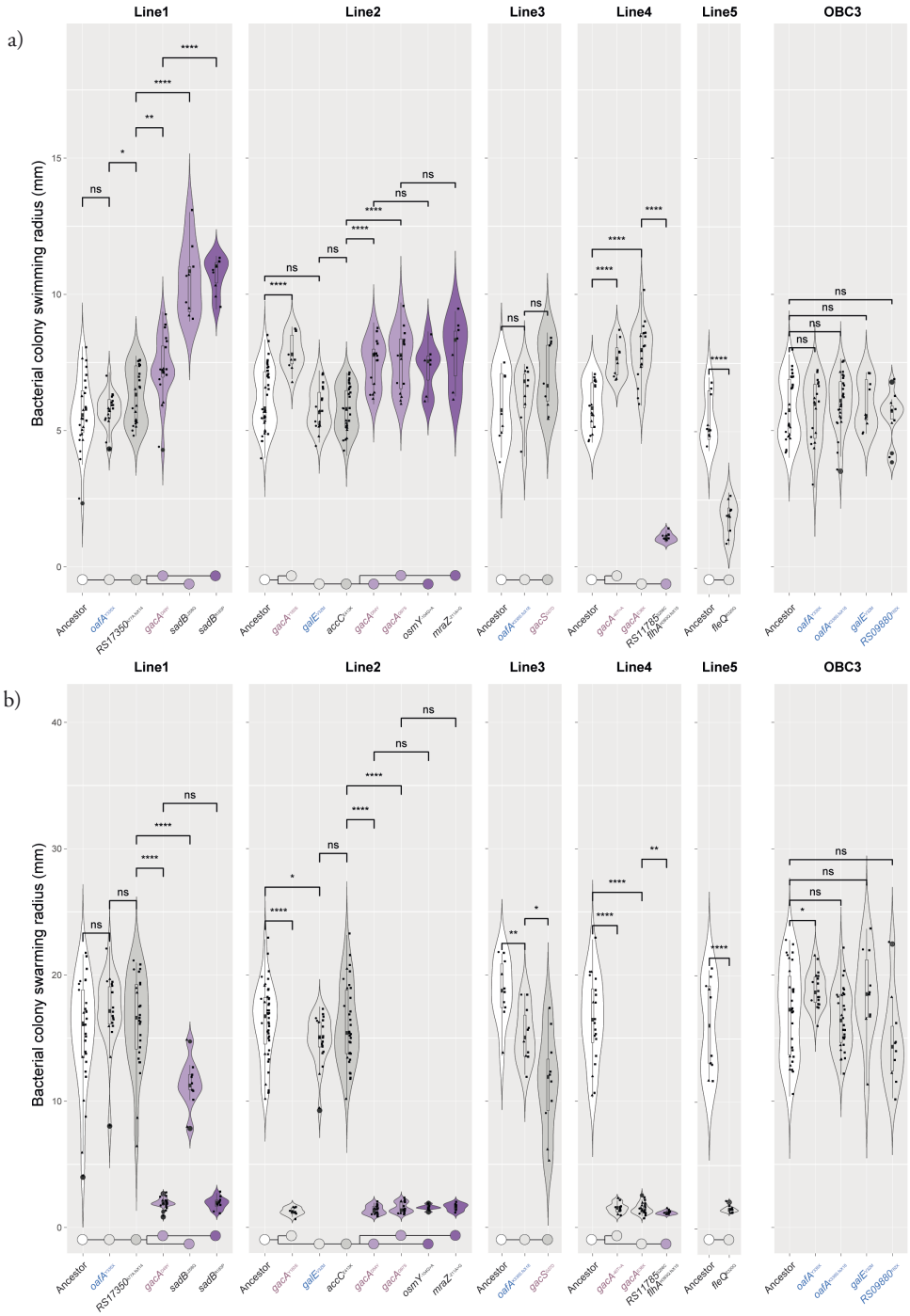

Figure 4 Evolved, root-competent mutant *P. protegens* CHA0 strains are characterized by enhanced swimming and impaired swarming.
(figure description on next page)

The accumulative effects of parallel and sequential mutations on swimming motility (panel a) and swarming motility (panel b) are shown. For each experimental line, strains carrying mutations that can be connected to bacterial motility, or that are the ancestor or descendants of such mutant strains, were studied using typical swimming and swarming assays on Cook's Cytophaga (CC) medium (Déziel *et al.*, 2001). The colony area as a measure for bacterial motility was determined using ImageJ. The combined data from three independent experiments is shown, and datapoints from each experiment can be discerned by their respective shape. The sample size, n, varies per genotype as related strains are combined on each plate, and we report the minimum and maximum n per replicate experiment. For swimming assays, circles represent replicate 1 ($2 \leq n \leq 6$) (excludes *osmY*$^{104G>A}$ and *mraZ*$^{211A>G}$), triangles replicate 2 ($3 \leq n \leq 15$), and squares replicate 3 ($4 \leq n \leq 20$). For swarming assays, circles represent replicate 1 ($1 \leq n \leq 3$) (excludes *osmY*$^{104G>A}$ and *mraZ*$^{211A>G}$), triangles replicate 2 ($2 \leq n \leq 6$), and squares replicate 3 ($7 \leq n \leq 35$). Obvious outliers were removed after pooling. Significant differences in motility between a genotype and its respective progenitor were determined by unpaired t-test analysis (swimming, $7 \leq n \leq 41$; swarming, $7 \leq n \leq 44$; * $\alpha = 0.05$, ** $\alpha = 0.01$, *** $\alpha = 0.005$, **** $\alpha = 0.001$, ns = non-significant) and the result is shown above each comparison. The genealogy of the mutations is shown below each experimental line highlighting both parallel (branching) and sequential mutations. Colors depict the number of acquired mutations relative to the ancestor (white), and these are light-grey: 1, grey: 2, light-purple:3 and purple: 4.

Dynamics of global phenotypic change

Since natural selection eventually operates at the phenotypic level, revealing bacterial global phenotypic evolutionary dynamics can help us to identify traits that are under selection. Moreover, beneficial genetic mutations can be predicted if they are linked to well-known root colonization traits. A broad range of 30 bacterial traits including different aspects of bacterial life-history traits, were examined for the sequenced isolates, which allows for genotype-phenotype association analysis.

As shown in Fig. 5a, the 30 bacterial traits separated into four clusters that share a similar pattern across the different mutant genotypes and this clustering is supported by model-based clustering analysis (Fig. S4). Growth of the bacteria in 1/3 strength King's B (KB) medium was positively correlated with siderophore and exoprotease production, tryptophan side oxidase activity, and growth inhibition of the bacterial plant pathogen *Ralstonia solanacearum*. Thus, this cluster, designated cluster 1, contains traits associated with bacterial social behavior, related to microbe-microbe communication and cooperation, such as the production of public goods. In a principal component analysis (Fig. S5a), the first principal component (PC1) is strongly correlated with all five traits, with a total explanation of 64.5% for all variables. Cluster 2 contains traits linked to carbon source utilization. For this cluster PC1 is strongly correlated with all carbon source usage-related traits, with a total explanation of 83.9% for all variables (Fig. S5b). A third cluster was observed for the bacterial ability to form a biofilm, to produce indole-3-acetic acid (IAA), and to inhibit the growth of two fungal plant pathogens, with a total explanation of 82.4% by PC1 (Fig. S5c). Finally, cluster 4 contains all seven traits that are related to bacterial resistance to biotic and abiotic stresses. The first principal component (PC1) is strongly correlated with all seven traits, with a total explanation of 53.9% for all variables (Fig. S5d). For

these four clusters, the PC1 (or -PC1) value is used as a proxy to present the general performance of all the traits that clustered together.

a)

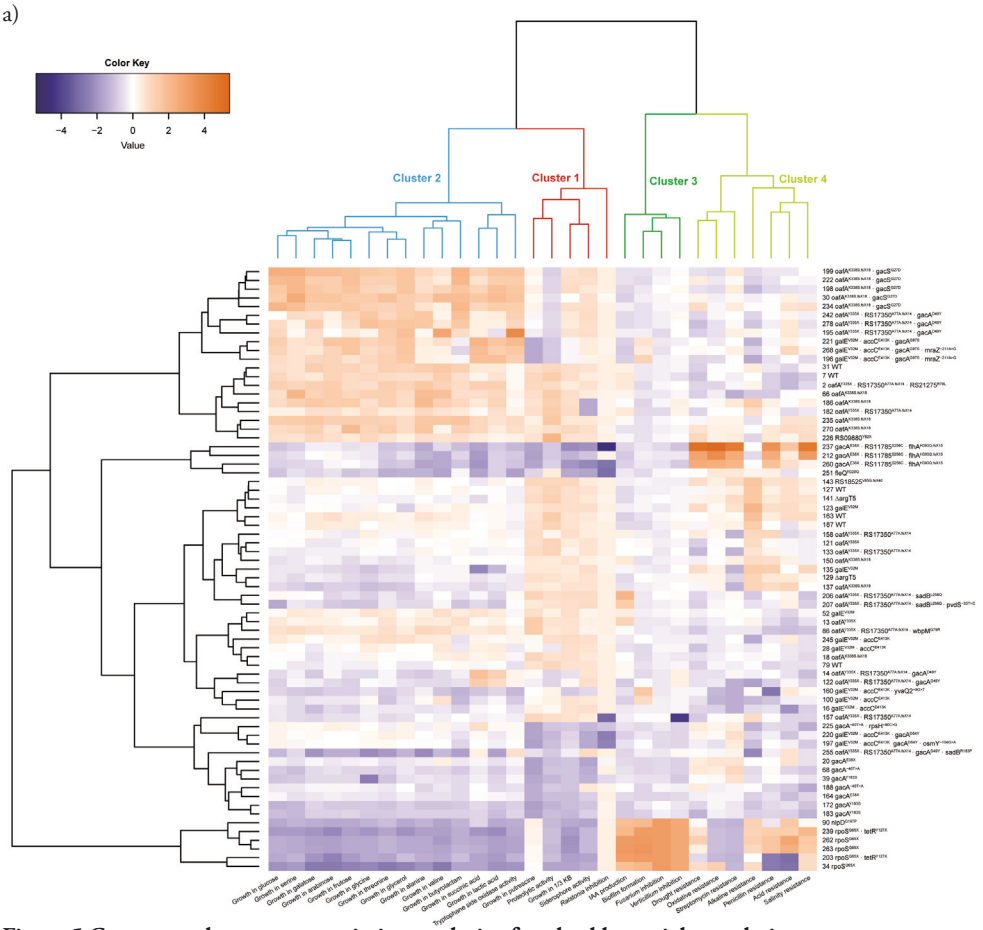

Figure 5 Genotype-phenotype association analysis of evolved bacterial populations.
(figure continued on next page)

Isolates without mutations or only with synonymous mutations were excluded for this association analysis a) Heatmap representing the performance of 30 life-history traits of six ancestral and 63 evolved isolates. The "ward.D2" method was used for hierarchical clustering, based on the dissimilarities of the set of objects being clustered. The four clusters depicted on top are model predicted. Each column illustrates one bacterial life-history trait, indicated on the bottom of the figure. Each row represents an isolate, indicated by its sample ID number and mutational events. b-e) Principal component analysis was applied to generate a general symbolic index for each model predicted cluster. The proxy values of each cluster were normalized, higher values represent better performance. To illustrate better the accumulative effects of each mutational event, ANOVA was applied to reveal the phenotypic change between each genotype and their identified nearest ancestor in each line (only applied for genotypes that have been detected more than once; n >= 2). Asterisks alongside the mutational events indicate significant differences (*α = 0.05, **α = 0.01, ***α = 0.001; n.s. = non-significant). Color-filled circles represent bacterial genotypes, with different colors representing independent evolving populations and the size denotes the number of replicates (n). The dashed line represents the average value of the ancestor.

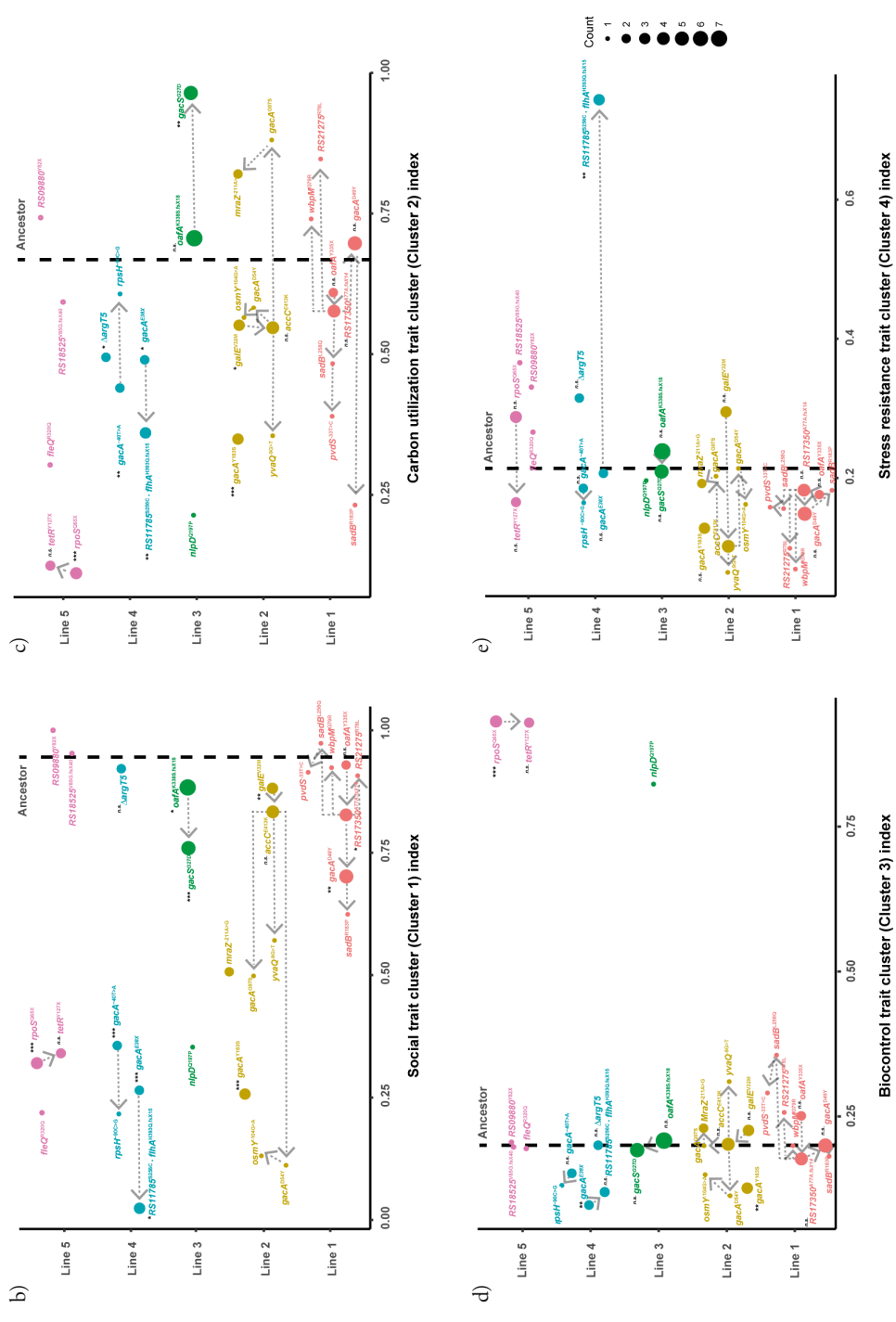
b)
Ancestor
Line 5
Line 4
Line 3
Line 2
Line 1
0.00
0.25
0.50
0.75
1.00
Social trait cluster (Cluster 1) index
c)
Ancestor
Line 5
Line 4
Line 3
Line 2
Line 1
0.25
0.50
0.75
1.00
Carbon utilization trait cluster (Cluster 2) index
d)
Ancestor
Line 5
Line 4
Line 3
Line 2
Line 1
0.25
0.50
0.75
Biocontrol trait cluster (Cluster 3) index
e)
Ancestor
Line 5
Line 4
Line 3
Line 2
Line 1
0.2
0.4
0.6
Stress resistance trait cluster (Cluster 4) index
Count
1
2
3
4
5
6
7

As is shown in Fig. 5b, all five evolutionary lines showed a parallel trend of accumulative decline of social traits. Mutations in *gacA, gacS,* and *rpoS* resulted in significantly decreased bacterial social traits, and this was also observed for the double mutant *RS11785*^{S256C} · *flhA*$^{H393Q.fsX15}$ relative to the background *gacA*^{E38X} mutation. *RS11785*, like *gacA*, encodes a LysR-type transcriptional regulator. In addition to these global regulators, earlier mutations in *oafA*, *galE* and *RS17350*$^{A77A.fsX14}$ encoding a putative methyltransferase, also resulted in a significant but relatively small decrease in social traits. This parallel decline of the bacterial social traits index suggests a negative selection of bacterial social behavior, especially the production of costly public goods such as siderophores and exoproteases.

All traits related to the utilization of 14 different carbon sources, that were selected based on their reported presence in root exudates of Arabidopsis (Chaparro *et al.*, 2013) grouped in one cluster (cluster 2; Fig. 5a). This suggests that carbon source utilization is co-regulated. Different mutations in *gacS* and *gacA* resulted in contrasting bacterial carbon source utilization. A mutation in the first N-terminal transmembrane domain of GacS (G27D) (Fig. 2) resulted in significant enhancement of carbon source utilization (Fig. 5a, c). A similar trend was observed for mutant *gacA*^{G97S}. In contrast, the majority of evolved genotypes, including most mutations in *gacA* and *rpoS*, showed a reduced ability to utilize carbon sources (Fig. 5a, c).

In contrast to the previous two clusters, traits in clusters 3 (Fig. 5d) and 4 (Fig. 5e) were more stable, as most genotypes behave like the ancestor. Only two *gacA* mutants, *gacA*^{E38X} and *gacA*^{Y183S}, were associated with a significant decline of bacterial traits associated with biocontrol, i.e., antifungal activity and biofilm formation, while the *rpoS*^{Q65X} mutation resulted in a significant increase for these traits. The double mutation *RS11785*^{S256C} · *flhA*$^{H393Q.fsX15}$, in the background of the disruptive *gacA*^{E38X} mutation (Fig. 5e), was the only mutational event that led to a significant increase of general resistance to various environmental stresses. *FlhA* encodes the flagellar biosynthesis protein FlhA and is linked to bacterial motility. The LysR-type transcriptional regulator RS11785 comprises a N-terminal HTH DNA-binding domain (PF00126) and a C-terminal substrate binding domain (PF03466). This substrate binding domain is linked to aromatic compound degradation and resembles that of the type 2 periplasmic binding proteins or PBP2s. PBP2s are responsible for binding and uptake of several substrates including polysaccharides and several amino acids. We used HHpred (Zimmermann *et al.*, 2018) for protein remote homology detection and three-dimensional structure analysis to assess the possible consequence of the S256C amino acid substitution. This analysis identified OxyR from *E. coli* as the best template for modeling (E-value: 2.9e-30, Score: 166.45). OxyR represents the master peroxide sensor in gram-negative bacteria, which operates via intramo-

lecular disulfide-bond formation in the regulatory PBP2-like domain. RS11785 is unlikely to represent the master peroxide sensor in *P. protegens* CHA0 because another CHA0 protein encoded by *PFLCHA0_RS030065* is much more similar to OxyR (89% percent pairwise sequence identity versus 29% for RS11785). Nevertheless, it is tempting to speculate that the serine (S, Ser) to cysteine (C, Cys) amino acid substitution (S256C) we observed here might influence regulatory activity by altered intramolecular disulfide-bond formation as such bonds are governed by pairs of cysteine residues. Lastly, RS11785 bears resemblance (37% sequence identity, 93% sequence coverage) to the LysR-type PBP2-domain containing regulator alsR which regulates the activity of the acetoin operon (*alsSD*) in response to several signals such as glucose and acetate in *Bacillus amyloliquefaciens*. Acetoin (3-hydroxy-2-butanone, a precursor for 2,3-butanediol) can elicit induced systemic resistance (Rudrappa *et al.*, 2010), and is linked to general plant growth promotion in *Bacilli*. In the absence of singular mutations in *flhA* and *RS11785*, the molecular mechanism underlying the observed enhanced environmental stress resistance in this double mutant remains to be clarified but we hypothesize that altered regulatory activity by RS11785^{256C} is the most likely cause.

Discussion

The rhizosphere is a nutrient-rich environment for root-associated bacteria. However, to access the available nutrients bacteria must overcome various challenges, including the plant immune system, presence of competing and/or predatory microorganisms, and abiotic stresses. In the gnotobiotic binary system used in this study we tracked changes in *P. protegens* CHA0 in the rhizosphere of Arabidopsis under reproducible and controlled conditions without interference of complex interactions with other microbes. Mutations affecting global regulators, bacterial cell surface structure, and motility accumulated in parallel in our evolutionary experiment, revealing at least three important strategies of bacterial adaptation to the rhizosphere.

Global regulators and rhizosphere adaptation

The GacS/GacA two-component regulator system controls the production of antimicrobial secondary metabolites, exoenzymes, and siderophores, but also biofilm formation, stress responses, motility, and quorum sensing (Heeb *et al.*, 2002; Haas & Keel, 2003; Haas & Défago, 2005; Raaijmakers *et al.*, 2010; Hassan *et al.*, 2010). In the present study, mutations in the GacS/GacA two-component regulator system caused dramatic changes in several bacterial phenotypic traits, including motility, carbon source utilization, and social traits (Fig. 4 and 5). The overall gain in swimming motility is not unexpected, as swimming motility, driven by the flagellum apparatus, has been repeatedly reported to be an important root colonization trait in root-

associated bacteria, including several *Pseudomonas* spp. (Lugtenberg *et al.*, 2001b; Colaianni *et al.*, 2021; Knights *et al.*, 2021; Parys *et al.*, 2021). In line with this, genome-wide transposon disruption mutant analysis by Cole and coworkers (2018) showed that the majority of motility-related genes in *P. simiae* WCS417 are positively associated with Arabidopsis root colonization (Cole *et al.*, 2017).

In contrast with the observed enhanced swimming motility across the evolutionary selection lines, swarming motility was found to be severely hampered throughout, and this appears to be the case especially for *gac* mutants. Swarming, like swimming, is driven by the flagellum but in addition depends on the production of several compounds, including quorum sensing molecules and biosurfactants. *P. protegens* CHA0 is a known producer of the biosurfactant orfamide A and the GacS/GacA two-component system is known to be an important regulator for its biosynthesis (Sobrero *et al.*, 2017). These results fit observations by Song and co-workers (Song *et al.*, 2016) in the closely related *P. protegens* strain Pf-5. During swarming motility, *gac* mutants emerged that lack production of the surfactant orfamide. These mutants cannot swarm, but they co-swarm with orfamide producing cells (Song *et al.*, 2016).

Remarkably, we also identified two completely non-motile mutants in our experiments with disruptions in the *fleQ* and *flhA* genes. Possibly, these mutants adhere much better to the root surface or might be able to form a biofilm more rapidly or strongly as these traits are often inversely correlated with bacterial motility (Simm *et al.*, 2004; Caiazza *et al.*, 2007; Romling *et al.*, 2013). Future experiments should reveal whether such trade-off between bacterial motility and root adherence indeed underlies our observations in this evolutionary experiment.

The decreased production of public goods, such as siderophores and exoproteases, which were observed in all independent evolutionary lines (Fig. 5), could be beneficial for bacterial fitness by saving energy and primary metabolites. For example, adaptation of *P. aeruginosa* to the human host through mutations in regulators was accompanied by loss of siderophore production, secreted proteases, and biofilm formation (Smith *et al.*, 2006; Winstanley *et al.*, 2016).

Cell surface structures as bacterial adaptation targets

Bacterial cell surface components are the first line of defense against environmental stress and interplay with hosts (Lerouge & Vanderleyden, 2001; Whitfield & Trent, 2014; Maldonado *et al.*, 2016). LPS is a central outer membrane component for gram-negative bacteria, and exhibits structural adaptability that is contributed especially by its O-antigen part (Lerouge & Vanderleyden, 2001; Maldonado *et al.*, 2016). Bacterial O-antigen structure modification plays an important role in evasion

of host immunity (Murray *et al.*, 2006), and has the potential to change host-bacteria interactions (Lerouge & Vanderleyden, 2001; Maldonado *et al.*, 2016; Ranf, 2016). In plant pathogenic bacteria, LPS components are important virulence determinants (Newman *et al.*, 2000; Di Lorenzo *et al.*, 2017), which can activate a variety of defense-related responses (Barton-Willis *et al.*, 1984; Newman *et al.*, 1995, 2000; Erbs & Newman, 2003). In *P. fluorescens* the O-antigen component has been implicated to induce systemic resistance in radish (Leeman *et al.*, 1995) and Arabidopsis (Van Wees *et al.*, 1997).

We observed parallel mutations in genes that are involved in LPS biosynthesis and structure modification. In three out of the five evolutionary lines, the first fixed mutations were identified in *oafA* and *galE* that are annotated as O-antigen biosynthesis and structure modification related (Table 1). *OafA* encodes an O-acetyltransferase, which is postulated to modify the O-antigen by acetylation (Allison & Verma, 2000). The enzyme GalE, UDP-galactose 4-epimerase, is involved in the interconversion of UDP-glucose to UDP-galactose, an essential intermediate for LPS core and O-antigen structures (Samuel & Reeves, 2003; Chang *et al.*, 2008; Liu *et al.*, 2008). Inactivation of *galE* in *Porphyromonas gingivalis* resulted in shortening of the O-antigen (Nakao *et al.*, 2006), and in *Bradyrhizobium japonicum*, disruption of *galE* resulted in the complete absence of O-antigen (Chang *et al.*, 2008). Thus, it is tempting to speculate that evasion of the plant's immune response plays a role in adaptation of CHA0 to the rhizosphere of Arabidopsis.

In conclusion, the observed bacterial genetic and phenotypic adaption dynamics emphasize important roles for global regulators, motility, and cell surface structure in bacterial adaptation to its host. The parallel emergence of mutations in similar genes resulted in specific fitness advantages for mutants in the rhizosphere, suggesting that this evolutionary process is driven by the rhizosphere environment.

Acknowledgments

This work was supported by China Scholarship Council fellowships (to E.L. and H.Z.), a postdoctoral fellowship of the Research Foundation Flanders (FWO 12B8116RN) (to R.D.J.), and a European Research Council Advanced Grant 269072 (to C.M.J.P.).

Materials and methods

Experimental setup

We set up an experimental evolution experiment with Arabidopsis ecotype Col-0 as host plant and *Pseudomonas protegens* CHA0 (CHA0) as the evolving bacterial strain. CHA0 (Ramette *et al.*, 2011) is a model strain originally isolated from roots of tobacco plants grown in soil naturally suppressive to black root rot (Stutz *et al.*, 1986). CHA0 was chromosomally tagged with GFP and a kanamycin resistance cassette (Jousset *et al.*, 2006) to enable consistent tracking of the strain and identification of contaminations. We previously described the setup of the evolutionary experiment in great detail (Li *et al.*, 2021a). In brief: the ancestral bacterial population (10^6 cells) was inoculated on Arabidopsis roots grown under gnotobiotic conditions inside ECO2 boxes in carbon-free silver sand. For each cycle, Arabidopsis seeds were surface sterilized using chlorine gas, germinated on modified Hoagland's agar medium, and grown for two weeks until transplantation into the ECO2 boxes, containing each two plants (Li *et al.*, 2021a). Inoculated two-week-old seedlings were then grown for an additional four weeks, after which the root-associated bacteria were collected in 10 mM $MgSO_4$ and subjected to fluorescence-based cell counting by flow cytometry yielding on average 10^7 cells/root. 10^6 cells of the evolved bacterial populations were then transferred to new plants and this cycle was repeated eight times. After each cycle, a small fraction of each population was plated on general-purpose, nonselective medium, 3 g/l tryptic soy agar (TSA), to assess for contaminations and to verify that all colonies carried the *GFP* marker gene, as observed under UV light, on the one hand, and to select individual isolates for phenotypic characterization on the other hand.

We previously picked sixteen random isolates from each of five experimental lines at cycles 2, 4 and 6 respectively plus sixteen isolates from the ancestor population, yielding a total set of 256 isolates (26). These 256 isolates were subsequently grouped into five distinct phenotypes based on their performance on a variety of bacterial life-history traits (Li *et al.*, 2021a). In the current study we selected six of these sixteen isolates per line, and per cycle, for genome sequence analysis. Isolates were selected to represent the breath of phenotypic diversity observed previously (26). Together with six isolates from the ancestor population we set out to obtain genome sequences of 96 isolates in total using the NextSeq-500 Illumina platform (2 x 75 bp paired-end). Sequencing of two isolates from line 4, cycle 4, however, failed and thus a final set of 94 genomes were retrieved. We then used the snippy pipeline (https://github.com/tseemann/snippy), integrating reference genome-based mapping of the Illumina reads by BWA-MEM, variant calling by SAMtools and FreeBayes, and variant impact analysis using SnpEff (Cingolani *et al.*, 2012), to identify single nucleotide polymorphisms (SNPs) and small indels and deletions (INDELs). Larger INDELs were identified

by calculating the breath of coverage of the mapped Illumina reads on the reference genome in a sliding window using bedtools (Quinlan & Hall, 2010). Regions with reduced coverage (<99%) were manually inspected in the Integrative Genome Viewer (IGV). Phylogenetic trees for each line were constructed manually with illustrator based on all detected mutations, the length of the branches representing the number of mutations. The genealogy and frequency of each lineage is shown in the Muller plots that are prepared with R package '*ggmuller'*.

Bacterial life-history traits

For the 94 sequenced isolates, a variety of bacterial life-history traits reflecting various aspects of bacterial physiological processes, were measured previously as part of all 256 isolates initially collected (Li *et al.*, 2021a). Briefly, we monitored optical density (OD) at a wavelength of 600 nm to estimate the bacterial yield after 72 hours of growth under different growth conditions in 96-well microplates. We measured bacterial growth yield and resistance to various stresses, including acidic (pH = 5) and alkaline (pH = 9) conditions, oxidative stress in 0.0025% H_2O_2, water potential stress (15% polyethylene glycol (PEG)-6000)), and salt stress (2% NaCl), and resistance to the antibiotics streptomycin (1 μg/ml), tetracycline (1 μg/ml), and penicillin (5 μg/ml). Bacterial carbon source utilization was quantified as growth yield in modified Ornston and Stanier (OS) minimal medium (Højberg *et al.*, 1999) supplemented with single carbon sources that have been reported to be abundant in Arabidopsis root exudates (Chaparro et al 2013). These included the following carbon sources; alanine, arabinose, butyrolactam, fructose, galactose, glucose, glycerol, glycine, lactic acid, putrescine, serine, succinic acid, threonine, and valine that were added to a final concentration of 0.5 g/l. In addition, we measured bacterial auxin (indole-3-acetic acid or IAA) production with a colorimetric test (Glickmann & Dessaux, 1995), iron-chelating ability using a modified chrome azurol S (CAS) assay (Alexander & Zuberer, 1991), proteolytic activity by the adapted assay from Smeltzer *et al.* (1993), tryptophan side chain oxidase activity using a colorimetric assay (Oberhänsli *et al.*, 1991), and biofilm formation using a modified Chrystal Violet staining assay (Moskowitz *et al.*, 2004). We measured the OD values reflecting the color intensities at specific wavelengths to quantify these traits. We further assessed bacterial antimicrobial activity by quantifying their effect on growth of the fungi *Verticillium dahliae* and *Fusarium oxysporum,* and the bacterium *Ralstonia solanacearum*.

Motility assays

Motility assays were undertaken in round petri dish plates containing Cook's Cytophaga medium (CC medium) (0.3% agar for swimming, 0.5% agar for swarming) (Christensen & Cook, 1972), using typical swimming and swarming assays as described by Déziel et al (Déziel *et al.*, 2001). All tested strains were grown on King's

B medium agar plates for 24 hours before inoculation. Swim and swarm plates were inoculated with the tested strains with a sterile toothpick. For swimming plates, the inoculum was introduced by gently piercing the agar such that the motility within the semisolid agar could be evaluated. For swarming plates, the inoculum was introduced on the agar surface enabling visualization of motility across the agar surface. Both swimming and swarming plates were imaged after 18 hours incubation at 21 °C with right-side-up. The radii of swimming and swarming motility were determined from the photographs by ImageJ, examining the inner circular turbid zone inside the 0.3% agar for swimming and the outer circular zone on top of the 0.5% agar surface for swarming.

Hierarchical and Model-based clustering of bacterial traits

Hierarchical clustering

A heatmap to illustrate the association patterns of bacterial genotypes and their measured traits was constructed in R using the *ggplot2* package. Isolates without mutations or only with synonymous mutations were excluded from the association analysis. Hierarchical clustering was performed using the Ward.D2 method, that is based on the squared dissimilarities of the set of objects being clustered (Murtagh & Legendre, 2014).

Model-based clustering

We applied a model-based clustering method to reveal the best fitting structures of trait covariance patterns. For example, some traits might be either directly or indirectly co-regulated by the same gene, which is expected for global regulators particularly which can co-regulate thousands of genes. We used the *mclust* package in R to run the model simulation (Scrucca *et al.*, 2016). This method assumes that the input data are distributed as a mixture of two or more clusters. The advantage of the model-based clustering method is that it avoids heuristic assumptions and uses a soft assignment that every data point has a possibility of falling to each cluster, which facilitates the best clustering solution. The so-called Bayesian Information Criterion (BIC) was used to select the best model. A large BIC score indicates a better fit of the model.

This result is in line with the outcome of hierarchical clustering with Adjusted Rand Index (ARI) set as 1, and k set as 4 in "ward.D2" as indicated in Fig. 5a. ARI is usually used to evaluate the match degree of a given clustering solution comparing to the model-based clustering result, with 0 reflecting a random partition and 1 the boundary of accuracy of a certain clustering solution (Scrucca *et al.*, 2016).

Genotype-phenotype association analysis

Bacterial traits within each model-predicted cluster have similar data distribution patterns and covaried together by the definition of the clustering method. Thus, we applied a linear regression-based method, i.e., principal component analysis (PCA), to reduce the dimensionality of data and generate a proxy for each model predicted cluster. These proxies were later used as the x-axis values in Fig. 5b-e. We applied the package *ggbiplot* in R to generate the PCA plots and PC1 index from the normalized datasets. The proxies were normalized for further analysis.

To examine the accumulative effects of each mutation on bacterial phenotype, ANOVA was used to compare cluster proxies of evolved genotypes with their direct ancestors. Only genotypes identified more than once ($n >= 2$) were included in this analysis.

Relative quantification of mutant frequency using HRM profile analysis

We used High-Resolution Melting (HRM) profile analysis with integrated LunaProbes to quantify the ratio of mutant to wild type genotypes (Lee *et al.*, 2011; Capper *et al.*, 2015; Zhong *et al.*, 2016). The probes and primers used in this study are listed in Table S2. Primers were designed using Primer3. Probes were designed with the single nucleotide polymorphism (SNP) located in the middle of the sequence, and the 3' end was blocked by carbon spacer C3. The primer asymmetry was set to 2:1 (excess primer: limiting primer) in all cases. Pre-PCR was performed in a 10-µl reaction system, with 0.25 µM excess primer, 0.125 µM limiting primer, 0.25 µM probe, 0.5 µl bacterial sample culture (100-fold diluted saved sample, OD_{600} is about 0.01), 1X LightScanner Master Mix (BioFire Defense). DMSO with the final concentration 5% was supplemented in all reactions to ensure the targeted melting domains are within the detection limit of the LightScanner (Idaho Technology Inc.). Finally, MQ water was used to supplement up to 10 µl. A 96-well black microtiter plate with white wells was used to minimize background fluorescence. Before amplification, 25 µl mineral oil was loaded in each well to prevent evaporation, and the plate was covered with a foil seal to prevent the degradation of fluorescent molecules. Amplification was initiated by a holding at 95 °C for 3 min, followed by 55 cycles of denaturation at 95 °C for 30 s, annealing at 60 °C for 30 s and extension at 72 °C for 30 s and then kept at 72 °C for 10 min. After amplification, samples were heated in a ThermalCycler (Bio-Rad) shortly to 95 °C for 30 s to denature all double-stranded structures followed by a rapid cooling to 25 °C for 30 s to facilitate successful hybridization between probes and the target strands. The plate was then transferred to a LightScanner (Idaho Technology Inc.). Melting profiles of each well were collected by monitoring the continuous loss of fluorescence with a steady increase of the temperature from 35 °C to 97 °C with a ramp rate of 0.1 °C /s. The relative quantification was based on the negative first derivative plots using software MATLAB. The areas of probe-target duplexes melting

peaks were auto-calculated by 'AutoFit Peaks I Residuals' function in software PeakFit (SeaSolve Software Inc.). The mutant frequency *X* was calculated using the formula shown below:

$$X = \frac{Area_{mutant}}{Area_{mutant} + Area_{WT}}$$

To validate the HRM method, standard curves were generated by measuring mixed samples with known proportions of mutant templates: 0%, 10%, 20%, 30%, 40%, 50%, 60%, 70%, 80%, 90% and 100%. Measurements for each sample were done in triplicate. Linear regression formula of each mutant between actual frequencies and measured frequencies were shown in Fig. S1. The high R^2 values, and nearly equal to 1 slope values of these equations, confirmed that the HRM method can accurately detect mutants' frequency in a mixed population.

Data availability

The *P. protegens* CHA0-GFP reference genome is deposited on GenBank: RCSR00000000.1. Raw sequencing data used in this study are deposited at the NCBI database under BioProject PRJNA473919. A conversion table for the CHA0-GFP to CHA0 gene annotations including recent NCBI accession codes is available here: https://doi.org/10.6084/m9.figshare.13295828.v2.

Supplementary information:

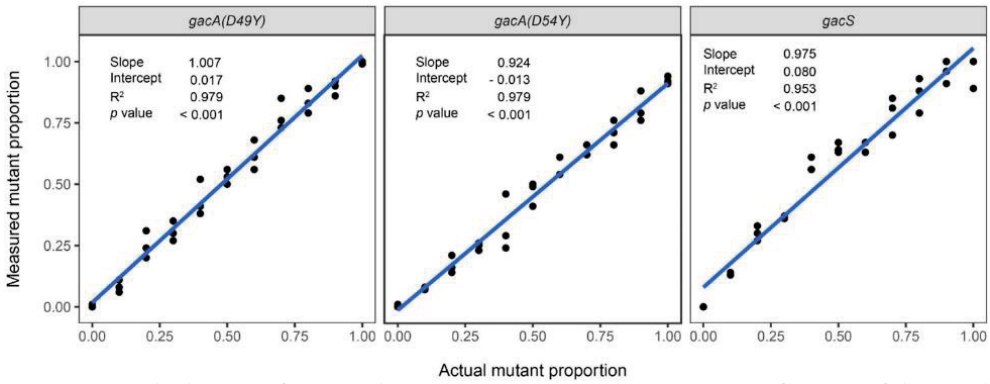

Figure S1 Standard curves of measured mutant versus ancestor proportion as a function of the actual proportion.
A series of mixed samples with known proportions, 0%, 10%, 20%, 30%, 40%, 50%, 60%, 70%, 80%, 90% and 100% of mutant frequency were illustrated. Relative densities of mutants *gacA*^{D49Y}, *gacA*^{D54Y}, and *gacS*^{G27D} were measured by PCR-based high-resolution melting (HRM) analysis. Measurements for each sample were performed in triplicate. In each plot, the black dots represent the measurements, the blue line the fit which was generated based on linear regression modelling.

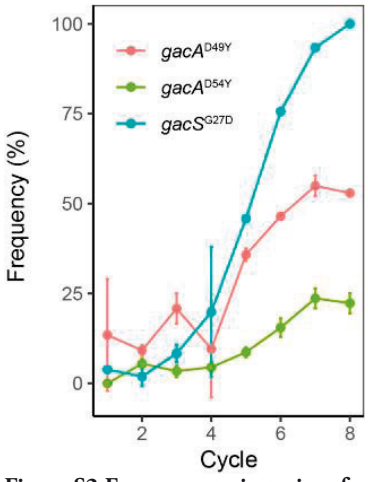

Figure S2 Frequency trajectories of *gacA*^{D49Y}, *gacA*^{D54Y} and *gacS*^{G27D} mutants during long-term rhizosphere adaption.
The X-axis represents the plant-to-plant transferring cycle of the bacterial population. Mutant frequency was determined by quantifying the ratio of mutant allele relative to wild-type allele, using PCR-based high-resolution melting (HRM) analysis. The data shown are the mean of two technical replicates, and error bars represent the standard deviation of the mean.

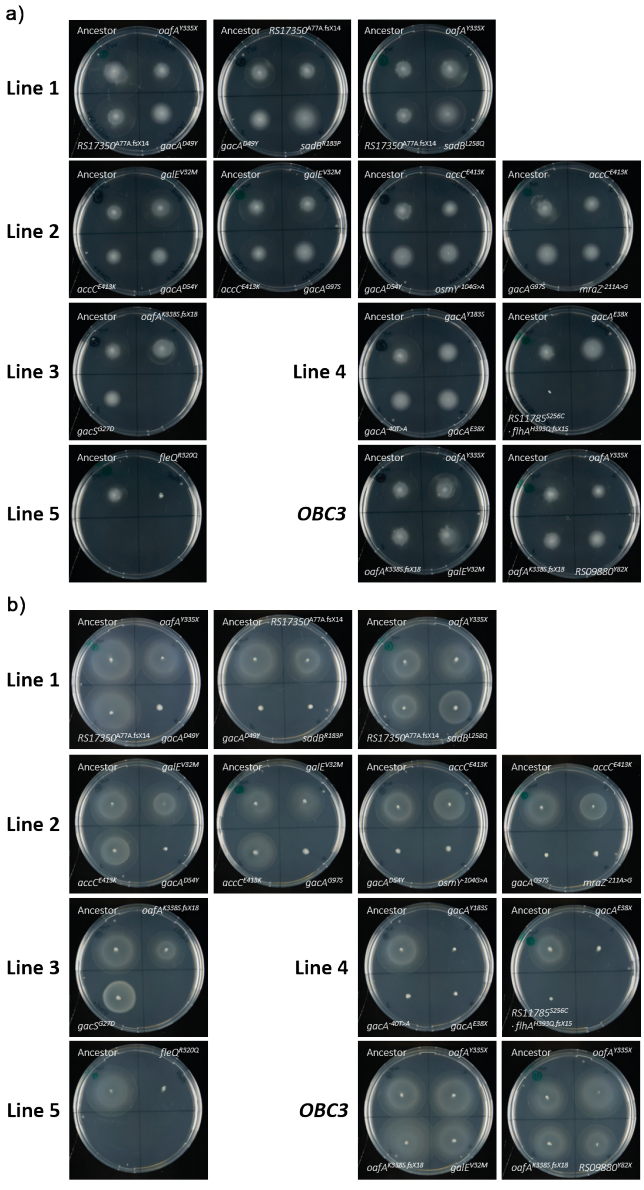

Figure S3 Representative photographs of a) swimming and b) swarming motility assays.
Photographs illustrate the experimental layout of motility assays in which every plate is inoculated with the ancestral strain alongside various sequential mutations clustered per experimental line (with the exception of *gacA*^{Y183S}, indicated by the red box, in line 4 which was identified in line 2). Genotypes are indicated in each respective corner. All plates were incubated with the right side up at 21 °C for 18 h and then photographed. In swimming and swarming plates, we observed double halos that we address to swarming behavior on the surface of the agar due to spill-over during inoculation and to surface colony growth, respectively. For swimming radii measurements, we only considered the inner circle, which we confirmed to be swimming within the agar by side-view inspection. For swarming radii measurements, on the other hand, we considered the outer circle.

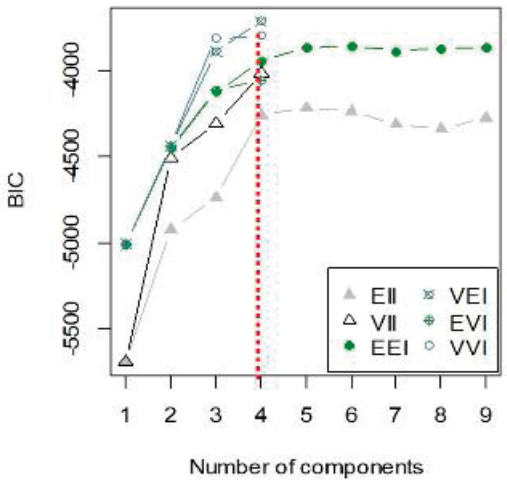

Figure S4 Selection of the best clustering model.
Bayesian Information Criterion (BIC) was used with the mclust R package (Scrucca *et al.*, 2016). A large BIC score indicates strong evidence for the corresponding model. The VEI model with 4 components best fits our data.

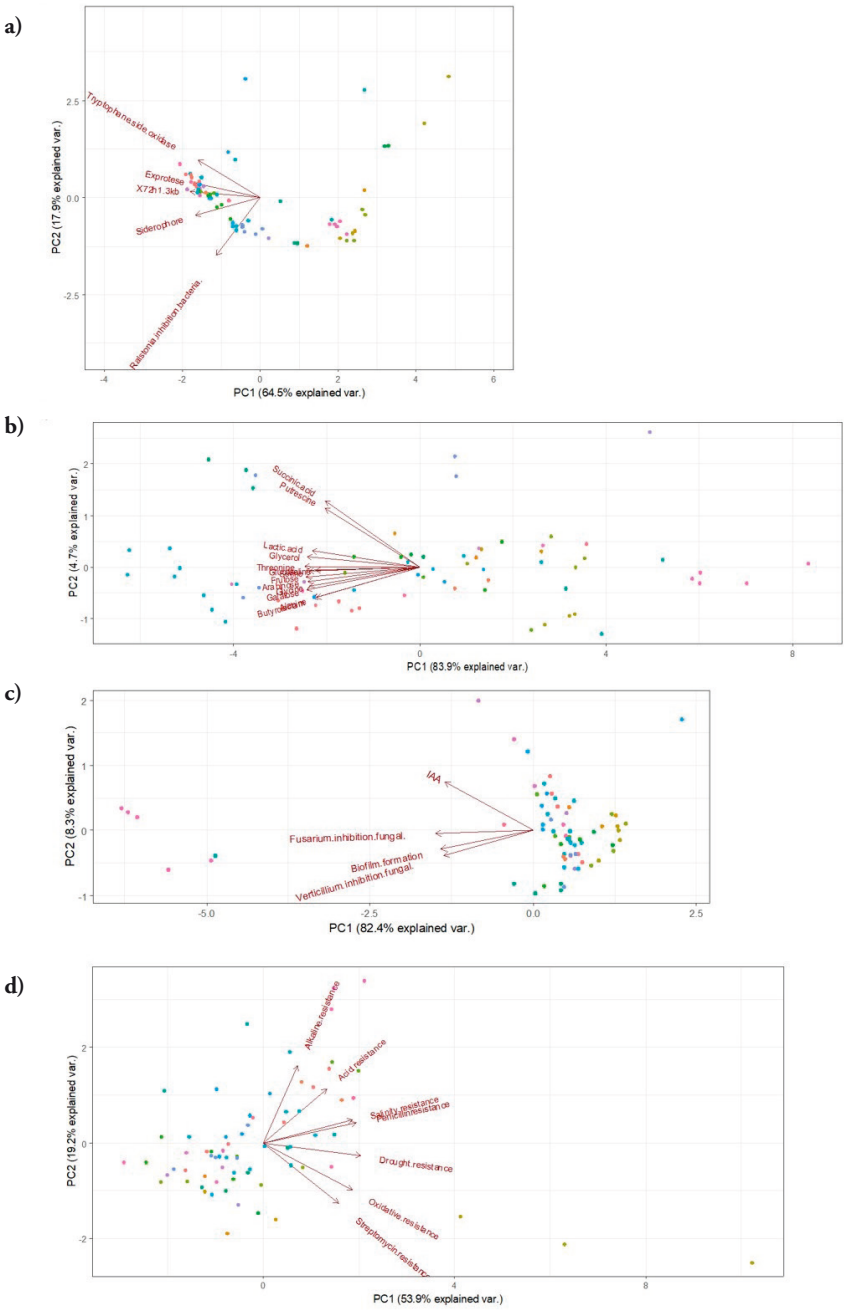

Figure S5 Coordinate axes transformation of each model predicted cluster using principal component analysis (PCA).

a) PCA plot of social trait cluster (cluster 1); b) PCA plot of carbon utilization trait cluster (cluster 2); c) PCA plot of biocontrol trait cluster (cluster 3); d) PCA plot of stress resistance trait cluster (cluster 4). Each dot represents one isolate.

Table S1 Genotypes of whole-genome sequenced CHA0 isolates

Sample ID	Line	Cycle	Genotype	NCBI SRR IDENTIFIER
61	1	2	WT	SRR13155042
169	1	2	WT	SRR13155041
13	1	2	*oafA*^{Y335X}	SRR13155030
121	1	2	*oafA*^{Y335X}	SRR13155019
133	1	2	*oafA*^{Y335X} · RS17350$^{A77A.fsX14}$	SRR8053478
157	1	2	*oafA*^{Y335X} · RS17350$^{A77A.fsX14}$	SRR13155008
158	1	4	*oafA*^{Y335X} · RS17350$^{A77A.fsX14}$	SRR13154997
182	1	4	*oafA*^{Y335X} · RS17350$^{A77A.fsX14}$	SRR13154986
14	1	4	*oafA*^{Y335X} · RS17350$^{A77A.fsX14}$ · gacA^{D49Y}	SRR13154981
122	1	4	*oafA*^{Y335X} · RS17350$^{A77A.fsX14}$ · gacA^{D49Y}	SRR13154980
86	1	4	*oafA*^{Y335X} · RS17350$^{A77A.fsX14}$ · wbpM^{G79R}	SRR8053477
2	1	4	*oafA*^{Y335X} · RS17350$^{A77A.fsX14}$ · RS21275^{R78L}	SRR13154979
195	1	6	*oafA*^{Y335X} · RS17350$^{A77A.fsX14}$ · gacA^{D49Y}	SRR13155040
242	1	6	*oafA*^{Y335X} · RS17350$^{A77A.fsX14}$ · gacA^{D49Y}	SRR8053476
278	1	6	*oafA*^{Y335X} · RS17350$^{A77A.fsX14}$ · gacA^{D49Y}	SRR13155039
255	1	6	*oafA*^{Y335X} · RS17350$^{A77A.fsX14}$ · gacA^{D49Y} · sadB^{R183P}	SRR13155038
206	1	6	*oafA*^{Y335X} · RS17350$^{A77A.fsX14}$ · sadB^{L258Q}	SRR13155037
207	1	6	*oafA*^{Y335X} · RS17350$^{A77A.fsX14}$ · sadB^{L258Q} · pvdS$^{-33T>C}$	SRR13155036
87	2	2	WT	SRR13155035
39	2	2	*gacA*^{Y183S}	SRR13155034
183	2	2	*gacA*^{Y183S}	SRR13155033
123	2	2	*galE*^{V32M}	SRR13155032
135	2	2	*galE*^{V32M}	SRR13155031
63	2	2	*tssM*$^{1336C>T}$	SRR13155029
172	2	4	*gacA*^{Y183S}	SRR8053471
52	2	4	*galE*^{V32M}	SRR8053473
16	2	4	*galE*^{V32M} · accC^{E413K}	SRR8053475
28	2	4	*galE*^{V32M} · accC^{E413K}	SRR8053474
100	2	4	*galE*^{V32M} · accC^{E413K}	SRR13155028
160	2	4	*galE*^{V32M} · accC^{E413K} · yvaQ2$^{-9G>T}$	SRR8053472
245	2	6	*galE*^{V32M} · accC^{E413K}	SRR13155027
220	2	6	*galE*^{V32M} · accC^{E413K} · gacA^{D54Y}	SRR8053470
197	2	6	*galE*^{V32M} · accC^{E413K} · gacA^{D54Y} · osmY$^{-104G>A}$	SRR13155026
221	2	6	*galE*^{V32M} · accC^{E413K} · gacA^{G97S}	SRR13155025
196	2	6	*galE*^{V32M} · accC^{E413K} · gacA^{G97S} · mraZ$^{-211A>G}$	SRR13155024
268	2	6	*galE*^{V32M} · accC^{E413K} · gacA^{G97S} · mraZ$^{-211A>G}$	SRR8053469

29	3	2	WT	SRR13155023
65	3	2	WT	SRR8053484
53	3	2	WT	SRR13155022
77	3	2	WT	SRR13155021
161	3	2	WT	SRR13155020
137	3	2	*oafA*$^{K338S.fsX18}$	SRR13155018
90	3	4	*nlpD*^{Q197P}	SRR8053486
18	3	4	*oafA*$^{K338S.fsX18}$	SRR13155017
66	3	4	*oafA*$^{K338S.fsX18}$	SRR8053483
150	3	4	*oafA*$^{K338S.fsX18}$	SRR13155016
186	3	4	*oafA*$^{K338S.fsX18}$	SRR13155015
30	3	4	*oafA*$^{K338S.fsX18}$ · gacS^{G27D}	SRR13155014
235	3	6	*oafA*$^{K338S.fsX18}$	SRR13155013
270	3	6	*oafA*$^{K338S.fsX18}$	SRR13155012
199	3	6	*oafA*$^{K338S.fsX18}$ · gacS^{G27D}	SRR13155011
222	3	6	*oafA*$^{K338S.fsX18}$ · gacS^{G27D}	SRR8053485
234	3	6	*oafA*$^{K338S.fsX18}$ · gacS^{G27D}	SRR13155010
198	3	6	*oafA*$^{K338S.fsX18}$ · gacS^{G27D}	SRR13155009
57	4	2	WT	SRR13155007
105	4	2	WT	SRR13155006
81	4	2	WT	SRR13155005
129	4	2	ΔargT5	SRR13155004
141	4	2	ΔargT5	SRR13155003
21	4	2	*hult*$^{786C>T}$	SRR8053480
80	4	4	WT	SRR8053482
152	4	4	WT	SRR13155002
188	4	4	*gacA*$^{-40T>A}$	SRR8053481
68	4	4	*gacA*$^{-40T>A}$ · RS11820$^{33C>T}$	SRR8053479
164	4	4	*gacA*^{E38X}	SRR13155001
20	4	4	*gacA*^{E38X} · *nudL*$^{288C>T}$	SRR13155000
225	4	6	*gacA*$^{-40T>A}$ · rpsH$^{-90C>G}$	SRR13154999
212	4	6	*gacA*^{E38X} · RS11785^{S256C} · flhA$^{H393Q.fsX15}$	SRR13154998
237	4	6	*gacA*^{E38X} · RS11785^{S256C} · flhA$^{H393Q.fsX15}$	SRR13154996
260	4	6	*gacA*^{E38X} · RS11785^{S256C} · flhA$^{H393Q.fsX15}$	SRR8053488
11	6	2	WT	SRR13154995
71	6	2	WT	SRR13154994
191	6	2	WT	SRR13154993
35	6	2	WT	SRR13154992
83	6	2	WT	SRR13154991

143	6	2	*RS18525*$^{V85G.fsX40}$	SRR13154990
70	6	4	WT	SRR8053461
106	6	4	WT	SRR13154989
142	6	4	WT	SRR13154988
58	6	4	WT	SRR8053487
190	6	4	WT	SRR13154987
34	6	4	*rpoS*^{Q65X}	SRR13154985
251	6	6	*fleQ*^{R320Q}	SRR8053463
262	6	6	*rpoS*^{Q65X}	SRR8053464
263	6	6	*rpoS*^{Q65X}	SRR8053465
203	6	6	*rpoS*^{Q65X} · tetR^{Y127X}	SRR13154984
239	6	6	*rpoS*^{Q65X} · tetR^{Y127X}	SRR8053462
226	6	6	*RS09880*^{Y82X} · RS12070$^{1389C>G}$	SRR13154983
7	ancestor	0	WT	SRR8053466
31	ancestor	0	WT	SRR8053467
79	ancestor	0	WT	SRR8053468
127	ancestor	0	WT	SRR8053459
163	ancestor	0	WT	SRR8053460
187	ancestor	0	WT	SRR13154982

Note: X, represents a stop codon (at its relative position in case of a shifted frame); fs, frame shift; del, deletion; DNA sequence change positions are relative to the cDNA.

Figure legends mentioned references: (Déziel et al., 2001; Noble, 2019)
Supplementary figure legends mentioned references: (Scrucca et al., 2016)

Table S2 Primers and probes used for high-resolution melting (HRM) analysis

Target gene	Strain ID	SNP locus	Forward primer (excess)	Reverse primer (limiting)	Amplicon size	Probe sequence	Probe length	Target strand	Perfect match/ mismatch	$_{\Delta}$Tm (°C)
gacA^{D49Y}	242	145 G>T	5'-ATCGATGGCCTGCAAG-TAGT-3'	5'-CGGGTAG-GAAAGGGATCTTC-3'	206 bp	5'-CATCAGGACCACATC-GGGCTTCAGCTCCCG-/C3/3'	30nt	WT	G::C / T::C	5.31
gacA^{D54Y}	220	160 G>T				5'-TGGCATCTTGACGTC-CATCAGGACCACATC-/C3/3'	30nt	WT	G::C / T::C	4.92
gacS^{G27D}	222	80 G>A	5'-GCGTACTGTTGCT-GACCTTG-3'	5'-AGCATCTGGGTGTT-GTGGTT-3'	178bp	5'-AGGTGAAGTAGCC-GCCCAGCACCAAAGCCA-/C3/3'	30nt	WT	G::C / A::C	4.83

For the two *gacA* mutants the same set of primers was used. Underlined bases indicate the position of the single nucleotide point (SNP) mutations within the probe sequences. ΔTm (°C) indicates the melting temperature difference between WT-probe duplex and mutant-probe duplex.

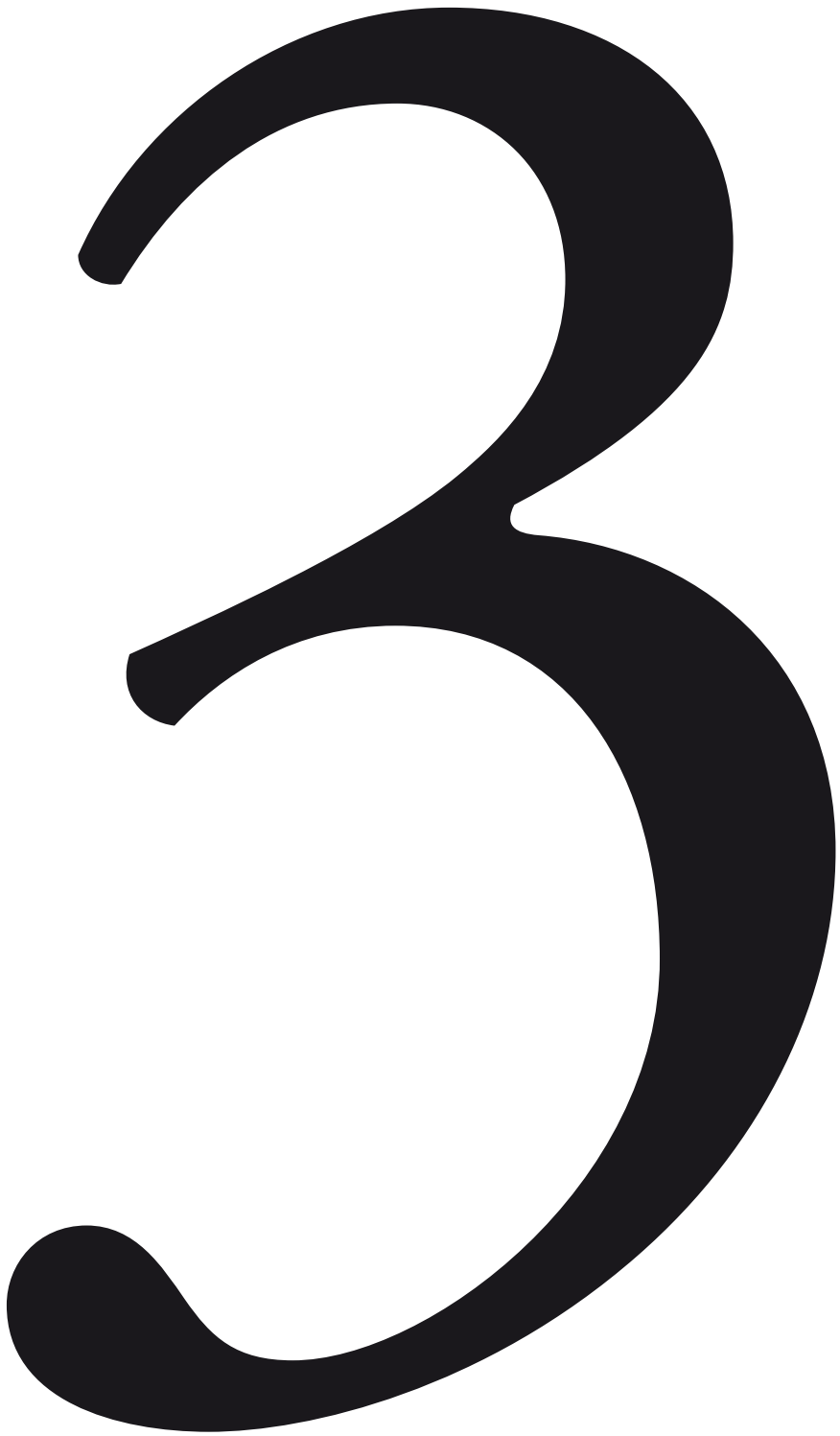

CHAPTER 3

OafA gene mutations in *Pseudomonas protegens* drive plant-adaptation by altering bacterial root attachment

Hao Zhang[1], Erqin Li[1], Sarah N. Tindall[2], Odile Reimeringer[1], Ado van Assche[3], Gavin H. Thomas[2], Bart Lievens[3], Corné M.J. Pieterse[1], Ronnie de Jonge[1,#]

[1]Plant-Microbe Interactions, Department of Biology, Science4Life, Utrecht University, Padualaan 8, 3584 CH, Utrecht, the Netherlands

[2]York Biomedical Research Institute, Department of Biology, University of York, United Kingdom

[3]CMPG Laboratory for Process Microbial Ecology and Bioinspirational Management (PME&BIM), Department M2S, KU Leuven, Leuven, Belgium

Abstract

Plant growth-promoting *Pseudomonas* spp. rhizobacteria display diverse plant-beneficial activities, highlighting their potential to support sustainable agriculture. The application of beneficial bacteria in the field, however, is hampered by significant variation in their performance, likely because of environmental conditions favoring local micro-organisms and the lack of adaptation to the relevant crop. To improve utilization of beneficial bacteria in agriculture, a better understanding of the mechanisms underlying host adaptation are therefore imperative. Effective plant root colonization is an important factor driving the success of beneficial microbes. Multiple relevant bacterial features are identified that contribute to host colonization, such as flagellin- and pili-driven motility and attachment, and exo- and membrane-bound polysaccharide-driven attachment. To study bacterial adaptation in the rhizosphere, we previously employed experimental evolution to track the physiological and genetic dynamics of root-dwelling *Pseudomonas protegens* CHA0 in the *Arabidopsis thaliana* rhizosphere under axenic conditions. Among 35 unique mutations, four mutations in three *OBC3* (O-antigenic polysaccharide biosynthesis cluster 3) genes were identified that can be associated with the decoration of the O-antigen, a major constituent of bacterial cell surface lipopolysaccharide. In this study, we investigated how mutations in *oafA*, a gene encoding a predicted O-antigen acetyltransferase, improve root colonization. We show that enhanced root colonization of *oafA* mutants can be reconstituted *in vitro*, and that improved bacterial fitness is specific for their growth in the root environment. Furthermore, we provide evidence that enhanced root colonization is driven by increased root attachment. We also found that one of the other two O-antigen decoration mutants in the gene *RS09880*, encoding a predicted glycosyl transferase, also displays increased root attachment. All together, these results highlight a role of O-antigen decoration in root colonization, likely by mediating bacterial root attachment.

Author contributions:

H.Z. is the lead author on this paper in terms of experimental design, execution of the experiments, data analysis, and the writing of the manuscript. H.Z., E.L., and R.D.J. designed experiments; H.Z. and O.R. performed experiments; S.N.T. and G.H.T. contributed to model development and illustration of the OafA protein; A.V.A. and B.L. contributed to experimental design and conduction of the Biolog® Phenotype MicroArrayTM for microbial cells; H.Z. and R.D.J. analyzed data; H.Z., E.L., C.M.J.P., and R.D.J. participated in content discussions and contributed to the final manuscript.

Introduction

The concept of 'the rhizosphere', the narrow region of soil surrounding the plant root, was first coined by Lorenz Hiltner in 1904. The observation of enriched diversity and enhanced activity of microorganisms in this region is referred to as 'the rhizosphere effect' (Hartmann *et al.*, 2008; Brink, 2016; Bakker *et al.*, 2020). From the time when the rhizosphere was first described, the understanding of its complexity and its role in both natural and agricultural ecosystem processes had increased significantly. Plant roots exude a significant proportion of photosynthetically-fixed carbon in the form of sugars, amino acids and organic acids in the rhizosphere, therewith fostering a large microbial community (Bais *et al.*, 2006a; Philippot *et al.*, 2013). As a hotspot for microbial interactions, the rhizosphere represents a critical battlefield for root-associated microorganisms and their activities affect plant growth and health in both positive and negative ways (Raaijmakers *et al.*, 2009). Meanwhile, abiotic variations in the rhizosphere driven by climatic and seasonal changes, and agricultural practices that include soil temperature, water content, porosity and pH also participate in the temporal dynamics of the rhizosphere (McNear, 2013; York *et al.*, 2016).

The microbial population in the rhizosphere consists of many diverse microbes that can have negative, neutral or positive effects on plant fitness. Whereas some of them can be pathogenic resulting in a reduction in plant fitness and when referring to agriculture, significant yield losses, others can be beneficial, promoting both plant growth, health and yield. Alongside the well-studied symbiotic nitrogen-fixing bacteria, many other naturally free-living bacteria in the rhizosphere can boost plant growth. These bacteria are called plant growth-promoting rhizobacteria or PGPR. Numerous PGPR have been described, primarily those from the genera *Pseudomonas*, *Bacillus* and *Streptomyces*. *Pseudomonas* spp., rod-shaped, motile, gram-negative bacteria, are among the oldest of described PGPR and are found in a wide variety of environments. They display high metabolic diversity and are found in the rhizosphere microbial communities of many plants, including crop species (Agaras *et al.*, 2015; Stringlis *et al.*, 2018c). PGPR *Pseudomonas* spp. display diverse plant-beneficial activities, such as plant growth-promotion, root architecture modification, biocontrol against pathogens, balancing plant iron homeostasis and triggering induced systemic resistance (ISR) (Zamioudis *et al.*, 2013; Pieterse *et al.*, 2014; Verbon *et al.*, 2017; Pieterse *et al.*, 2021). These observations highlight their potential as biofertilizers, biopesticides and phytostimulators in agriculture, which would further contribute to sustainable agriculture and global food security. Nevertheless, the translation of these scientific discoveries into agricultural application has been hindered as a consequence of their inconsistent performance in the field (Morrissey *et al.*, 2004; Mark *et al.*, 2006; Martínez-Viveros *et al.*, 2010; Bashan *et al.*, 2014; Vejan *et al.*, 2016). One of

the main factors for this inconsistency is believed to be inadequate colonization and activity of applied bacteria under field conditions. Insufficient bacterial colonization further attenuates bacterial activity, e.g., it reduces the accumulation of required bacterial metabolites which are needed to achieve sufficient biocontrol or plant growth promotion (Lugtenberg & Dekkers, 1999; Chin-A-Woeng *et al.*, 2000; Mark *et al.*, 2006).

The ability of beneficial bacteria to colonize and persist in the rhizosphere, referred to as rhizosphere competence, has been the subject of studies for a long time. In *Pseudomonas* spp., a vast array of relevant traits have been identified that include high metabolic versatility (the ability to utilize a wide variety of organic compounds), motility-driven chemotactic behavior, the capacity to form a strong biofilm, being stress resistant, having an array of secondary metabolites with antibiotic characteristics, and effective manipulation of host immune responses (Lam *et al.*, 1990; Barret *et al.*, 2011; Zboralski & Filion, 2020). Root attachment is a critical initial step of successful rhizosphere colonization, and in addition to the beforementioned traits involves flagellin- and pili-mediated root surface adhesion and the production of a variety of species-specific polysaccharides such as EPS (exopolysaccharide) and LPS (lipopolysaccharide) (Rodríguez-Navarro *et al.*, 2007; Berne *et al.*, 2015; Wheatley & Poole, 2018).

Previously, we used experimental evolution to track the physiological and genetic dynamics of root- dwelling *Pseudomonas protegens* CHA0 bacteria (CHA0) in the *Arabidopsis thaliana* (Arabidopsis) Col-0 rhizosphere. We observed that evolved CHA0 bacteria over up to eight plant generations are primarily affected in global regulators, in motility, and in genes responsible for cell surface decoration (**Chapter 2**). Here we focus on the genes responsible for cell surface decoration and investigate how they contribute to enhanced rhizosphere competence. Specifically, we identified four mutations in three cell surface decoration genes, and each mutation was found in a separate population (an independent experimental evolutionary line). Two of these mutations are in the predicted O-antigen acetyltransferase *oafA* gene, one in the UDP-glucose 4-epimerase-encoding gene *galE* and the fourth mutation in a candidate glycosyl transferase-encoding gene, *RS09880* (**Chapter 2**). All three genes localize within close proximity of each other in the genome of CHA0 in a region that was previously named O-antigenic polysaccharide biosynthesis cluster 3 (OBC3), because of its role in the biosynthesis of O-antigen polysaccharide. O-antigen is one of the three major structural components of LPS in addition to a lipid-A moiety and a core oligosaccharide (Kupferschmied *et al.*, 2016). Whereas the structures of the lipid-A and core oligosaccharide are highly conserved among bacterial genera, the O-antigenic portion of the LPS can vary significantly, even within a single bacterial species (Lerouge & Vanderleyden, 2001). Given the observation that the *oafA* gene was

mutated twice in our experimental evolution approach, we here set out to investigate the evolutionary benefit of these *oafA* mutations specifically. We conducted *in vitro*, *in vivo*, and *in silico* experiments to investigate *oafA* mutants' metabolic versatility, root colonization and attachment to obtain mechanistic insight into the observed, enhanced rhizosphere competence. We show that strong early-stage bacterial root attachment of the *oafA* mutants drives increased root colonization. Further analysis shows that a similar enhanced root attachment trait can be observed in *RS09880* mutant bacteria, one of the other *OBC3* mutants in the evolutionary experiment. Collectively, these results support the hypothesis that adaptation of cell surface decoration for increased root attachment by fine-tuning the decoration of exposed O-antigen represents an important rhizosphere competence trait.

Results

oafA encodes a candidate two-domain, AT3-SNGH, O-antigen acetyltransferase

Ninety individual colonies derived from the rhizosphere bacterial community of experimentally evolving CHA0 were previously subjected to next-generation sequencing, and variant analysis led to the identification of thirty-five mutations distributed over twenty-eight genes (**Chapter 2**). Affected genes encoded several global regulators, as well as key regulators of cellular motility, but also several proteins that are implicated in cell surface decoration, specifically biosynthesis of lipopolysaccharide (LPS). Four out of the thirty-five mutations were located in an O-antigen (O-PS; one of three structural components of LPS) biosynthesis gene cluster previously depicted as *OBC3* for O-PS biosynthesis cluster 3 (**Chapter 2**) (Kupferschmied *et al.*, 2016). Two mutations were found to disrupt the coding sequence of *oafA*, encoding the predicted O-antigen acetylase OafA, resulting in a premature stop at more or less halfway the gene in both cases (Fig. 1a, b). The other two *OBC3*-mutations, yielding an amino-acid substitution (V32M) and a premature stop (Y82*), were located in *galE*, encoding a UDP-glucose 4-epimerase, and in *RS09880*, encoding a glycosyl transferase, respectively (Fig. 1a). All four *OBC3*-mutations were identified in separate evolutionary CHA0 lines, and three of them were observed already early-on in the evolutionary experiment (i.e., in the second root colonization cycle). These three early mutations (two in *oafA*, one in *galE*) spread through their respective populations quickly, reaching fixation before the end of the evolution experiment; the eighth plant generation (cycle). The fourth mutation in *RS09880* occurred later in the evolutionary experiment (after the sixth root colonization cycle) limiting our ability to observe its possible fixation (**Chapter 2**). Given the observation that the *oafA* gene was mutated twice, independently, we set out to characterize these adaptative mutations in more detail to better understand their evolutionary and physiological significance for CHA0 biology in the rhizosphere.

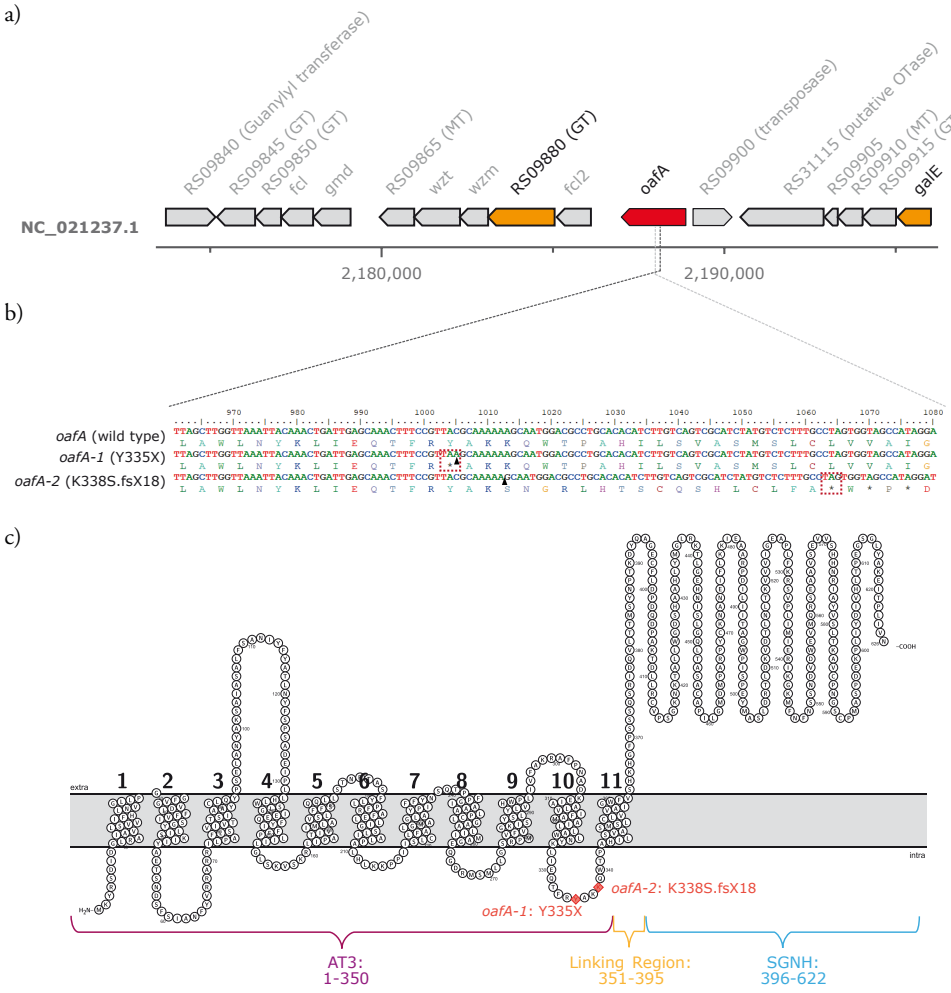

Figure 1 *P. protegens* CHA0 OafA (OafA-CHA0) is a membrane-bound O-acetyltransferase with a linked AT3-SGNH domain topology.
a) The *oafA* gene is located in the *OBC3* (O-antigen biosynthesis cluster 3) gene cluster, which encodes multiple genes involved in the biosynthesis of the O-antigenic portion of lipopolysaccharide (adapted from Li *et al.* 2020a). Putative functions of encoded proteins or gene names in the *OBC3* gene cluster are indicated above the corresponding genes and the genes are drawn to scale. b) Two *oafA* mutants found in two independent evolutionary lines are indicated, i.e., $oafA^{Y335X}$ (*oafA-1*), a mutant with a TAC>TAA substitution (black triangle), resulting in an early stop codon replacing a Tyrosine-335 (Y335X) (red dash-line box), and $oafA^{K338S.fsX18}$ (*oafA-2*), a deletion at Lysine-338 resulting in a frame shift (black triangle indicated one of six adenines from this region is missing) and a premature stop 18 codons downstream (red dash-line box). c) The predicted protein topology of OafA-CHA0 containing two domains, an acyltransferase-3 (AT-3) domain (IPR002656) and a SGNH hydrolase domain (IPR036514). The AT3 domain consists of 11 transmembrane helices (TMH), the 11th of which is presumably required to localize the fused extracytoplasmic SGNH domain in the periplasm (Pearson *et al.*, 2020). Both *oafA* mutations (red colored) disrupt the open reading frame and are located in the linker region. (***figure continued on next page***)

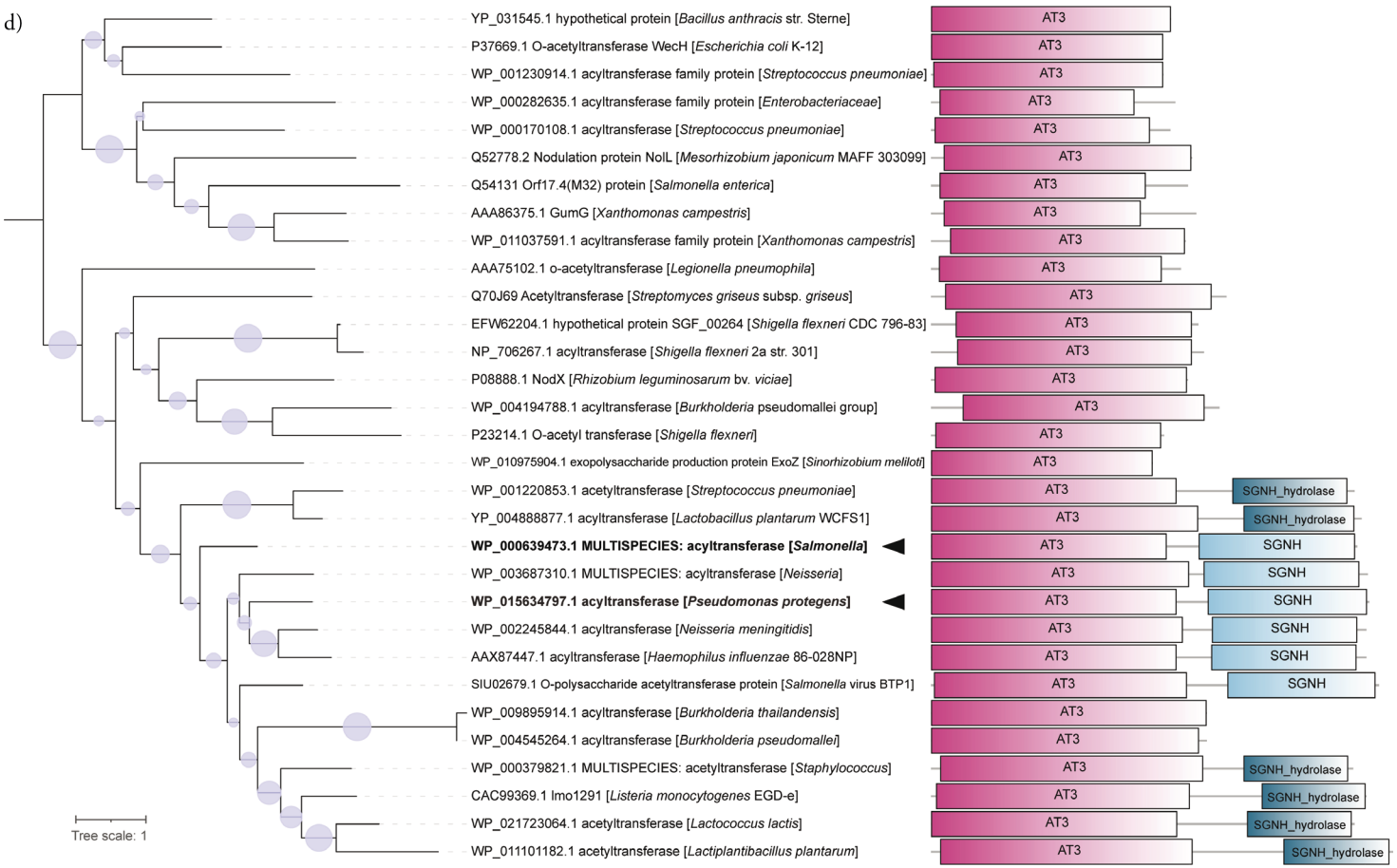

(**Fig. 1** *continued*) d) Maximum likelihood phylogenetic analysis of OafA-CHA0 (black triangle) and 30 well-characterized AT3 domain-containing proteins (Pearson *et al.*, 2020) places OafA-CHA0 alongside *Salmonella enterica subspecies enterica serovar* Typhimurium OafA (OafA-S.Tym) (black triangle).

The endogenous CHA0 OafA polypeptide (OafA-CHA0) is 626 amino acids long and consists of two distinct protein domains, i.e., a membrane-bound acetyltransferase-3 (AT3; IPR002656) domain and a SGNH hydrolase domain (IPR036514) (Fig. 1c) (Pearson *et al.*, 2020). AT3 domain-containing proteins are implicated in O-acetylation of a variety of carbohydrates across all domains of life, including acetylation of the O-antigenic portion of the LPS. SGNH hydrolase domains are less well characterized and lend their name from the strict conservation of four residues, Ser, Gly, Asn and His that sets them apart from a larger superfamily of GDSL hydrolases (Akoh *et al.*, 2004). Two distinct protein domain architectures are described for AT3-type acetyltransferases, those with only the AT3 domain (AT3-only; (Pearson *et al.*, 2020)) and those in which the AT3 domain is linked to the SGNH hydrolase domain (AT3-SGNH) (Fig. 1d). *Shigella* Oac (Oac-Shigella) is an example of an AT3-only O-antigen acetyltransferase (Clark *et al.*, 1991), and *Staphylococcus* OatA is a well characterized AT3-SGNH O-acetyltransferase of peptidoglycan (Bera *et al.*, 2005). Transmembrane (TM) prediction by TMHMM (version 2.0; (Krogh *et al.*, 2001)) identified eleven TMs in the C-terminal AT3 domain of OafA-CHA0 that anchor the protein in the plasma membrane separating cytoplasm and periplasm in this gram-negative bacterium. To better understand the potential functional role of OafA-CHA0, we compared its amino-acid sequence with that of a selected set of 30 AT3 domain-containing proteins that have been experimentally characterized (11 AT3-SGNH proteins and 19 AT3-only proteins; Fig. 1d) (Pearson *et al.*, 2020). Phylogenetic analysis of the common AT3 part of these proteins by maximum likelihood places OafA-CHA0 next to one *Salmonella enterica* OafA among all other AT3-SGNH fusion proteins, which is OafA of *Salmonella enterica* subspecies *enterica* serovar Typhimurium (*S.*Tym), OafA-S.Tym (WP_000639473.1) (Fig. 1d). OafA-S.Tym acetylates the 2-hydroxyl group on the abequose moiety of the O-antigen which is unique to the *S.* Typhimurium serovar (Slauch *et al.*, 1995). Although global protein similarity between OafA-CHA0 and OafA-S.Tym is relatively low (29.2%), the conserved overall protein topology supports a role for OafA-CHA0 in O-antigen acetylation in CHA0. Both mutations in *oafA*, Y335* (*oafA-1*), and K338S.fs*18 (*oafA-2*), a deletion at Lysine-338 resulting in a frame shift and a premature stop 18 amino acids downstream, are located in between the predicted AT3 and SGNH hydrolase domains (Fig. 1b, c) and disrupt the open reading frame. Therefore, we presume that at least the SGNH hydrolase domain is no longer synthesized. In the absence of expression data (transcript or protein level), however, we don't know whether the AT3 domain on its own is produced in the *oafA* mutant CHA0 cells.

OafA mutants rapidly accumulate in the Arabidopsis rhizosphere

Experimental evolutionary analysis of microbes has provided a way to identify beneficial mutations and corresponding genes (Rozen *et al.*, 2002). A study which

examined the fitness of *Pseudomonas fluorescens* SBW25 mutants that were selected under nutrient stress, suggested that particularly early-appearing and subsequently fixed mutations tend to have larger selective advantage, compared with later appeared mutations (Barrett *et al.*, 2006). Previously we examined six bacterial colonies from each evolutionary line at root colonization cycles 2, 4 and 6, and both *oafA* mutants discussed here were among the first observed mutants in the evolutionary experiment (**Chapter 2**). The *oafA* mutants were identified in colonies isolated from the second cycle and onwards and a clear increase of *oafA* mutant frequency was shown over subsequent cycles reaching fixation at the sixth cycle (**Chapter 2**) (Fig. 2). In order to improve the resolution of *oafA* mutants' frequency over the consecutive cycles of the CHA0 experimental evolution experiment (**Chapter 2**), we conducted high resolution melt curve analysis (HRM) on each cycle of the bacterial population containing the *oafA-1* mutation. HRM is a PCR-based analysis which incorporates sequence-specific probes to quantify the frequency of a specific sequence variant (Dames *et al.*, 2007; DeSilva & Blackett, 2007). Previously we used this approach to reveal rhizosphere-specific competence of several evolved *gac* mutants (Li *et al.*, 2021a) and their frequency in the respective populations over multiple root colonization cycles (**Chapter 2**).

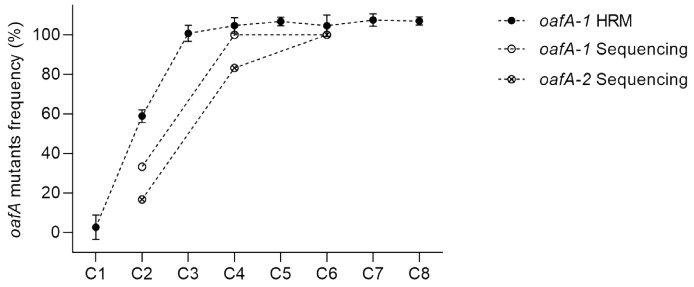

Figure 2 Frequency of *oafA-1* and *oafA-2* mutants increases rapidly during microbial adaptation on Arabidopsis roots.
Black dots represent *oafA-1* mutant frequency across eight cycles as determined by high resolution melting (HRM) curve analysis (*n* represents technical measurement replicates wherein, 2 <= *n* <= 3). Open circles indicate the frequency of *oafA-1* and *oafA-2* as determined by whole-genome sequencing of individual colonies (Li *et al.*, 2021a). Six bacterial colonies were sequenced from each evolutionary line at cycle 2, 4, and 6, and *oafA-1* frequency (open circles) and *oafA-2* frequency (open circles with cross) were calculated from their occurrence among single colony-based whole-genome sequences (Li *et al.* 2021a).

To detect the substitution (c.1005C>A) in *oafA-1* using HRM, specifically, we designed probe CHA0_wt_*oafA-1* (AACTTTCCGTTACGCAAAAAAGCAAT) (Fig. 1b) in combination with primers *oafA-1*_forward (CGCACTGGTGATTTTTGCAATG) and *oafA-1*_reverse (CTGACAAGATGTGTGCAGGC). For *oafA-2* (c.1013delA), unfortunately, five adenine nucleotides flank the deletion of one of them, making HRM analysis much less accurate and therefore unsuitable. HRM analysis using probe CHA0_wt_*oafA-1* showed that the *oafA-1* frequency was negligible in cycle one,

increased to approximately 60% in cycle two (Fig. 2), and reached fixation (frequency at 100%) from cycle three and onwards, demonstrating its rapid spread through its respective population. The rapid increase in *oafA-1* frequency illustrates its enhanced ability to colonize the rhizosphere as compared to its CHA0 wild-type ancestor. Given the difficulty of tracking *oafA-2* mutant frequency by HRM analysis, and similarity to *oafA-1* in terms of its position in the *oafA* gene (Fig. 1b, c), we decided to use the *oafA-1* mutant as a representative for both *oafA* mutants in subsequent experiments.

The *oafA-1* mutant has unaltered metabolic versatility

Bacterial cell surface decoration by LPS is important for the selective permeability of the outer membrane by supporting membrane integrity and by providing a barrier to prevent the uptake of toxic compounds (Murata *et al.*, 2007). As a consequence, it aids bacterial resistance to antimicrobial peptides like polymyxin B (Yi *et al.*, 2014; Cullen *et al.*, 2015) and plays an important role in general physiology and adaptation to dynamic environmental conditions, such as pH, oxygen levels, osmotic pressure and salinity (Lloret *et al.*, 1995; Jofré *et al.*, 2004; Schwechheimer & Kuehn, 2015; Simpson & Trent, 2019; Huszczynski *et al.*, 2020). In order to identify the biological mechanisms underlying the evolutionary selection of the *oafA* mutations in our experiment, we decided to first quantify several general physiological parameters such as growth, tolerance to stress, and behavior of both wild type and mutant cells.

Initially, we examined bacterial growth in standard King's B (KB) medium and one-tenth ($1/10^{th}$) strength KB medium, representing nutrient rich and poor conditions, respectively. In addition, we assayed bacterial growth in the reciprocal genotype culture filtrate, i.e., growth of the wild type bacteria in the culture filtrate of an *oafA-1* overnight culture, and that of *oafA-1* in the wild type culture filtrate. We reasoned that the filtrates of bacterial overnight cultures contain less nutrients plus a mixture of synthesized and exuded secondary metabolites that could potentially have an antagonistic effect (Ramesh *et al.*, 2009; Kumar *et al.*, 2012). Three bacterial suspensions, that of the wild type, the *oafA-1* mutant, and a mixture of wild type and *oafA-1* cells (WT:*oafA-1*) at equal density (1:1) were inoculated separately in the abovementioned growth conditions, both in pure nutrient conditions and in culture filtrate, for 23 h incubation. We observed identical growth among the wild type, the *oafA-1* mutant and the mixture of these two in all tested growth conditions (Fig. S1). To examine whether the underlying growth dynamics were indeed comparable, we made use of the Gompertz regression model (Tjørve & Tjørve, 2017). This model describes the relation between bacterial incubation time (h) and bacterial optical density at 600 nm (OD_{600} value) and allows inference of the final cell density (Y_m), initial cell density (Y_0), bacterial growth rate coefficient (K), and the inflection time point (1/K). Inflection refers to the time point when bacterial growth rate switches from an increasing trend

towards a decreasing trend (Table 1). No significant difference was observed between the growth of wild type CHA0 and the *oafA-1* mutant in standard KB medium, 1/10th KB medium and culture filtrate of wild type CHA0. The *oafA-1* mutant bacteria had a significantly higher cell density (Y_m) than wild type CHA0 in the culture filtrate of *oafA-1* mutant, which is probably due to a significant longer inflection time (1/K) for *oafA-1* (Table 1). All three bacterial treatment populations achieved the highest final cell density in standard KB medium and the lowest in 1/10th strength KB as expected due to the lower nutrient availability in this medium. Reversely, in line with observations in diverse microbial systems, both wild type and *oafA-1* mutant bacteria had the highest growth-rate and shortest inflection time point in 1/10th strength KB confirming that the maximal rate of bacterial nutrient uptake occurs under conditions of low nutrient availability (Bisson & Fraenkel, 1984; Bonachela *et al.*, 2012; Nev *et al.*, 2021). Notably, the WT/*oafA-1* mixture had the longest inflection time point (1/K) and significant higher final cell density (Y_m) compared to single genotype bacterial growth under three nutrient limited media, suggesting that microbe-microbe competition, potentially driven by lack of kin recognition (Stefanic *et al.*, 2015), interferes with growth when the two genotypes were mixed. In contrast, WT/*oafA-1* mixture had a similar final cell density as wild type CHA0, but significantly lower of that compared to *oafA-1* in KB medium (Table 1). These indicate the nutrient availability might affect this microbe-microbe competition.

Table 1 Growth kinetics parameters of the *oafA-1* mutant cultured in four tested media support its unaltered growth compared to the wild type progenitor

The wild type, *oafA-1* mutant and WT/*oafA-1* (1:1) mixes were cultured in 1/10th strength KB medium, and full strength KB medium, and in the culture filtrates of the wild type and the *oafA-1* mutant that were pre-grown in full strength KB medium. Bacterial cell suspensions (10 µl of 10^7 cfu/ml) were added to 190 µl growth medium or culture filtrates in a 96-well plate (cell density OD_{600} equal to 0.005, $n = 6$). Bacterial cell density was recorded every hour for 23 hours of continuous growth at 28 ºC ($0 \leq t \leq 23$). The Gompertz function was used to perform bacterial fitness data regression analysis (Tjørve & Tjørve, 2017). The best-fit values of the Gompertz function for different bacterial genotypes cultured in four growth conditions are shown. *Gompertz function $Y= Y_m * (Y_0/Y_m)^{(exp(-K*t))}$, where Y_m is the maximum cell density (same units as OD value), Y_0 is the initial cell density (same units as OD value), K is a growth-rate coefficient, which determines the lag time (units as per hour, maximum relative growth rate K/e, maximum absolute growth rate $K*Y_m/e$) and 1/K is the inflection time point (units as hour). Statistical tests in each parameter panel was carried out using two-way ANOVA followed with Tukey's multiple comparison test for each medium treatment subpanel ($\alpha = 0.05$; different lowercase letters indicate significant differences; $n = 6$).

Growth Condition	Treatments	Best-fit values (Gompertz function*)			
		Y_m	Y_0	K	1/K
KB medium	WT	2.962^{ab}	0.000975^{a}	0.155^{a}	6.461^{a}
	oafA-1	3.016^{a}	0.000434^{a}	0.158^{a}	6.344^{a}
	WT:*oafA-1* (1:1)	2.927^{b}	0.000930^{a}	0.157^{a}	6.380^{a}
1/10th KB medium	WT	1.017^{b}	0.000891^{ab}	0.204^{a}	4.907^{b}
	oafA-1	1.052^{b}	0.000373^{b}	0.198^{ab}	5.066^{ab}
	WT:*oafA-1* (1:1)	1.129^{a}	0.001389^{a}	0.188^{b}	5.357^{a}
Culture filtrate of wild type CHA0	WT	1.667^{b}	0.000359^{a}	0.162^{a}	6.189^{b}
	oafA-1	1.706^{b}	0.000308^{a}	0.157^{a}	6.380^{ab}
	WT:*oafA-1* (1:1)	1.792^{a}	0.000370^{a}	0.152^{a}	6.598^{a}
Culture filtrate of the *oafA-1* mutant	WT	1.636^{c}	0.000285^{a}	0.159^{a}	6.295^{b}
	oafA-1	1.733^{b}	0.000323^{a}	0.149^{ab}	6.724^{a}
	WT:*oafA-1* (1:1)	1.838^{a}	0.000329^{a}	0.144^{b}	6.970^{a}

To examine the growth dynamics and/or yield of wild type CHA0 and the *oafA-1* mutant bacteria across many different growth conditions, the Biolog® Phenotype MicroArray™ (PM) system was used. This system consists of various bacterial growth modifiers such as diverse carbon sources, osmotic and ionic stressors, pH effect mediators and multiple antibiotics, to facilitate high-throughput characterization of bacterial genotypes (Dunkley *et al.*, 2019). We tested the growth of the wild type and the *oafA-1* mutant in PM Biolog plates PM1 and PM2 (different carbon sources; Fig. 3a and 3b), in PM9 and PM10 (different osmotic, ionic and pH modifiers; Fig. 3c and 3d) and in PM12B (various chemical stressors; Fig. 3e). Across the 480 tested conditions, growth dynamics and yield of the wild type and the *oafA-1* mutant bacteria were similar and accordingly we did not observe significant differences between their growth among all tested conditions (adjust $p < 0.05$; Fig. 3). It was previously shown that *Pseudomonas* bacteria lower the environmental pH when colonizing the root to suppress local host immune responses (Yu *et al.*, 2019), and thus we hypothesized

that pH might affect bacterial growth. However, again we did not observe significant differential-growth between wild type *oafA-1* mutant bacteria cultured across the tested pH range modulated by various pH modifiers. Kupferschmied and coworkers suggested that CHA0 O-PS is important for resistance towards a class of cationic antimicrobial peptides, known as AMPs (Kupferschmied *et al.*, 2016). Given the predicted role of OafA-CHA0 in O-antigen acetylation, we carefully assessed the growth dynamics of the wild type and the *oafA-1* mutant bacteria in PM Biology plate PM12B. PM12B, amongst many other compounds, contains polymyxin B (PMB), which is a bacterial AMP, and a reference compound for AMP research (Cole *et al.*, 2017). Similar to bacterial performance observed in the pH modifiers' assay, the *oafA-1* mutant displayed unaltered growth compared to the wild type in PMB. It should be noted, however, that the concentration used in the PM12B plate is possibly too low to exert an effect as CHA0 is highly resistant to PMB at concentrations as high as 1 mg/ml (Kupferschmied *et al.*, 2016; Dunkley *et al.*, 2019). Unaltered sensitivity towards PMB was also observed in another O-antigen defective CHA0 mutant, the Δ*fcl* mutant which lacks the entire long O-PS (Kupferschmied *et al.*, 2016), suggesting that PMB resistance in CHA0 does not appear to be mediated by the long O-PS. Altogether, the analysis of bacterial growth in the presence or absence of external stressors shows that *oafA-1* mutant bacteria are metabolically as versatile and competent as the wild type, which suggests that the enhanced root competence of the *oafA* mutants observed in the evolutionary experiment cannot be readily explained by growth penalties or metabolic deficiencies present in the wild type and is therefore likely driven explicitly by processes that are important during colonization of the plant roots. This is further corroborated by *in vitro* bacterial motility experiments on these CHA0 genotypes which demonstrated that the identified *OBC3* gene cluster mutants, including *oafA-1* and *oafA-2*, displayed unaltered motility compared to the wild type (**Chapter 2**).

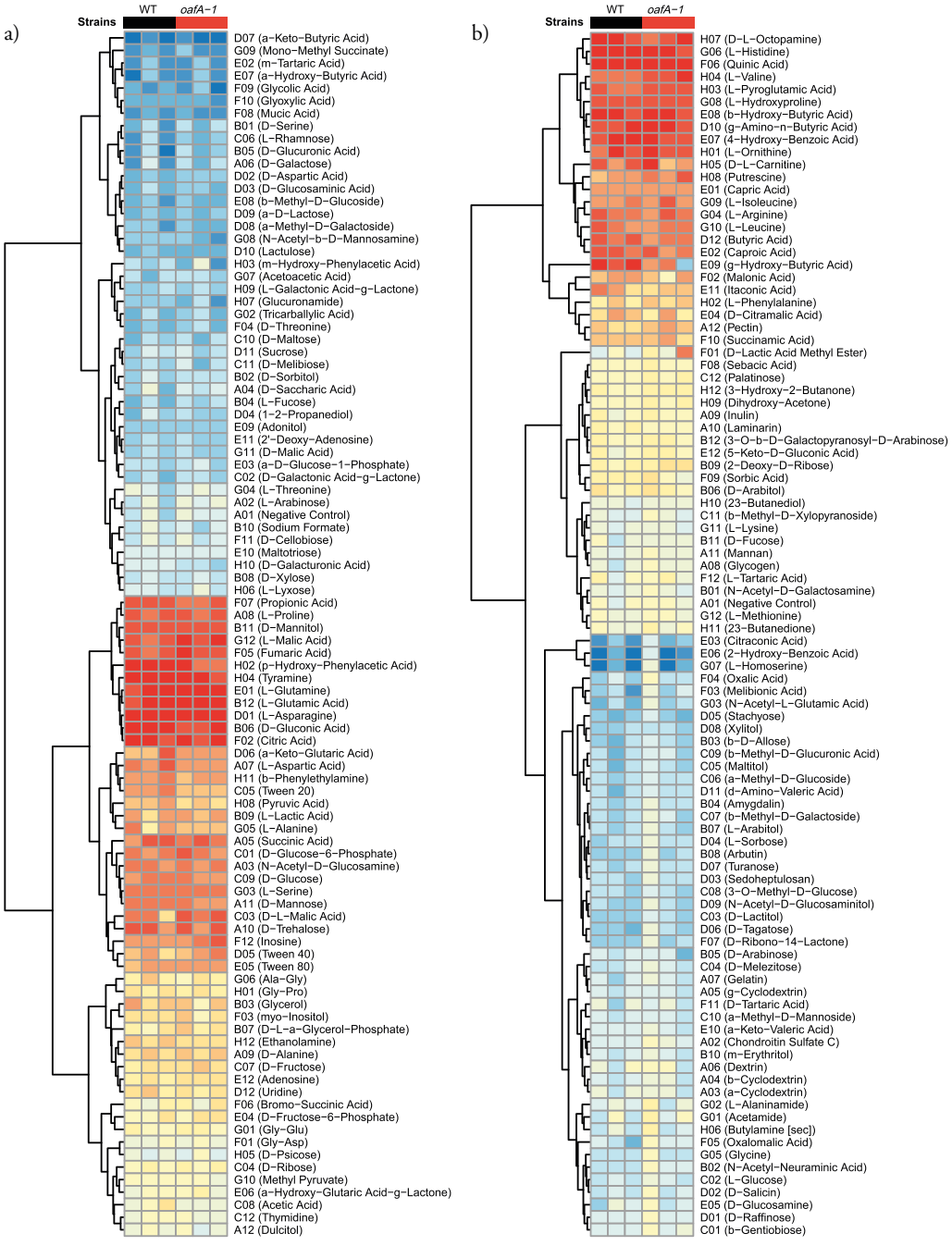
a)
Strains
WT
oafA−1
D07 (a−Keto−Butyric Acid)
G09 (Mono−Methyl Succinate)
E02 (m−Tartaric Acid)
E07 (a−Hydroxy−Butyric Acid)
F09 (Glycolic Acid)
F10 (Glyoxylic Acid)
F08 (Mucic Acid)
B01 (D−Serine)
C06 (L−Rhamnose)
B05 (D−Glucuronic Acid)
A06 (D−Galactose)
D02 (D−Aspartic Acid)
D03 (D−Glucosaminic Acid)
E08 (b−Methyl−D−Glucoside)
D09 (a−D−Lactose)
D08 (a−Methyl−D−Galactoside)
G08 (N−Acetyl−b−D−Mannosamine)
D10 (Lactulose)
H03 (m−Hydroxy−Phenylacetic Acid)
G07 (Acetoacetic Acid)
H09 (L−Galactonic Acid−g−Lactone)
H07 (Glucuronamide)
G02 (Tricarballylic Acid)
F04 (D−Threonine)
C10 (D−Maltose)
D11 (Sucrose)
C11 (D−Melibiose)
B02 (D−Sorbitol)
A04 (D−Saccharic Acid)
B04 (L−Fucose)
D04 (1−2−Propanediol)
E09 (Adonitol)
E11 (2'−Deoxy−Adenosine)
G11 (D−Malic Acid)
E03 (a−D−Glucose−1−Phosphate)
C02 (D−Galactonic Acid−g−Lactone)
G04 (L−Threonine)
A02 (L−Arabinose)
A01 (Negative Control)
B10 (Sodium Formate)
F11 (D−Cellobiose)
E10 (Maltotriose)
H10 (D−Galacturonic Acid)
B08 (D−Xylose)
H06 (L−Lyxose)
F07 (Propionic Acid)
A08 (L−Proline)
B11 (D−Mannitol)
G12 (L−Malic Acid)
F05 (Fumaric Acid)
H02 (p−Hydroxy−Phenylacetic Acid)
H04 (Tyramine)
E01 (L−Glutamine)
B12 (L−Glutamic Acid)
D01 (L−Asparagine)
B06 (D−Gluconic Acid)
F02 (Citric Acid)
D06 (a−Keto−Glutaric Acid)
A07 (L−Aspartic Acid)
H11 (b−Phenylethylamine)
C05 (Tween 20)
H08 (Pyruvic Acid)
B09 (L−Lactic Acid)
G05 (L−Alanine)
A05 (Succinic Acid)
C01 (D−Glucose−6−Phosphate)
A03 (N−Acetyl−D−Glucosamine)
C09 (D−Glucose)
G03 (L−Serine)
A11 (D−Mannose)
C03 (D−L−Malic Acid)
A10 (D−Trehalose)
F12 (Inosine)
D05 (Tween 40)
E05 (Tween 80)
G06 (Ala−Gly)
H01 (Gly−Pro)
B03 (Glycerol)
F03 (myo−Inositol)
B07 (D−L−a−Glycerol−Phosphate)
H12 (Ethanolamine)
A09 (D−Alanine)
C07 (D−Fructose)
E12 (Adenosine)
D12 (Uridine)
F06 (Bromo−Succinic Acid)
E04 (D−Fructose−6−Phosphate)
G01 (Gly−Glu)
F01 (Gly−Asp)
H05 (D−Psicose)
C04 (D−Ribose)
G10 (Methyl Pyruvate)
E06 (a−Hydroxy−Glutaric Acid−g−Lactone)
C08 (Acetic Acid)
C12 (Thymidine)
A12 (Dulcitol)
b)
Strains
WT
oafA−1
H07 (D−L−Octopamine)
G06 (L−Histidine)
F06 (Quinic Acid)
H04 (L−Valine)
H03 (L−Pyroglutamic Acid)
G08 (L−Hydroxyproline)
E08 (b−Hydroxy−Butyric Acid)
D10 (g−Amino−n−Butyric Acid)
E07 (4−Hydroxy−Benzoic Acid)
H01 (L−Ornithine)
H05 (D−L−Carnitine)
H08 (Putrescine)
E01 (Capric Acid)
G09 (L−Isoleucine)
G04 (L−Arginine)
G10 (L−Leucine)
D12 (Butyric Acid)
E02 (Caproic Acid)
E09 (g−Hydroxy−Butyric Acid)
F02 (Malonic Acid)
E11 (Itaconic Acid)
H02 (L−Phenylalanine)
E04 (D−Citramalic Acid)
A12 (Pectin)
F10 (Succinamic Acid)
F01 (D−Lactic Acid Methyl Ester)
F08 (Sebacic Acid)
C12 (Palatinose)
H12 (3−Hydroxy−2−Butanone)
H09 (Dihydroxy−Acetone)
A09 (Inulin)
A10 (Laminarin)
B12 (3−O−b−D−Galactopyranosyl−D−Arabinose)
E12 (5−Keto−D−Gluconic Acid)
B09 (2−Deoxy−D−Ribose)
F09 (Sorbic Acid)
B06 (D−Arabitol)
H10 (23−Butanediol)
C11 (b−Methyl−D−Xylopyranoside)
G11 (L−Lysine)
B11 (D−Fucose)
A11 (Mannan)
A08 (Glycogen)
F12 (L−Tartaric Acid)
B01 (N−Acetyl−D−Galactosamine)
A01 (Negative Control)
G12 (L−Methionine)
H11 (23−Butanedione)
E03 (Citraconic Acid)
E06 (2−Hydroxy−Benzoic Acid)
G07 (L−Homoserine)
F04 (Oxalic Acid)
F03 (Melibionic Acid)
G03 (N−Acetyl−L−Glutamic Acid)
D05 (Stachyose)
D08 (Xylitol)
B03 (b−D−Allose)
C09 (b−Methyl−D−Glucuronic Acid)
C05 (Maltitol)
C06 (a−Methyl−D−Glucoside)
D11 (d−Amino−Valeric Acid)
B04 (Amygdalin)
C07 (b−Methyl−D−Galactoside)
B07 (L−Arabitol)
D04 (L−Sorbose)
B08 (Arbutin)
D07 (Turanose)
D03 (Sedoheptulosan)
C08 (3−O−Methyl−D−Glucose)
D09 (N−Acetyl−D−Glucosaminitol)
C03 (D−Lactitol)
D06 (D−Tagatose)
F07 (D−Ribono−14−Lactone)
B05 (D−Arabinose)
C04 (D−Melezitose)
A07 (Gelatin)
A05 (g−Cyclodextrin)
F11 (D−Tartaric Acid)
C10 (a−Methyl−D−Mannoside)
E10 (a−Keto−Valeric Acid)
A02 (Chondroitin Sulfate C)
B10 (m−Erythritol)
A06 (Dextrin)
A04 (b−Cyclodextrin)
A03 (a−Cyclodextrin)
G02 (L−Alaninamide)
G01 (Acetamide)
H06 (Butylamine [sec])
F05 (Oxalomalic Acid)
G05 (Glycine)
B02 (N−Acetyl−Neuraminic Acid)
C02 (L−Glucose)
D02 (D−Salicin)
E05 (D−Glucosamine)
D01 (D−Raffinose)
C01 (b−Gentiobiose)

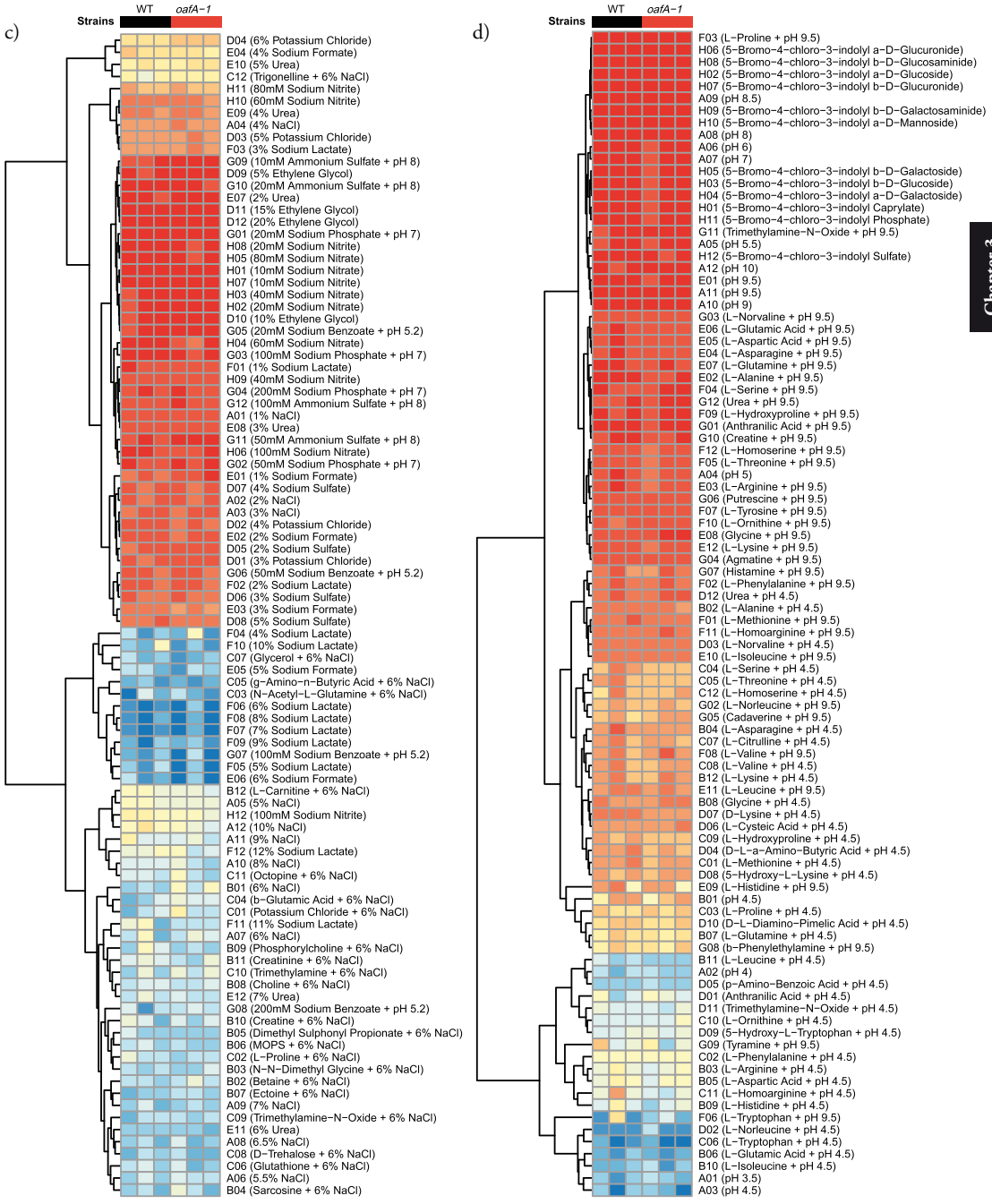
c)
Strains
WT
oafA−1
D04 (6% Potassium Chloride)
E04 (4% Sodium Formate)
E10 (5% Urea)
C12 (Trigonelline + 6% NaCl)
H11 (80mM Sodium Nitrite)
H10 (60mM Sodium Nitrite)
E09 (4% Urea)
A04 (4% NaCl)
D03 (5% Potassium Chloride)
F03 (3% Sodium Lactate)
G09 (10mM Ammonium Sulfate + pH 8)
D09 (5% Ethylene Glycol)
G10 (20mM Ammonium Sulfate + pH 8)
E07 (2% Urea)
D11 (15% Ethylene Glycol)
D12 (20% Ethylene Glycol)
G01 (20mM Sodium Phosphate + pH 7)
H08 (20mM Sodium Nitrite)
H05 (80mM Sodium Nitrate)
H01 (10mM Sodium Nitrate)
H07 (10mM Sodium Nitrite)
H03 (40mM Sodium Nitrate)
H02 (20mM Sodium Nitrate)
D10 (10% Ethylene Glycol)
G05 (20mM Sodium Benzoate + pH 5.2)
H04 (60mM Sodium Nitrate)
G03 (100mM Sodium Phosphate + pH 7)
F01 (1% Sodium Lactate)
H09 (40mM Sodium Nitrite)
G04 (200mM Sodium Phosphate + pH 7)
G12 (100mM Ammonium Sulfate + pH 8)
A01 (1% NaCl)
E08 (3% Urea)
G11 (50mM Ammonium Sulfate + pH 8)
H06 (100mM Sodium Nitrate)
G02 (50mM Sodium Phosphate + pH 7)
E01 (1% Sodium Formate)
D07 (4% Sodium Sulfate)
A02 (2% NaCl)
A03 (3% NaCl)
D02 (4% Potassium Chloride)
E02 (2% Sodium Formate)
D05 (2% Sodium Sulfate)
D01 (3% Potassium Chloride)
G06 (50mM Sodium Benzoate + pH 5.2)
F02 (2% Sodium Lactate)
D06 (3% Sodium Sulfate)
E03 (3% Sodium Formate)
D08 (5% Sodium Sulfate)
F04 (4% Sodium Lactate)
F10 (10% Sodium Lactate)
C07 (Glycerol + 6% NaCl)
E05 (5% Sodium Formate)
C05 (g−Amino−n−Butyric Acid + 6% NaCl)
C03 (N−Acetyl−L−Glutamine + 6% NaCl)
F06 (6% Sodium Lactate)
F08 (8% Sodium Lactate)
F07 (7% Sodium Lactate)
F09 (9% Sodium Lactate)
G07 (100mM Sodium Benzoate + pH 5.2)
F05 (5% Sodium Lactate)
E06 (6% Sodium Formate)
B12 (L−Carnitine + 6% NaCl)
A05 (5% NaCl)
H12 (100mM Sodium Nitrite)
A12 (10% NaCl)
A11 (9% NaCl)
F12 (12% Sodium Lactate)
A10 (8% NaCl)
C11 (Octopine + 6% NaCl)
B01 (6% NaCl)
C04 (b−Glutamic Acid + 6% NaCl)
C01 (Potassium Chloride + 6% NaCl)
F11 (11% Sodium Lactate)
A07 (6% NaCl)
B09 (Phosphorylcholine + 6% NaCl)
B11 (Creatinine + 6% NaCl)
C10 (Trimethylamine + 6% NaCl)
B08 (Choline + 6% NaCl)
E12 (7% Urea)
G08 (200mM Sodium Benzoate + pH 5.2)
B10 (Creatine + 6% NaCl)
B05 (Dimethyl Sulphonyl Propionate + 6% NaCl)
B06 (MOPS + 6% NaCl)
C02 (L−Proline + 6% NaCl)
B03 (N−N−Dimethyl Glycine + 6% NaCl)
B02 (Betaine + 6% NaCl)
B07 (Ectoine + 6% NaCl)
A09 (7% NaCl)
C09 (Trimethylamine−N−Oxide + 6% NaCl)
E11 (6% Urea)
A08 (6.5% NaCl)
C08 (D−Trehalose + 6% NaCl)
C06 (Glutathione + 6% NaCl)
A06 (5.5% NaCl)
B04 (Sarcosine + 6% NaCl)
d)
Strains
WT
oafA−1
F03 (L−Proline + pH 9.5)
H06 (5−Bromo−4−chloro−3−indolyl a−D−Glucuronide)
H08 (5−Bromo−4−chloro−3−indolyl b−D−Glucosaminide)
H02 (5−Bromo−4−chloro−3−indolyl a−D−Glucoside)
H07 (5−Bromo−4−chloro−3−indolyl b−D−Glucuronide)
A09 (pH 8.5)
H09 (5−Bromo−4−chloro−3−indolyl b−D−Galactosaminide)
H10 (5−Bromo−4−chloro−3−indolyl a−D−Mannoside)
A08 (pH 8)
A06 (pH 6)
A07 (pH 7)
H05 (5−Bromo−4−chloro−3−indolyl b−D−Galactoside)
H03 (5−Bromo−4−chloro−3−indolyl b−D−Glucoside)
H04 (5−Bromo−4−chloro−3−indolyl a−D−Galactoside)
H01 (5−Bromo−4−chloro−3−indolyl Caprylate)
H11 (5−Bromo−4−chloro−3−indolyl Phosphate)
G11 (Trimethylamine−N−Oxide + pH 9.5)
A05 (pH 5.5)
H12 (5−Bromo−4−chloro−3−indolyl Sulfate)
A12 (pH 10)
E01 (pH 9.5)
A11 (pH 9.5)
A10 (pH 9)
G03 (L−Norvaline + pH 9.5)
E06 (L−Glutamic Acid + pH 9.5)
E05 (L−Aspartic Acid + pH 9.5)
E04 (L−Asparagine + pH 9.5)
E07 (L−Glutamine + pH 9.5)
E02 (L−Alanine + pH 9.5)
F04 (L−Serine + pH 9.5)
G12 (Urea + pH 9.5)
F09 (L−Hydroxyproline + pH 9.5)
G01 (Anthranilic Acid + pH 9.5)
G10 (Creatine + pH 9.5)
F12 (L−Homoserine + pH 9.5)
F05 (L−Threonine + pH 9.5)
A04 (pH 5)
E03 (L−Arginine + pH 9.5)
G06 (Putrescine + pH 9.5)
F07 (L−Tyrosine + pH 9.5)
F10 (L−Ornithine + pH 9.5)
E08 (Glycine + pH 9.5)
E12 (L−Lysine + pH 9.5)
G04 (Agmatine + pH 9.5)
G07 (Histamine + pH 9.5)
F02 (L−Phenylalanine + pH 9.5)
D12 (Urea + pH 4.5)
B02 (L−Alanine + pH 4.5)
F01 (L−Methionine + pH 9.5)
F11 (L−Homoarginine + pH 9.5)
D03 (L−Norvaline + pH 4.5)
E10 (L−Isoleucine + pH 9.5)
C04 (L−Serine + pH 4.5)
C05 (L−Threonine + pH 4.5)
C12 (L−Homoserine + pH 4.5)
G02 (L−Norleucine + pH 9.5)
G05 (Cadaverine + pH 9.5)
B04 (L−Asparagine + pH 4.5)
C07 (L−Citrulline + pH 4.5)
F08 (L−Valine + pH 9.5)
C08 (L−Valine + pH 4.5)
B12 (L−Lysine + pH 4.5)
E11 (L−Leucine + pH 9.5)
B08 (Glycine + pH 4.5)
D07 (D−Lysine + pH 4.5)
D06 (L−Cysteic Acid + pH 4.5)
C09 (L−Hydroxyproline + pH 4.5)
D04 (D−L−a−Amino−Butyric Acid + pH 4.5)
C01 (L−Methionine + pH 4.5)
D08 (5−Hydroxy−L−Lysine + pH 4.5)
E09 (L−Histidine + pH 9.5)
B01 (pH 4.5)
C03 (L−Proline + pH 4.5)
D10 (D−L−Diamino−Pimelic Acid + pH 4.5)
B07 (L−Glutamine + pH 4.5)
G08 (b−Phenylethylamine + pH 9.5)
B11 (L−Leucine + pH 4.5)
A02 (pH 4)
D05 (p−Amino−Benzoic Acid + pH 4.5)
D01 (Anthranilic Acid + pH 4.5)
D11 (Trimethylamine−N−Oxide + pH 4.5)
C10 (L−Ornithine + pH 4.5)
D09 (5−Hydroxy−L−Tryptophan + pH 4.5)
G09 (Tyramine + pH 9.5)
C02 (L−Phenylalanine + pH 4.5)
B03 (L−Arginine + pH 4.5)
B05 (L−Aspartic Acid + pH 4.5)
C11 (L−Homoarginine + pH 4.5)
B09 (L−Histidine + pH 4.5)
F06 (L−Tryptophan + pH 9.5)
D02 (L−Norleucine + pH 4.5)
C06 (L−Tryptophan + pH 4.5)
B06 (L−Glutamic Acid + pH 4.5)
B10 (L−Isoleucine + pH 4.5)
A01 (pH 3.5)
A03 (pH 4.5)

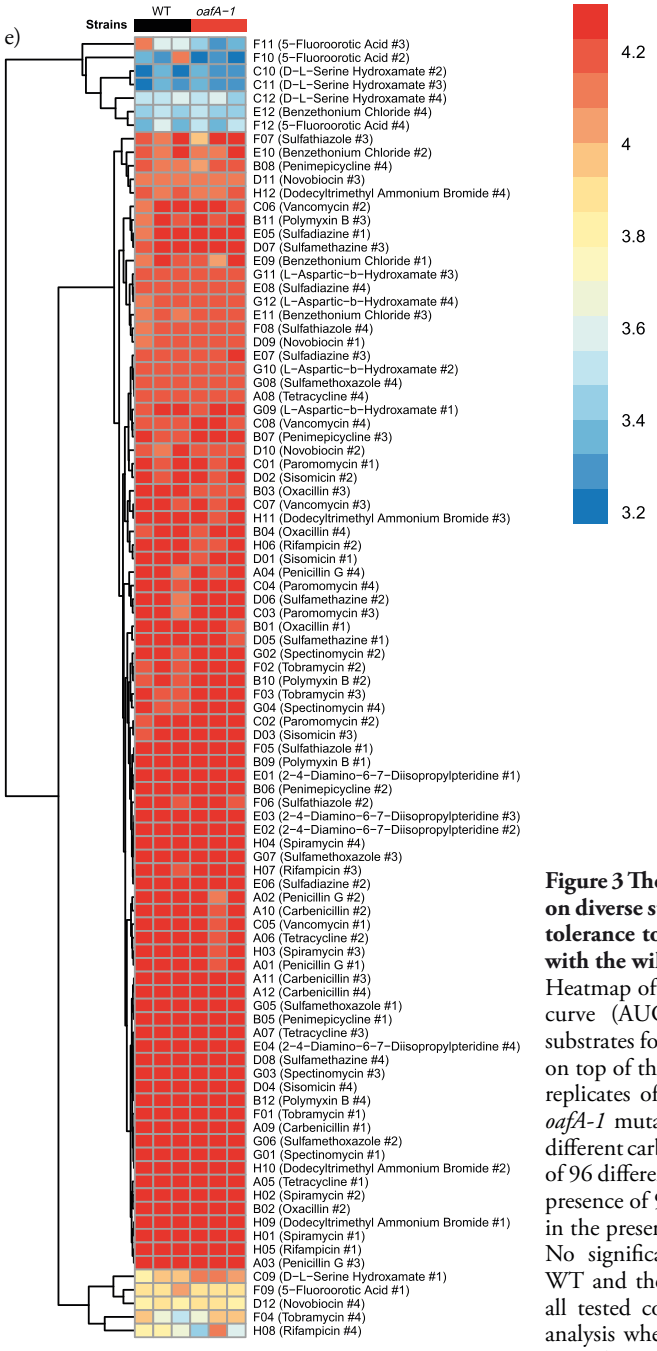

Figure 3 The *oafA-1* mutant grows equally well on diverse substrates and displays comparable tolerance to several stressors when compared with the wild type progenitor.
Heatmap of the area under the bacterial growth curve (AUC, $\log_{10}$ transformed) on diverse substrates for 72 hours (25 ºC). Squared legends on top of the heatmaps indicate three biological replicates of wild type (WT) (black) and the *oafA-1* mutant (red). a) and b) growth on 192 different carbon sources c) growth in the presence of 96 different osmotic stressors d) growth in the presence of 96 different pH modifiers e) growth in the presence of 96 various chemical stressors. No significant difference in growth between WT and the *oafA-1* mutant was found among all tested conditions based on unpaired t-test analysis when corrected for multiple testing (n = 3, adjusted p-value < 0.05).

Root colonization and inhibition of Arabidopsis growth are unaltered in *oafA* mutant bacteria

To test whether plants indeed are the driving force behind the selection of the *oafA* mutants, we used a gnotobiotic, agar-based setup involving Arabidopsis seedlings to study plant-bacteria interactions in detail. Such setup has been used extensively to study binary, one plant-one bacterium interactions allowing for high reproducibility and detailed characterization (Zamioudis *et al.*, 2013, 2015; Stringlis *et al.*, 2018a; Li *et al.*, 2021a). Arabidopsis seedlings of 12-days-old were inoculated with an equal cell number of the wild type, the *oafA-1* mutant or a wild type/*oafA-1* mixture in equal ratio (1:1) on the root-shoot junction. All bacteria-treated plants showed similar, reduced growth phenotypes upon treatment (Fig. 4a, b), displaying shorter primary roots at 3 dpi (Fig. 4d), and overall growth inhibition at 7 dpi (significant at $\alpha = 0.05$ for both plant shoot and root weight and primary root length; Fig. 4b-d). This is in line with our previous work in which we recorded plant growth retardation by CHA0 overall, with the notable exception of evolved, mutualistic CHA0 bacteria carrying mutations in several global regulators (Li *et al.*, 2021a).

To assess bacterial root colonization ability, we examined the bacterial density on the roots of collected Arabidopsis seedlings. We observed that the *oafA-1* bacterial density was higher at 3 dpi, when compared to the wild type or WT/*oafA-1* mixed populations (Fig. 5a, b). At 7 dpi, however, this difference had disappeared but now the WT/*oafA-1* mixed population density was significantly lower compared to root bacterial density of the wild type or the *oafA-1* single genotype inoculation (Fig. 5a, b). With the data collected from several replicated experiments, we were able to assess the correlation between the weight of, and the bacterial density on, roots treated with different bacteria at 7 dpi. There was no significant correlation observed between these two parameters. However, the root bacterial density of the wild type and the *oafA-1* mutant single-genotype inoculation demonstrated a positive trend with plant root weight, while the WT/*oafA-1* mixed population displays a negative trend with plant root weight (Fig. 6, Table S1). These results suggest that the mixed population triggers a different plant response when compared to single-genotype application. Such response could be triggered by microbe-microbe competition leading to release of selective compounds that repress plant growth. Or, alternatively, it could be that the mixture consumes the available plant root exudates faster than single genotype application, similar to our observations of growth in low nutrient media due to the lack of kin recognition (Table 1). Such behavior leads to an accelerated transition to the final, death phase of the bacterial population which is associated with a decline in bacterial cells. Elevated bacterial density of the *oafA-1* mutant at 3 dpi, compared to

the wild type, was repeatedly observed, albeit not always significantly, suggesting that this mutant has the potential to outcompete the wild type by accelerated colonization.

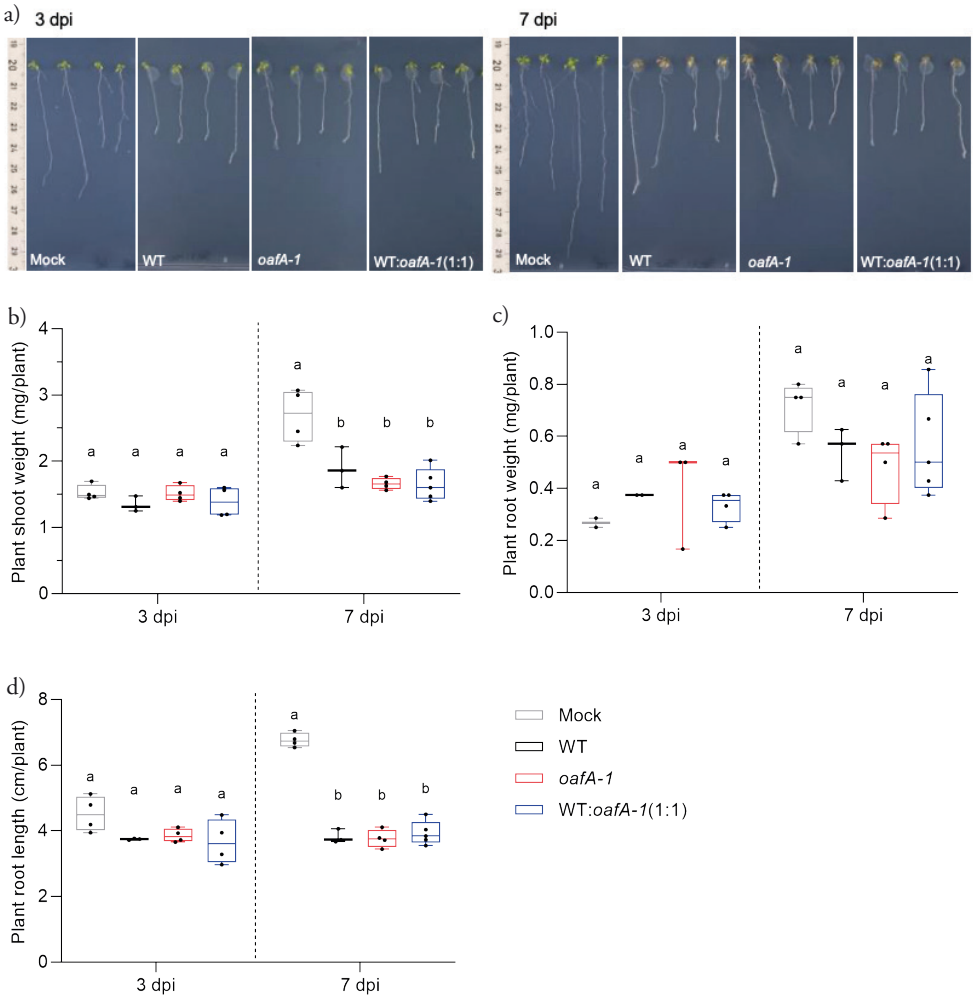

Figure 4 Effect of the *oafA-1* mutant and a mixture of wild type and mutant *oafA-1* on Arabidopsis are comparable to wild type mono-application.
Twelve-day-old Arabidopsis seedlings are inoculated with bacterial cell suspensions (10 µl of 10^7 cfu/ml) of wild type (WT), the *oafA-1* mutant, or a mixture of the two genotypes (1:1) on the root-shoot junction. The mock treatment used 10 µl 10 mM $MgSO_4$ instead. a) Arabidopsis phenotypes at 3- and 7-days post inoculation (dpi). b-d) Fresh shoot weight in mg/plant at 3 and 7 dpi, fresh root weight in mg/plant at 3 and 7 dpi, and primary root length in cm/plant at 3 dpi and 7 dpi, respectively. Statistical tests in all panels of each time point was carried out using one-way ANOVA followed by Tukey's multiple comparison test ($\alpha = 0.05$; different lowercase letters indicate significant differences; $2 \leq n \leq 5$).

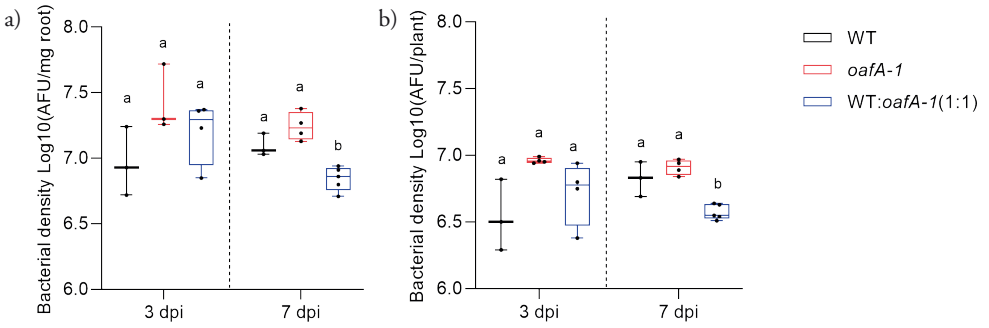

Figure 5 Increased early Arabidopsis colonization by *oafA-1* mutant bacteria.
Twelve-day-old Arabidopsis seedlings were treated with bacterial cell suspensions (10 µl of 10^7 cfu/ml) of wild type (WT), the *oafA-1* mutant, or a mixture of the two genotypes (1:1) on the root-shoot junction. The mock treatment used 10 µl 10 mM $MgSO_4$ instead. Bacterial density is depicted in Active Fluorescent Units (AFU) per mg root weight (a) or AFU/plant (b) in log_{10} scale. Statistical tests in all panels of each time point was carried out using one-way ANOVA followed by Tukey's multiple comparison test ($\alpha = 0.05$; different lowercase letters indicate significant differences; $3 \leq n \leq 4$).

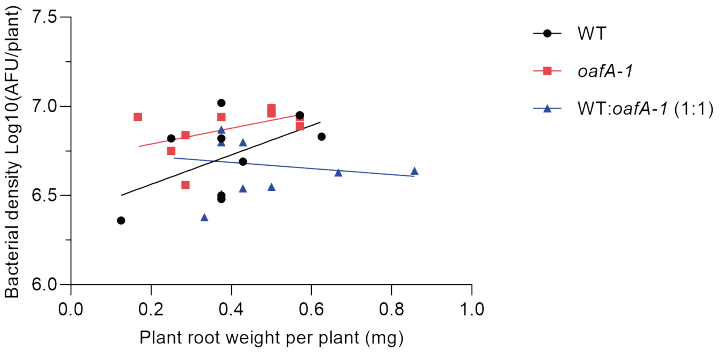

Figure 6 Root colonization of the mixture of wild type and *oafA-1* bacterial cells, in contrast to single-genotype colonization, shows no correlation with plant root weight.
Twelve-day-old seedlings were treated with bacterial cell suspensions (10 µl of 10^7 cfu/ml) of wild type (WT), the *oafA-1* mutant bacteria (*oafA-1*), or the mixture of the two genotypes (1:1) on the root-shoot junction. The root bacterial density (measured by flow cytometry as the Active Fluorescent Unit (AFU)/plant, log_{10} transformed) at 3 dpi days post inoculation (dpi) and 7 dpi for each bacterial treatment is plotted against the corresponding root sample weight (mg/plant) ($8 \leq n \leq 11$). Different colors and shapes represent different treatment groups (WT, black dot; *oafA-1*, read square; WT:*oafA-1* (1:1), blue triangle). A linear regression model is determined for each treatment and depicted in the same color (WT: $R^2 = 0.34$, $p = 0.17$; *oafA-1*: $R^2 = 0.45$, $p = 0.10$; WT/*oafA-1*(1:1): $R^2 = 0.06$, $p = 0.56$).

The *oafA-1* mutant outcompetes the wild type only in the rhizosphere

The elevated *oafA-1* population density observed at 3 dpi suggests that this mutant can colonize the Arabidopsis root faster than the wild type. Meanwhile, the significantly lower root bacterial density of WT/*oafA-1* mixture at 7 dpi and its different correlation to plant root weight indicate bacteria-bacteria interaction between wild type CHA0 and the *oafA-1* mutant. Naturally, we assessed the frequency of the *oafA-1* mutant

in the WT/*oafA-1* mixed populations from the rhizosphere samples of both at 3 dpi and 7 dpi using HRM curve analysis. For comparison, we included in this analysis the mixed populations sampled from *in vitro* culture media and culture filtrates, in which we did not detect differences in growth dynamics between wild type CHA0 and the *oafA-1* mutant. We found that the *oafA-1* frequency averages around 55% for all *in vitro*-mixed culture samples at the final time point of the experiments (Fig. 7a). In contrast, the frequency of *oafA-1* reached up to 70% for the mixed populations when sampled from plant roots. A 40% relative increase, compared to the initial 50% frequency, was observed for both 3 dpi and 7 dpi root bacterial samples (Fig. 7a). Although WT/*oafA-1* mixture behaved differently as single genotype *in vitro* (Table 1), the *oafA-1* mutant frequency did not increase in these samples. Comparably, the significantly increased *oafA-1* mutant frequency on root indicates a much stronger competence between wild type CHA0 progenitor and the *oafA-1* mutant on plant roots (Fig. 7a).

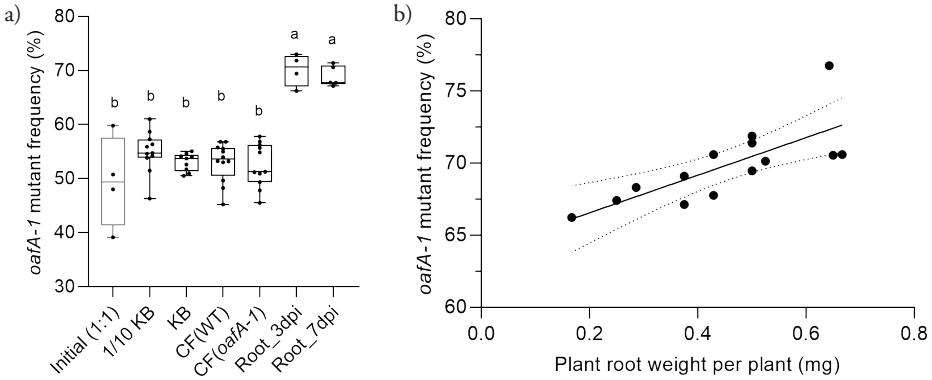

Figure 7 The *oafA-1* mutant outcompetes the wild type only on Arabidopsis roots, and its frequency during mixed, competitive colonization is positively correlated with root weight.
a) The frequency of *oafA-1* mutant bacteria in wild type (WT)/*oafA-1* mixed samples (initial 1:1) obtained from different growth media or the rhizosphere. The *oafA-1* frequency in the WT/*oafA-1* (1:1) initial sample was determined for one experiment only (cell density OD_{600} equal to 0.01; grey, $n = 4$). The growth media were one-tenth strength KB ($1/10^{th}$ KB, $n = 12$), full strength KB (KB, $n = 12$), culture filtrate of the wild type (CF_{WT}, $n = 12$), and culture filtrate of the *oafA-1* mutant (CF_{oafA-1}, $n = 12$). Bacterial cell suspensions (10 µl of 10^7 cells/ml) of WT/*oafA-1* (1:1) were inoculated into 190 µl growth medium in a 96-well plate for incubation at 28 ºC (final cell density OD_{600} equal to 0.005). After 23 hours of growth in the listed conditions, bacterial samples were collected and subjected to mutant frequency determination by HRM curve analysis. For root bacterial samples, 12-day-old seedlings were inoculated with bacterial cell suspensions (10 µl of 10^7 cells/ml) of WT/*oafA-1* (1:1) on the root-shoot junction. The samples are collected at 3- and 7-days post inoculation (dpi) ($n \geq 4$). Statistical analysis across all panels was carried out using one-way ANOVA followed by Tukey's multiple comparison test ($\alpha = 0.05$; different lowercase letters indicate significant differences; $4 \leq n \leq 12$). b) Frequency of the *oafA-1* mutant from root samples inoculated with the mixed (1:1) WT/*oafA-1* samples is positively correlated with plant root weight (mg/plant). The black line indicates the linear regressions with 95% confidence intervals (dotted black lines; $n = 14$, $R^2 = 0.56$, $p = 0.002$).

In addition, there was a significant positive correlation between the *oafA-1* frequency in the rhizosphere of the WT/*oafA-1* mixture and root weight, when replicated experiments were analyzed altogether at 3 and 7 dpi (Fig. 7b). It suggests plant roots play a role in this selection preference, in which root size directly or indirectly affect the increase levels. Due to the initial density of wild type CHA0 and *oafA-1* are equal, we could not exclude the possibility that the increased *oafA-1* frequency is a result of more decreased wild type CHA0 population in a mixed population.

The *oafA-1* mutant bacterial competence is root-size dependent

To clarify whether the increased *oafA-1* frequency is due to the enhanced competence of the *oafA-1* mutant, we decided to reduce the initial percentage of the *oafA-1* cells from 50% to 20%, corresponding to an initial ratio of 8:2 WT:*oafA-1* bacterial cells. Furthermore, we compared bacterial population density and specifically, *oafA-1* colonization, on older, and therefore larger plants. If plants indeed play a role in this selection preference as we hypothesized, we would expect to observe a bigger relative increase for *oafA-1* frequency. In addition, if the dramatic decrease of the WT/*oafA-1* mixed population from 3 dpi to 7 dpi is the result of faster metabolism, we would expect to observe a less decreased bacterial density of the mixture on bigger plant roots, which have more root exudation, in absolute levels. We took 18-day-old seedlings alongside 12-day-old seedlings for this comparison, that on average are 40% heavier in terms of root weight and have 30% longer primary root length at the end of the experiment.

As observed previously, bacterial colonization inhibited the growth of 12-day-old initial (12D) seedlings, irrespective of bacterial genotype (Fig. 8a, b). In contrast, a reduced level of bacteria-induced plant growth inhibition was observed on 18-day-old initial (18D) seedlings at 7 dpi, as plant shoot and root weights were not significantly impaired by bacterial colonization when compared with the mock-treatment (Fig. 8b, c). Yet, at both plant ages, bacteria-treated plants displayed shorter primary roots (Fig. 8d). The bacterial density of wild type and mutant cells on the roots of 12D and 18D seedlings was comparable, suggesting that the bacteria-induced growth retardation observed on 12D seedlings does not affect bacterial carrying capacity significantly in this setup and over the examined time window (Fig. 9a). Given the increased weight of 18D seedlings, the absolute number of bacterial cells on the roots of 18D seedlings is higher than that on the 12D seedlings (Fig. 9b). In other words, the 18D initial seedlings have higher root bacterial carrying capacity than that of 12D initial seedlings, but the relative bacterial colonization appears consistent over both two types of seedlings. Intriguingly, the higher bacterial carrying capacity and relative healthy of 18D seedlings' roots contains significantly lower bacterial density of the WT/*oafA-1* (8:2) mixed population (Fig. 8a, 9a, b). In contrast, the mixed

bacterial population is comparable with single genotypes' bacteria on 12D seedlings (Fig. 9a, b). These observations suggest that a lower initial ratio of the *oafA-1* mutant, - 20% compared to earlier 50% -, relieved the competition between wild type and *oafA-1* mutant cells, while bigger and older plants exacerbated this microbe-microbe interaction. In addition, the combined analysis of 12D and 18D seedlings, indicates that root colonization by wild type and *oafA-1* mutant cells, when applied on their own, positively correlates with plant root weight (R^2 = 0.91 and 0.88 respectively; Fig. 9c, Table S2), and this correlation is lost when both genotypes were applied as a mix (R^2 = 0.01; Fig. 9c, Table S2). Thus, the lower bacterial population density of mixed wild type and mutant cells on roots might not be linked to the amount of root exudates produced, but to other, hitherto unknown, features of the plant roots together with the microbe-microbe competition between both genotypes.

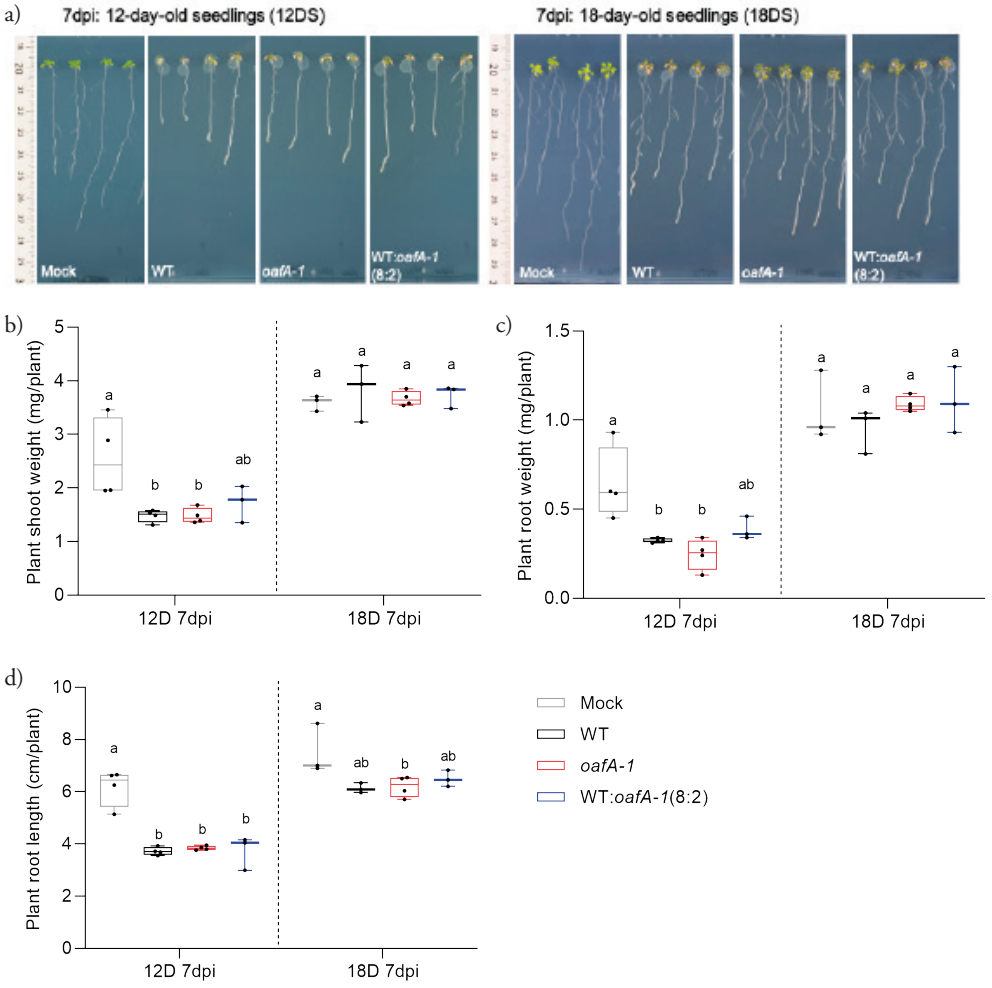

Figure 8 Effects of the *oafA-1* mutant and a mixture of wild type and *oafA-1* (8:2) cells on different ages of Arabidopsis plants are comparable to application of wild type cells.
Twelve-day-old (12D) and 18-day-old (18D) seedlings were inoculated on the root-shoot junction with bacterial cell suspensions (10 µl of 10^7 cells/ml) of wild type (WT), *oafA-1* mutant bacteria (*oafA-1*), or a mixture of the two genotypes at a ratio of 8:2 (WT/*oafA-1*). The mock treatment used 10 µl 10 mM $MgSO_4$ instead. a) Representative pictures of 12D (a, left) and 18D (a, right) Arabidopsis seedlings at 7 days post inoculation (dpi) by bacterial cells or a mock solution. b-d) Fresh shoot weight in mg/plant at 7 dpi, fresh root weight in mg/plant at 7 dpi, and primary root length in cm/plant at 7 dpi, respectively. Statistical tests in all panels of each time point was carried out using one-way ANOVA followed by Tukey's multiple comparison test ($\alpha = 0.05$; different lowercase letters indicate significant differences; $3 \leq n \leq 5$).

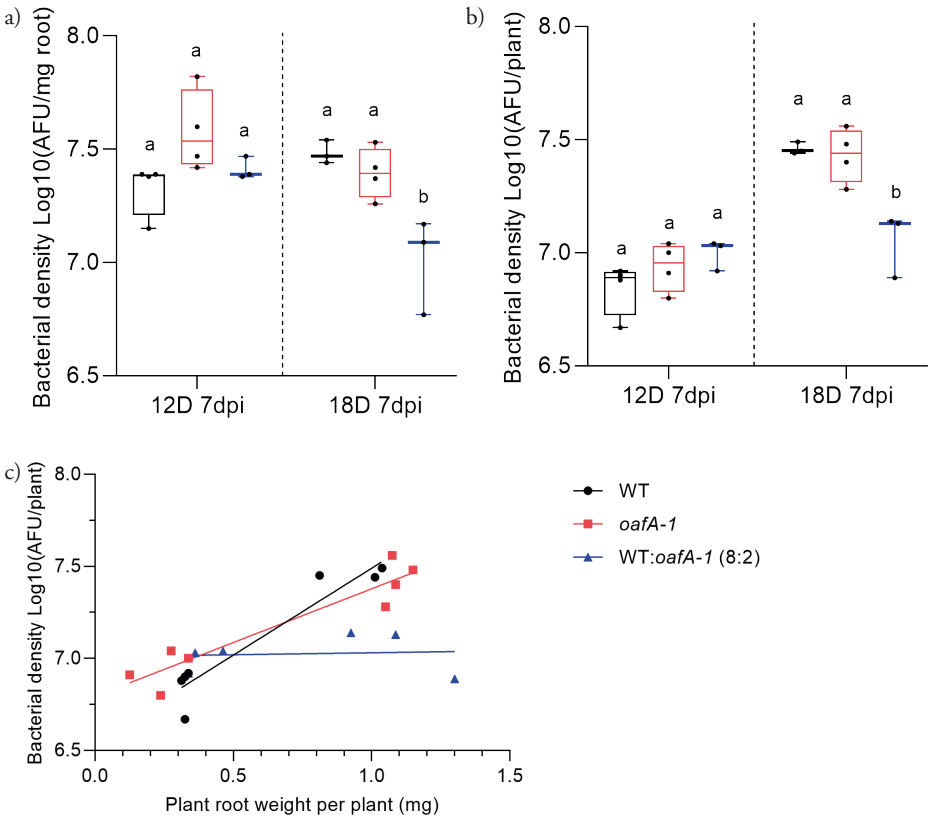

Figure 9 Mixture of wild type CHA0 and the *oafA-1* mutant, unlike single genotype, displays no-correlation with seedling age and consequently weight.
Twelve-day-old (12D) initial seedlings and 18-day-old (18D) initial seedlings were treated with cell suspensions (10 µl of 10^7 cfu/ml) of wild type (WT), the *oafA-1* mutant bacteria, or a mixture of both genotypes (WT/*oafA-1*; 8:2) on the root-shoot junction. The mock treatment used 10 µl 10 mM $MgSO_4$ instead. The bacterial density is depicted in a) Active Fluorescent Units (AFU)/grams root weight or b) AFU/plant in log_{10} scale. Statistical tests in a and b panels were carried out using one-way ANOVA followed by Tukey's multiple comparison test ($\alpha = 0.05$; different lowercase letters indicate significant differences; $3 \leq n \leq 4$) c) Root colonization by wild type and *oafA-1* mutant bacteria is positively correlated with seedling root weight, while the mixture of both genotypes (WT/*oafA-1*; 8:2) did not ($6 \leq n \leq 8$). For all panels, different colors and shapes represent different bacterial treatments (WT, black, $R^2 = 0.91$, $p = 0.0009$; *oafA-1*, red, $R^2 = 0.88$, $p = 0.0005$; mixture of WT/*oafA-1* (8:2), blue, $R^2 = 0.008$, $p = 0.87$).

Next, we examined the frequency of the *oafA-1* mutant in the mixed populations on the 12D and 18D seedlings using HRM curve analysis (Fig. 10). We observed that the *oafA-1* frequency increased in both populations, seven days after inoculation, although only significant for 18D. Given the initial 20% *oafA-1* in the mixed inoculum we observed a 50% relative increase in *oafA-1* frequency on 12D seedlings, which is comparable to the previously observed 40% in the initial 1:1 mixed inoculations. Notably, we observe a staggering 80% relative increase on 18D seedlings with an initial 20% *oafA-1* frequency (Fig. 7 and Fig. 10a). Altogether, these results suggest

that the increased *oafA-1* frequency is a result of enhanced bacterial competence of the *oafA-1* mutant, and bacterial expansion of *oafA-1* mutant in a mixed population depends on plant size, likely root carrying capacity. This is corroborated by our earlier observations that *oafA-1* frequency only reached 100% after three growth cycles of four weeks each in the evolutionary experiment (Fig. 2).

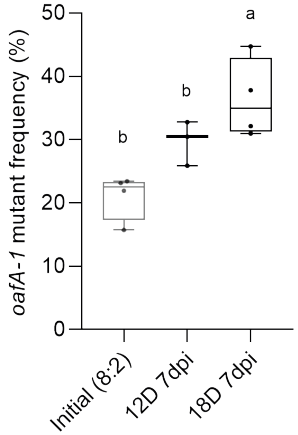

Figure 10 Frequency of *oafA-1* increases most strongly on the roots of 18-day-old seedlings compared to that on smaller 12-day-old seedlings.
Twelve-day-old (12D) initial seedlings and 18-day-old (18D) initial seedlings were treated with cell suspensions (10 µl of 10^7 cells/ml) of a mixture of wild type and *oafA-1* mutant bacteria (8:2) on the root-shoot junction. The frequency of *oafA-1* was measured at 7 dpi of both 12D and 18D seedlings. The *oafA-1* frequency in the initial mixture was measured directly from the inoculation samples before dilution (Cell density OD_{600} equal to 0.1). Statistical tests were carried out using one-way ANOVA followed by Tukey's multiple comparison test ($\alpha = 0.05$; different lowercase letters indicate significant differences; $3 \leq n \leq 4$).

OafA mutants have significantly faster root attachment

The rapid, increased frequency of the *oafA-1* mutant on plant roots, both when applied as a single genotype and when applied as a mixture with wild type CHA0 progenitor, and further accelerated by the use of larger seedlings, suggests that the here described *oafA* mutations affect especially the early phases of colonization. As bacterial motility is unaffected in *OBC3* mutants altogether, including both *oafA* mutants (**Chapter 2**), we questioned whether bacterial root attachment is affected by these *oafA* mutations. From several experimental systems, including those involving bacteria from the *Pseudomonas* genus, it is known that primary attachment, characterized by weak, reversible binding of bacteria to the root surface, and secondary attachment, characterized by a switch to stronger, irreversible binding of bacterial cells on the plant root surface, are modulated by adhesive pili, outer membrane porins and extracellular fibrils such as exopolysaccharides (Rodríguez-Navarro *et al.*, 2007; Wheatley & Poole, 2018; Carroll *et al.*, 2020; Knights *et al.*, 2021). It is therefore not unlikely that mutations potentially affecting LPS structure could alter root attachment. Thus, here we set out to assess bacterial attachment of the *oafA* mutants. To this end, we dipped

10-day-old (10D) seedlings in cell suspensions of the wild type, *oafA-1* and *oafA-2* bacteria for 0.5 hr and 2.5 hr followed by quantification of the stably attached bacterial cells on the root. We observed significantly higher cell density of the *oafA-1* and *oafA-2* mutant compared to the wild type at 0.5 hr post dipping (Fig. 11). At 2.5 hr post dipping, these differences had disappeared and we observed similar cell density for all genotypes (Fig. 11). To test whether other cell surface decoration (*OBC3*) mutants from the evolutionary experiment, i.e., the *galE* mutant and the *RS09880* mutant, had similar effects on bacterial root attachment, we conducted another attachment experiment with these two mutants (Fig. S3). Interestingly, the *galE* mutant did not show a significantly higher bacterial attachment on roots when compared to the wild type in both time points, while the *RS09880* mutant did at 2.5 hr post dipping. Considering three out of four cell surface decoration mutants show better attachment in early phases of colonization, we speculate that such decoration represents an important evolutionary strategy for enhanced root competence of rhizobacteria such as CHA0 on Arabidopsis in gnotobiotic conditions (**Chapter 2**).

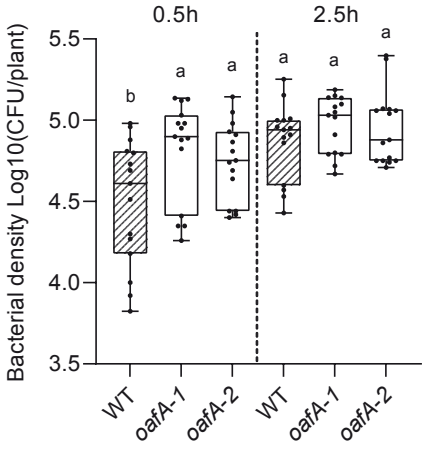

Figure 11 Faster attachment of *oafA* mutant bacteria to Arabidopsis roots .
Ten-day-old seedlings were dipped in bacterial cell suspensions (1 ml of 10^7 cfu/ml) of the wild type or the *oafA-1* or *oafA-2* mutants. The root-associated bacteria were quantified after 0.5 hours and 2.5 hours. Statistical tests of each time point was carried out using one-way ANOVA followed by Tukey's multiple comparison test ($\alpha = 0.05$; different lowercase letters indicate significant differences; $n = 15$).

Discussion

Successful application of plant-beneficial microbes in the field relies on bacterial colonization to fully exert their plant-beneficial functions. Bacterial rhizosphere competence reflects the ability of bacteria to interact with the plant root, to compete with other microorganisms, and to adapt to soil edaphic factors such as pH and organic matter levels. The bacterial cell surface and modifications thereof contribute to almost all these interactions (Clark *et al.*, 1991; Lerouge & Vanderleyden, 2001; Kupferschmied *et al.*, 2016; Simpson & Trent, 2019; Knights *et al.*, 2021). Despite

multiple studies that established an important role for lipopolysaccharide (LPS) in plant-bacteria interactions, studies on the physiological effects of O-antigen modification, one of three functional domains of LPS, and contribution to enhanced rhizosphere competence are rare. In this study, we conducted a series of *in vitro* and *in vivo* experiments to characterize two recently identified CHA0 O-antigen acetyltransferase (*oafA*) mutants that arose during experimental evolution in the rhizosphere of Arabidopsis (**Chapter 2**). We assessed the metabolic versatility of these mutants, examined their ability to colonize the roots of Arabidopsis plants, and quantified their effect on plant development. Our study extends our understanding of the role of LPS, specifically O-antigen modification, in plant-microbe interactions, by using spontaneous mutants that appeared during long-term evolution of CHA0 on Arabidopsis plants (**Chapter 2**) (Li *et al.*, 2021a).

Diverse functions of LPS O-antigen in plant-microbe interactions

As an integral component of the cell envelope, LPS localizes on the outer membrane in gram-negative bacteria. In plant-microbe interactions, LPS and its derivatives can be recognized by plants as microbe-associated molecular patterns (MAMPs), which induce innate immune responses of plants (Newman *et al.*, 1995; Zeidler *et al.*, 2004; Silipo *et al.*, 2005). It should be noted however, that most research used purified LPS preparations to study LPS activity *in vitro*, and might therefore not fully represent the spectrum of natural LPS activities (Zeidler *et al.*, 2004). Kutschera and coworkers, e.g., recently found that LPS-copurified medium-chain 3-hydroxy fatty acids (mc-3-OH-FA), are in fact the main constituents of elicitor-active LPS preparations. Consequently, it appeared that the previously identified receptor for LPS, LIPOOLIGOSACCHARIDE-SPECIFIC REDUCED ELICITATION (LORE), in fact represents a mc-3-OH-FA receptor (Kutschera *et al.*, 2019). Interestingly, mc-3-OH-FA appears to be a weak elicitor of MAMP-triggered immunity (MTI), as it elicited only about one fifth of differential expressed genes (DEGs) when compared with the flagellin epitope flg22 at about double the amount of time (Bjornson *et al.*, 2021). Based on these discoveries it appears that plants possess only low affinity for LPS. In the present study, we found that *oafA* mutants had unaltered effects on plant performance when compared with wild type bacteria and thus we hypothesize that O-antigen modification in these mutants did not result in altered bacteria-induced plant immunity. In addition, the less-growth-inhibited 18D seedlings, compared to same bacteria-treated 12D seedlings at 7 dpi, had a consistent single bacterial genotype colonization cell density, but a significantly lower mixture population in 18D seedlings at 7 dpi (Fig. 9a, b). This finding provides additional evidence that the selection of *OBC3* mutants in the evolutionary experiment cannot be attributed to an altered plant immunity response.

Other than its MAMP activity, LPS integrity, especially that of the O-antigen, plays an important role in bacterial fitness in the rhizosphere (Dekkers *et al.*, 1998). Dekkers and coworkers found that O-antigen mutants with complete loss of O-antigen, showed impaired growth in artificial culture medium and in root exudates relative to wild type bacteria (Dekkers *et al.*, 1998). Furthermore, another mutant, with a shorter O-antigen chain, was identified which showed unaltered growth in these *in vitro* conditions yet displayed defective colonization on tomato roots (Dekkers *et al.*, 1998). In contrast, the *oafA* mutants described in the present study showed better rather than worse root colonization. We found that spontaneous mutant *oafA-1* has unaltered *in vitro* growth potential compared to the CHA0 wild type across several tested growth conditions, and enhanced colonization capacity in the rhizosphere which was particularly obvious when it was competing directly with the wild type progenitor. Previously it was shown that disruption of the *OBC3*-encoded *GDP-L-fucose synthase*, led to a complete loss of long O-antigen on the LPS but this, in turn, did not affect root colonization which was comparable to the wild type (Kupferschmied *et al.*, 2016). From these and our results, we speculate that not only O-antigen integrity, but also its composition can affect bacterial root competence. The O-antigenic portion of the LPS can vary considerably within one bacterial strain as a result of the incorporation of different types and numbers of repeating units, specifically sugar moieties, along the polysaccharide chain. Auxiliary modifications such as acetylation and methylation lead to further intra-organism diversity (Lerouge & Vanderleyden, 2001), and as a result the LPS of a single bacterium can be highly heterogenous.

OafA-CHA0 is an AT3-SGNH fused protein

Unlike some other root-associated pseudomonads, CHA0 lacks the classical Common Polysaccharide Antigen (CPA) O-antigen biosynthesis gene cluster and contains a markedly reduced O-Specific Antigen (OSA) cluster (Lam *et al.*, 2011; Kupferschmied *et al.*, 2016). Instead, it encodes alternative O-antigen biosynthesis gene clusters, i.e., *OBC1* and *OBC3*, predicted to contribute to ABC-transporter-dependent biosynthesis of polysaccharides, and *OBC2*, containing genes for the biosynthesis of polysaccharides through a Wzx/Wzy-dependent pathway (Kupferschmied *et al.*, 2016). Partial deletion of the *OBC3* gene cluster, including deletion of *RS09880* but not *oafA* or *galE*, resulted in an O-antigen defective CHA0 mutant (Kupferschmied *et al.*, 2016). Comparison of OafA-CHA0 with well-studied O-antigen acetyltransferase proteins revealed its notable similarity to OafA-S.Tym (Fig. 1d), which, like OafA-CHA0, is composed of an AT3-SGNH fused domain architecture, and it was recently demonstrated that the OafA-S.Tym SGNH domain is necessary for the acetylation of O-antigen (Pearson *et al.*, 2020). As OafA-CHA0 is also an AT3-SGNH fused protein and both *oafA* mutants encode a premature stop in between the regions encoding the AT3 and SGNH domains, we speculate that these mutations convert OafA-CHA0

into an AT3-only protein which could potentially still act to acetylate the O-antigen at atypical moieties or even alternative substrates altogether (Fig. 1c).

LPS O-antigen modification alters bacterial attachment *in vitro* and *in vivo*

Diverse representations of the O-antigen are likely to affect various aspects of bacterial physiology and behavior mediated by environmental factors or via interactions with host organisms such as plants. Proteomics analysis of *Pseudomonas aeruginosa* attached to glass wool fibers revealed profound changes in the bacterial cell envelope, including over-accumulation of outer membrane proteins, periplasmic folding proteins and O-antigen chain length regulators (Crouzet *et al.*, 2017). In the present study, altered bacteria-host interaction through O-antigen decoration changes was demonstrated that is likely driven by faster root attachment (Fig. 11, S3). As a prerequisite for microbial colonization; root attachment anchors bacteria in the nutrient-rich environment of the plant rhizosphere, securing a prime location for the subsequent development of more intimate associations (Knights *et al.*, 2021). The importance of root attachment and the role of LPS is further exemplified by observations in *Azospirillum brasilense* and *Herbaspirillum seropedicae*. In these species, altered LPS composition, mediated by disruption of dTDP-rhamnose biosynthesis, resulted in impaired attachment to maize roots and consequently reduced root colonization (Jofré *et al.*, 2004; Balsanelli *et al.*, 2010, 2013). Rhamnose is an important constituent of LPS and disruption of rhamnose biosynthesis genes results in a modified LPS core structure and atypical colony morphology (Jofré *et al.*, 2004). Interestingly, the LPS mutant of *H. seropedicae*, which lacks the central monosaccharide rhamnose in the O-antigen chain, displayed reduced maize root attachment while displaying unaltered attachment on a glass fiber matrix (Balsanelli *et al.*, 2010). In addition, Mitra and coworkers reported that an *rffB* mutant of *Rhizobium sp.* IRBG74 with defects in the rhamnose-containing O-antigen had diminished rice root attachment and colonization, but not impaired attachment on polypropylene plates (Mitra *et al.*, 2016). These observations indicate that LPS or its constituents in these organisms are not required for general surface attachment, but that they do play a critical role in the attachment to the plant surface.

LPS attachment also alters bacteria-bacteria interactions. For example, contrasting outcomes of the interaction between *Acinetobacter sp.* C6 and *Pseudomonas putida* KT2440 in a biofilm flow chamber were shown to be directly correlated to the LPS structure of KT2440 (Hansen *et al.*, 2007b,a). In the absence of an O-antigen side chain on its LPS, specifically, KT2440 suppressed the growth of C6 while such suppression was not observed with intact LPS. In the present study, we observed that root colonization by a mixture of wild type and *oafA-1* mutant cells tended to yield a smaller bacterial population when compared to singular application (Fig. 5, 9). This suggests that bacteria-bacteria interactions between both genotypes might also play

a role during root colonization in our experiments. This competitive relation was noticeable (Table 1), but not significant under the tested *in vitro* conditions (Fig. S1).

OBC3 mutants have altered secondary root attachment

A common biphasic root attachment mechanism consists of two phases: primary attachment, characterized by reversible binding of bacteria to the root surface, followed by secondary attachment which results in their irreversible adhesion. The specific root attachment stage at which *oafA* and other *OBC3* mutations are preferentially selected is yet to be revealed. We conducted our root attachment assay over a relatively short time period, i.e., no longer than 2.5 hours, which was previously suggested to be representative of primary root attachment (Carroll *et al.*, 2020). Yet, we did include a washing step in the attachment assay, therewith specifically enriching for cells that are stably attached to the plant root. Thus, we speculate that *OBC3* mutations altered, at least in part, also secondary root attachment.

Bacterial motility and chemotaxis are defined by the movement towards the root and bacterial adhesion to the root depends on the efficiency of attachment. As the *oafA* mutants do not display altered growth or motility (**Chapter 2**), yet still outcompete the CHA0 wild type after mixed application, we believe that the increased root attachment by these mutants is the main driver of their selection in the evolutionary experiment. Currently it is not clear whether *oafA*-mediated modifications in CHA0 O-antigen play a significant role during later proliferation phases on the root, but we hypothesize that the increased initial attachment ability might be sufficient for *oafA* mutants to fully outcompete the wild type. In a competitive environment, faster root attachment enables *oafA* mutants to quickly occupy the nutrient-rich niche at the site of inoculation and spread into available sites more rapidly. Due to the significant plant growth inhibition from wild type and mutant colonization, we could not test above-mentioned assumptions, as we didn't observe extinction of the wild type in the current experimental setup that only lasted one week. Future research on the *OBC3* mutants should focus on competitive root and surface attachment, revealing the relative role and advantage of said mutants in biofilm formation and biofilm matrix development on biotic and abiotic surfaces. It will further aid our understanding of the biological function of O-antigen diversity and heterogeneity of CHA0. Such knowledge would benefit the application of beneficial *Pseudomonas* spp. in agriculture as fast and efficient colonization of plant roots is imperative to attain their plant-beneficial functions.

Acknowledgments

This work was supported by China Scholarship Council fellowships (to H.Z. and E.L.). We thank Hans van Pelt for taking photographs. We also thank Peter Veenhuizen

from the Ecology and Biodiversity group at Utrecht University for providing support with the operation of the microplate reader and flow cytometer.

Materials and methods

Bacterial colonization in rhizosphere

Seed sterilization and plant seedling growth conditions

Arabidopsis Col-0 seeds were surface sterilized by exposure to chlorine gas for 3.5 h in a jar. The gas was formed upon mixing 100 ml bleach with 3.2 ml hydrochloric acid fuming (37%) (Van Wees *et al.*, 2013). Sterilized seeds were then sown on modified Hoagland medium containing 3 mM KNO_3, 0.5 mM $MgSO_4$, 1.5 mM $CaCl_2$, 1.5 mM K_2SO_4, 1.5 mM NaH_2PO_4, 25 μM H_3BO_3, 1 μM $MnSO_4$, 0.5 mM $ZnSO_4$, 0.05 μM $(NH_4)_6Mo_7O_{24}$, 0.3 mM $CuSO_4$, 0.05% 2-ethanesulfonic acid (MES; Duchefa Biochemie, Haarlem, the Netherlands), 50 μM FeNaEDTA and 1% plant agar (Duchefa Biochemie) (Li *et al.*, 2021a). Before autoclaving, potassium hydroxide was used to adjust the pH of the medium to 5.8. After sowing, seeds were stratified at 4 ºC in the dark for 2 days. After stratification, we transferred and placed the plates in a vertical position in a growth chamber (21 ºC; light intensity 100 μmol/($m^2 \cdot s$)) for a 10-hour light/14-hour dark daily regime (Millet *et al.*, 2010).

Bacterial strains preparation

In the previous evolutionary experiment (**Chapter 2**) (Li *et al.*, 2021a), we used *P. protegens* CHA0 as the ancestral strain (Ramette *et al.*, 2011), which was chromosomally tagged with GFP and a kanamycin resistance cassette to enable specific tracking of the strain and detection of contaminations (Jousset *et al.*, 2006). In the present study, we cultured the same CHA0-derived, tagged ancestral strain (further denoted as the wild type) and evolved mutant strains on King's medium B (KB) agar plates in a 28 ºC incubator (King *et al.*, 1954), prior to the experiment. After 24 h of growth, a single colony of each strain from the KB plate was separately collected and transferred to 15 ml KB liquid medium in a 50-ml tube. Then, we put the tubes in a shaking incubator with 225 revolutions per minute (rpm) at 28 ºC. After 18 h of growth, cells were collected in 10 mM $MgSO_4$, and washed twice through centrifugation for 10 min at 3000 rpm. The washing eliminates any carry-over nutrient supplementation in the media. The washed bacterial pellet was resuspended in 10 mM $MgSO_4$ and adjusted to a final density of OD_{600} equal to 0.1 (corresponding to $8 \cdot 10^7$ colony-forming units (cfu) per ml) for subsequent use.

Root colonization assay

Bacterial root colonization assays were performed under similar conditions and on similar media as described for Arabidopsis seedling growth. We cooled the medium to a temperature near solidification point (around 40-45 ºC) then poured it into square 15-cm square plates and allowed agar to solidify, after which selected, uniformly sized 12-day-old (12D) or 18-day-old (18D) seedlings were transplanted onto them in one row with equal spacing. The prepared bacterial suspension was then inoculated on the root-shoot junction of each plant by applying 10 µl of 10^7 cfu/ml. For the mock treatment we used 10 µl of 10 mM $MgSO_4$ instead. Following bacterial inoculation on Arabidopsis seedlings, we stored an aliquot of the WT/*oafA-1* inoculum in the freezer for verification of the initial *oafA-1* frequency at a later time. To assess bacterial root colonization, we collected plant roots after 3 days and after 7 days. Before collection, we also recorded the plant phenotypes by photographing and measuring shoot and root weight.

Collected root samples were weighed in a sterilized 2-ml Eppendorf tube with glass beads, after which 1 ml of 10 mM $MgSO_4$ was added. We used a TissueLyser II (Qiagen, US, Cat. No. / ID: 85300) to wash of, and resuspend bacteria from the samples. The TissueLyser II was programmed for 2 cycles of 30 seconds with a frequency of 28 cycles per second. Following sample resuspension, we used a flow cytometer C6 (BD Accuri™ C6 Plus, thresholds for FSC:2000, SSC: 8000) to count the active fluorescence units (AFUs) per sample using GFP fluorescence as a proxy for the number of bacterial cells (Li *et al.*, 2021a). To verify the quality of bacterial density results using flow cytometer, we compared AFUs numbers with counts of bacterial colony forming units (CFUs) on KB agar. We plated serial dilutions (10x, 100x, 1000x, 10000x dilutions) for each collected sample with five technical replicates. After overnight incubation at 28 ºC, CFUs were determined by counting the number of colonies. Both methods yielded similar results.

Root attachment assay

A. thaliana Col-0 seeds were sown on modified Hoagland medium plates as described before, but this time with 1% sucrose to achieve better growing, uniform plants. Following stratification, plants were grown for 10 days under the before-described Arabidopsis growth conditions. For root attachment assays, six-well plates were prepared by filling them with 1 ml of the relevant bacterial suspension at a final density of 10^7 cfu/ml. Then, three 10-day-old (10D) seedlings were gently removed from the Hoagland agar plates and immerged in the bacterial suspension in each of the wells of the six-well plates. We included 3 replicate wells for each bacterial treatment. After 0.5 hour and 2.5 hours of co-incubation of plants and bacteria with gentle vertical shaking (Speed 5, BioDancer, New Brunswick Scientific Co. INC®, at room temperature), we replaced the bacterial suspension with 1 ml of 10 mM $MgSO_4$

followed by 10 minutes of gentle shaking at the same speed. This washing step was performed twice to remove non-stably attached bacterial cells on the roots. Finally, stably attached bacteria were washed off the roots using a TissueLyser II at a frequency of 28 Hz per second for 1 min (1680 oscillations/minute), serially diluted in 10 mM $MgSO_4$ and plated on KB plates for CFU counting as described before.

Relative quantification of the *oafA-1* mutant frequency using HRM profile analysis

We used high-resolution melting (HRM) curve profile a nalysis w ith i ntegrated LunaProbes to quantify the *oafA-1* mutant frequency in mixed populations of wild type and *oafA-1* mutant cells (Lee *et al.*, 2011; Capper *et al.*, 2015; Zhong *et al.*, 2016).

Primers and probe design

The primers and probe used in this study are listed in Table S3. Primers were designed using the program Primer3. The probe was designed with the *oafA-1* single-nucleotide polymorphism (c.1005C>A) located in the center of the sequence, and the 3′ end was blocked by carbon spacer C3, which prohibits polymerase extension and prevents exonuclease-dependent oligo cleavage.

Pre-PCR and frequency quantification

We set the primer asymmetry to 2:1 (excess primer: limiting primer) in all cases to obtain a surplus of single strand DNA in the target sequence, which hybridizes to the probe during the next steps in the PCR. The HRM pre-PCR was performed in a 10-µl reaction that included 0.25 µM excess primer, 0.125 µM limiting primer, 0.25 µM probe, 0.5 µl bacterial sample (for cell suspensions used during the inoculation with OD_{600} estimated above 0.01; for root bacterial cell samples, the input was diluted 10-fold, and their OD_{600} differs among treatments), and 1× LightScanner Master Mix (BioFire Defense). Dimethyl sulfoxide (DMSO) was added to all reactions at a final concentration of 5%. This ensures the target products are within the detection limit of the LightScanner (Idaho Technology Inc.). Milli-Q water (BioFire Defense) was used to raise the volume up to 10 µl. We used 96-well black microtiter plates with white wells to minimize background fluorescence (Bio-Rad, Hard-Shell® HSP9665). To prevent evaporation, we loaded 25 µl mineral oil into the each well containing a sample and sealed the plate with PCR sealing film before amplification. Thermocycling conditions are listed in Table 2.

Table 2 Thermocycling conditions for the HRM pre-PCR

Step	Temperature	Time
Initial Denaturation	95 °C	3 minutes
55 cycles		
Denaturation	95 °C	30 seconds
Annealing	60 °C	30 seconds
Extension	72 °C	30 seconds
Final Extension	72 °C	10 minutes
Hold	4 °C	

After amplification, samples were heated shortly to 90 °C for 30 s in a ThermalCycler (Bio-Rad) to denature all double-stranded structures. Then, we used rapid cooling to 25 °C for 30 s to facilitate successful hybridization between the probe and the target strand. After cooling down the plate, we transferred it to a LightScanner to heat up slowly. The LightScanner collects the melting profiles of each well by monitoring the continuous loss of fluorescence coming from denatured double-stranded DNA and bound probe. It is set to steadily increase the temperature from 35 °C to 97 °C with a ramp rate of 0.1 °C per second.

Calculation and analysis

The relative quantification of the *oafA*-1 mutant frequency was derived from the negative first derivative plots using MATLAB (MathWorks Software Inc.). The area-under-the-curve of the probe-target duplex melting peak was auto-calculated using the 'AutoFit Peaks I Residuals' function in the software PeakFit (SeaSolve Software Inc.). The mutant frequency X was subsequently calculated using the following formula:

$$X = \frac{\text{Area}_{\text{mutant}}}{\text{Area}_{\text{mutant}} + \text{Area}_{\text{wildtype}}}$$

To validate the RQ-HRM method for the *oafA-1* probe, we prepared standard curves by measuring wild type and mutant mixed samples with known proportions of the *oafA-1* mutant templates: 0, 10.00, 33.33, 50.00, 66.67, 90.00, and 100.00%. Measurements for each sample contain at least three replicates. The linear regression formula for each mutant relating actual frequency and measured frequency is shown in Fig. S2. The sufficiently high R^2 values, and close to 1 slope values of these equations, confirmed that the RQ-HRM method can accurately detect mutants' frequency in a mixed population. The RQ-HRM-determined frequencies were also quantified by shotgun sequencing data analysis (Table S4).

The absolute and relative increase of the *oafA-1* frequency was calculated using the following formulas:

$$\text{Absolute increase} = \text{Final frequency}_{oafA-1} - \text{Initial frequency}_{oafA-1}$$

$$\text{Relative increase} = \frac{\text{Final frequency}_{oafA-1} - \text{Initial frequency}_{oafA-1}}{\text{Initial Frequency}_{oafA-1}}$$

Supplementary information

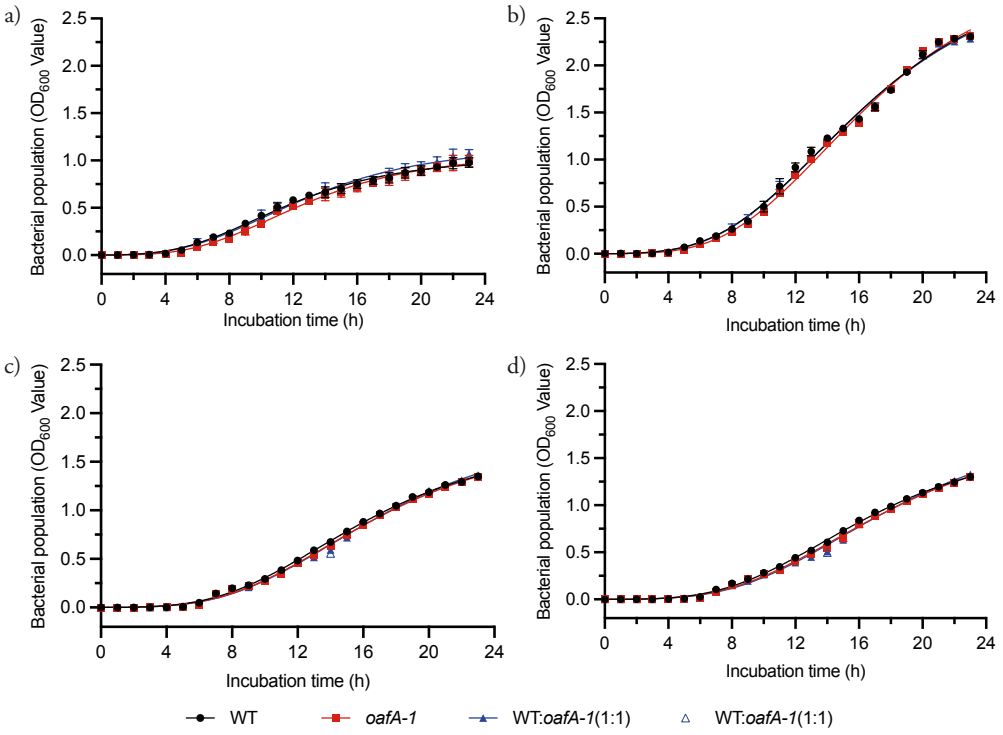

Figure S1 The *oafA-1* mutant and WT&*oafA-1* mix (1:1) have identical growth curves as that of wild type (WT) in four tested media.
The growth media are a) 1/10 strength KB medium, b) full strength KB medium, c) culture filtrates of wild type and d) culture filtrates of the *oafA-1*. Bacterial cell suspensions (10 µl of 10^7 cfu/ml) were mixed into 190 µl growth medium or culture filtrates in a 96 well plate (cell density OD_{600} equal to 0.005). The cell density was recorded every hour for 23 hours growth at 28 ºC. Solid black circles represent the wild type, solid red squares represent the *oafA-1* and solid blue triangles represent the WT/*oafA-1* (1:1) mixture (n=6 for each time point). Outlier values are shown as empty symbols correspondingly.

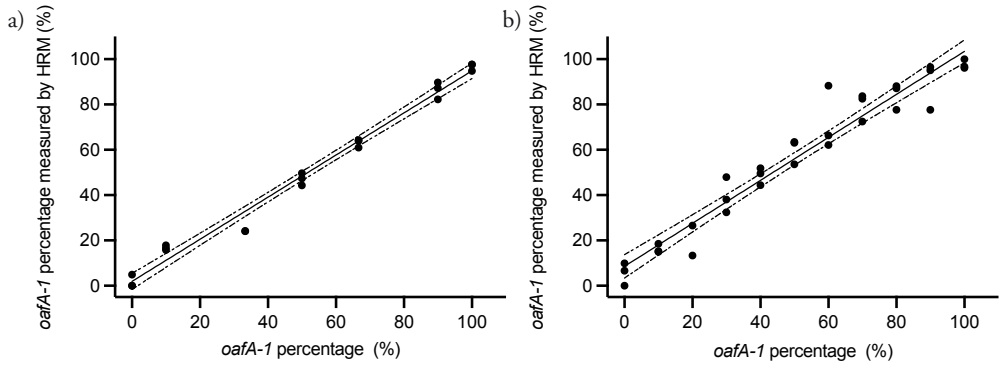

Figure S2 Standard curves for high resolution melting (HRM) curve analysis of *oafA-1*.
Graphs show the corresponding standard curves used in: a) The *oafA-1* frequency within wild type (WT)/ *oafA-1* (1:1) mixed samples from different growth medium and rhizosphere samples (Slope = 0.9294, R^2 = 0.9851, p < 0.0001). b) The *oafA-1* frequency within WT/*oafA-1* (8:2) mixed rhizosphere samples at 7 dpi on 12-day-old seedlings and 18-day-old seedlings (Slope = 0.9491, R^2 = 0.9439, p < 0.0001).

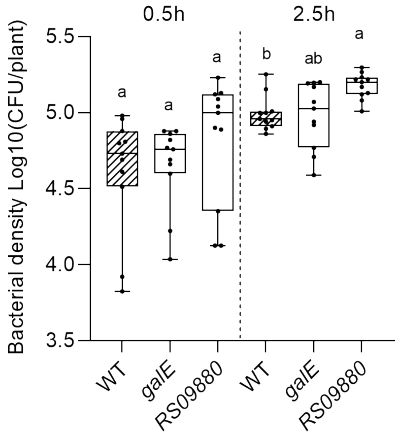

Figure S3 Disruption of *OBC3* gene *RS09880* also results in stronger bacterial adherence to Arabidopsis roots compared to wild type cells.
Ten-day-old seedlings were dipped in bacterial cell suspensions (1 ml of 10^7 cfu/ml) of the wild type, or of *galE* or *RS09880* mutants. Root-associated bacteria were plated for colony form unit (CFU) quantification after 0.5 hours and 2.5 hours. Statistical testing of each time point was carried out using one-way ANOVA followed by Tukey's multiple comparison test (α = 0.05; different lowercase letters indicate significant differences; n = 11)

Table S1 Bacterial root colonization of a wild type (WT)/*oafA-1* mixed inoculum (1:1 initial) shows a different correlation with plant root weight compared to mono-strain inoculation.
Linear regression parameters for the correlation between wild type (WT), the *oafA-1* mutant and a mixture of the two in 1:1 ratio bacterial population densities and plant root weight for 12-day-old seedlings at 7 dpi (8 <= n <= 11).

Treatments	Best-fit values (Simple linear regression)				Goodness of Fit		p value
	Slope	Y-intercept	X-intercept	1/slope	R squared	Sy.x	
WT	0.6545	6.533	-9.982	1.528	0.1963	0.1939	0.1723
oafA-1	0.2590	6.786	-26.20	3.861	0.07453	0.1373	0.4166
WT:*oafA-1* (1:1)	-0.1603	6.739	42.05	-6.240	0.05482	0.1387	0.5768

Table S2 Bacterial root colonization of a wild type (WT)/*oafA-1* mixed inoculum (8:2 initial) is not correlated with plant root weight for 12-day-old initial seedlings and 18-day-old initial seedlings
Linear regression parameters for the correlation between wild type (WT), the *oafA-1* mutant and the mixture of the two in 8:2 ratio bacterial population densities and plant root weight for 12-day-old initial seedlings and 18-day-old initial seedlings at 7 dpi (6 <= n <= 8).

Treatments	Best-fit values (Simple linear regression)				Goodness of Fit		p value
	Slope	Y-intercept	X-intercept	1/slope	R squared	Sy.x	
WT	0.9411	6.549	-6.959	1.063	0.9090	0.1125	0.0009
oafA-1	0.5843	6.794	-11.63	1.711	0.8849	0.1038	0.0005
WT: *oafA-1* (8:2)	0.02211	7.008	-317.0	45.22	0.007775	0.1155	0.8681

Table S3 Primers and probe used for the quantification of *oafA-1* frequency by HRM curve analysis

Oligo Name	Orientation	5' Modification	Seq (5'- 3')	3' Modification
113*oafA-1*	Forward	None	CGCACTGGTGATTTTTG-CAATG	None
	Reverse	None	CTGACAAGATGTGTGCAGGC	None
CHA0_wt_*oafA-1*	Forward	None	AACTTTCCGTTACG-CAAAAAAGCAAT	/3SpC3/

Table S4 Quantification of the *oafA* mutant frequency in different WT/*oafA-1* mixtures by metagenomic shotgun sequencing provides independent support for HRM curve analysis-based quantification.

The final *oafA-1* frequency of a wild type (WT)/*oafA-1* mixed inoculum from multiple experiments at the end of the experiments were quantified by metagenomic shotgun sequencing analysis (Seq.), and by high-resolution melting (HRM) curve analysis. The frequency of the *oafA-2* mutation could not be detected by HRM curve analysis due to the specific mutation and its flanking sequence. NA, not applicable. R1-R5 refer to biological replicate root microbial samples in each experiment.

Treatments	Methods	3dpi					7dpi				
		R1	R2	R3	R4	R5	R1	R2	R3	R4	R5
WT: *oafA-1*	Seq.	77%	69%	100%	80%	/	86%	83%	87%	100%	NA
(1:1)	HRM	69%	68%	71%	68%	/	74%	73%	72%	72%	74%
WT: *oafA-1*	Seq.	74%	NA	100%	54%	/	85%	81%	44%	76%	73%
(1:1)	HRM	66%	69%	73%	72%	/	67%	68%	68%	71%	71%
WT: *oafA-1*	Seq.	NA	45%	38%	/	/	11%	48%	50%	NA	/
(8:2)	HRM	33%	31%	26%	/	/	31%	45%	38%	32%	/
WT: *oafA-2*	Seq.	60%	50%	67%	100%	57%	59%	64%	40%	89%	/
(1:1)	HRM	NA	NA	NA	NA	NA	NA	NA	NA	NA	/

Figure legends mentioned references: (Pearson *et al.*, 2020; Li *et al.*, 2021a)

4

CHAPTER 4

OBC3-controlled lipopolysaccharide diversity in *Pseudomonas protegens*: a multifunctional toolbox

Hao Zhang[1], Jordan Vacheron[2], Jan P. M. Tommassen3, Clara M. Heiman[2], Christoph J. Keel[2], Corné M.J. Pieterse[1], Ronnie de Jonge[1,#]

[1]Plant-Microbe Interactions, Department of Biology, Science4Life, Utrecht University, Padualaan 8, 3584 CH, Utrecht, the Netherlands

[2]Department of Fundamental Microbiology, University of Lausanne, Lausanne, Switzerland

[3]Microbiology, Department of Biology, Science4Life, Utrecht University, Padualaan 8, 3584 CH, Utrecht, the Netherlands

Abstract

We previously characterized four experimentally evolved O-antigenic polysaccharide biosynthesis cluster 3 (*OBC3*) mutants of *Pseudomonas protegens* CHA0 (CHA0) which displayed enhanced rhizosphere competence via increased plant root attachment. In the present study, we characterized the distribution and conservation of the *OBC3* gene cluster among environmental strains of *P. protegens* spp., revealing similar *OBC3* mutants in several of them. Considering the occurrence of such mutations in the absence of plant hosts, we hypothesized that alternative sources of selection might be present in the environment. Besides its role in cell adhesion, bacterial cell envelop structures also represent important receptors for bacteriophage recognition and attachment. Bacteriophages are viruses that widely occur in any environment where their bacterial hosts are present. To cope with these viruses, bacteria evolved various mechanisms, one of which is preventing phage recognition through altering the cell surface-exposed lipopolysaccharide (LPS) structure. Genomic analysis reveals that the CHA0 genome encodes four predicted prophages, bacterial genome-integrated phage regions, one of which is located in the vicinity of the *OBC3* gene cluster and two are likely part of one larger phage. To evaluate a possible interaction between the *OBC3* mutations and phage susceptibility we assessed mutant sensitivity towards an environmental phage as well as to the prophages encoded by CHA0 itself by prophage activation experiments. Two out of four *OBC3* mutants, i.e., those in *OBC3* genes *galE*, and *RS09880*, showed significantly reduced sensitivity towards the environmental phage GP100. Mitomycin C-driven activation of CHA0 prophages did not indicate altered phage susceptibility in *oafA* mutants although lack of prophage activation cannot be excluded. Notably, GP100-resistant CHA0 mutants in *galE* and *RS09880* displayed a shortened or complete lack of the long O-antigenic side chain of the LPS, respectively, whereas the GP100-susceptible mutants in *oafA* displayed unaltered LPS thus confirming a correlation between the integrity of the LPS and phage susceptibility. Analysis of whole-genome shotgun sequencing data of evolved CHA0 populations and mixes of wildtype and mutant strains under plant-selective conditions did not indicate activation of any of the CHA0 prophages. In conclusion, we found that *OBC3* mutations are widespread in nature, and occasionally can contribute to resistance to environmental phages.

Author contributions:

H.Z. was responsible for experimental design, execution of the experiments, data analysis, and the writing of the manuscript. H.Z. and R.D.J. designed experiments; H.Z. performed experiments; J.V., C.M.H., and C.J.K. contributed to the design and execution of phage-plaque assays. J.P.M.T. contributed to the design of LPS extraction and visualization experiment and the analysis of the result; H.Z. and R.D.J. analyzed data; H.Z., C.M.J.P., and R.D.J. participated in content discussion and contributed to the final manuscript.

Introduction

Plants are surrounded by numerous microbes, and reversely, plant-associated microbes face selection pressure from their plant host. In nature, microbes also encounter other microbes and predators such as protists and viruses such as bacteriophages for bacteria. Consequently, microbes evolved countless adaptations depending on these various selection pressures, which in turn shaped their phenotypes and affected their interactions with plant hosts. Bacteriophages, also known as phages in short, are ubiquitous and highly abundant. There are over 100 million phage species and about 10^{31} phage particles estimated to be present in the biosphere (Rohwer, 2003; McNair *et al.*, 2012; Rohwer & Segall, 2015). Phages impact on bacterial populations in several ways, including predation and alteration of bacterial phenotype by genetic interactions. The corresponding phage behaviors are represented by the phage lytic cycle, in which phages directly kill and solubilize host bacteria, and the phage lysogenic cycle which embodies the integration of the phage genome into the bacterial host genome or they exist as plasmids inside host cells. Both types of phages shape the composition, ecological function and evolution of bacterial communities in nature (De Smet *et al.*, 2017; Chevallereau *et al.*, 2022), therefore, phages play a crucial role in maintaining bacterial diversity in the environment. The classical Kill-the-Winner (KtW) model of Thingstad (Thingstad, 2000) states that virulent phage infection hinders the continuous increase of the population of a high abundant bacterial species in a microbial community, resulting in a decrease in the population of this species. Evidence shows that phages prevent one species from dominating the environment by modulating bacterial population dynamics (Weinbauer & Rassoulzadegan, 2004; Rodriguez-Valera *et al.*, 2009; Maslov & Sneppen, 2017). This has been demonstrated in several *in vitro* experiments that study the coevolution of bacteria and phages (Gómez & Buckling, 2011; Scanlan, 2017). In addition, phages can transfer genes horizontally to their bacterial hosts, which can enhance the host's ability to withstand infection by other phages (Menouni *et al.*, 2015; Koskella & Taylor, 2018; Ramisetty & Sudhakari, 2019) and/or increase the bacterial host's virulence (Evans *et al.*, 2010b; Davies *et al.*, 2016). Phages can also affect bacterial populations through their lytic cycle, although this occurs at a low rate in the case of endogenous or temperate phages (Nanda *et al.*, 2015). Prophage induction, - activation of the lytic cycle of temperate phages -, is typically associated with the detection of host bacterial cell's DNA damage. Severely damaged DNA, sensed by RecA, initiates the SOS response, including autocleavage of SOS repressor genes like *lexA*, and result in de-repression of prophage genes (Craig & Roberts, 1980; Waldor & Friedman, 2005; Asadulghani *et al.*, 2009; Kaushik *et al.*, 2022). DNA damage may occur due to antimicrobial actions, such as UV light, extreme pH environment and starvation, and other external cues like presence of acyl-homoserine lactones (AHLs), quorum sensing signaling

molecules (Little, 2014; Feiner *et al.*, 2015; Howard-Varona *et al.*, 2017; Liang *et al.*, 2020). Overall, phages play a key role in shaping the dynamics and structure of microbial communities through their influence on bacterial populations (Bossi *et al.*, 2003; Koskella & Brockhurst, 2014; Nanda *et al.*, 2015; Fernández *et al.*, 2018; Koskella & Taylor, 2018; Naureen *et al.*, 2020).

For phage infection to occur, phages must adsorb to the bacterial cell surface by binding to phage receptors, and injecting their genome. Phage receptors typically refer to bacterial structures that phages could dock on to, including peptidoglycan and teichoic acids of the gram-positive cell wall, and glycolipid moieties and lipopolysaccharide (LPS) of the gram-negative cell wall, or a wide array of integral membrane proteins and appendages, such as pili and flagella (De Smet *et al.*, 2017; Gordillo Altamirano & Barr, 2021). To prevent phage's adsorption, bacteria evolve to alter or disguise receptors through surface modification, for instance, LPS modification in gram-negative bacteria. LPS is an outer-membrane structure of gram-negative bacteria, which displays a high intra-organism diversity, and O-antigen polysaccharide, one of three components of LPS, contributes the most to LPS diversity (Knirel & Valvano, 2011; Knirel *et al.*, 2015). Kulikov *et al.* conducted experiments examining a panel of *Escherichia coli* strain 4 s mutants, with deficiencies for O-antigen modification, O-antigen biosynthesis or core-oligosaccharide biosynthesis, for their susceptibility towards different bacteriophages. This analysis demonstrated that the bacterial O-antigen structure mediates resistance towards bacteriophages (Kulikov *et al.*, 2019). O-antigen variation can be observed at multiple levels, including large variation by length, or small modifications by incorporation of glucosyl or fucosyl residues-type sugar moieties, or with non-carbohydrate substituents, like the addition of acetyl and methyl groups (Lerouge & Vanderleyden, 2001). Some of these modifications are regulated by prophage genes. For instance, prophage *SfX* in *Shigella flexneri* encodes several genes that affect bacterial host O-antigen glucosylation (Guan *et al.*, 1999). Similarly, *Pseudomonas aeruginosa* was reported to gain resistance towards environmental phages through prophage-mediated defenses, including O-antigen modification (Bondy-Denomy *et al.*, 2016). The high abundance of bacteriophages in the environment, combined with the function of O-antigen as a receptor for these phages, supports the idea that the O-antigen has adaptive significance (Lam *et al.*, 2011; Knirel *et al.*, 2015; Bertani & Ruiz, 2018).

Bacteria can adapt to their host environment in various ways, but these adaptations may not always align with their ability to resist phages. In fact, trade-offs between these adaptations are often observed. For example, bacterial motility and phage resistance may be inversely related, as increased motility can come at the expense of phage resistance (Koskella *et al.*, 2011). Similarly, bacterial virulence and phage resistance

may also be negatively correlated, with increased virulence potentially compromising the ability of bacteria to resist phages (Evans *et al.*, 2010a; Kupferschmied *et al.*, 2016). In *P. protegens*, O-antigen biosynthesis gene clusters (*OBCs*) have been shown to contribute to virulence with regards to their insecticidal activities. It was further hypothesized that these *OBCs* were acquired through horizontal gene transfer (Kupferschmied *et al.*, 2016).

We previously described four *P. protegens* CHA0 (CHA0) mutants that originated from an *in vivo* evolution experiment, with mutations located in three O-antigenic polysaccharide biosynthesis-related genes, i.e., *oafA* (twice), *galE* and *RS09880* (Li *et al.*, 2021a,b). All four mutations reside in the O-antigenic polysaccharide biosynthesis cluster 3 (*OBC3*), which is involved with the biosynthesis of O-antigen polysaccharide (**Chapter 2**) (Kupferschmied *et al.*, 2016). The four mutants were each identified in independent biological replicates suggesting that evolution in the analyzed environment was reproducible, likely due to strong natural selection (**Chapter 2**). To identify the critical selective forces operating in this environment, comprised of CHA0 bacteria on *Arabidopsis thaliana* (Arabidopsis) roots in the absence of other microorganisms, we previously characterized these *OBC3* mutants with regards to plant root adaptive traits such as growth on plant root exudates, plant root adherence, and bacterial motility (**Chapter 2**). We concluded that especially root adherence plays an important role in the selection of these mutants. However, we could not exclude the possibility that also phages could play a role, especially given the nature of the mutations. In this study, the distribution of the *OBC3* gene cluster within multiple strains of *P. protegens* was investigated, as well as the potential trade-offs between the gained fitness of *OBC3* mutants and their sensitivity towards phages. Additionally, the study aimed to determine whether the selection of *OBC3* mutants in the evolution experiment was due to the presence of phages. The results of this study may provide insight into the evolutionary processes and mechanisms underlying the adaptation of *P. protegens* to its environment and the role of phages in shaping its evolution.

Results

Spontaneous mutations in *oafA* are observed among naturally occurring *P. protegens* strains

P. protegens CHA0 *oafA* encodes a two-domain protein (CHA0-OafA) consisting of an N-terminal, transmembrane-localized acetyltransferase-3 domain (AT3) and a C-terminal, periplastic SGNH hydrolase domain (SGNH). Based on the conserved domain topology and overall sequence similarity, we previously hypothesized that CHA0-OafA, like *Salmonella enterica* subspecies *enterica* serovar Typhimurium (S. Typhimurium) OafA (OafA-S.Tym) encodes a single protein, two domain AT3-SGNH

O-antigen acetyltransferase. OafA-S.Tym is involved in the acetylation of the O-antigen via the consecutive activity of the AT3 domain, i.e., transfer of an acetyl moiety across the cell membrane and onto the SGNH domain, and the SGNH domain, i.e., attachment of the acetyl moiety to the respective O-antigen target (**Chapter 3**)(Pearson *et al.*, 2020). Both spontaneous *oafA* mutations that arose during adaptation to the Arabidopsis rhizosphere are found in between the regions encoding the AT3 and SGNH domain, and resulted in a premature stop. We hypothesized that, as a result, the SGNH domain is no longer active and only the AT3 domain may be active (**Chapter 3**).

AT3-only acetyltransferases are not uncommon, but their distribution within *P. protegens* is unknown (Pearson *et al.*, 2020). Therefore, we examined both the distribution and domain architecture of *oafA* homologs among publicly available *P. protegens* genomes by BLASTp (protein query to protein database) and tBLASTn (protein query to genome database) analysis (%identity ≥ 40%, %coverage ≥ 30%), and CD-search using the conserved domain database (CDD), respectively. Among 71 *P. protegens* genomes (including CHA0) available through the NCBI Genomes database (November 2021), 52 lack an *oafA* gene copy, 14 genomes encode a full-length copy of the *oafA* gene and 5 encode a AT3-only OafA protein (Fig. 1a, b). *P. protegens* strains carrying *oafA* are distributed along the tree, indicatives of frequent gains or losses of this gene. The tBLASTn analysis, in addition to identifying these AT3-only OafA proteins, identified significant similarity to the CHA0-OafA SGNH domain downstream of the AT3 sequence in these AT3-only protein-coding genes. Alignment of this region revealed its high conservation, both at the nucleotide and at the protein level. Surprisingly, all five strains encoding this truncated *oafA* gene, 1B1, H78, UMG3145, BIGb0404, JUb28, carry, in addition to several other mutations, a thymine (T) insertion at position 1,083 in the open reading frame (ORF), yielding a premature stop, splitting the AT3 domain from the SGNH domain (Fig. 2). The genome-predicted ORF in these strains is accordingly annotated as a pseudogene in the NCBI Genomes database. These five *P. protegens* strains were isolated from diverse locations and years (Table S1), but are phylogenetically closely related (Fig. 1). These observations indicate that this shared mutation was present in the last common ancestor of these strains and must have originated at least 15 years ago (the age of the oldest of these five strains), and persisted for another 6 years. Conservation of the C-terminal SGNH sequence as observed across these years suggests that it might be under stabilizing selection and consequently might still be active. In addition to the naturally occurring *oafA* mutations that split the domains of AT3-SGNH, the same type of mutation was also identified in CHA0 *oafA* mutants from the evolution experiment (Fig. 1) (**Chapter 3**). The presence of these diverse *oafA* mutations suggests that the disruption of the AT3-SGNH fusion may have a general benefit for bacterial fitness beyond the previously described root attachment-enhancement (**Chapter 3**).

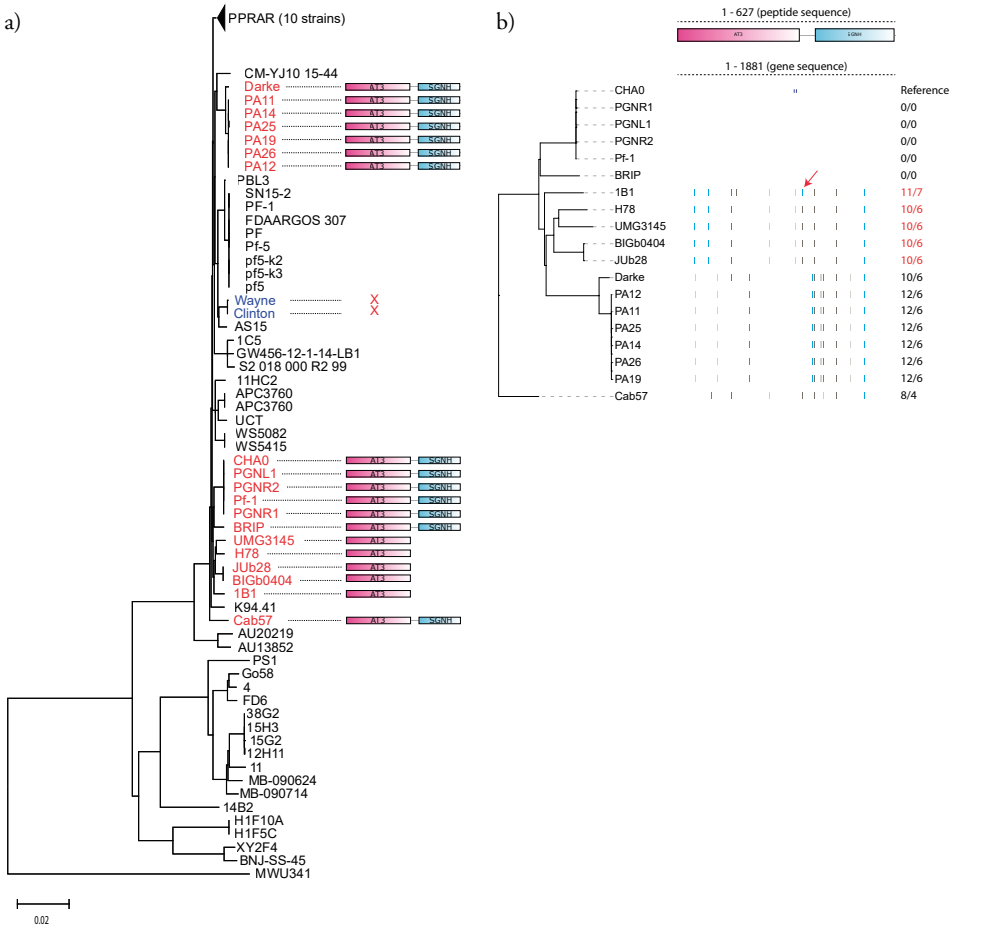

Figure 1 Spontaneous mutations in *oafA* are observed in naturally occurring *P. protegens* strains.
a) Spontaneous mutations in *oafA* homologs of eighteen *P. protegens* strains. The phylogenetic tree, represented by the cladogram, is built by Phylip from Mash-derived genome-to-genome pair-wise distances (Ondov *et al.*, 2016). The mutations in each line are indicated by vertical lines and their total number are demonstrated on the right side (total number/ number of mutations that alter the peptide sequence). Both mutations in CHA0-*oafA* (blue vertical lines , reference line) yield a premature stop codon, splitting the AT3 domain from the SGNH domain. Five strains (red labels on the right) contain a thymine (T) insertion at position 1,083 disrupting the open reading frame (blue vertical line, pointed out by the red arrow), which also yields a premature stop, separating both domains. The predicted ORF in these strains is simultaneously annotated as a pseudogene in the NCBI GenBank repository. b) The distribution and variation of *oafA* homologs among 71 *P. protegens* genomes. CHA0-OafA contains two domains, an N-terminal, transmembrane-localized acetyltransferase-3 domain (AT3, red background label) and a C-terminal, periplastic SGNH hydrolase domain (SGNH, blue background label) (Top panel). *P. protegens* Wayne and Clinton strains (blue label) don't contain the *oafA* gene, yet do contain remnants of the *OBC3* gene cluster. Nineteen strains (red labels), including *P. protegens* CHA0, contain *oafA*. All strains were collected from natural environments and genome sequence data were obtained from NCBI GenBank. The phylogenetic tree, represented by a cladogram, is built by Phylip from Mash-derived genome-to-genome pair-wise distances like in (a) (Ondov *et al.*, 2016).

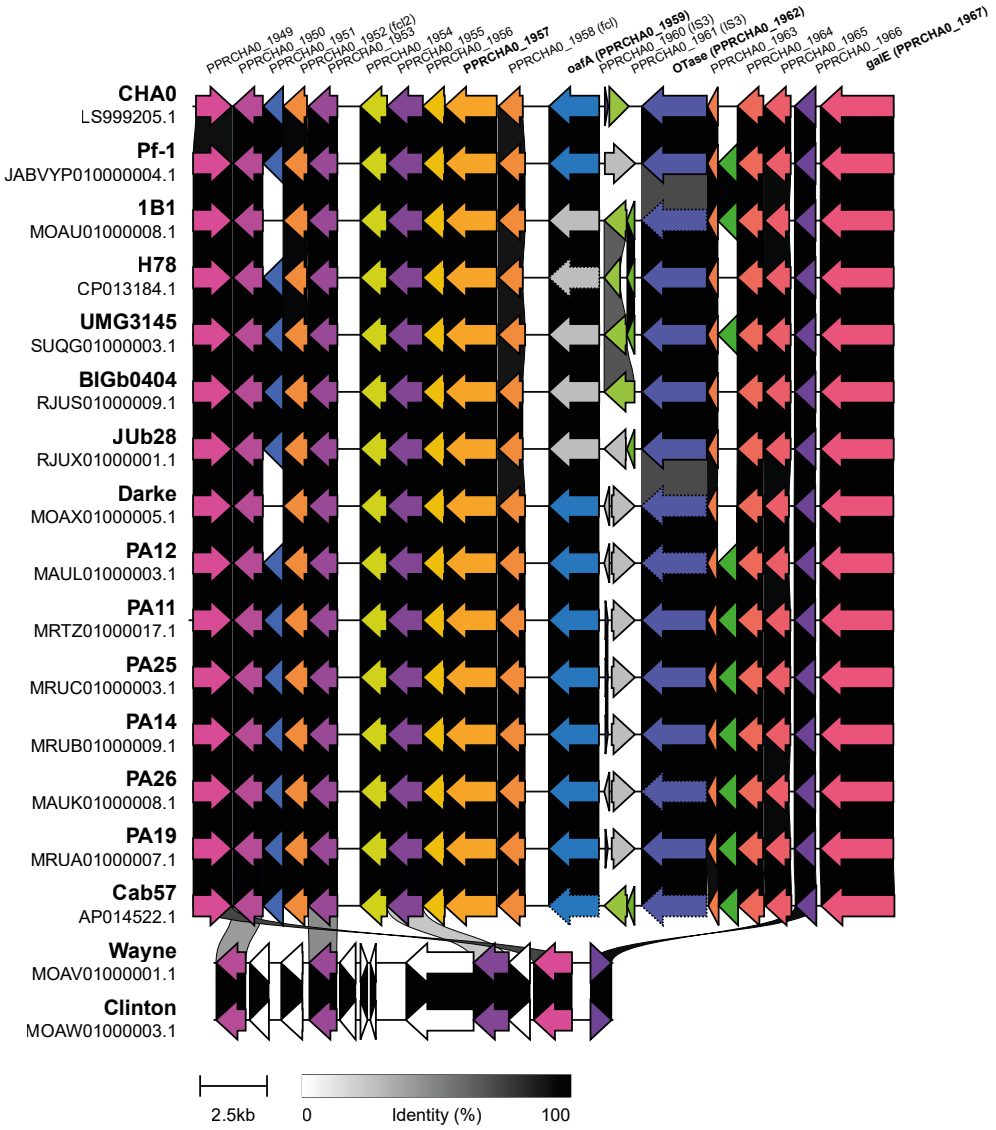

Figure 2 Variations of the *OBC3* gene cluster in diverse *P. protegens* strains.
Alignment of the complete *P. protegens* CHA0 *OBC3* gene cluster (on the top, from 5' to 3' direction, left = Guanylyl transferase, right = *galE*) with the genomic regions of *P. protegens* Pf-1, 1B1, H78, UMG3145, BIGb0404, JUb28, Darke, PA12, PA11, PA25, PA14, PA26, PA19, Cab57, Wayne and Clinton (top to bottom) using protein-to-protein BLASTp analysis. Homologous genes are indicated with a similar color. The percentage identity of homologous proteins between strains are indicated by the white (0%) to black (100%) gradient. *P. protegens* strains Wayne and Clinton contain a few *OBC3* genes, possible remnants of evolution. Rearrangements of the *IS3* transposase region involving PPRCHA0_1960 and PPRCHA0_1961 were identified among several strains highlighted by the green and grey arrows in oppositive orientation. Dash-outlined arrows indicate manual annotation of a gene, and grey highlighting indicates pseudogenes. All strains were collected from natural environments and genome sequence data were obtained from NCBI GenBank.

Concurrent mutation of *OBC3* genes among environmental *P. protegens* isolates

In addition to the *oafA* mutants, several other CHA0 mutants were identified from the evolution experiment in the Arabidopsis rhizosphere. These mutants include two that carried mutations in genes nearby *oafA*, i.e., in *galE*, encoding a UDP-glucose 4-epimerase, and in *PPRCHA0_1957* (alternative ids: RS09880|PPRCHA0_RS10110), encoding a putative glycosyltransferase (**Chapter 2**). Together with *oafA*, these genes are part of the same gene cluster, known as the O-antigenic polysaccharide biosynthesis cluster 3 (*OBC3*) (Li *et al.*, 2021a). This gene cluster is named after its role in the biosynthesis of O-antigen polysaccharide (one of three structural components of LPS) and it is present in several *P. protegens* strains that are closely related to CHA0, i.e., BRIP, PGNR1, Cab57 and *Pseudomonas* sp. CMR5c (Kupferschmied *et al.*, 2016).

Given the occurrence of natural *oafA* mutants, we wondered whether *P. protegens* strains that contain the *OBC3* gene cluster carry additional mutations that could explain said mutations. Therefore, we aligned the sequence of the CHA0 *OBC3* genomic region by BLASTn (Altschul & Koonin, 1998) against a subset of the genome sequences of the *P. protegens* strains previously noted as available via the NCBI non-redundant (nr) database (Fig. S1). This analysis confirmed the presence of a frame-shifting mutation in *oafA* in all five natural *oafA* mutant strains (Fig. 2, Fig. S1). In addition, it highlights the lack of alignment in the region directly upstream *oafA* encoding a IS3 transposase. In the same set of *P. protegens* strains, a high number of mutations were observed in another upstream region, encoding a putative oligosaccharyltransferase (Otase) (Kupferschmied *et al.*, 2016). OTases are enzymes that play a crucial role in glycoprotein biosynthesis, as they are required for the final glycosylation step in the synthesis of these proteins. This step involves the transfer of pre-assembled glycan chains onto lipid carriers, which are then transferred onto protein acceptors to form the final glycoprotein structure (Hug & Feldman, 2011). Glycoproteins are frequent mediators of interactions between bacterial cells and their environment (Ristl *et al.*, 2015). The presence of these mutations in the *otase* gene may affect the ability of the bacteria to produce functional glycoproteins, which could have implications for their fitness and virulence.

Notably, both type of alterations, lack of alignment in the *IS3 transposase* region, and a high number of mutations in *otase*, are only observed in bacterial isolates with a disrupted *oafA* open reading frame (Fig. S1). Thus, there might be a connection between the loss or the activity of the *IS3* transposase gene, and mutations in the *oafA* and *otase* genes. Hug & Feldman reviewed and proposed evolutionary connections between bacterial O-antigen synthesis and bacterial protein glycosylation pathways through analysis of shared homologous components (Hug & Feldman, 2011). One

example involves two closely related ATP-binding cassette transporters (ABC transporters) which participate in the general N-glycosylation system in *Campylobacter jejuni* and LPS biosynthesis in *Helicobacter pylori* (Hug & Feldman, 2011). Although the region encoding the putative Otase in strains 1B1, H78, BIGb0404, JUb28 and UMG3145 is riddled with mutations when compared to the CHA0 (Fig. S1), analysis of the predicted genes in their respective genomic regions revealed the encoding of a full-length Otase with similar length to the CHA0 Otase in all of them (Fig. 2). On average the Otase of these strains are 76% similar to CHA0 Otase on the nucleotide and on the amino acid level, which is considerably lower than that of the similarity of the other *OBC3* gene cluster genes, signifying accelerated evolution of this genomic region (Fig. S1; Fig. 2). As both OafA and Otase potentially alter the bacterial cell surface structure, the observed mutations likely contribute to adaptation to the environment.

The *OBC3* gene cluster is located in the vicinity of a *P. protegens* CHA0 prophage

In addition to its role in bacterial surface attachment, LPS, and particularly the O-antigen polysaccharide chain, also plays a critical role in bacteria-virus interactions. The O-antigen polysaccharide chain can be decorated with a variety of different sugars, proteins, and other molecules, which can affect the ability of bacteriophages (viruses that infect bacteria) to recognize and attach to the bacterial cell. By modulating the decoration of its LPS, a bacterium may be able to avoid recognition by bacteriophages and increase its chances of survival in a viral environment (Knirel *et al.*, 2015; Herman, 2015; Hampton *et al.*, 2020). Therefore, we wondered whether *OBC3* mutations might be driven by bacteria-virus interactions in the environment and thus that mutants might have altered bacteriophage sensitivity. Prophages, bacteriophage genomes that are integrated inside bacterial genomes, could be a direct source of viral particles in the bacterial environment via their genomic activation, commonly referred to as prophage induction (Nanda *et al.*, 2015). To assess a potential role for bacteriophages in the emergence of *OBC3* mutants, we first investigated the presence of prophages in the CHA0 genome by using the prophage prediction tool PHASTER (PHAge Search Tool Enhanced Release) (Arndt *et al.*, 2016). PHASTER detected two intact prophages, one questionable prophage and one incomplete prophage based on the presence/absence pattern of various critical phage particles components (Table 1).

Table 1 The *P. protegens* CHA0 genome encodes four prophage regions

Four prophage regions are predicted through PHASTER within the *P. protegens* CHA0 genome. Two intact prophage regions, one questionable and one incomplete region were detected. The *OBC3* gene cluster region length and position were listed, which demonstrate a close location next to predicted prophage region 2. (accession number NZ_LS999205.1; genome length 6,868,303 bp)

	Region	Region Length	Completeness	#Total Proteins	Specific Keyword	Region Position	Most Common Phage	Attachment Site	GC %
Predicted phage	1	33.4 Kb	intact	38	plate, tail, protease	1,389,266-1,422,721	PHAGE_Salmon_118970_sal3_NC_031940(11)	No	62.39%
	2	40.8 Kb	questionable	49	integrase	2,250,071-2,290,905	PHAGE_Pseudo_Dobby_NC_048109(28)	Yes	58.56%
	3	36.5 Kb	intact	41	tail, virion, capsid, head, portal, transposase	4,272,657-4,309,214	PHAGE_Pseudo_YMC11/02/R656_NC_028657(11)	No	58.73%
	4	17 Kb	incomplete	11	NA	4,316,594-4,333,596	PHAGE_Pseudo_PMG1_NC_016765(3)	Yes	54.87%
OBC3 cluster		22.3 Kb				2,173,937-2,196,258			50.09%
Whole Genome		6.87 Mb				1 - 6,868,303			63.4%

Region Length: the length of the regions is indicated in Kbp.
Completeness: a prediction of whether the region contains an intact or incomplete prophage based on the following criteria, intact (score > 90), questionable (score 70-90) and incomplete (score < 70). The detailed criteria for scoring prophage regions is described in material and methods.
#Total Proteins: the number of ORFs present in the region.
Specific Keyword: the specific phage-related keyword(s) found in protein name(s) in the region.
Region Position: the start and end positions of the region on the bacterial chromosome.
Most Common Phage: the phage(s) with the highest number of proteins most similar to those in the region.
Attachment Site: the putative phage attachment site.
GC%: the percentage of GC nucleotides of the region.

The predicted, intact region 1 phage is similar to *Salmonella* phage 118970_sal3 (32/38 phage proteins) (NCBI accession number NC_031940, GenBank no. KU927493) which belongs to the *Myoviridae* family. *Salmonella* phage 118970_sal3 was first isolated from water buffalo feces in southern Italy and exhibits lytic activity against *Salmonella enterica* serovar Typhimurium (Paradiso *et al.*, 2016). The second intact phage encoded by region 3 has the highest similarity to *Pseudomonas* phage YMC11/02/R656 (35/41 phage proteins) (NCBI accession number NC_028657) which is an unclassified phage from the *Siphoviridae* family. It was reported in the genome of *Achromobacter ruhlandii* strain 8173 isolated from cystic fibrosis patients (Rodrigues *et al.*, 2016). The incomplete phage encoded by region 4 is predicted to be similar to *Pseudomonas* phage PMG1 (9/11 phage proteins) (NCBI accession number NC_016765), which was identified in the genome of *Brucella canis* strain BCB018 isolated from dogs (Kaden *et al.*, 2014). The predicted, questionable, prophage in region 2 is most similar to *Pseudomonas* phage Dobby (38/49 phage proteins) (NCBI accession number NC_048109). Dobby was found in *P. aeruginosa* strain UMB2738 which is cultured from a calcium oxalate kidney stone. It is a ΦCTX-like phage lacking the ability to produce cytotoxin (CTX) (Johnson *et al.*, 2019). Dobby's genome is most similar to prophages within the genomes of three *P. aeruginosa* strains isolated from clinical samples, but it has a significantly shorter sequence than these closely related ΦCTX-like phages. The missing part from Dobby's sequence encodes the *rfbA*, *rfbB* and *rfbD* genes at the 3' end of an O-antigen biosynthetic gene cluster (Johnson *et al.*, 2019). In CHA0 this predicted prophage region is coined questionable due to the absence of several key prophage genes. These genes are important for O-antigen modifications. Notably, in the *P. protegens* CHA0 genome, the *OBC3* gene cluster is located in close proximity to this predicted prophage (Table 1).

Both intact prophage regions did not contain putative attachment sites, while the questionable prophage and incomplete prophage region had putative attachment sites and integrase genes (Table 1). Integrase genes play a key role in phage lysogeny establishment, maintenance and prophage induction (Ramisetty & Sudhakari, 2019). The "attL" and "attR" attachment sites in bacterial DNA are thought to be involved in site-specific genetic recombination. These sites are believed to correspond to the phage attachment sites ("attB" and "attP" sites, respectively) that are used by phages to integrate their genome into the genome of their host bacterium during infection (Menouni *et al.*, 2015; Ramisetty & Sudhakari, 2019). These sites are essential regulatory sequences for excision of the prophage during prophage induction. Altogether these results suggest that both incomplete or questionable prophages could still be activated to become lytic phages, although the virulence might be comprised as a consequence of several missing genes (Vacheron *et al.*, 2021).

The *oafA-1* mutant demonstrates unaltered mitomycin C sensitivity

Prophages are maintained in the quiescent state, and typically DNA damage is required to activate them. Upon DNA damage, bacterial cells initiate a response known as the SOS response which can lead to de-repression of prophage genes. To investigate whether prophages encoded by the CHA0 genome are responsible for the selection of *oafA* mutants we used mitomycin C (MmC) to activate the SOS response and stimulate prophage induction. MmC is commonly used for prophage induction under laboratory conditions (Muschel & Schmoker, 1966; Pratama & Van Elsas, 2017). We conducted bacterial growth assays of *oafA-1* bacterial cells and wild type cells under increasing concentrations of MmC, *in vitro*. We found that the growth of *oafA-1* mutant cells was comparable to wild type cells, and that increasing concentrations of MmC led to bacterial death but also reduced optical density (Fig. 3). The observed phenotypic alterations were comparable for both mutant and wild type cells suggesting that the mutation does not alter its sensitivity towards its own prophages. However, we observed significant bacterial cell death already at 0.5 µg/ml MmC, which is considerably lower than the 3.0 µg/ml MmC used in other studies for prophage induction (Chene *et al.*, 2006; Vacheron *et al.*, 2021), which could mean that the level of prophage induction might be too small in our experiment to exert a differential effect.

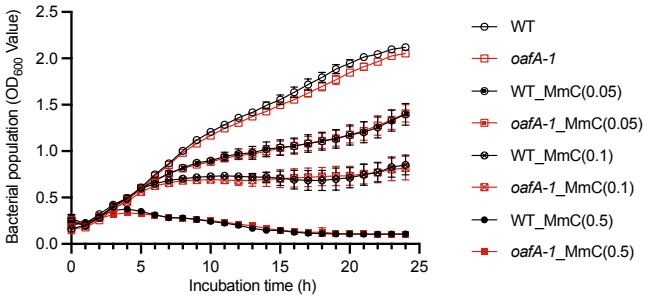

Figure 3 Mutant *oafA-1* cells display unaltered growth under mitomycin C treatment.
Representative growth curve profiles observed for wild type (WT) and *oafA-1* mutant cells at increasing concentrations of mitomycin C (MmC). Cell density was recorded every hour for 24 hours at 28 ºC. Open black circles represent the wild type (WT), and open red squares represent the *oafA-1* mutant (n = 6 for each time point, each treatment, and each strain).

In general, the stability of a prophage is tightly coupled with the physiology of the host cell. To investigate whether prophages were induced during the evolution experiment, we sequenced the rhizosphere microbial communities from generations 2 and 6 from the original experiment (**Chapter 2**) (Li *et al.*, 2021a). In addition, we also sequenced rhizosphere microbial communities of wild type and *oafA-1* mixed populations (both initial 1:1 and initial 8:2), which were stored from experiments conducted in **Chapter 3**. Analysis of the relative abundance of prophage genomic regions when compared to the remainder of the CHA0 genome using PropagAtE (Kieft & Anantharaman,

2022), demonstrated the lack of prophage activation in these experiments (Sup. Table 1). Because bacterial populations consisted of only one bacterial species, and as no plasmids or large genomic islands have been detected in the *P. protegens* CHA0 genome, we excluded the potential role of mobile genetic elements in explaining the phenotypic variation.

Phage-resistant *OBC3* mutants display altered LPS structure

As we were unable to confirm the activation of endogenous CHA0 prophages and concomitantly sensitivity of the *OBC3* mutants to said prophages, we made use of an environmental phage, named ΦGP100 to verify whether *OBC3* mutants have altered phage sensitivity. ΦGP100 belongs to the *Podoviridae* family. It was isolated from rhizosphere soil in Switzerland and found to infect *P. protegens* CHA0 and related strains of the same species (Vacheron *et al.*, 2018). By conducting phage plaque assays (Hockett & Baltrus, 2017), we were able to observe clear lysis of the CHA0 wild type, confirming that it is sensitive to ΦGP100 (Fig. 4) (Vacheron *et al.*, 2018). Identical lysis circles were observed for both *oafA* mutants, while *galE* and *RS09880* mutant cells appeared resistant to ΦGP100 as no lysis was observed (Fig. 4).

Figure 4 Differential sensitivity towards ΦGP100 among *OBC3* mutants.
OBC3 mutants were exposed to *P. protegens* CHA0 environmental phage ΦGP100 using a phage plaque assay. Specifically, a 5-µl spot of purified viral ΦGP100 was deposited on top of a 25 µl/ml bacterial film on LB soft agar. The plates were incubated overnight at 25°C. Wild-type and *oafA* mutants showed clear lysis by ΦGP100 inoculation (red squares; indicating sensitivity), whereas *galE* and *RS09880* mutants' cells show no lysis (green squares; indicating resistance).

Given the role of *OBC3* in LPS biosynthesis and LPS's role on phage recognition, we hypothesized that the altered phage sensitivity observed for the *OBC3* mutants, *galE* and *RS09880*, could be mediated by an altered LPS structure. Therefore, we used sodium dodecyl sulphate-polyacrylamide (SDS) gel electrophoresis (SDS-PAGE) followed by silver staining to visualize the LPS patterns of wild type and mutant cell envelopes. Separation and visualization of the LPS of wild type and mutant cells revealed a profile with a dominant low-molecular-weight band below 20 kDa and a smear comprising molecules with high-molecular-weight up to around 120 kDa (Fig. 5). The mutation in *RS09880*, encoding a putative glycosyl transferase, resulted in the complete loss of the bands above 25 kDa (Fig. 5). It suggests that this mutation completely disrupts the biosynthesis of long O-antigen. Comparable loss of long O-antigen was reported previously upon deletion of the GDP-L-fucose synthase-

encoding gene, *fcl*, and upon a partial deletion of *OBC3* which among several other genes included *fcl* highlighting the relative importance of this gene (Kupferschmied *et al.*, 2016). The mutation in *galE*, encoding a UDP-glucose 4-epimerase which catalyzes the interconversion between UDP-galactose and UDP-glucose, displayed a downwards-shift of the high-molecular-weight bands by several kDa (Fig. 5). In contrast, analysis of the LPS of both *oafA* mutants revealed no recognizable changes with that of the wild type. However, we cannot exclude the possibility that the resolution of this analysis was insufficient to observe subtle modifications executed by OafA, such as the addition of an acetyl group. In other systems, like *Salmonella*, O-antigen modifications can typically only be visualized by the use of specific antibodies that recognize the specific modification (Pearson *et al.*, 2020).

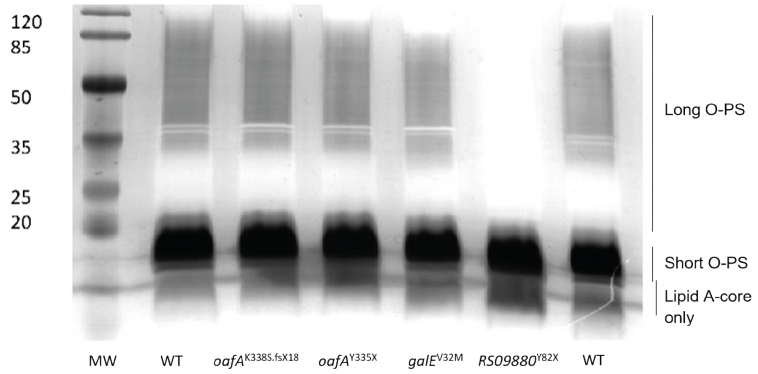

Figure 5 *OBC3* mutants display diverse LPS structures.
Silver-stained patterns of LPS of *P. protegens* CHA0 *OBC3* mutants *oafA-1*, *oafA-2, galE,* and *RS09880*. All strains were grown at 28 ºC to late stationary growth phase in King's medium Broth, followed by LPS extraction, purification, and SDS-polyacrylamide gel electrophoresis. Molecular weights in kDa are depicted on the left of the gel and predicted compositions of LPS molecules on the right.

Discussion

Biological control strain *P. protegens* CHA0 was isolated from a tobacco field soil in Switzerland in 1986, and characterized for its capacity against tobacco black root rot disease (Stutz *et al.*, 1986). Its biocontrol activities can be attributed to its large variety of bioactive secondary metabolites (Keel *et al.*, 1992; Ramette *et al.*, 2011), including several molecules that can be potentially harmful for plants as well. Production of these molecules results in an opportunistic-pathogen behavior for CHA0 on axenically grown Arabidopsis plants (**Chapter 3**) (Li *et al.*, 2021a). Adaptation of CHA0 on Arabidopsis plants yielded the emergence of many mutualistic *gac* mutants that, in contrast to the CHA0 ancestor, are beneficial for Arabidopsis, likely mediated by a reduction in the biosynthesis of these harmful molecules (**Chapter 2**) (Li *et al.*, 2021a). Besides these mutualistic mutants, the majority of bacterial colonies picked during the first cycles

of the experiment contained mutations in a small genomic window depicted as the O-antigen biosynthesis gene cluster 3 (*OBC3*) (**Chapter 2**). *OBC3* is involved in the biosynthesis of the O-antigenic side chain of bacterial lipopolysaccharide (LPS). LPS is important for bacterial cell wall integrity and bacterial interactions with the environment. Previously, we characterized *OBC3* mutants in relation to *in vitro* bacterial growth and root colonization ability, revealing its role in bacterial root attachment (**Chapter 3**). Specifically, we found that several *OBC3* mutants attach faster to axenic Arabidopsis roots relative to the ancestor, which potentially explains their enhanced root competence (**Chapter 3**). O-antigen variation plays an important role in bacterial adaptation to the environment (Lerouge & Vanderleyden, 2001; Wang *et al.*, 2010; De Smet *et al.*, 2017). Besides bacterial host adhesion, O-antigen variation affects virulence of pathogenic bacteria. For instance, changes in the relative proportion of O-antigen side chains as well as the complete loss of O-antigen resulted in reduced virulence of *P. aeruginosa* towards mice (Ivanov *et al.*, 2011) and reduced insecticidal virulence of *P. protegens* CHA0 towards insects (Kupferschmied *et al.*, 2016).

OBC3 was first described by Kupferschmied and co-workers revealing its distribution in several pseudomonads, i.e., *P. protegens* strains BRIP, PGNR1, Cab57 and *P. sp.* CMR5c in addition to CHA0 (Kupferschmied *et al.*, 2016). To elaborate on the general role of O-antigen among *P. protegens*, we here examined the distribution of the *oafA* gene and of the entire *OBC3* gene cluster among 71 *P. protegens* strains using whole-genome comparisons and gene sequence alignment. These 71 strains derive from diverse environments including plant- and non-plant-associated ones. Surprisingly, among several *P. protegens* strains from diverse environments, identical *oafA* mutations were identified that were similar to the *oafA* mutations we identified from the Arabidopsis rhizosphere (**Chapter 2**) (Fig. 1). These naturally occurring mutated *oafA* sequences encode a conserved thymine (T) insertion at position 1,083 disrupting the open reading frame and yielding a premature stop. As a consequence of this premature stop, the AT3 domain is disconnected from the SGNH domain in the OafA protein comparable to the spontaneous mutants described in this thesis.

Given the phylogenetic relatedness of the strains and the strict conservation of this mutation it appears most likely that this mutation occurred in a common ancestor of all of these strains, at least 15 years ago (Sup. Table 1). It has been reported that the SGNH domain of AT3-SGNH-fused domain-containing proteins is both necessary and sufficient for LPS acetylation (Pearson *et al.*, 2020). Thus, we hypothesize that these natural *oafA* mutants probably have dysregulated O-antigen acetylation, benefiting the respective bacteria by providing a general adaptive advantage. The high sequence similarity in the *oafA* gene sequence downstream of the disruptive mutation that is responsible for encoding of the SGNH domain, suggests that this part of the *oafA* gene might still be

active, potentially yielding a disconnected, SGNH-only protein. Among these strains, we also observed parallel mutations in the genes flanking *oafA* and forming the *OBC3* gene cluster (Fig. 2), which is reminiscent of the various spontaneous CHA0 mutants that target *OBC3* in our evolution experiment (**Chapter 3**).

As not all environmental *P. protegens* are plant-associated, nor surface-associated, O-antigen modification-driven altered adhesion cannot easily explain their appearance across the diverse environments. Besides adhesion, O-antigen also serves as critical docking station for bacteriophages (phages) (Lerouge & Vanderleyden, 2001; Herman, 2015; Hampton *et al.*, 2020). Phages are ubiquitous viral particles that can infect and kill bacterial cells, and they consequently play important roles in maintenance and evolution of bacterial populations in nature. Modification of the O-antigen, among many other traits, therefore, mediates bacterial susceptibility towards phages making it an important target of adaptive evolution in bacteria (Lam *et al.*, 2011; Knirel *et al.*, 2015; Bertani & Ruiz, 2018). For example, spontaneous mutations of *Escherichia coli* 4s, which are found within O-antigen biosynthesis genes, induced bacterial host resistance to bacteriophage G7C and also altered bacterial interactions with several other bacteriophages (Knirel *et al.*, 2015).

To test whether the here discussed *oafA* variants affect phage susceptibility, we first examined candidate endogenous prophages, bacterial genome-integrated phage regions, within the CHA0 genome. We identified four such prophages, two complete, and two incomplete ones (Table 1). This is in contrast to previous findings that report three complete ones (Jousset *et al.*, 2014), with two of them being inducible (Vacheron *et al.*, 2021). However, the CHA0 genome also encodes two tailocins (Vacheron *et al.*, 2021), phage tail-like structures that can be used to ward off competing bacteria, that are considered remnants of earlier bacteriophage integration and could therefore affect the identification of genome-encoded phages (Ghequire *et al.*, 2015).

Noting the existence of several prophages, we set out to examine the potential of *in vitro* and *in vivo* CHA0 prophage activation, and attempted to quantify the abundance of phage particles from the evolution experiment. In addition, we assessed the sensitivity of wild type and mutant bacterial cells to environmental phage particles. We were unable to demonstrate or detect prophage activation *in vitro*, corroborated by the lack of active phage particle detection from both the experimental evolutionary populations and from *in vivo* plant root colonization assays using shotgun metagenome sequencing. As a result, we reject our hypothesis that prophage activation might be driving selection of spontaneous *OBC3* mutants. Phage sensitivity tests using the environmental *P. protegens* phage ΦGP100 (Vacheron *et al.*, 2018), on the other hand, revealed a diverse pallet of sensitivities among these *OBC3* mutants. Both o*afA*

mutants displayed unaltered sensitivities compared to the CHA0 wild type, while the two other *OBC3* mutants, *galE*^{V32M} and *RS09880*^{Y82X}, both became fully resistant. A link between the O-antigen structure and phage sensitivity was revealed (Lerouge & Vanderleyden, 2001; Herman, 2015; Kulikov *et al.*, 2019). Therefore, we set out to visualize the LPS structure of the *OBC3* mutants via SDS-PAGE analysis (Tsai & Frasch, 1982; Lee *et al.*, 1995). Notably, we observed that LPS integrity, particularly the long O-antigen, fully correlated with ΦGP100 sensitivity (Fig. 4, 5). Specifically, LPS of *oafA* mutants was visually indistinguishable from the wild type, while *galE* and *RS09880* mutants had abnormal or even completely missing long O-antigen, respectively (Fig. 5). Although the GalE enzyme, encoding an UDP-galactose 4-epimerase, is suggested to play a role in the biosynthesis of the exopolysaccharide, and the core oligosaccharide part of LPS rather than the O-antigen (Fry *et al.*, 2000; Nesper *et al.*, 2001; Nakao *et al.*, 2006), the *galE*'s localization in the *OBC3* gene cluster corroborates it's potential role in O-antigen biosynthesis, which is what we found here. *RS09880* encodes a putative glycosyltransferase that is predicted to be involved in the assembly of the repeating units of LPS using nucleotide-activated sugars. These sugars are activated by the attachment of a nucleotide, such as ATP or UDP, in order to facilitate their transfer to another molecule during the synthesis of complex carbohydrates like LPS. Disruption of another glycosyltransferase in CHA0, *wbpL*, has also been shown to result in a disruption of both short and long O-antigen (Kupferschmied *et al.*, 2016). The LPS profile of both *oafA* mutants appeared to be indistinguishable from the wild type, yet it should be noted that this might be caused by a lack of resolution. Small modifications, like the addition of an acetyl group, usually requires the use of modification-specific antibodies. For example, Pearson and coworkers (Pearson *et al.*, 2020) used the O:5 antibody to probe OafA-dependent O-antigen abequose acetylation in *Salmonella enterica* serovar Typhimurium (*S.* Typhimurium) that is otherwise invisible. Nevertheless, phage plaque assays involving the *OBC3* mutants showed that apparent O-antigen modification can be linked to phage sensitivity.

The SGNH domain of *S.* Typhimurium OafA has been shown to acetylate the abequose of the O-antigen on its own (Pearson *et al.*, 2020). This raises the possibility that the potentially active, but disconnected CHA0 SGNH-only protein in the *oafA* mutants may translocate other acetyl groups to different targets in the periplasm, such as extracellular polysaccharides (EPS). EPS are produced by bacteria and other microorganisms and found in the extracellular environment. It forms a sticky, gel-like substance that helps to protect and support the bacterial cells, and can also act as a barrier to prevent the attachment of other microorganisms. Similarly, Otase-regulated glycoprotein biosynthesis might affect EPS synthesis and release. For instance, glomalin, a glycoprotein, is produced by arbuscular mycorrhiza fungi (AMF) and is deposited in large amounts on their hyphae and spores in soil and on plant roots. It is

thought to form a biofilm-like substance that enhances the size and stability of AMF aggregates, helping these fungi to better attach to surfaces and protect themselves from environmental stresses. The ability of glomalin to increase the stability of AMF aggregates may also enhance the ability of these fungi to form beneficial associations with plants (Agnihotri *et al.*, 2022).

In conclusion, we identified conserved *OBC3* gene clusters in a variety of *P. protegens* genomes, some of which encode surprisingly similar mutations in the *oafA* gene to the ones we previously identified in experimentally evolved, spontaneous CHA0 mutants. Similar to those mutants, naturally occurring *oafA* mutations result in either a complete loss of C-terminal SGNH domain functionality or alternatively yield a disconnection between the N-terminal AT3 domain and the SGNH domain. Such modification likely provides a selective benefit in their respective environments, possibly by mediating interactions with environmental phages although we didn't observe any change in phage resistance in our CHA0 *oafA* mutants. Mutations in *galE* and *RS09880*, on the other hand, do alter phage resistance, corroborated by visible changes in LPS integrity. Overall, given the lack of active phage detection in the evolution experiment, as well as during the *in vivo* competition experiments on the plant root; and in the absence of altered phage susceptibility in the case of *oafA-1* and *oafA-2* it appears that phage selection did not play a role during the evolution experiment.

Acknowledgments

This work was supported by a China Scholarship Council fellowship (to H.Z.). We thank Ria Tommassen from the Microbiology group at Utrecht University for extraction and visualization of lipopolysaccharides.

Materials and methods

Genomic analysis

Seventy available genomes of *Pseudomonas protegens* environmental strains, excluding *Pseudomonas protegens* CHA0, were obtained from the NCBI GenBank database and analyzed for the presence of homologous *oafA* genes and the *OBC3* gene cluster. A combination of BLASTp (protein query to protein database) and tBLASTn (protein query to translated nucleotide database) analysis was used to identify *oafA*- and *OBC3*-positive genome sequences. We used Mash-derived genome-to-genome pairwise distances to build strain/genome-level phylogenetic trees (version 2.3) (Ondov *et al.*, 2016). Cblaster (version 1.3.12) and Clinker (version 0.0.23) (Gilchrist & Chooi, 2021) were used to visualize the *OBC3* gene cluster structure, by aligning the *OBC3* protein sequences of CHA0 together with all *OBC3*-positive *P. protegens* strains.

The genome of *P. protegens* CHA0 was analyzed with PHASTER (Arndt *et al.*, 2016) to search for sequences encoding prophages. For each prophage sequence detected, it reveals its possible phage sources and determines the presence of critical phage genes.

Bacterial phage sensitivity assays

Bacteria preparation

To conduct bacterial growth sensitivity experiments, we cultured *P. protegens* CHA0 wild type and mutant strains on King's medium B (KB) agar plates in a 28 ºC incubator (King *et al.*, 1954). After 24 h of growth, a single colony of each strain from the KB plate was separately collected and transferred to 15 ml KB liquid medium in a 50-ml tube. Then, we put the tubes in a shaking incubator with 225 revolutions per minute (rpm) at 28 ºC. After 18 h of growth, cells were collected in 10 mM $MgSO_4$, and washed twice through centrifugation for 10 min at 3000 rpm. The washing eliminates any carry-over nutrient supplementation in the media. The washed bacterial pellet was resuspended in 10 mM $MgSO_4$ and adjusted to a final density of OD_{600} equal to 0.1 (corresponding to $8 \bullet 10^7$ colony-forming units (cfu) per ml) for subsequent use.

Growth kinetics and mitomycin C sensitivity of wild type and oafA-1 mutant bacterial cells

Wild type and *oafA-1* mutant bacterial suspensions were inoculated in 200 µl liquid KB medium per well with a final optical density OD_{600} equal to 0.2 in 96-well plate, separately. Both strains were treated with an additional final concentration of 0.05, 0.1 and 0.5 µg/ml of mitomycin C (MmC) separately, or an equal amount of 10mM $MgSO_4$ as control treatment. Bacterial growth was monitored for 24 h by measuring the OD_{600} every hour in a SPECTROstar Nano Microplate Reader (BMG LABTECH, Germany). This growth kinetic assay was performed once with six biological replicates.

Phage-plaque soft agar assay

The environmental phage ΦGP100 was found to infect specifically *P. protegens* CHA0 and related strains of the same species (Vacheron *et al.*, 2018). To test the sensitivity of the different *OBC3* mutants to ΦGP100, soft agar assays were performed using an adaptation of a protocol from Hockett and Baltrus, 2017 (Hockett & Baltrus, 2017). Following overnight incubation, 500 µl of each bacterial culture was mixed with 20 ml of LB soft agar in a 50-ml Falcon tube by inverting the tube. This mixture was poured into an empty Petri dish (diameter of 90-mm). Once the agar solidified, spots of 5 µl of purified viral particles of ΦGP100 were deposited onto the bacterial overlay. The plates were then incubated overnight at 25°C. Sensitivity of the bacteria towards ΦGP100 was assessed using the following scale: clear lysis (sensitive), semi-clear lysis, opaque lysis and no lysis (resistant).

Active prophage detection through metagenomes

Metagenomes from rhizosphere microbial samples were analyzed in this study for the presence of active phages. Two samples, from generations 2 and 6, were obtained from the original evolution experiment replicate line 1 in which *oafA-1* evolved. Additional samples include those obtained from competitive root colonization assays described in **Chapter 3**. For metagenomic sequencing, Illumina libraries were prepared using the HackFlex procedure (Gaio *et al.*, 2022), and around 1 M reads were generated per sample. PropagAtE (Prophage Activity Estimator; version 1.1.0) (Kieft & Anantharaman, 2022) was used to quantify the abundance of active prophages from all selected samples. It uses the genomic coordinates of integrated prophage sequences in combination with whole-genome shotgun sequencing reads to estimate whether a given prophage is dormant active.

LPS extraction and visualization

The method described by Tsai and Frasch (1982) was used with some modifications for the extraction and visualization of LPS (Tsai & Frasch, 1982). Bacteria were sampled for LPS extraction after being cultured for 16 hours in 10 ml of KB at 28 ℃ with 200 rpm shaking, reaching the late exponential growth phase, and suspended as 1.5 ml suspensions with an optical density at 600 nm (OD_{600}) of 5.0. After 1-hour incubation with the proteinase K at 60 ℃, the extracted samples were immediately subjected to sodium dodecyl sulfate polyacrylamide gel electrophoresis (SDS-PAGE). SDS-PAGE was performed using 14% (bis)acrylamide gels, followed by silver-staining for 10 minutes with the silver-solution, and washing with Milli-Q water for 3 times, each for 15 minutes. Finally, a picture of the gel was taken.

Supplementary information

Table S1 List of the nineteen *P. protegens* genomes containing *oafA* homologues

Strain	Geographic Origin	Habitat/Host	Collection date (year)	Genome sequenced	BioSample Number	Biocontrol ability	Reference/ BioProject
P. protegens PGNR1	Ghana	Tobacco	~1998	Jousset *et al.* (2014)	SAMN03891657	Antifungal activity	(Keel *et al.*, 1996)
P. protegens PGNL1	Ghana	Root/Tobacco	~1996	ETH Zurich; 2020	SAMN15098418	Antifungal activity	(Keel *et al.*, 1996)
P. protegens PGNR2	Ghana	Root/Tobacco	~1996	ETH Zurich; 2020	SAMN15098418	Antifungal activity	(Keel *et al.*, 1996)
P. protegens Pf-1	Switzerland	Root/Tobacco	~1988	ETH Zurich; 2020	SAMN15098417	NA	(Compeau *et al.*, 1988)
P. protegens BRIP	Switzerland	Cyclops	2014	Justus Liebig University Giessen; 2015	SAMN03891658	Antifungal activity; Insecticidal activity	(Ruffner *et al.*, 2015; Flury *et al.*, 2016)
P. protegens 1B1	USA	Mississippi River	2008	Ohio State University; 2016	SAMN05933917	Antibiotic activity	(de Freitas & Taylor, 2022)
P. protegens H78	China	Rape field soil	2012	Shanghai Jiao Tong University; 2019	SAMN04240923	Antibiotic activity	(Huang *et al.*, 2017)
P. protegens UMG3145	Portugal	Forest soil	2013	Universidade do Minho; 2019	SAMN1147945	NA	PRJNA534200
P. protegens BIGb0404	France	Rotting Petasites stem	2009	Joint Genome Institute; 2018	SAMN10361489	NA	(Samuel *et al.*, 2016)
P. protegens JUb28	France	Rotting Hawthorn fruits	2007	Joint Genome Institute; 2018	SAMN10361497	NA	(Samuel *et al.*, 2016)
P. protegens Darke	USA, Ohio	Soil	2001	Ohio State university	SAMN05933920	NA	PRJNA342848
P. protegens PA12	Mexico	Flower/Piper auritum	2012	Centro de Investigacion y de Estudios Avanzados del IPN; 2016	SAMN05302429	Antifungal activity	(Gutiérrez-García *et al.*, 2017)
P. protegens PA11	Mexico	Leaf/Piper auritum	2012	Centro de Investigacion y de Estudios Avanzados del IPN; 2016	SAMN06111856	Antifungal activity	(Gutiérrez-García *et al.*, 2017)

P. protegens PA25	Mexico	Stem/Piper auritum	2012	Centro de Investigacion y de Estudios Avanzados del IPN; 2016	SAMN06111859	Antifungal activity	(Gutiérrez-García *et al.*, 2017)
P. protegens PA14	Mexico	Stem/Piper auritum	2012	Centro de Investigacion y de Estudios Avanzados del IPN; 2016	SAMN06111858	Antifungal activity	(Gutiérrez-García *et al.*, 2017)
P. protegens PA26	Mexico	Leaf/Piper auritum	2012	Centro de Investigacion y de Estudios Avanzados del IPN; 2016	SAMN05302430	Antifungal activity	(Gutiérrez-García *et al.*, 2017)
P. protegens PA19	Mexico	Leaf/Piper auritum	2012	Centro de Investigacion y de Estudios Avanzados del IPN; 2016	SAMN06111857	Antifungal activity	(Gutiérrez-García *et al.*, 2017)
P. protegens Cab57	Japan	Rhizosphere/ Shepherd's purse	~2014	DDBJ; 2016	SAMD00061024	Antibiotic activity	(Takeuchi *et al.*, 2014)

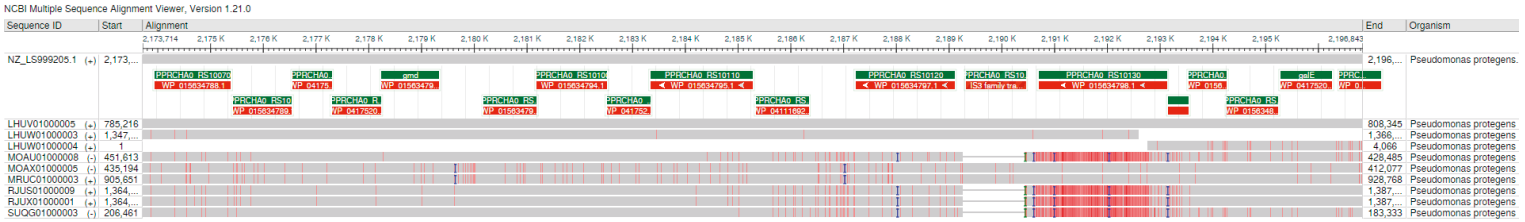

Figure S1 Alignment of the *OBC3* gene cluster in closely related *P. protegens* strains.
Alignment of the complete *P. protegens* CHA0 *OBC3* gene cluster (on the top, from 5' to 3' direction, left = Guanylyl transferase, right = *galE*) with genomic regions in *P. protegens* strains PGNR, BRIP (twice, involving two contigs), 1B1, Darke, PA25, BIGb0404, JUb28, and UMG3145 (top to bottom). All strains were collected from natural environments and genome sequence data were obtained from NCBI GenBank. The BLASTn nucleotide-to-nucleotide alignment shows absence of alignment (gapped alignment indicated by long horizontal lines) for the *IS3* transposase region in the four strains that have an insertion in the *oafA* gene (blue vertical bar at position 2,188 K) and the presence of many (disruptive) mutations in the putative *otase* (the gene downstream of the gap). The red vertical lines indicate mismatches/differences with respect to the CHA0 reference query.

Figure legends mentioned references: (Ondov *et al.*, 2016)

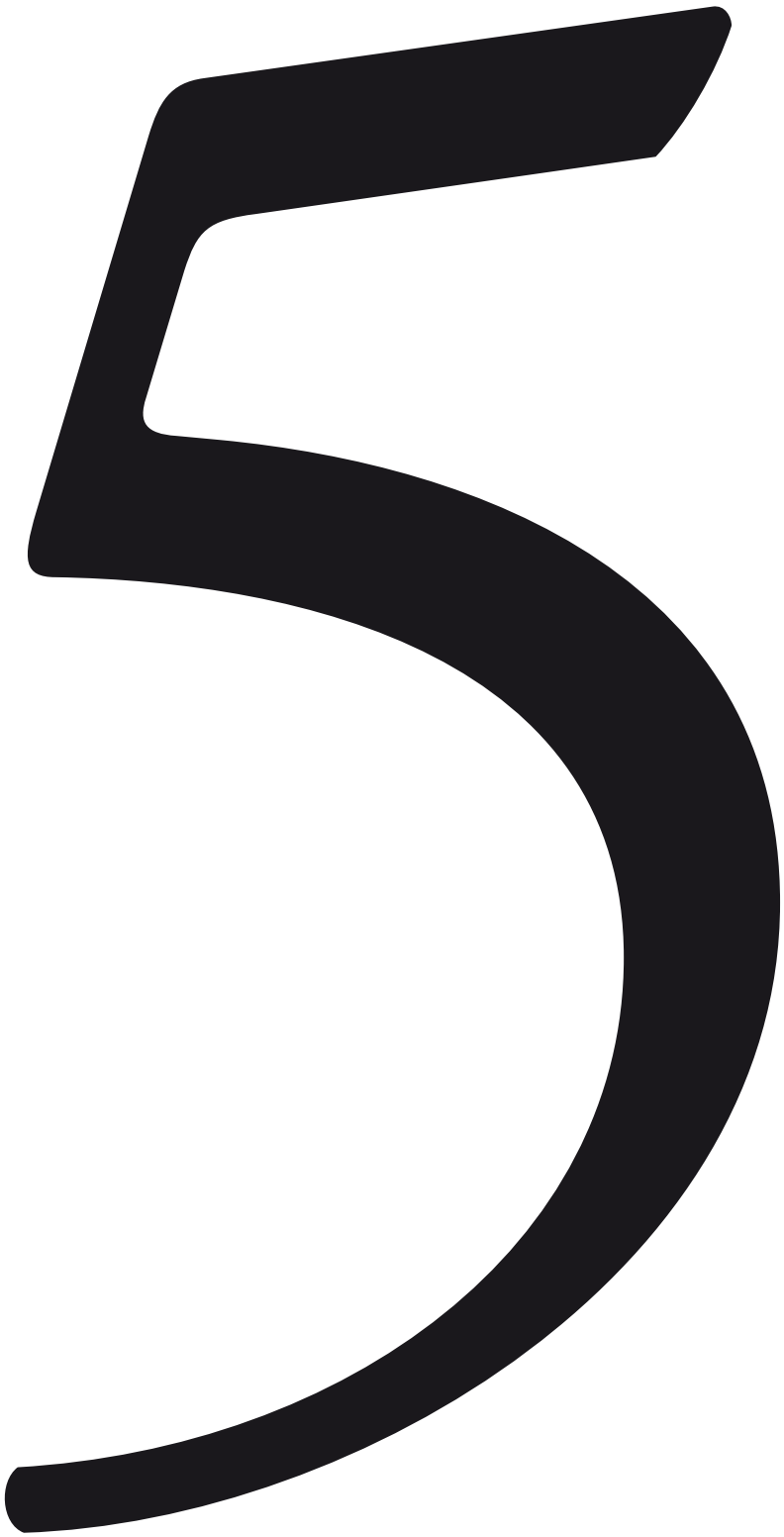

CHAPTER 5

Summarizing discussion

Hao Zhang[1]

[1]Plant-Microbe Interactions, Department of Biology, Science4Life,
Utrecht University, Padualaan 8, 3584 CH, Utrecht, the Netherlands

Author contributions:

H.Z. wrote the summarizing discussion and prepared all illustrations.

Exploring the potential of rhizobacterial rhizosphere adaptation for sustainable agriculture

Global food security is threatened in face of the constant increasing human population (Misselhorn *et al.*, 2012). Since the green revolution (Evenson & Gollin, 2003), we have gotten accustomed to use synthetic fertilizers to improve plant nutrient availability and synthetic pesticides to control pathogenic microbes and insects. As a result, crop growth and yield have improved, in turn supporting significant population growth. However, the use of these synthetic compounds brings a big burden to natural systems because they can leak out of the soil into aquatic environments, or are biological stable for long periods of time, therewith negatively affecting the environment (Baweja *et al.*, 2020). Modernized food production is required to achieve a more sustainable system, both for the environment and for human health, while simultaneously fulfilling the increasing needs of food quantity, quality and variety for the global human population. Crops like cereals and vegetables form the main components of human daily food. Therefore, crop growth and yield directly affect food availability, and developments towards improving these traits attract research and economic interest.

Plants are surrounded by numerous microorganisms. Through characterization of their effects on the plant, they can be classified as either beneficial, pathogenic or neutral. Pathogenic microbes and pests, such as insect herbivores, heavily impair plant growth and production, causing up to twenty percent of yield loss in major crops like wheat, rice and potato (Savary *et al.*, 2019). In the course of evolution, plants developed a sophisticated immune system to help them fight against these threats. A two-branched plant innate immune system model was proposed by Jones and Dangl (Jones & Dangl, 2006). The first branch describes the recognition of common microbial molecules, also known as MAMPs or PAMPs for microbe or pathogen-associated molecular patterns, and subsequent activation of basal defense. This branch is commonly referred to as PAMP-triggered immunity or PTI. The second branch, which is known as effector-triggered immunity or ETI, involves the recognition of specialized effector molecules and is associated with elevated levels of defense (Jones & Dangl, 2006). In addition to plant innate immunity, many beneficial rhizobacteria were found that aid in plant health protection. These bacteria, typically referred to as plant growth-promoting rhizobacteria or PGPR have attracted considerable attention over the past decades due to their promising biocontrol and plant growth-promotion functions (Lugtenberg & Kamilova, 2009; Martínez-Viveros *et al.*, 2010; Barret *et al.*, 2011; Vejan *et al.*, 2016; Pieterse *et al.*, 2021). One well-known PGPR genus is the ubiquitous *Pseudomonas* genus, members of which have been isolated from a plethora of plant species and which have been further characterized with respect to their plant-beneficial traits and promising role as biocontrol agents. Successful root colonization

of specific *Pseudomonas* spp. triggers induced systemic resistance (ISR) of plants, which protect plants against future attacks from aboveground pests and pathogens (Pieterse *et al.*, 2014; Verbon *et al.*, 2017; Stringlis *et al.*, 2018b). Furthermore, PGPR mediate plant nutrient acquisition and aid in iron homeostasis (Verbon *et al.*, 2017; Stringlis *et al.*, 2018b). Given the beneficial activities of many of these root-associated microorganisms, it is not surprising that evidence is accumulating that plants are able to shape the microbial community or microbiome on their roots to their own benefit and skillfully utilize their functional repertories (Berendsen *et al.*, 2012, 2018; Reinhold-Hurek *et al.*, 2015; Sasse *et al.*, 2018).

As rhizobacterial *Pseudomonas* spp. can provide the plant with many growth-promoting and protective traits, the translation of these discoveries into agricultural application has been the topic of extensive research. Unfortunately, such translation has been hindered due to their inconsistent performance in the field (Morrissey *et al.*, 2004; Mark *et al.*, 2006; Vejan *et al.*, 2016). This reminds us about the complexity of soil, its chemical composition, water content, climatic conditions, and more importantly, the knowledge gap on adaptation of introduced bacterial strains in complex environments.

The present research focuses on characterizing bacterial rhizosphere-adaptation-traits of several *Pseudomonas protegens* CHA0 (CHA0) isolates which evolved during a laboratory evolution experiment (Li *et al.*, 2021a). CHA0 is a well-known and well-studied biocontrol strain that was identified in Switzerland in 1986 from tobacco field soil with natural resistance against tobacco black root rot disease (Stutz *et al.*, 1986). Following its identification, CHA0 was demonstrated to be the driver of said resistance, and moreover, subsequent studies showed that its biocontrol activities can be attributed to the large variety of secondary metabolites it produces (Keel *et al.*, 1992; Ramette *et al.*, 2011). Despite its biocontrol activities, application of CHA0 on plant roots is not necessarily beneficial as some of its metabolites (Flury *et al.*, 2016), e.g., hydrogen cyanide, are also potentially harmful to the plant (Defago *et al.*, 1990; Siegień & Bogatek, 2006). To better understand how microorganisms adapt to a new environment and investigate whether plants are able to steer such adaptation, Li and colleagues (2021a) set out to study the adaptation of CHA0 to a new host plant, *Arabidopsis thaliana* Col-0 (Arabidopsis), that was known to be sensitive to this strain via an approach known as experimental evolution (Li *et al.*, 2021a). Experimental evolution is described as the use of controlled laboratory, or field experiments to explore the dynamics of evolution. It provides a powerful tool to study microbial adaptation to different environments in real-time (Kawecki *et al.*, 2012; Lenski, 2017). Here, the colonization of Arabidopsis roots by CHA0 was carried out under gnotobiotic conditions in the lab. The experiment involved five independent replicated lines, and

it ran over eight cycles of four weeks each (**Chapter 2**) (Li *et al.*, 2021a). Replicated lines represent parallel evolution experiments with an identical start. In each following cycle, CHA0 cells were harvested from an Arabidopsis seedling at the end of the four weeks and introduced on a new one. As expected, initial application of CHA0 on Arabidopsis resulted in a negative plant-microbe interaction, in which the plant suffered from CHA0 colonization (Li *et al.*, 2021a). However, repeated introduction of evolving CHA0 populations on new Arabidopsis plants drove the emergence of CHA0 bacterial cells that were increasingly less harmful to the plant. Ultimately, CHA0 strains evolved that were beneficial, promoting rather than inhibiting plant growth. Concomitantly, plants were able to accommodate larger bacterial populations demonstrating that both plants and bacteria benefitted from the bacterial adaptations.

Adaptative mechanisms of root-colonizing microbes

Several adaptive strategies were identified by the characterization of the evolved strains. These strategies included alteration of motility, cell surface modification, and reduction of synthesized secondary metabolites. The third strategy appeared to be one of the key adaptations in relation to the observed plant-beneficial effects of evolved isolates (**Chapter 2**). The corresponding genetic changes underlying these adaptations have been identified and are discussed extensively in this thesis (**Chapters 2, 3 and 4**). Better understanding of these bacterial adaptation traits aids important knowledge on bacterial evolution and bacterial competition in the rhizosphere and on the plant root.

Impaired motility: contradictory results for bacterial rhizosphere adaptation?

We found that the independent lines converge on similar evolutionary trajectories involving overlapping biological processes and molecular mechanisms. For instance, a trend of enhanced swimming and worsened swarming was observed for evolved mutants in each independent line (**Chapter 2**). Enhanced swimming motility of evolved CHA0 isolates is not unexpected as there is ample evidence for its importance in rhizosphere colonization. Swimming is a motile behavior which refers to individual movement in liquid, powered by rotating flagella, while swarming is described as multicellular surface movement that is also powered by flagella but involves a variety of additional cues like quorum sensing (Kearns, 2010). Both swimming and swarming motility are driven by chemotaxis, a mechanism enabling the bacteria to move in response to a gradient of extracellular signals (Sampedro *et al.*, 2015). Successful bacterial colonization of new environments relies on bacterial chemotaxis and associated motility to reach nutrient-rich niches or avoid regions depleted of nutrients or rich in toxic compounds (De Weert *et al.*, 2002). Accordingly, inactivation of bacterial chemotaxis or motility was previously shown to hinder efficient bacterial colonization

in the rhizosphere (De Weert *et al.*, 2002; Capdevila *et al.*, 2004; Martínez-Granero *et al.*, 2006; Oku *et al.*, 2012, 2014; Allard-Massicotte *et al.*, 2016; Pieterse *et al.*, 2021). Likewise, a recent study of competitive colonization of Arabidopsis roots involving thousands of *Pseudomonas simiae* WCS417r (WCS417r) mutant bacteria highlighted the relative importance of motility genes as such genes were overrepresented among genes mutated in colonization-depleted WCS417r variants (Cole *et al.*, 2017). Swimming was also reported to be an important trait for early colonization in root-associated bacteria *Bacillus subtilis* (Allard-Massicotte *et al.*, 2016).

Similar to the present research, altered bacterial motility of evolved isolates during adaptation was reported in an evolution experiment involving the gram-positive rhizobacterium, *B. subtilis* DK1042 (DK1042) (Nordgaard *et al.*, 2021). DK1042 rapidly adapted to Arabidopsis following 12 consecutive transfers from seedling to seedling in a hydroponic system. Evolved DK1042 isolates displayed increased root-colonization ability, which was associated with robust biofilm formation in response to the plant polysaccharide xylan. Surprisingly, in contrast with the *Pseudomonas* mutants from the present study, DK1042 mutants were significantly impaired in both swimming and swarming motility (Nordgaard *et al.*, 2021). In another experimental evolutionary study involving *Bacillus thuringiensis* 407 Cry$^-$ (Bt407) and Arabidopsis, and using the same hydroponic setup as described by Nordgaard *et al.* (2021) but performed over 40 cycles, led to the emergence of isolates with reduced swimming and enhanced swarming motility in two out of five lineages (Lin *et al.*, 2021). These findings support the notion that swimming motility is not an important competence trait in the hydroponic environment. It is possible that the combination of hydroponic growth and continuous shaking facilitated random contact between bacterial cells and seedlings therewith reducing the importance of motile behavior for bacterial fitness (Lin *et al.*, 2021; Nordgaard *et al.*, 2021). Our current hypothesis is that bacteria are likely to benefit from bacterial swimming ability when host plants are grown in a static environment, like sand in the present research using *P. protegens* CHA0.

Swarming, like swimming, is driven by the flagellum but in addition depends on the production of several compounds, including quorum-sensing molecules and biosurfactants. Swarming motility describes a rapid multicellular movement of surfactin-aided rafts of cells across a surface (Kearns, 2010). Bacterial swarming motility plays an important role in biofilm formation, which is a prerequisite for bacterial proliferation on roots (Hansen *et al.*, 2007a). Interestingly, several evolved CHA0 isolates from four out of five independent lines demonstrated a worsened ability to swarm (**Chapter 2**). In addition, the previously mentioned Arabidopsis-Bacilli evolutionary studies revealed that swarming motility of DK1042 and Bt407 evolved to opposite directions under identical conditions (Lin *et al.*, 2021; Nordgaard *et al.*, 2021). In addition to

enhanced swarming ability of Bt407 isolates, these isolates gained a stronger ability to aggregate to form microcolonies, which in turn benefits their ability to form a strong biofilm on colonized Arabidopsis roots and a faster biofilm on fresh seedlings (Lin *et al.*, 2021). In combination with the worsened swimming ability in these mutants, these results are indicative for a fundamental trade-off between swimming and swarming (Lin *et al.*, 2021). Such trade-off was also observed in CHA0 isolates in the present research, but then in a reverse manner (**Chapter 2**).

In contrast to the trade-off between swimming and swarming of evolved CHA0 or Bt407 isolates, the evolved DK1042 showed both worsened swimming and swarming motility. Nordgaard *et al.* concluded that bacterial motility is not important for root colonization in this environment based on the appearance of motility-impaired isolates in multiple independent populations (Nordgaard *et al.*, 2021). By reviewing these isolates in detail, disruptive mutations in several flagellum biosynthesis genes, i.e., *fliF*, *fliK*, *fliM*, and *hag*, were identified (Nordgaard *et al.*, 2021), which explained the worsened swimming and swarming behavior for the same isolates. In comparison, evolved motility-altered Bt407 isolates are the result of mutations in the global regulator *Rho* (Lin *et al.*, 2021), which indirectly regulates bacterial motility. This suggests that the phenotypically similar impairment of motility can derive from highly diverse genetic adaptations. Altogether, this suggests that mere description of the morphological changes of bacterial motility might not be sufficient to explain bacterial adaptation strategy in rhizosphere. In the present research, swarming-impaired isolates encoded disruptive mutations in the two-component sensor system *gacS*/*gacA*, in the flagellin biosynthesis gene *flhA*, and in the transcriptional regulator *fleQ*. *FlhA* and *fleQ* are directly involved in flagellum biosynthesis (Fig. 1a, IV). It was previously reported that mutants of *P. fluorescens* F113, with mutations in flagellar filament synthesis regulatory genes *fliC*, *fliS*, *fleQ* and *fliT*, showed reduced or completely blocked motility and therefore had lower competitive alfalfa root colonization (Capdevila *et al.*, 2004). Similarly, mutations in *flhA*, which encodes a component of the flagellar export apparatus, eliminated swarming motility of *P. protegens* Pf-5 (Song, 2015). Consistent with these reports, evolved CHA0 *flhA* and *fleQ* mutants described in **Chapter 2** and the evolved flagellum synthesis mutants of *B. subtilis* DK1042 showed impaired motility for both swimming and swarming (Nordgaard *et al.*, 2021). As flagellum rotation is essential for both types of motilities, disruptive mutations in flagellum biosynthesis genes are expected to result in motility-impaired bacteria. Instead, swarming-deficient CHA0 *gacS* or *gacA* isolates display enhanced swimming motility, which suggests the existence of distinct rhizosphere adaptation strategies that depend on the intricate regulation of swarming behavior whilst maintaining swimming motility. In Bt407, *Rho* possibly represents an analogous regulatory mechanism (Lin *et al.*, 2021).

It is also possible that mutants with altered motility benefit from other bacteria that do not encode the underlying mutations. For example, Song and coworkers (2016) showed that *P. protegens* Pf-5 (Pf-5) *gac* mutants that completely lost the ability to swarm emerged during a swarming experimental evolutionary assay (Song *et al.*, 2016). In this assay, bacterial cells were inoculated in the center of an agar plate and allowed to swarm. Subsequently, cells from the edge of the swarming colony were obtained and used for the next evolutionary cycle on a new agar plate. The appearance of swarming-deficient mutants therefore was surprising. Further analysis showed that the lack of production of the biosurfactant, orfamide, was critical for the loss of swarming motility. Bacterial surfactants are secreted molecules that can reduce surface tension and enable the spread of bacteria (Kearns, 2010). Surprisingly, the Pf-5 *gac* mutants which cannot swarm on their own, can in fact co-swarm with orfamide-producing wild type cells, if they move to the edge of swarming zone first (Song *et al.*, 2016). Such behavior is oftentimes referred to as (social) cheating, and it is frequently associated with a decrease in overall performance, which is also observed in this evolution experiment, i.e., accumulation of *gac* mutants resulted in overall decreased swarming of Pf-5 colonies. CHA0 is also a known producer of orfamide A (Sobrero *et al.*, 2017), and it is possible that the evolved CHA0 *gac* mutants achieve swarming functionality through a similar strategy as Pf-5 *gac* mutants.

Evidence to support this hypothesis derive from the observation that swarming-deficient CHA0 *gac* mutants always coexisted with swarming-proficient isolates (**Chapter 2**) (Li *et al.*, 2021b). For example, $gacA^{D49Y}$ (a swarming-deficient isolate) and the succeeding mutant $gacA^{D49Y}$ · $sadB^{R183P}$ (a swarming-deficient isolate) coexisted with *RS21275* (a suspected, yet untested, swarming-proficient isolate) and $sadB^{L258Q}$ (a swarming-proficient, albeit reduced, isolate) in line 1 (**Chapter 2**). Similar coexisting isolates were observed in line 2 in which $gacA^{Y183S}$ (a swarming-deficient isolate) appeared with $galE^{V32M}$ (a swarming-proficient, albeit reduced, isolate), $gacA^{D54Y}$ (a swarming-deficient isolate), and $gacA^{G97S}$ (a swarming-deficient isolate) appeared with *galE* · *accC* (a swarming-proficient, albeit reduced, isolate). Although we didn't measure motility of other mutants in line 4 except the $gacA^{-40T>A}$ and $gacA^{E38X}$ mutants (swarming-deficient isolates), we observed that both *gacA* mutants coexisted with mutants in *hutI* and in *argT5* that we speculate are swarming-proficient before *gacA* mutants fully dominated the population (**Chapter 2**). Surprisingly, $gacS^{G27D}$ (a swarming-proficient, albeit reduced, isolate) mutant was observed in line 3 from cycle 3 and onwards without the presence of coexisting isolates in the community. This isolate, however, only has slightly impaired swarming motility while maintaining a same level of swimming ability as the ancestor and thus likely does not depend on other cells for its motility. Alternatively, CHA0 *gac* mutants might benefit from reduced swarming motility through a functional trade-off with another beneficial trait, biofilm formation, which will be discussed in a later section.

We also identified another possible adaptive strategy that relates to bacterial motility. Specifically, we identified several mutants that are involved with the regulation of flagellar rotation (Fig. 1a, IV). The first one is *RS17350*. This gene encodes a methyltransferase domain-containing protein which might act in a similar way as methyltransferase *CheR*. CheR is involved in flagella-driven chemotaxis. It constitutively transfers methyl groups to methyl-accepting chemotaxis proteins (MCPs), therewith it increases CheA autophosphorylation, finally resulting in a clockwise rotation of flagella. López-Farfán *et al.* demonstrated that the expression of *MCP* genes in *P. putida* KT2440 is inversely correlated with proximity to maize root exudates (López-Farfán *et al.*, 2019), suggesting that chemotactic responses become less important closer to the root. Similarly, *yvaQ2* from CHA0 evolved isolates, encoding a methyl-accepting chemotaxis protein, and *fliM* from DK1042 evolved isolates, encoding a flagellar motor switch protein, regulate proton-driven clockwise rotation of the flagellum. Mutations in these genes result in partial impairment of bacterial motility. These findings also illustrate how fine-tuning of motility could play a role in bacterial root adaptation.

Temporal organization of mutant selection in the rhizosphere?

Throughout the evolution experiment we identified 35 mutations, including single-nucleotide polymorphisms, insertions, and deletions, that are distributed over 28 genes (**Chapter 2**). Most of the mutations were distributed evenly across the CHA0 genome, and as expected for independently evolving populations, all of the mutations we identified were unique for each population. Given the limited number of mutations we assume that recurrent mutation of the same gene or genetic region is indicative of strong selection pressure. Notably, we observed such recurrent mutations in several of the same genes and/or pathways, including *gacA* and *gacS*, the *OBC3* gene cluster (*oafA* (twice), *galE*, and *RS09880*), a putative pyoverdine siderophore biosynthesis cluster (*pvdS* and *RS21275*) and also *sadB.* Thus, we assume that the associated processes are critical for CHA0 fitness in the Arabidopsis rhizosphere in the experimental setup used.

In a stable environment, bacterial populations are thought to gradually approach a phenotypic optimum likely involving stepwise substitution of favorable mutations. In three independent evolutionary lines, adaptive mutations in *OBC3* genes and in *gac* genes evolved in a seemingly, structured temporal fashion, i.e., we always observed the emergence of *OBC3* mutants before the emergence of *gac* mutants. Specifically, the *gacA*^{D49Y} mutation evolved in the *oafA*^{Y335X} background in line 1 and both *gacA*^{D54Y} and *gacA*^{G97S} mutations evolved in the background of the *galE*^{V32M} mutation in line 2. Notably, mutant *gacA*^{Y183S} evolved in line 2 at cycle 2, independent of *galE*^{V32M}, but this mutant was outcompeted by the *galE* · *gacA* double mutant in later cycles. Only in line 4, *gacA* mutants evolved without a preceding *OBC3* mutation. These results

suggest a possible genetic interaction between *OBC3* and *gac* genes during bacterial rhizosphere competence. The fact that we never found *gac* mutants appear before *OBC3* mutations might just be a coincidence due to the limited number of evolved isolates, but alternatively, it could indicate that *OBC3* mutations are essential for *gac* mutants to establish their strong competitive advantage.

An adaptation model proposed by Sir Ronald Fisher suggests that small phenotypic effects are more likely to bring a population closer to its fitness optimum, rather than those having larger effects (Orr, 1998). This could be explained by emphasizing the pleiotropic nature of most mutations. Pleiotropism is defined as the phenomenon that a single mutation affects multiple wild-type traits in a seemingly untargeted way (Stearns, 2010). Following our previous assumption on the temporal nature of adaptation, early selected *OBC3* mutations could be more important for bacterial root adaptation than the later arrived two-component regulatory system *gac* mutants.

Recurrent mutations in the cell surface decoration *OBC3* gene cluster and in the GacS/GacA two-component regulator system drive rhizosphere adaptation

Cell envelope modification altered bacterial fitness

The bacterial cell envelope serves an important role to maintain bacterial cellular integrity and it is the first point of interaction with the environment. It supports structural stability, affects self-recognition, influences motility, protects against invaders, and affects many other processes such as exopolysaccharide exudation by the embedding of specific proteins (Simpson & Trent, 2019). In Gram-negative bacteria, the cell envelope largely consists of heterogeneous glycolipids, namely lipopolysaccharides (LPS). Bacteria evolved to fine-tune the modification of LPS structures to quickly adapt to diverse and often hostile environments. Consequently, a high diversity of LPS structures is observed between and within bacterial species (Lam *et al.*, 2011; Kutschera & Ranf, 2019). Modification of the O-antigen domain of the LPS, one of the three functional domains of LPS, represents the majority of LPS diversity (Lerouge & Vanderleyden, 2001; Raymond *et al.*, 2002; Lam *et al.*, 2011).

In the present study, several mutations were found in a single gene cluster responsible for the biosynthesis of long O-antigen, i.e., *OBC3*, one of the clusters which is responsible for O-antigen polysaccharide biosynthesis in *P. protegens* (Kupferschmied *et al.*, 2016). Identification of mutations in *OBC3* genes in four out of five evolutionary lines strongly suggests that LPS modification plays an important role in the adaptation of CHA0 to the Arabidopsis root rhizosphere (Fig.1a, II). Also, in *B. thuringiensis* it was reported that isolates with mutations in genes related to peptidoglycan biosynthesis evolved in

multiple lineages during adaptation to the plant rhizosphere (Lin *et al.*, 2021), further corroborating the importance of envelope modification during bacterial adaptation in the rhizosphere.

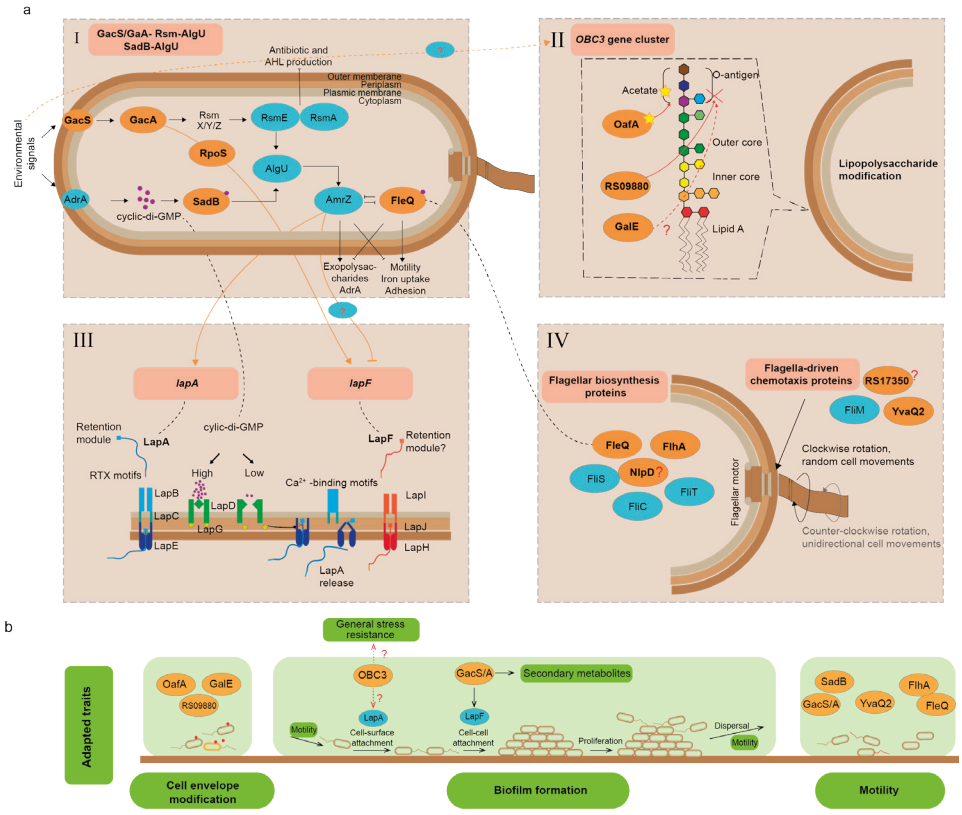

Figure 1 Rhizosphere adaptation of *P. protegens* CHA0.
a) Adapted genes and linked pathways of CHA0 during rhizosphere adaptation. I, The Gac-Rsm-AlgU and SadB-AlgU pathways in plant-beneficial *Pseudomonas* spp. for the regulation of bacterial motility and metabolism. II, *OBC3* gene cluster regulates O-antigen modification. III, mechanism of the large adhesion proteins LapA and LapF regulating bacterial attachment in *P. putida* KT2440. LapA regulation is mediated by transcription factors such as FleQ and GacA, while FleQ and RpoS are important for the regulation of LapF. FleQ and SadB regulatory activity is also determined by cyclic-di-GMP levels. IV, two groups of proteins are involved in flagella-driven chemotaxis in gram-negative bacteria. b) Adapted bacterial traits of CHA0 during rhizosphere adaptation. Three major changes are bacterial cell envelope modification regulated by *OBC3* gene cluster, bacterial biofilm formation alteration through LapA and LapF, and bacterial motility alteration from GacS/GacA, SadB and fleQ mutations. The proteins with bold names (orange background) are targeted in the here described evolution experiment. The question marks indicate a here-speculated function and/or an unknown protein based on prediction and protein similarity. *OBC3*: O-antigen biosynthesis gene cluster 3; Cyclic-di-GMP: cyclic dimeric guanosine monophosphate; RTX: repeats-in-toxin; RsmX/Y/Z: small non-coding RNA. Figure 1a is adapted from Zboralski & Filioin 2020.

High diversity of the O-antigen influences bacterial adaptation in a variety of conditions. Previous research on the role of O-antigen during host-microbe interactions

particularly focused on its potential to act as a MAMP, and how its' integrity affects virulence on various hosts (Lerouge & Vanderleyden, 2001; Knirel *et al.*, 2015; Maldonado *et al.*, 2016; Huszczynski *et al.*, 2020). MAMPs are conserved microbial structures or chemical patterns which can be recognized by plants, which include bacterial LPS, flagellin, lipoproteins, peptidoglycans, and conserved proteins such as EF-Tu (elongation factor Tu) (Jones & Dangl, 2006; Choi & Klessig, 2016). In the present study, we demonstrated that O-antigen modification benefits CHA0 during bacterial root attachment (**Chapter 3**). This, in turn, explains their potential to outcompete the ancestral strain and aligns with our observation that *oafA* and *galE* mutations became fixed in the evolution experiment (Chapters 2 & 3). In contrast to the observed reduction in bacterial fitness of LPS mutants from other studies (De Weger *et al.*, 1989a; Kupferschmied *et al.*, 2016; Rapicavoli *et al.*, 2018), our study on mutant *oafA-1*, one of four observed spontaneous *OBC3* mutants, revealed its unaltered metabolic versatility compared to the wild type (**Chapter 3**). We studied all *OBC3* mutants in more detail with respect to their resistance to various environmental stresses, such as drought, oxidative, alkaline, acid and antibiotics like penicillin, streptomycin. The results revealed that all of them have comparable resistance to the ancestral CHA0 wild type (**Chapter 2**).

Besides influencing interactions with the host, O-antigen also serves as a critical site of recognition for bacteriophages (Knirel *et al.*, 2015; Herman, 2015). Bacteriophages, or shortly phages, are viruses that can infect and replicate within bacteria. They are ubiquitous in nature and modulate bacterial populations by driving the abundance and diversity of bacteria, but also their activities (Buckling & Rainey, 2002; Naureen *et al.*, 2020). Bacterial fitness trade-offs among important traits, while they are adapting in a complex environment, have been observed. For instance, bacterial fitness trade-offs between bacterial motility and phage resistance (Koskella *et al.*, 2011), or between bacterial virulence and phage resistance (Evans *et al.*, 2010a; Kupferschmied *et al.*, 2016) were reported. To investigate whether *OBC3* mutation-driven changes in the O-antigen affect phage susceptibility, we assessed the susceptibility of all *OBC3* mutants towards the established CHA0-compatible environmental phage, ΦGP100 (**Chapter 4**). Phage plaque assays revealed that some of the evolved *OBC3* mutants indeed display altered phage sensitivity. While *oafA* mutants display unaltered phage sensitivity, the mutations in *galE* and *RS09880* are completely resistant to ΦGP100 infection. We then used SDS-polyacrylamide gel electrophoresis to further analyze the LPS structure of *OBC3* mutants. Surprisingly, we found that the integrity of the LPS corresponds fully with phage-sensitivity, as changes in said integrity, as seen in the *galE* and *RS09980* mutants, correspond directly with reduced phage sensitivity (**Chapter 4**). Initially we pondered whether phage contamination could have been a driver for the emergence of *OBC3* mutations, yet, the observation that *oafA* mutants

– which evolved in two independent lines – are as susceptible as the wild type to phage predation whilst also showing no obvious differences in LPS structure suggested to us that this was not the case. This hypothesis is further corroborated through the analysis of population sequencing data, derived from the evolution experiment and follow-up competition experiments, which revealed neither environmental phage particles nor an indication for prophage induction (**Chapter 4**). We thus conclude that although the *OBC3* mutation-based LPS modifications can result in phage-sensitivity changes, this is likely a side-effect of the LPS structure change evolved to increase root attachment. Interestingly, we further found that the *OBC3* gene cluster is located in close proximity to a prophage region in the CHA0 genome and is characterized by similar genomic characters such as GC skew (**Chapter 4**) (Jousset *et al.*, 2014). Although not a definitive proof, it suggests that the *OBC3* gene cluster, or at least some of its genes, might derive from genetic recombination or horizontal gene transfer during phage-genome integration which is further corroborated by the presence of a centrally-positioned transposase gene in the *OBC3* gene cluster (**Chapter 4**). In the present study, we did however not find a direct link between the *OBC3* gene cluster or any of the prophage regions.

OafA serves as a switch for acetylation of diverse polysaccharides?

OafA encodes an acetyltransferase, predicted to be involved in the acetylation of the O-antigen on the bacterial cell surface. To obtain a better understanding of *oafA* functionality and its evolutionary origin, we identified and characterized homologous *oafA* genes from multiple environmental *P. protegens* strains by computational analysis. Intriguingly, some of them appear to have acquired similar mutations as the ones we identified in the evolution experiment (**Chapter 4**). Since these strains originate from diverse environments, i.e., not only the rhizosphere but also from a river and from decaying fruits, we hypothesize that *oafA* and its associate mutations serve to enhance bacterial fitness in a broader sense for *P. protegens*.

The site of mutation, which refers to the position in the gene that is mutated, is located between the genetic regions encoding two functionally separate protein domains. As a result of the mutation, a premature stop codon is introduced disconnecting both domains. In *P. protegens, oafA* encodes a protein with an N-terminal acetyltransferase-3 (AT3) domain and a C-terminal SNGH domain. OafA AT3-SGNH fusion acetyltransferases, like CHA0 OafA, are common among bacteria, yet in a variety of organisms also AT3-only acetyltransferases can be found (Pearson *et al.*, 2020). In *Salmonella enterica* serotype Typhimurium (*S.* Typhimurium), it was shown that the fusion of the AT3 domain with the SGNH domain is essential for appropriate acetylation of the O-antigen. In this system the AT3 domain is responsible for the transfer of an acetyl group across the membrane and the SGNH domain for the transfer of this

group to the appropriate position on the O-antigen. Interestingly, acetylation of the correct O-antigen moiety could be reconstituted by the SGNH domain alone, i.e., without the presence of the normally-fused AT3 domain. Reversely, expression of the AT3-only equivalent resulted in promiscuous acetylation suggesting that the SGNH domain plays a critical role in substrate specificity (Pearson *et al.*, 2020).

Given the location of *oafA* mutations and the specific protein domain functionalities, we speculate whether loss or change of specificity of the CHA0 OafA AT3-only acetyltransferase results in the acetylation of a different target carbohydrate such as the peptidoglycan or extracellular polysaccharides (exopolysaccharides or EPS). Since CHA0 is a gram-negative bacterium, the peptidoglycan layer is not exposed to the environment, which we believe is unlikely to explain the altered rhizosphere competence via increased root attachment as we observed in *oafA* mutants. Instead, we hypothesize that OafA AT3-only mutant protein results in the acetylation of the exopolysaccharide near the outer membrane. The altered exopolysaccharide could boost bacterial biofilm formation, strength and self-recognition (Dragoš *et al.*, 2018; Pearson *et al.*, 2022). This would fit with our observation that *OBC3* mutants display enhanced root attachment, commonly associated with stronger biofilm formation. Furthermore, such genetic regulation of OafA could serve a much broader role in adaptive bacterial fitness in diverse environments (Fig. 1b). Till now, we did not obtain evidence to show that differentially acetylated exopolysaccharide could enhance bacterial biofilm formation in CHA0, but this is an interesting and important topic for future research.

GacS/GacA global regulators: an important pleiotropic switch

Many *Pseudomonas* species exhibit phenotypic variation resulting from spontaneous mutation in the *gacS/gacA* regulatory system, as was previously reported by Van Den Broek and coworkers (Van Den Broek *et al.*, 2005). Such mutants appeared in CHA0 in the present study during adaptation to the plant rhizosphere (**Chapter 2**), but also in *P. protegens* Pf-5 when evolved *in vitro* on agar as described by Song and coworkers (Song *et al.*, 2016). *GacS* and *gacA* encode for the sensor kinase GacS and the transcriptional response regulator GacA, respectively. Together, they regulate the production of antimicrobial secondary metabolites, exoenzymes, and siderophores, and also control biofilm formation, stress responses, motility, and quorum sensing (Bull *et al.*, 2001; Heeb & Haas, 2001; Workentine *et al.*, 2009). Strains carrying *gac* mutations are hypothesized to have a reduced metabolic load compared with their ancestors, and consequently, mutants generally have a growth advantage (Van Den Broek *et al.*, 2005). In the present study, mutations in the GacS/GacA two-component regulator system caused dramatic changes in several bacterial phenotypic traits, including enhanced swimming and reduced swarming motility, reduced bacterial carbon source utilization and diminished social traits, such as proteolytic activity and siderophore production

(**Chapter 2**). In addition, *gac* mutants also display reduced production of several, potentially toxic, secondary metabolites, which benefits plant growth (**Chapter 2**) (Li *et al.*, 2021a). These findings suggest an important pleiotropic switch function of GacS/GacA two-component system for enabling bacterial adaptation within a certain environment.

Revisit evolved adaptive mutations: a possible bacterial range expansion strategy with a thinner biofilm structure?

When rhizosphere-inhabiting bacteria are in the vicinity of plant roots, they switch from a planktonic to a sessile lifestyle to better benefit from the root exudates. This change is made possible by chemotaxis towards exudates, enabling the bacteria to get closer to the roots, and by biofilm formation, allowing them to attach to the roots and to develop fixed colonies (Danhorn & Fuqua, 2007).

Motility regulatory genes also affect biofilm formation

Bacterial biofilm development is a multi-step process starting from reversible attachment, followed by irreversible attachment, micro-colony formation to finally biofilm maturation and dispersal of bacteria (Castiblanco & Sundin, 2016) (Fig. 1b). Adhesins are adhesive structures, mostly proteins, expressed on the bacterial surface to promote attachment to a surface, a host or to other bacteria (Monds & O'Toole, 2009). We observed enhanced bacterial attachment of evolved *OBC3* mutants and propose that this is caused by increased irreversible attachment as the collected bacteria were still firmly attached on the root following multiple wash steps (**Chapter 3**). Several mutations we found were in genes that can be linked to the regulation of motility, namely, *gacS/gacA*, *fleQ*, *sadB* (twice), *rpoS* and *nlpD* (Fig. 1a, IV). Surprisingly, all of these genes directly or indirectly regulate the protein pair LapA and LapF (Zboralski & Filion, 2020) (Fig. 1a, III). LapA and LapF are large adhesion proteins, which are found in many rhizosphere-associated *Pseudomonas* spp. (Hinsa *et al.*, 2003; Martínez-Gil *et al.*, 2010, 2014). Fox *et al.* demonstrated that in *P. protegens* Pf-5, *lapA* was essential for wheat root colonization but dispensable for survival in soil (Fox *et al.*, 2016).

LapA belongs to the repeats-in-toxin (RTX) adhesion protein family, produced at the beginning of biofilm formation to promote cell-surface attachment; the highly similar protein, LapF, is synthesized at a later stage of biofilm formation, allowing cell-cell attachment (Hinsa *et al.*, 2003; Martínez-Gil *et al.*, 2010, 2014; Zboralski & Filion, 2020). Both *lapA* and *lapF* are under the control of the two-component regulatory system GacS/GacA, and their transcription is responsive to the intracellular levels of the second messenger cyclic dimeric GMP (c-di-GMP) in opposing ways (Martínez-Gil

et al., 2014). C-di-GMP is a ubiquitous, intracellular signalling molecule, mediating bacterial lifestyle transition from a planktonic motile one, to a non-motile, sessile one (Valentini & Filloux, 2016). It interacts with several key components in the bacterial cell, including the beforementioned transcriptional regulars FleQ and SadB (Fig. 1a, I). FleQ is a c-di-GMP-binding protein that in response to c-di-GMP binding functions as a transcriptional regulator (Muriel *et al.*, 2019). SadB, a regulator involved in the control of flagellum biosynthesis acts upstream of FleQ, and is positively regulated by c-di-GMP levels (Caiazza & O'Toole, 2004; Martínez-Granero *et al.*, 2012; Muriel *et al.*, 2019). It specifically binds c-di-GMP at the physiological levels and with an affinity that is much higher than that of FleQ (Muriel *et al.*, 2019). Once c-di-GMP is sensed by SadB, it activates *algU* transcription (Martínez-Granero *et al.*, 2012), and further regulates the transcription of the *fleQ* transcriptional repressor *AmrZ* (Martínez-Granero *et al.*, 2012; Muriel *et al.*, 2018). In *P. fluorescens* F113 and in *Pseudomonas aeruginosa* PAO1, the hub AmrZ/FleQ was shown to be a transcriptional repressor which controls the expression of flagellum biosynthesis genes (Martínez-Granero *et al.*, 2012; Jones *et al.*, 2014; Blanco-Romero *et al.*, 2018). Thus, high levels of c-di-GMP represses flagellum biosynthesis through binding of FleQ directly or indirectly via the SadB – AlgU pathway, activating in turn genes like *lapA* for the production of exopolysaccharides related to biofilm formation (Baraquet *et al.*, 2012; Muriel *et al.*, 2019; Zboralski & Filion, 2020) (Fig. 1a, III).

Given its role in flagellum biosynthesis, we expected that the *fleQ* mutant to be impaired in both swimming and swarming motility, and our observation in **Chapter 2** confirmed this. Conversely, we expected that *sadB* mutation would lead to increased motility behavior, both swimming and swarming, but our observations in **Chapter 2** showed that the isolated *oafA* · *RS17350* · *sadB* triple mutant displayed enhanced swimming and worsened swarming compared to its direct progenitor. The worsened swarming of this triple mutant might be caused by yet unknown group behavior, driven by biosurfactant production for example (Caiazza *et al.*, 2005), or by a hitherto unidentified genetic interaction with *oafA* or *RS17350*. It was previously reported that a *S.* Typhimurium *rpoE* mutant, a homolog of *algU* in pseudomonads, relied on intact LPS O-antigen for its protective role of the cell envelope, although *rpoE* itself is not essential in *S.* Typhimurium (Amar *et al.*, 2018). Considering the alterations in O-antigen structure in the *galE* mutant used in Amar's research and in the *oafA* mutant in the current study, we hypothesize that a similar interaction between *sadB* and *oafA* could underlie the worsened-swarming motility. In addition, AlgU is converged upon by both Gac-Rsm and SadB signal transduction pathways to downregulate motility in *P. fluorescens* 113 (Martínez-Granero *et al.*, 2012) (Fig. 1a, I). This is in alignment with our observation of enhanced swimming motility of all *gacA* mutants and specifically with the stepwise increase in swimming motility observed for the *oafA* · *RS17350*

double mutant, the *oafA · RS17350 · gacA* triple mutant to the *oafA · RS17350 · gacA · sadB* quadruple mutant (**Chapter 2**). In the end, both pathways that converge upon AlgU to downregulate motility have been disrupted. Based on these comparisons with *P. fluorescens* F113 and *P. aeruginosa* PAO1, we hypothesize that the worsened swarming motility of *gac* mutants might result from the enhanced expression of the downstream biofilm formation gene, *lapF*, which regulates bacterial cell-cell attachment and therewith limits swarming (Fig. 1a, III).

The GacS/GacA system positively regulates the expression of biofilm-associated genes *lapA* and *lapF*, along with genes involved in biosynthesis of many antibiotic compounds and extracellular enzymes. LapF is required for biofilm maturation and its three-dimensional development, and shown to respond to the stationary-phase RNA polymerase sigma factor RpoS (Martínez-Gil *et al.*, 2014). A *lapF* mutant is still able to irreversibly attach to a surface but is unable to form micro-colonies and mature biofilms, and to competitively colonize plant roots. The transcriptional regulator FleQ is required for the modulation of *lapA* expression by c-di-GMP but has a minor influence on *lapF*. Since *lapA* and *lapF* are regulated by both the GacS/GacA system and the c-di-GMP – FleQ pathway, disruption of each pathway would reduce bacterial biofilm formation. Mutations in *fleQ, rpoS* or *gacS/gacA* can result in downregulation of *lapA* and *lapF*, which is expected to reduce bacterial biofilm formation either during cell-surface interaction (*fleQ*), cell-cell interaction (*rpoS*) or both kinds of interactions (*gacS/gacA*). In the present research, all these mutants appeared separately, in different independent lines, which could indicate that these adaptive trajectories are mutually exclusive in the sense that combined disruption reduces competitiveness and are potentially deleterious.

An altered bacterial biofilm structure as bacterial rhizosphere adaptation strategy?

The *gac* mutants evolved in four out of five independent lines and the *fleQ* and *rpoS* mutants in the fifth. Altered bacterial motility in isolates carrying these mutations has been confirmed, while altered biofilm formation is hypothesized. A somewhat comparable adaptive strategy was found in *B. thuringiensis* during evolution in the rhizosphere. Specifically, evolved isolates displayed stronger aggregation during the formation of microcolonies (Lin *et al.*, 2021). These isolates could not form a mature biofilm, which possibly allows bacteria to form small communities that can protect the individual cells in the community on the one hand, and to spread faster during colonization as new cells won't attach onto the current layer of biofilm on the other hand. Such morphological adaptation fits general observations with respect to the *gac* mutants. Firstly, it has been reported that *gac* mutants typically display no significant differences during planktonic growth (Parkins *et al.*, 2001), neither do they displace

wild type cells in nutrient-rich liquid media or in sterile soil (Chancey *et al.*, 2002; Driscoll *et al.*, 2011). Secondly, while not losing its fitness with regards to growth, a *gacA* mutant of *P. aeruginosa* PA14 is defective in biofilm development, which is probably due to its inability to aggregate into microcolonies (Parkins *et al.*, 2001). Lastly, several studies point to the formation of mixed biofilms composed of wild type cells and *gac* mutant cells in which *gac* mutants form a connected biofilm with their wildtypes but do not overlay the wildtype-biofilm (Driscoll *et al.*, 2011; Song *et al.*, 2016). This is reminiscent of reduced cell-cell attachment in *gac* mutants as discussed previously. Summarizing, we hypothesize that *gac* mutations alter bacterial biofilm structure rather than quantity. Specifically, *gac* mutants might form a thin layer of biofilm without developing into a mature three-dimensional structure. With the same growth rate as their ancestral strains, *gac* mutants therefore benefit by forming a thinner biofilm in exchange for faster expansion. If this speculation is true, it is reasonable to think that other motility mutations could result in a similar phenotype, which, in total, suggests that biofilm restructuring is an important strategy for CHA0 adaptation in the rhizosphere.

The stepwise adaptation in the rhizosphere

I would like to propose a model for the bacterial stepwise adaptation in the rhizosphere that we observed and describe in this thesis. Since we observed most variation, both genetic and phenotypic, in independent line one from the present research, I will describe this stepwise adaptative model based on the bacterial evolution that occurred in this line (Fig. 2). At first, CHA0 cells colonize Arabidopsis and exploit the available root-derived carbohydrates for their growth in an otherwise nutrient-sparse environment. As a consequence of said exploitation, plants suffer, activate root immunity (Stringlis *et al.*, 2018a), boost toxic secondary metabolites production and reduce exudation of carbohydrates from the root. These changes impose the first selective pressure. Bacteria now sense and experience this hardened environment resulting in the selection of cell surface decoration mutants that are beneficial for three potential purposes: 1) the modified cell envelope could enhance resistance against the toxic metabolites, and 2) changes in the MAMP LPS structure that are released by cellular lysis could attenuate plant immunity, and finally 3) increased attachment to the nutrient-rich area in root environment. Our research on the cell envelope decoration mutants, e.g., $oafA^{Y335X}$ in line one, corroborate this third hypothesis: $oafA^{Y335X}$ mutant cells strongly and rapidly attach to the root cell.

Following this first adaptation, the *oafA* · *RS17350* double mutant appeared, which due to the predicted role of *RS17350*, encoding a methyltransferase, in flagella rotation, could be selected as a consequence of reduced random-cell movement therewith saving energy and forming a more stable colony in the present location. During

subsequent cycles, the *oafA* · *RS17350* · *gacA* triple mutant appeared and we predict that this mutant could form a thinner biofilm layer, therewith enhancing bacterial proliferation on the growing root by spreading faster to uncharted territory as small aggregated communities. Concomitantly, *gacA* mutation reduced bacterial secondary metabolite production, including many toxic ones (Li *et al.*, 2021a), relieving stress to the plants therewith benefiting the plant-microbe interaction as a whole. These triple mutant cells become the dominant genotype in the rhizosphere microbe population. Next, isolates with enhanced swimming ability such as the quadruple mutant carrying a *sadB* mutation are selected (Fig. 2).

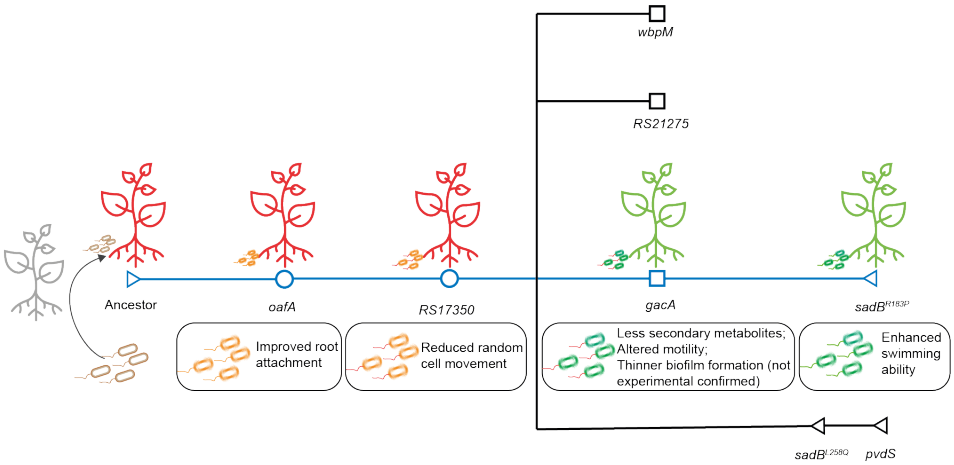

Figure 2 Stepwise adaptation of *P. protegens* CHA0 in the rhizosphere.
Genealogy of the evolved mutants in experimental line one that are selected in cycles 2 (circle symbol), 4 (square symbol) and 6 (reverse-arrow symbol) and ancestral strain from the initial phase (arrow symbol). The adaptation steps described in texts are marked as blue. The mutations and corresponding bacterial trait changes for the evolved mutants are illustrated (above the line) and described (under the line). The mutants' bacterial plant performance are illustrated above the line by color (red, plant growth inhibition; green, plant growth promotion). As the microbial community in the rhizosphere is composed of a mix of multiple genotypes, the presented plant-microbe interaction might not be representative for the whole community.

Figure legends mentioned references: (Zboralski & Filion, 2020)

Conclusion

Phenotypic and genotypic variation in the single strain bacterial community

Bacterial phenotypic variation, cells within an isogenic population displaying variable expression patterns, is a common phenomenon that occurs in almost any bacterial culture (Smits *et al.*, 2006). It brings new subpopulations in an overall genetically homogeneous population, which might increase the overall fitness of the bacterial community (Van Den Broek *et al.*, 2005; Smits *et al.*, 2006; Grote *et al.*, 2015). This variation is a regulatory mechanism at the DNA level which usually results in high frequency, reversible switches between colonies with a distinct phenotype. Under certain circumstances, like when experiencing unfavorable conditions such as presented by low-nutrient availability, extreme changes in the pH, or when switching between hosts, transcription-level-regulated phenotypic variation might be insufficient for adapting to these changes. In such event, beneficial mutations that arise across bacterial populations by chance can become selected. As an example, phenotypic variation resulting from spontaneous *gac* mutations were found in many rhizosphere-derived *Pseudomonas* spp. (Van Den Broek *et al.*, 2005; Song *et al.*, 2016). At the community level, bacteria growing in biofilms show a high degree of spatial and temporal heterogeneity (Branda *et al.*, 2005). Changes in the biofilm structure not only alter bacterial community fitness but also affect cell-to-cell interactions via processes like quorum-sensing, which further modify bacterial physiology (Parsek & Greenberg, 2005; Diggle *et al.*, 2007; Goo *et al.*, 2015). As for the multi-host strain *P. protegens* CHA0, a fast adaptive population strategy such as biofilm structure change is useful to adapt to changing environmental conditions or when switching between hosts. We speculate that bacterial genotypic variation, similar to bacterial phenotypic variation, supports bacterial fitness in a community and is likely ubiquitous in nature. With the rapid improvement of single-cell technologies including sequencing and metabolomics, we might be able to track natural variation of single bacterial species on a small spatial and short temporal scale.

From lab to nature: microbial evolution in a microbial community context

Although the evolution experiments in the Arabidopsis rhizosphere with CHA0 yielded novel information about microbial evolution in the rhizosphere, the question remains to what extend the discovered features play a role in microbial evolution in a microbial community context. Interestingly, we did detect certain lab-evolved mutants, like *oafA* mutants, that have also been discovered in environmental *Pseudomonas* strains. Additionally, spontaneous GacS/GacA mutants were also found in *in vitro* experiments of CHA0 (Song *et al.*, 2016) and in several other studies with plant-associated bacteria, such as *Pseudomonas* sp. PCL1171, *P. fluorescens* F113, *Bordetella*

bronchiseptica and *Asospirillum lipoferum* (Van Den Broek *et al.*, 2005). While in our study GacS/GacA mutations were related to *oafA*-regulated LPS decoration, in the other studies these mutants were found to be affected in different bacterial adaptation traits, like alteration of bacterial motility and biofilm formation, which fits the global regulatory nature of GacS/GacA. In a microbial community context, evolution of individual microbiota members will not only be influenced by the host plant, but also by microbe-microbe interactions in the rhizosphere microbial community. This would likely lead to completely different plant-microbe and microbe-microbe interaction dynamics when compared to evolution of a single microbe in a mono-association. In a microbial community context, CHA0 would interact with many other microbes in rhizosphere, resulting in regional antagonistic or symbiotic bacteria-bacteria interactions, different plant responses triggered by other microbes in the rhizosphere, and corresponding regional changes in root exudates profiles. This will likely shape CHA0 evolution differently than in the present study. Hence, future research should focus on increasing our understanding of bacterial adaptation in progressively more complex environments. This is especially important when considering sustainable agriculture that is supported by robust, rhizosphere-competent bioinoculants for the protection of plants against pests and pathogens and for the improved uptake of nutrients and water.

Acknowledgments

This work was supported by a China Scholarship Council fellowship (to H.Z.). I thank Corné Pieterse and Ronnie de Jonge for providing valuable comments and suggestions on the draft manuscript, and Sanne Poppeliers, Juan José Sanchez-Gil, and Gijs Selten for suggestions on the illustrations.

References

Agaras BC, Scandiani M, Luque A, Fernández L, Farina F, Carmona M, Gally M, Romero A, Wall L, Valverde C. 2015. Quantification of the potential biocontrol and direct plant growth promotion abilities based on multiple biological traits distinguish different groups of *Pseudomonas* spp. isolates. *Biological Control* **90**: 173–186.

Agnihotri R, Sharma MP, Prakash A, Ramesh A, Bhattacharjya S, Patra AK, Manna MC, Kurganova I, Kuzyakov Y. 2022. Glycoproteins of arbuscular mycorrhiza for soil carbon sequestration: review of mechanisms and controls. *Science of the Total Environment* **806**: 1–13.

Ahmad NH, Mustafa S, Man YBC. 2015. Microbial polysaccharides and their modification approaches: A review. *International Journal of Food Properties* **18**: 332–347.

Akoh CC, Lee GC, Liaw YC, Huang TH, Shaw JF. 2004. GDSL family of serine esterases/lipases. *Progress in Lipid Research* **43**: 534–552.

Alexander DB, Zuberer DA. 1991. Use of chrome azurol S reagents to evaluate siderophore production by rhizosphere bacteria. *Biology and Fertility of Soils* **12**: 39–45.

Allard-Massicotte R, Tessier L, Lécuyer F, Lakshmanan V, Lucier JF, Garneau D, Caudwell L, Vlamakis H, Bais HP, Beauregard PB. 2016. *Bacillus subtilis* early colonization of *Arabidopsis thaliana* roots involves multiple chemotaxis receptors. *mBio* **7**: e01664-16.

Allison GE, Verma NK. 2000. Serotype-converting bacteriophages and O-antigen modification in *Shigella flexneri*. *Trends in Microbiology* **8**: 17–23.

Altschul SF, Koonin E V. 1998. Iterated profile searches with PSI-BLAST - a tool for discovery in protein databases. *Trends in Biochemical Sciences* **23**: 444–447.

Amar A, Pezzoni M, Pizarro RA, Costa CS. 2018. New envelope stress factors involved in σ^E activation and conditional lethality of *rpoE* mutations in *Salmonella enterica*. *Microbiology* **164**: 1293–1307.

Arndt D, Grant JR, Marcu A, Sajed T, Pon A, Liang Y, Wishart DS. 2016. PHASTER: a better, faster version of the PHAST phage search tool. *Nucleic Acids Research* **44**: W16–W21.

Asadulghani M, Ogura Y, Ooka T, Itoh T, Sawaguchi A, Nakayama K, Hayashi T. 2009. The defective prophage pool of *Escherichia coli* O157 : prophage – prophage interactions potentiate horizontal transfer of virulence determinants. *PLoS Pathogens* **5**: 1–15.

Aznar A, Chen NWG, Thomine S, Dellagi A. 2015. Immunity to plant pathogens and iron homeostasis. *Plant Science* **240**: 90–97.

Aznar A, Dellagi A. 2015. New insights into the role of siderophores as triggers of plant immunity: what can we learn from animals? *Journal of Experimental Botany* **66**: 3001–3010.

Bais HP, Park SW, Weir TL, Callaway RM, Vivanco JM. 2004. How plants communicate using the underground information superhighway. *Trends in Plant Science* **9**: 26–32.

Bais HP, Weir TL, Perry LG, Gilroy S, Vivanco JM. 2006a. The role of root exudates in rhizosphere interactions with plants and other organisms. *Annual Review of Plant Biology* **57**: 233–266.

Bais HP, Weir TL, Perry LG, Gilroy S, Vivanco JM. 2006b. The role of root exudates in rhizosphere interations with plants and other organisms. *Annual Review of Plant Biology* **57**: 233–266.

Bakker PAHM, Berendsen RL, Van Pelt JA, Vismans G, Yu K, Li E, Van Bentum S, Poppeliers SWM, Sanchez Gil JJ, Zhang H, *et al.* 2020. The soil-borne identity and microbiome-assisted agriculture: looking back to the future. *Molecular Plant* **13**: 1394–1401.

Bakker PAHM, Peer van R, Schippers B. 1990. Specificity of siderophores and siderophore receptors and biocontrol by *Pseudomonas* spp. *Biological control of soil-borne plant pathogens.*: 131–142.

Bakker PAHM, Pieterse CMJ, de Jonge R, Berendsen RL. 2018. The soil-borne legacy. *Cell* **172**: 1178–1180.

Balsanelli E, Serrato R V., de Baura VA, Sassaki G, Yates MG, Rigo LU, Pedrosa FO, de Souza EM, Monteiro RA. **2010**. *Herbaspirillum seropedicae rfbB* and *rfbC* genes are required for maize colonization. *Environmental Microbiology* **12**: 2233–2244.

Balsanelli E, Tuleski TR, de Baura VA, Yates MG, Chubatsu LS, de Oliveira Pedrosa F, de Souza EM, Monteiro RA. **2013**. Maize root lectins mediate the interaction with *Herbaspirillum seropedicae* via N-Acetyl glucosamine residues of lipopolysaccharides. *PLoS ONE* **8**: e77001-9.

Baraquet C, Murakami K, Parsek MR, Harwood CS. **2012**. The FleQ protein from *Pseudomonas aeruginosa* functions as both a repressor and an activator to control gene expression from the *pel* operon promoter in response to c-di-GMP. *Nucleic Acids Research* **40**: 7207–7218.

Barret M, Morrissey JP, O'Gara F. **2011**. Functional genomics analysis of plant growth-promoting rhizobacterial traits involved in rhizosphere competence. *Biology and Fertility of Soils* **47**: 729–743.

Barrett RDH, MacLean RC, Bell G. **2006**. Mutations of intermediate effect are responsible for adaptation in evolving *Pseudomonas fluorescens* populations. *Biology Letters* **2**: 236–238.

Barton-Willis PA, Wang MC, Holliday MJ, Long MR, Keen NT. **1984**. Purification and composition of lipopolysaccharides from *Pseudomonas syringae*. pv. *glycinea*. *Physiological Plant Pathology* **25**: 387–398.

Bashan Y, de-Bashan LE, Prabhu SR, Hernandez JP. **2014**. Advances in plant growth-promoting bacterial inoculant technology: formulations and practical perspectives (1998-2013). *Plant and Soil* **378**: 1–33.

Bastián F, Cohen A, Piccoli P, Luna V, Bottini R, Baraldi R, Bottini R. **1998**. Production of indole-3-acetic acid and gibberellins A1 and A3 by *Acetobacter diazotrophicus* and *Herbaspirillum seropedicae* in chemically-defined culture media. *Plant Growth Regulation* **24**: 7–11.

Baweja P, Kumar S, Kumar G. **2020**. Fertilizers and pesticides: their impact on soil health and environment. In: Giri B, Varma A, eds. Soil Health. Cham: Springer International Publishing, 265–285.

Bedini E, De Castro C, Erbs G, Mangoni L, Dow JM, Newman MA, Parrilli M, Unverzagt C. **2005**. Structure-dependent modulation of a pathogen response in plants by synthetic O-antigen polysaccharides. *Journal of the American Chemical Society* **127**: 2414–2416.

Bera A, Herbert S, Jakob A, Vollmer W, Götz F. **2005**. Why are pathogenic staphylococci so lysozyme resistant? The peptidoglycan O-acetyltransferase OatA is the major determinant for lysozyme resistance of *Staphylococcus aureus*. *Molecular Microbiology* **55**: 778–787.

Berendsen RL, Pieterse CMJ, Bakker PAHM. **2012**. The rhizosphere microbiome and plant health. *Trends in Plant Science* **17**: 478–486.

Berendsen RL, van Verk MC, Stringlis IA, Zamioudis C, Tommassen J, Pieterse CMJ, Bakker PAHM. **2015**. Unearthing the genomes of plant-beneficial *Pseudomonas* model strains WCS358, WCS374 and WCS417. *BMC Genomics* **16**: 1–23.

Berendsen RL, Vismans G, Yu K, Song Y, De Jonge R, Burgman WP, Burmølle M, Herschend J, Bakker PAHM, Pieterse CMJ. **2018**. Disease-induced assemblage of a plant-beneficial bacterial consortium. *ISME Journal* **12**: 1496–1507.

Berne C, Ducret A, Hardy GG, Brun YV. 2015. Adhesins involved in attachment to abiotic surfaces by gram-negative bacteria. In: Ghannoum M, Parsek M, Whiteley M, Mukherjee PK, eds. Microbial Biofilms. Washington D.C.: ASM Press, 163–199.

Berry MC, McGhee GC, Zhao Y, Sundin GW. **2009**. Effect of a *waaL* mutation on lipopolysaccharide composition, oxidative stress survival, and virulence in *Erwinia amylovora*. *FEMS Microbiology Letters* **291**: 80–87.

Bertani B, Ruiz N. **2018**. Function and biogenesis of lipopolysaccharides. *EcoSal Plus* **8**: 1–33.

Bisson LF, Fraenkel DG. **1984**. Expression of kinase-dependent glucose uptake in *Saccharomyces cerevisiae*. *Journal of bacteriology* **159**: 1013–1017.

Bitas V, Kim H-S, Bennett JW, Kang S. 2013. Sniffing on microbes: diverse roles of microbial volatile organic compounds in plant health. *Molecular Plant-Microbe Interactions* **26**: 835–843.

Bjornson M, Pimprikar P, Nürnberger T, Zipfel C. 2021. The transcriptional landscape of *Arabidopsis thaliana* pattern-triggered immunity. *Nature Plants* **7**: 579–586.

Blanco-Romero E, Redondo-Nieto M, Martínez-Granero F, Garrido-Sanz D, Ramos-González MI, Martín M, Rivilla R. 2018. Genome-wide analysis of the FleQ direct regulon in *Pseudomonas fluorescens* F113 and *Pseudomonas putida* KT2440. *Scientific Reports* **8**: 1–13.

Blin K, Wolf T, Chevrette MG, Lu X, Schwalen CJ, Kautsar SA, Suarez Duran HG, de Los Santos ELC, Kim HU, Nave M, *et al.* 2017. antiSMASH 4.0-improvements in chemistry prediction and gene cluster boundary identification. *Nucleic Acids Research* **45**: W36--W41.

Blom D, Fabbri C, Connor EC, Schiestl FP, Klauser DR, Boller T, Eberl L, Weisskopf L. 2011. Production of plant growth modulating volatiles is widespread among rhizosphere bacteria and strongly depends on culture conditions. *Environmental Microbiology* **13**: 3047–3058.

Bonachela JA, Raghib M, Levin SA. 2012. Dynamic model of flexible phytoplankton nutrient uptake. *Proceedings of the National Academy of Sciences of the United States of America* **108**: 20633–20638.

Bondy-Denomy J, Qian J, Westra ER, Buckling A, Guttman DS, Davidson AR, Maxwell KL. 2016. Prophages mediate defense against phage infection through diverse mechanisms. *ISME Journal* **10**: 2854–2866.

Bossi L, Fuentes JA, Mora G, Figueroa-Bossi N. 2003. Prophage contribution to bacterial population dynamics. *Journal of Bacteriology* **185**: 6467–6471.

Bowden SD, Hale N, Chung JCS, Hodgkinson JT, Spring DR, Welch M. 2013. Surface swarming motility by *Pectobacterium atrosepticum* is a latent phenotype that requires O antigen and is regulated by quorum sensing. *Microbiology* **159**: 2375–2385.

Branda SS, Vik Å, Friedman L, Kolter R. 2005. Biofilms: the matrix revisited. *Trends in Microbiology* **13**: 20–26.

Brencic A, McFarland KA, McManus HR, Castang S, Mogno I, Dove SL, Lory S. 2009. The GacS/GacA signal transduction system of *Pseudomonas aeruginosa* acts exclusively through its control over the transcription of the RsmY and RsmZ regulatory small RNAs. *Molecular Microbiology* **73**: 434–445.

Brink SC. 2016. Unlocking the secrets of the rhizosphere. *Trends in Plant Science* **21**: 169–170.

Van Den Broek D, Bloemberg G V., Lugtenberg B. 2005. The role of phenotypic variation in rhizosphere *Pseudomonas* bacteria. *Environmental Microbiology* **7**: 1686–1697.

Brown D. 2010. A mathematical model of the Gac/Rsm quorum sensing network in *Pseudomonas fluorescens*. *BioSystems* **101**: 200–212.

Browne P, Rice O, Miller SH, Burke J, Dowling DN, Morrissey JP, O'Gara F. 2009. Superior inorganic phosphate solubilization is linked to phylogeny within the *Pseudomonas fluorescens* complex. *Applied Soil Ecology* **43**: 131–138.

Buckling A, Rainey PB. 2002. The role of parasites in sympatric and allopatric host diversification. *Nature* **420**: 496–499.

Bulgarelli D, Schlaeppi K, Spaepen S, van Themaat E, Schulze-Lefert P. 2013. Structure and functions of the bacterial microbiota of plants. *Annual Review of Plant Biology* **64**: 807–838.

Bull CT, Duffy B, Voisard C, Défago G, Keel C, Haas D. 2001. Characterization of spontaneous *gacS* and *gacA* regulatory mutants of *Pseudomonas fluorescens* biocontrol strain CHA0. *Antonie van Leeuwenhoek, International Journal of General and Molecular Microbiology* **79**: 327–336.

C. Hider R, Kong X. 2010. Chemistry and biology of siderophores. *Natural Product Reports* **27**: 637–657.

Caiazza NC, Merritt JH, Brothers KM, O'Toole GA. 2007. Inverse regulation of biofilm formation and swarming motility by *Pseudomonas aeruginosa* PA14. *Journal of Bacteriology* **189**: 3603–3612.

Caiazza NC, O'Toole GA. 2004. SadB is required for the transition from reversible to irreversible attachment during biofilm formation by *Pseudomonas aeruginosa* PA14. *Journal of Bacteriology* **186**: 4476–4485.

Caiazza NC, Shanks RMQ, O'Toole GA. 2005. Rhamnolipids modulate swarming motility patterns of *Pseudomonas aeruginosa*. *Journal of Bacteriology* **187**: 7351–7361.

Capdevila S, Martínez-Granero FM, Sánchez-Contreras M, Rivilla R, Martín M. 2004. Analysis of *Pseudomonas fluorescens* F113 genes implicated in flagellar filament synthesis and their role in competitive root colonization. *Microbiology* **150**: 3889–3897.

Capper RL, Jin YK, Lundgren PB, Peplow LM, Matz M V., van Oppen MJH. 2015. Quantitative high resolution melting: two methods to determine SNP allele frequencies from pooled samples. *BMC Genetics* **16**: 1–13.

Carroll SB. 2008. Evo-devo and an expanding evolutionary synthesis: a genetic theory of morphological evolution. *Cell* **134**: 25–36.

Carroll D, Holden N, Gifford ML, Dupuy LX, Carvalhais LC. 2020. Framework for quantification of the dynamics of root colonization by *Pseudomonas fluorescens* isolate. **11**: 1–16.

Castiblanco LF, Sundin GW. 2016. New insights on molecular regulation of biofilm formation in plant-associated bacteria. *Journal of Integrative Plant Biology* **58**: 362–372.

Cecchini DA, Laville E, Laguerre S, Robe P, Leclerc M, Doré J, Henrissat B, Remaud-Siméon M, Monsan P, Potocki-Véronèse G. 2013. Functional metagenomics reveals novel pathways of prebiotic breakdown by human gut bacteria. *PLoS ONE* **8**: e72766.

Challis GL. 2005. A widely distributed bacterial pathway for siderophore biosynthesis independent of nonribosomal peptide synthetases. *ChemBioChem* **6**: 601–611.

Chancey ST, Wood DW, Pierson EA, Pierson LS. 2002. Survival of GacS/GacA mutants of the biological control bacterium *Pseudomonas aureofaciens* 30-84 in the wheat rhizosphere. *Applied and Environmental Microbiology* **68**: 3308–3314.

Chang W-S, Park K-M, Koh S-C, So J-S. 2008. Characterization of the *Bradyrhizobium japonicum galE* gene: its impact on lipopolysaccharide profile and nodulation of soybean. *FEMS Microbiology Letters* **280**: 242–249.

Chaparro JM, Badri D V., Bakker MG, Sugiyama A, Manter DK, Vivanco JM. 2013. Root exudation of phytochemicals in *Arabidopsis* follows specific patterns that are developmentally programmed and correlate with soil microbial functions (K Wu, Ed.). *PLoS ONE* **8**: e55731.

Chapelle E, Mendes R, Bakker PAH, Raaijmakers JM. 2016. Fungal invasion of the rhizosphere microbiome. *ISME Journal* **10**: 265–268.

Chene F, Wang K, Stewart J, Belas R. 2006. Induction of multiple prophages from a marine bacterium: a genomic approach. *Applied and Environmental Microbiology* **72**: 4995–5001.

Cheng X, Cordovez V, Etalo DW, van der Voort M, Raaijmakers JM. 2016. Role of the GacS sensor kinase in the regulation of volatile production by plant growth-promoting *Pseudomonas fluorescens* SBW25. *Frontiers in Plant Science* **7**: 1706.

Chevallereau A, Pons BJ, van Houte S, Westra ER. 2022. Interactions between bacterial and phage communities in natural environments. *Nature Reviews Microbiology* **20**: 49–62.

Chin-A-Woeng TFC, Bloemberg G V., Mulders IHM, Dekkers LC, Lugtenberg BJJ. 2000. Root colonization by phenazine-1-carboxamide-producing bacterium *Pseudomonas chlororaphis* PCL1391 is essential for biocontrol of tomato foot and root rot. *Molecular Plant-Microbe Interactions* **13**: 1340–1345.

Choi HW, Klessig DF. 2016. DAMPs, MAMPs, and NAMPs in plant innate immunity. *BMC Plant Biology* **16**: 1–10.

Christensen PJ, Cook FD. 1972. The isolation and enumeration of cytophagas. *Canadian journal of microbiology* **18**: 1933–1940.

Cingolani P, Platts A, Wang LL, Coon M, Nguyen T, Wang L, Land SJ, Lu X, Ruden DM. 2012. A program for annotating and predicting the effects of single nucleotide polymorphisms, SnpEff: SNPs in the genome of *Drosophila melanogaster* strain *w1118; iso-2; iso-3*. *Fly* **6**: 80–92.

Clark CA, Beltrame J, Manning PA. 1991. The oac gene encoding a lipopolysaccharide O-antigen acetylase maps adjacent to the integrase-encoding gene on the genome of *Shigella flexneri* bacteriophage Sf6. *Gene* **107**: 43–52.

Colaianni NR, Parys K, Lee HS, Conway JM, Kim NH, Edelbacher N, Mucyn TS, Madalinski M, Law TF, Jones CD, *et al.* 2021. A complex immune response to flagellin epitope variation in commensal communities. *Cell Host and Microbe* **29**: 635-649.e9.

Cole BJ, Feltcher ME, Waters RJ, Wetmore KM, Mucyn TS, Ryan EM, Wang G, Ul-Hasan S, McDonald M, Yoshikuni Y, *et al.* 2017. Genome-wide identification of bacterial plant colonization genes. *PLoS Biology* **15**: 1–24.

Compeau G, Al-Achi BJ, Platsouka E, Levy SB. 1988. Survival of rifampin-resistant mutants of *Pseudomonas fluorescens* and *Pseudomonas putida* in soil systems. *Applied and Environmental Microbiology* **54**: 2432–2438.

Cordovez V, Carrion VJ, Etalo DW, Mumm R, Zhu H, van Wezel GP, Raaijmakers JM. 2015. Diversity and functions of volatile organic compounds produced by *Streptomyces* from a disease-suppressive soil. *Frontiers in Microbiology* **6**: 1081.

Cordovez V, Mommer L, Moisan K, Lucas-Barbosa D, Pierik R, Mumm R, Carrion VJ, Raaijmakers JM. 2017. Plant phenotypic and transcriptional changes induced by volatiles from the fungal root pathogen *Rhizoctonia solani*. *Frontiers in Plant Science* **8**: 1262.

Cornelis P, Dingemans J. 2013. *Pseudomonas aeruginosa* adapts its iron uptake strategies in function of the type of infections. *Frontiers in Cellular and Infection Microbiology* **3**: 75.

Craig NL, Roberts JW. 1980. *E. coli* recA protein-directed cleavage of phage lambda repressor requires polynucleotide. *Nature* **283**: 26–30.

Crouzet M, Claverol S, Lomenech AM, Le Sénéchal C, Costaglioli P, Barthe C, Garbay B, Bonneu M, Vilain S. 2017. *Pseudomonas aeruginosa* cells attached to a surface display a typical proteome early as 20 minutes of incubation. *PLoS ONE* **12**: 1–24.

Cullen TW, Schofield WB, Barry NA, Putnam EE, Rundell EA, Trent MS, Degnan PH, Booth CJ, Yu H, Goodman AL. 2015. Antimicrobial peptide resistance mediates resilience of prominent gut commensals during inflammation. *Science* **347**: 170–175.

D'aes J, Kieu NP, Léclère V, Tokarski C, Olorunleke FE, De Maeyer K, Jacques P, Höfte M, Ongena M. 2014. To settle or to move? The interplay between two classes of cyclic lipopeptides in the biocontrol strain *Pseudomonas* CMR12a. *Environmental Microbiology* **16**: 2282–2300.

van Dam NM, Weinhold A, Garbeva P. 2016. Calling in the dark: the role of volatiles for communication in the rhizosphere. In: Signaling and Communication in Plants. Deciphering Chemical Language of Plant Communication. Springer, Cham, 175–210.

Dames S, Margraf RL, Pattison DC, Wittwer CT, Voelkerding K V. 2007. Characterization of aberrant melting peaks in unlabeled probe assays. *Journal of Molecular Diagnostics* **9**: 290–296.

Damkiaer S, Yang L, Molin S, Jelsbak L. 2013. Evolutionary remodeling of global regulatory networks during long-term bacterial adaptation to human hosts. *Proceedings of the National Academy of Sciences of the United States of America* **110**: 7766–7771.

Danhorn T, Fuqua C. 2007. Biofilm formation by plant-associated bacteria. *Annual Review of Microbiology* **61**: 401–422.

Davies E V., James CE, Williams D, O'Brien S, Fothergill JL, Haldenby S, Paterson S, Winstanley C, Brockhurst MA. 2016. Temperate phages both mediate and drive adaptive evolution in pathogen biofilms. *Proceedings of the National Academy of Sciences of the United States of America* **113**: 8266–8271.

Defago G, Berling CH, Burger U, Haas D, Kahr G, Keel C, Voisard C, Wirthner P, Wiithrich B. 1990. Suppression of black root rot of tobacco and other root diseases by strains of *Pseudomonas fluorescens*: potential applications and mechanisms. *Biological control of soil-borne plant pathogens*: 93–108.

Dekkers LC, Van Der Bij AJ, Mulders IHM, Phoelich CC, Wentwoord RAR, Glandorf DCM, Wijffelman CA, Lugtenberg BJJ. 1998. Role of the O-antigen of lipopolysaccharide, and possible roles of growth rate and of NADH:ubiquinone oxidoreductase (nuo) in competitive tomato root-tip colonization by *Pseudomonas fluorescens* WCS365. *Molecular Plant-Microbe Interactions* **11**: 763–771.

DeSilva D, Blackett J. 2007. Assay: high-resolution melting & unlabeled probes. *Genetic Engineering and Biotechnology News* **27**: 1–11.

Déziel E, Comeau Y, Villemur R. 2001. Initiation of biofilm formation by *Pseudomonas aeruginosa* 57RP correlates with emergence of hyperpiliated and highly adherent phenotypic variants deficient in swimming, swarming, and twitching motilities. *Journal of Bacteriology* **183**: 1195–1204.

Dicke M, Sabelis MW. 1988. Infochemical terminology: based on cost-benefit analysis rather than origin of compounds? *Functional Ecology* **2**: 131–139.

Dieppois G, Opota O, Lalucat J, Lemaitre B. 2015. *Pseudomonas entomophila*: a versatile bacterium with entomopathogenic properties. In: *Pseudomonas*. Springer, Dordrecht, 25–49.

Diggle SP, Griffin AS, Campbell GS, West SA. 2007. Cooperation and conflict in quorum-sensing bacterial populations. *Nature* **450**: 411–414.

Dodds PN, Rathjen JP. 2010. Plant immunity: towards an integrated view of plant-pathogen interactions. *Nature Reviews. Genetics* **11**: 539–548.

Dragoš A, Kiesewalter H, Martin M, Hsu CY, Hartmann R, Wechsler T, Eriksen C, Brix S, Drescher K, Stanley-Wall N, *et al.* 2018. Division of labor during biofilm matrix production. *Current Biology* **28**: 1903-1913.e5.

Driscoll WW, Pepper JW, Pierson LS, Pierson EA. 2011. Spontaneous *gac* mutants of *Pseudomonas* biological control strains: cheaters or mutualists? *Applied and Environmental Microbiology* **77**: 7227–7235.

Duca D, Lorv J, Patten CL, Rose D, Glick BR. 2014. Indole-3-acetic acid in plant-microbe interactions. *Antonie Van Leeuwenhoek* **106**: 85–125.

Dunkley EJ, Chalmers JD, Cho S, Finn TJ, Patrick WM. 2019. Assessment of Phenotype Microarray plates for rapid and high-throughput analysis of collateral sensitivity networks. *PLoS ONE* **14**: 1–12.

Eisen JA. 1998. Phylogenomics: improving functional predictions for uncharacterized genes by evolutionary analysis. *Genome Research* **8**: 163–167.

Erbs G, Newman M-A. 2003. The role of lipopolysaccharides in induction of plant defence responses. *Molecular Plant Pathology* **4**: 421–425.

Evans TJ, Ind A, Komitopoulou E, Salmond GPC. 2010a. Phage-selected lipopolysaccharide mutants of *Pectobacterium atrosepticum* exhibit different impacts on virulence. *Journal of Applied Microbiology* **109**: 505–514.

Evans TJ, Trauner A, Komitopoulou E, Salmond GPC. **2010b**. Exploitation of a new flagellatropic phage of *Erwinia* for positive selection of bacterial mutants attenuated in plant virulence: towards phage therapy. *Journal of Applied Microbiology* **108**: 676–685.

Evenson RE, Gollin D. **2003**. Assessing the impact of the Green Revolution, 1960 to 2000. *Science* **300**: 758–762.

Falardeau J, Wise C, Novitsky L, Avis TJ. **2013**. Ecological and mechanistic insights into the direct and indirect antimicrobial properties of *Bacillus subtilis* lipopeptides on plant pathogens. *Journal of Chemical Ecology* **39**: 869–878.

Farace G, Fernandez O, Jacquens L, Coutte F, Krier F, Jacques P, Clément C, Barka EA, Jacquard C, Dorey S. **2015**. Cyclic lipopeptides from *Bacillus subtilis* activate distinct patterns of defence responses in grapevine. *Molecular Plant Pathology* **16**: 177–187.

Feiner R, Argov T, Rabinovich L, Sigal N, Borovok I, Herskovits AA. **2015**. A new perspective on lysogeny: prophages as active regulatory switches of bacteria. *Nature Reviews Microbiology* **13**: 641–650.

Fernández L, Rodríguez A, García P. **2018**. Phage or foe: an insight into the impact of viral predation on microbial communities. *ISME Journal* **12**: 1171–1179.

Flury P, Aellen N, Ruffner B, Péchy-Tarr M, Fataar S, Metla Z, Dominguez-Ferreras A, Bloemberg G, Frey J, Goesmann A, *et al.* 2016. Insect pathogenicity in plant-beneficial pseudomonads: phylogenetic distribution and comparative genomics. *ISME Journal* **10**: 2527–2542.

Flury P, Vesga P, Péchy-Tarr M, Aellen N, Dennert F, Hofer N, Kupferschmied KP, Kupferschmied P, Metla Z, Ma Z, *et al.* 2017. Antimicrobial and insecticidal: cyclic lipopeptides and hydrogen cyanide produced by plant-beneficial *Pseudomonas* strains CHA0, CMR12a, and PCL1391 contribute to insect killing. *Frontiers in Microbiology* **8**.

Fox AR, Soto G, Valverde C, Russo D, Lagares A, Zorreguieta Á, Alleva K, Pascuan C, Frare R, Mercado-Blanco J, *et al.* 2016. Major cereal crops benefit from biological nitrogen fixation when inoculated with the nitrogen-fixing bacterium *Pseudomonas protegens* Pf-5 X940. *Environmental Microbiology* **18**: 3522–3534.

de Freitas CC, Taylor CG. **2022**. Biological control of hairy root disease using beneficial *Pseudomonas* strains. *Biological Control* **177**: 1–11.

Fry BN, Feng S, Chen YY, Newell DG, Coloe PJ, Korolik V. **2000**. The *galE* gene of *Campylobacter jejuni* is involved in lipopolysaccharide synthesis and virulence. *Infection and Immunity* **68**: 2594–2601.

Gaio D, Anantanawat K, To J, Liu M, Monahan L, Darling AE. **2022**. Hackflex: low-cost, high-throughput, Illumina Nextera Flex library construction. *Microbial Genomics* **8**: 1–16.

Galperin MY, Makarova KS, Wolf YI, Koonin E V. 2015. Expanded microbial genome coverage and improved protein family annotation in the COG database. *Nucleic Acids Research* **43**: D261–D269.

García E, Alonso Á, Platas G, Sacristán S. **2013**. The endophytic mycobiota of *Arabidopsis thaliana*. *Fungal Diversity* **60**: 71–89.

Ghequire MGK, Dillen Y, Lambrichts I, Proost P, Wattiez R, De Mot R. **2015**. Different ancestries of R tailocins in rhizospheric *Pseudomonas* isolates. *Genome Biology and Evolution* **7**: 2810–2828.

Gilchrist CLM, Chooi YH. **2021**. Clinker & clustermap.js: automatic generation of gene cluster comparison figures. *Bioinformatics* **37**: 2473–2475.

Giraud A, Arous S, De Paepe M, Gaboriau-Routhiau V, Bambou JC, Rakotobe S, Lindner AB, Taddei F, Cerf-Bensussan N. **2008**. Dissecting the genetic components of adaptation of *Escherichia coli* to the mouse gut. *PLoS Genetics* **4**: 0052–0061.

Glick BR. **2014**. Bacteria with ACC deaminase can promote plant growth and help to feed the world. *Microbiological Research* **169**: 30–39.

Glickmann E, Dessaux Y. **1995**. A critical examination of the specificity of the salkowski reagent for indolic compounds produced by phytopathogenic bacteria. *Applied and environmental microbiology* **61**: 793–796.

Göhre V, Robatzek S. **2008**. Breaking the barriers: microbial effector molecules subvert plant immunity. *Annual Review of Phytopathology* **46**: 189–215.

Gómez P, Buckling A. **2011**. Bacteria-phage antagonistic coevolution in soil. *Science* **332**: 106–109.

Goo E, An JH, Kang Y, Hwang I. **2015**. Control of bacterial metabolism by quorum sensing. *Trends in Microbiology* **23**: 567–576.

Gordillo Altamirano FL, Barr JJ. **2021**. Unlocking the next generation of phage therapy: the key is in the receptors. *Current Opinion in Biotechnology* **68**: 115–123.

Goswami RS, Kistler HC. **2005**. Pathogenicity and in planta mycotoxin accumulation among members of the *Fusarium graminearum* species complex on wheat and rice. *Phytopathology* **95**: 1397–1404.

Großkinsky DK, Tafner R, Moreno M V., Stenglein SA, De Salamone IEG, Nelson LM, Novák O, Strnad M, Van Der Graaff E, Roitsch T. **2016**. Cytokinin production by *Pseudomonas fluorescens* G20-18 determines biocontrol activity against *Pseudomonas syringae* in Arabidopsis. *Scientific Reports* **6**: 1–11.

Grote J, Krysciak D, Streit WR. **2015**. Phenotypic heterogeneity, a phenomenon that may explain why quorum sensing does not always result in truly homogenous cell behavior. *Applied and Environmental Microbiology* **81**: 5280–5289.

Guan S, Bastin D, Verma NK. **1999**. Glucosylation gene cluster of *Shigella flexneri*. *Microbiology* **145**: 1263–1273.

Gutiérrez-García K, Neira-González A, Pérez-Gutiérrez RM, Granados-Ramírez G, Zarraga R, Wrobel K, Barona-Gómez F, Flores-Cotera LB. **2017**. Phylogenomics of 2,4-diacetylphloroglucinol-producing Pseudomonas and novel antiglycation endophytes from Piper auritum. *Journal of Natural Products* **80**: 1955–1963.

Haas D, Défago G. **2005**. Biological control of soil-borne pathogens by fluorescent pseudomonads. *Nature Reviews Microbiology* **3**: 307–319.

Haas D, Keel C. **2003**. Regulation of antibotic production in root-colonizing *Pseudomonas* spp. and relavance for biological control of plant disease. *Annu. Rev. Phytopathol.* **41**: 117–153.

Hacquard S, Kracher B, Hiruma K, Münch PC, Garrido-Oter R, Thon MR, Weimann A, Damm U, Dallery J-F, Hainaut M, *et al.* 2016. Survival trade-offs in plant roots during colonization by closely related beneficial and pathogenic fungi. *Nature Communications* **7**: 11362.

Hampton HG, Watson BNJ, Fineran PC. **2020**. The arms race between bacteria and their phage foes. *Nature* **577**: 327–336.

Han AW, Sandy M, Fishman B, Trindade-Silva AE, Soares CAG, Distel DL, Butler A, Haygood MG. **2013**. Turnerbactin, a novel triscatecholate siderophore from the shipworm endosymbiont *Teredinibacter turnerae* T7901. *PloS One* **8**: e76151.

Hansen SK, Haagensen JAJ, Gjermansen M, Jørgensen TM, Tolker-Nielsen T, Molin S. **2007a**. Characterization of a *Pseudomonas putida* rough variant evolved in a mixed-species biofilm with *Acinetobacter sp.* strain C6. *Journal of Bacteriology* **189**: 4932–4943.

Hansen SK, Rainey PB, Haagensen JAJ, Molin S. **2007b**. Evolution of species interactions in a biofilm community. *Nature* **445**: 533–536.

Hartmann A, Rothballer M, Schmid M. **2008**. Lorenz Hiltner, a pioneer in rhizosphere microbial ecology and soil bacteriology research. *Plant and Soil* **312**: 7–14.

Hassan KA, Johnson A, Shaffer BT, Ren Q, Kidarsa TA, Elbourne LDH, Hartney S, Duboy R, Goebel NC, Zabriskie TM, *et al.* 2010. Inactivation of the GacA response regulator in *Pseudomonas fluorescens* Pf-5 has far-reaching transcriptomic consequences. *Environmental Microbiology* **12**: 899–915.

Heeb S, Blumer C, Haas D. 2002. Regulatory RNA as mediator in GacA/RsmA-dependent global control of exoproduct formation in *Pseudomonas fluorescens* CHA0. *Journal of bacteriology* **184**: 1046–1056.

Heeb S, Haas D. 2001. Regulatory roles of the GacS/GacA two-component system in plant-associated and other gram-negative bacteria. *The American Phytopathological Society* **14**: 1351–1363.

Heeb S, Valverde C, Haas D. 2005. Role of the stress sigma factor RpoS in GacA/RsmA-controlled secondary metabolism and resistance to oxidative stress in Pseudomonas fluorescens CHA0. *FEMS Microbiology Letters* **243**: 251–258.

Herman R. 2015. Characterisation of lipopolysaccharide O-antigen acetyltransferases in the bacterium *Salmonella*.

Hinsa SM, Espinosa-Urgel M, Ramos JL, O'Toole GA. 2003. Transition from reversible to irreversible attachment during biofilm formation by *Pseudomonas fluorescens* WCS365 requires an ABC transporter and a large secreted protein. *Molecular Microbiology* **49**: 905–918.

Hiruma K, Gerlach N, Sacristán S, Nakano RT, Hacquard S, Kracher B, Neumann U, Ramírez D, Bucher M, O'Connell RJ, *et al.* 2016. Root endophyte colletotrichum tofieldiae confers plant fitness benefits that are phosphate status dependent. *Cell* **165**: 464–474.

Hockett KL, Baltrus DA. 2017. Use of the soft-agar overlay technique to screen for bacterially produced inhibitory compounds. *Journal of Visualized Experiments* **2017**: 1–5.

Højberg O, Schnider U, Winteler H V, Sørensen J, Haas D. 1999. Oxygen-sensing reporter strain of *Pseudomonas fluorescens* for monitoring the distribution of low-oxygen habitats in soil. *Applied and Environmental Microbiology* **65**: 4085–4093.

Howard-Varona C, Hargreaves KR, Abedon ST, Sullivan MB. 2017. Lysogeny in nature: mechanisms, impact and ecology of temperate phages. *ISME Journal* **11**: 1511–1520.

Huang X, Wang Z, Liu Y, Zhang X. 2017. Complete genome sequence of the *Pseudomonas protegens* H78, a plant growth-promoting rhizobacterium. *Genome Announcements* **5**: 1–2.

Hug I, Feldman MF. 2011. Analogies and homologies in lipopolysaccharide and glycoprotein biosynthesis in bacteria. *Glycobiology* **21**: 138–151.

Hunter P. 2008. The great leap forward. *EMBO reports* **9**: 608–611.

Huszczynski SM, Lam JS, Khursigara CM. 2020. The role of *Pseudomonas aeruginosa* lipopolysaccharide in bacterial pathogenesis and physiology. *Pathogens* **9**: 1–22.

Ivanov IE, Kintz EN, Porter LA, Goldberg JB, Burnham NA, Camesano TA. 2011. Relating the physical properties of *Pseudomonas aeruginosa* lipopolysaccharides to virulence by atomic force microscopy. *Journal of Bacteriology* **193**: 1259–1266.

Jofré E, Lagares A, Mori G. 2004. Disruption of dTDP-rhamnose biosynthesis modifies lipopolysaccharide core, exopolysaccharide production, and root colonization in *Azospirillum brasilense*. *FEMS Microbiology Letters* **231**: 267–275.

Johnson G, Wolfe AJ, Putonti C. 2019. Characterization of the φCTX-like *Pseudomonas aeruginosa* phage Dobby isolated from the kidney stone microbiota. *Access Microbiology* **1**: 1–4.

Jones JDG, Dangl JL. 2006. The plant immune system. *Nature* **444**: 323–329.

Jones CJ, Newsom D, Kelly B, Irie Y, Jennings LK, Xu B, Limoli DH, Harrison JJ, Parsek MR, White P, *et al.* 2014. ChIP-Seq and RNA-Seq reveal an AmrZ-mediated mechanism for cyclic di-GMP synthesis and biofilm development by *Pseudomonas aeruginosa*. *PLoS Pathogens* **10**: e1003984.

De Jonge R, Ebert MK, Huitt-Roehl CR, Pal P, Suttle JC, Spanner RE, Neubauer JD, Jurick WM, Stott KA, Secor GA, *et al.* 2018. Gene cluster conservation provides insight into cercosporin biosynthesis and extends production to the genus *Colletotrichum*. *Proceedings of the National Academy of Sciences of the United States of America* **115**: E5459–E5466.

Jousset A, Lara E, Wall LG, Valverde C. 2006. Secondary metabolites help biocontrol strain *Pseudomonas fluorescens* CHA0 to escape protozoan grazing. *Applied and Environmental Microbiology* **72**: 7083–7090.

Jousset A, Schuldes J, Keel C, Maurhofer M, Daniel R, Scheu S, Thuermer A. 2014. Full-genome sequence of the plant growth-promoting bacterium *Pseudomonas protegens* CHA0. *Genome Announcements* **2**: e00322-14.

Kaden R, Ågren J, Båverud V, Hallgren G, Ferrari S, Börjesson J, Lindberg M, Bäckman S, Wahab T. 2014. Brucellosis outbreak in a Swedish kennel in 2013: determination of genetic markers for source tracing. *Veterinary Microbiology* **174**: 523–530.

Kang S-M, Radhakrishnan R, Khan AL, Kim M-J, Park J-M, Kim B-R, Shin D-H, Lee I-J. 2014. Gibberellin secreting rhizobacterium, *Pseudomonas putida* H-2-3 modulates the hormonal and stress physiology of soybean to improve the plant growth under saline and drought conditions. *Plant physiology and biochemistry: PPB* **84**: 115–124.

Kaushik V, Tiwari M, Tiwari V. 2022. Interaction of RecA mediated SOS response with bacterial persistence, biofilm formation, and host response. *International Journal of Biological Macromolecules* **217**: 931–943.

Kawecki TJ, Lenski RE, Ebert D, Hollis B, Olivieri I, Whitlock MC. 2012. Experimental evolution. *Trends in Ecology and Evolution* **27**: 547–560.

Kearns DB. 2010. A field guide to bacterial swarming motility. *Nature Reviews Microbiology* **8**: 634–644.

Keel C, Schnider U, Maurhofer M, Voisard C, Laville J, Burger U, Wirthner P, Haas D, Défago G. 1992. Suppression of root disease by *Pseudomonas fluorescens* CHA0: importance of the bacterial secondary metabolite 2,4-diacetylphloroglucinol. *Molecular Plant-Microbe Interactions* **5**: 4–13.

Keel C, Weller DM, Natsch A, Défago G, Cook RJ, Thomashow LS. 1996. Conservation of the 2,4-diacetylphloroglucinol biosynthesis locus among fluorescent *Pseudomonas* strains from diverse geographic locations. *Applied and Environmental Microbiology* **62**: 552–563.

Khan R, Shah MD, Shah L, Lee PC, Khan I. 2022. Bacterial polysaccharides - a big source for prebiotics and therapeutics. *Frontiers in Nutrition* **9**.

Kieft K, Anantharaman K. 2022. Deciphering active prophages from metagenomes. *mSystems* **7**: 1–15.

King EO, Ward MK, Raney DE. 1954. Two simple media for the demonstration of pyocyanin and fluorescin. *The Journal of Laboratory and Clinical Medicine* **44**: 301–307.

Knights HE, Jorrin B, Haskett TL, Poole PS. 2021. Deciphering bacterial mechanisms of root colonization. *Environmental Microbiology Reports* **13**: 428–444.

Knirel YA, Prokhorov NS, Shashkov AS, Ovchinnikova OG, Zdorovenko EL, Liu B, Kostryukova ES, Larin AK, Golomidova AK, Letarov A V. 2015. Variations in O-antigen biosynthesis and O-acetylation associated with altered phage sensitivity in *Escherichia coli* 4s. *Journal of Bacteriology* **197**: 905–912.

Knirel YA, Valvano MA. 2011. Bacterial lipopolysaccharides: structure, chemical synthesis, biogensis and interaction with host cells (YA Knirel and MA Valvano, Eds.). Springer Science & Business Media.

Koskella B, Brockhurst MA. 2014. Bacteria-phage coevolution as a driver of ecological and evolutionary processes in microbial communities. *FEMS Microbiology Reviews* **38**: 916–931.

Koskella B, Taylor TB. 2018. Multifaceted impacts of bacteriophages in the plant microbiome. *Annual Review of Phytopathology* **56**: 361–380.

Koskella B, Taylor TB, Bates J, Buckling A. 2011. Using experimental evolution to explore natural patterns between bacterial motility and resistance to bacteriophages. *ISME Journal* **5**: 1809–1817.

Krogh A, Larsson B, Von Heijne G, Sonnhammer ELL. 2001. Predicting transmembrane protein topology with a hidden Markov model: application to complete genomes. *Journal of Molecular Biology* **305**: 567–580.

Kulikov EE, Golomidova AK, Prokhorov NS, Ivanov PA, Letarov A V. 2019. High-throughput LPS profiling as a tool for revealing of bacteriophage infection strategies. *Scientific Reports* **9**: 1–10.

Kumar P, Dubey RC, Maheshwari DK. 2012. *Bacillus* strains isolated from rhizosphere showed plant growth promoting and antagonistic activity against phytopathogens. *Microbiological Research* **167**: 493–499.

Kupferschmied P, Chai T, Flury P, Blom J, Smits THM, Maurhofer M, Keel C. 2016. Specific surface glycan decorations enable antimicrobial peptide resistance in plant-beneficial pseudomonads with insect-pathogenic properties. *Environmental Microbiology* **18**: 4265–4281.

Kutschera A, Dawid C, Gisch N, Schmid C, Raasch L, Gerster T, Schäffer M, Smakowska-Luzan E, Belkhadir Y, Corina Vlot A, *et al.* 2019. Bacterial medium-chain 3-hydroxy fatty acid metabolites trigger immunity in *Arabidopsis* plants. *Science* **364**: 178–181.

Kutschera A, Ranf S. 2019. The multifaceted functions of lipopolysaccharide in plant-bacteria interactions. *Biochimie* **159**: 93–98.

Lam KN, Cheng J, Engel K, Neufeld JD, Charles TC. 2015. Current and future resources for functional metagenomics. *Frontiers in Microbiology* **6**: 1–8.

Lam ST, Ellis DM, Ligon JM. 1990. Genetic approaches for studying rhizosphere colonization. *Plant and Soil* **129**: 11–18.

Lam JS, Taylor VL, Islam ST, Hao Y, Kocíncová D. 2011. Genetic and functional diversity of *Pseudomonas aeruginosa* lipopolysaccharide. *Frontiers in Microbiology* **2**: 1–25.

Lapouge K, Schubert M, Allain FH-T, Haas D. 2007. Gac/Rsm signal transduction pathway of γ-proteobacteria: from RNA recognition to regulation of social behaviour. *Molecular Microbiology* **67**: 241–253.

Lee HK, Lee CK, Loh TP, Tang JWT, Tambyah PA, Koay ESC. 2011. High-resolution melting approach to efficient identification and quantification of H275Y mutant influenza H1N1/2009 virus in mixed-virus- population samples. *Journal of Clinical Microbiology* **49**: 3555–3559.

Lee NG, Sunshine MG, Engstrom JJ, Gibson BW, Apicella MA. 1995. Mutation of the htrB locus of *Haemophilus influenzae* nontypable strain 2019 is associated with modifications of lipid A and phosphorylation of the lipo-oligosaccharide. *Journal of Biological Chemistry* **270**: 27151–27159.

Leeman M, Pelt JA van, Ouden FM den, Heinsbroek M, Bakker PAHM, Schippers B. 1995. Induction of systemic resistance against *Fusarium wilt* of radish by lipopolysaccharides of *Pseudomonas fluorescens*. *Phytopathology (USA)* **85**: 1021–1027.

Lenski RE. 2017. Experimental evolution and the dynamics of adaptation and genome evolution in microbial populations. *ISME Journal* **11**: 2181–2194.

Lerouge I, Vanderleyden J. 2001. O-antigen structural variation: mechanisms and possible roles in animal/plant-microbe interactions. *FEMS Microbiology Reviews* **26**: 17–47.

Li E, de Jonge R, Liu C, Jiang H, Friman V-P, Pieterse CMJ, Bakker PAHM, Jousset A. 2021a. Rapid evolution of bacterial mutualism in the plant rhizosphere. *Nature Communications* **12**: 1–13.

Li Y, Wang Z, Liu X, Song Z, Li R, Shao C, Yin Y. 2016. Siderophore biosynthesis but not reductive iron assimilation is essential for the dimorphic fungus *Nomuraea rileyi* conidiation, dimorphism transition, resistance to oxidative stress, pigmented microsclerotium formation, and virulence. *Frontiers in Microbiology* **7**: 931.

Li E, Zhang H, Jiang H, Pieterse CMJ, Jousset A, Bakker PAHM, de Jonge R. 2021b. Experimental-Evolution-Driven identification of *Arabidopsis* rhizosphere competence genes in *Pseudomonas protegens*. *mBio* **12**: e00927-21.

Liang X, Wagner RE, Li B, Zhang N, Radosevich M. 2020. Quorum sensing signals alter in vitro soil virus abundance and bacterial community composition. *Frontiers in Microbiology* **11**: 1–13.

Lin Y, Alstrup M, Pang JKY, Maróti G, Er-Rafik M, Tourasse N, Økstad OA, Kovács ÁT. 2021. Adaptation of *Bacillus thuringiensis* to plant colonization affects differentiation and toxicity. *mSystems* **6**: e00864-21.

Little JW. 2014. Lysogeny, prophage Induction, and lysogenic conversion. In: Phages. 37–54.

Liu B, Knirel YA, Feng L, Perepelov A V., Senchenkova SN, Wang Q, Reeves PR, Wang L. 2008. Structure and genetics of *Shigella* O antigens. *FEMS Microbiology Reviews* **32**: 627–653.

Lloret J, Bolanos L, Lucas MM, Peart JM, Brewin NJ, Bonilla I, Rivilla R. 1995. Ionic stress and osmotic pressure induce different alterations in the lipopolysaccharide of a *Rhizobium meliloti* strain. *Applied and Environmental Microbiology* **61**: 3701–3704.

Lofgren LA, LeBlanc NR, Certano AK, Nachtigall J, LaBine KM, Riddle J, Broz K, Dong Y, Bethan B, Kafer CW, *et al.* 2018. *Fusarium graminearum*: pathogen or endophyte of North American grasses? *New Phytologist* **217**: 1203–1212.

Loper JE, Hassan KA, Mavrodi D V., Davis EW, Lim CK, Shaffer BT, Elbourne LDH, Stockwell VO, Hartney SL, Breakwell K, *et al.* 2012. Comparative genomics of plant-associated *Pseudomonas* spp.: insights into diversity and inheritance of traits involved in multitrophic interactions. *PLoS Genetics* **8**: e1002784.

López-Farfán D, Reyes-Darias JA, Matilla MA, Krell T. 2019. Concentration dependent effect of plant root exudates on the chemosensory systems of *Pseudomonas putida* KT2440. *Frontiers in Microbiology* **10**: 1–15.

de Lorenzo V, Neilands JB. 1986. Characterization of *iucA* and *iucC* genes of the aerobactin system of plasmid ColV-K30 in *Escherichia coli*. *Journal of Bacteriology* **167**: 350–355.

Di Lorenzo F, Silipo A, Andersen Gersby LB, Palmigiano A, Lanzetta R, Garozzo D, Boyer C, Pruvost O, Newman MA, Molinaro A. 2017. *Xanthomonas citri* pv. *citri* pathotypes: LPS structure and function as microbe-associated molecular patterns. *ChemBioChem* **18**: 772–781.

Ludwig-Müller J. 2015. Bacteria and fungi controlling plant growth by manipulating auxin: balance between development and defense. *Journal of Plant Physiology* **172**: 4–12.

Lugtenberg BJJ, Dekkers LC. 1999. What makes *Pseudomonas* bacteria rhizosphere competent? *Environmental Microbiology* **1**: 9–13.

Lugtenberg BJJ, Dekkers L, Bloemberg G V. 2001a. Molecular determinants of rhizosphere colonization by *Pseudomonas*. *Annual Review of Phytopathology* **39**: 461–490.

Lugtenberg BJJ, Dekkers L, Bloemberg G V. 2001b. Molecular determinants of rhizosphere colonization *Pseudomonas*. *Annual Review of Phytopathology* **39**: 461–490.

Lugtenberg B, Kamilova F. 2009. Plant-Growth-Promoting Rhizobacteria. *Annual Review of Microbiology* **63**: 541–556.

Ma Z, Geudens N, Kieu NP, Sinnaeve D, Ongena M, Martins JC, Höfte M. 2016a. Biosynthesis, chemical structure, and structure-activity relationship of orfamide lipopeptides produced by *Pseudomonas protegens* and related species. *Frontiers in Microbiology* **7**: 1–27.

Ma Z, Hua GKH, Ongena M, Höfte M. 2016b. Role of phenazines and cyclic lipopeptides produced by *pseudomonas* sp. CMR12a in induced systemic resistance on rice and bean. *Environmental Microbiology Reports* **8**: 896–904.

Ma Z, Ongena M, Höfte M. 2017. The cyclic lipopeptide orfamide induces systemic resistance in rice to *Cochliobolus miyabeanus* but not to *Magnaporthe oryzae*. *Plant Cell Reports* **36**: 1731–1746.

Madala NE, Molinaro A, Dubery IA. **2012**. Distinct carbohydrate and lipid-based molecular patterns within lipopolysaccharides from *Burkholderia cepacia* contribute to defense-associated differential gene expression in *Arabidopsis thaliana*. *Innate Immunity* **18**: 140–154.

Maddamsetti R, Lenski RE, Barrick JE. **2015**. Adaptation, clonal interference, and frequency-dependent interactions in a long-term evolution experiment with *Escherichia Coli*. *Genetics* **200**: 619–631.

Maldonado RF, Sá-Correia I, Valvano MA. **2016**. Lipopolysaccharide modification in gram-negative bacteria during chronic infection. *FEMS Microbiology Reviews* **40**: 480–493.

Mark GL, Morrissey JP, Higgins P, O'Gara F. **2006**. Molecular-based strategies to exploit *Pseudomonas* biocontrol strains for environmental biotechnology applications. *FEMS Microbiology Ecology* **56**: 167–177.

Martínez-Gil M, Ramos-González MI, Espinosa-Urgel M. **2014**. Roles of cyclic Di-GMP and the Gac system in transcriptional control of the genes coding for the *Pseudomonas putida* adhesins LapA and LapF. *Journal of Bacteriology* **196**: 1484–1495.

Martínez-Gil M, Yousef-Coronado F, Espinosa-Urgel M. **2010**. LapF, the second largest *Pseudomonas putida* protein, contributes to plant root colonization and determines biofilm architecture. *Molecular Microbiology* **77**: 549–561.

Martínez-Granero F, Navazo A, Barahona E, Redondo-Nieto M, Rivilla R, Martín M. **2012**. The Gac-Rsm and SadB signal transduction pathways converge on Algu to downregulate motility in *Pseudomonas fluorescens*. *PLoS ONE* **7**: e31765.

Martínez-Granero F, Rivilla R, Martín M. **2006**. Rhizosphere selection of highly motile phenotypic variants of *Pseudomonas fluorescens* with enhanced competitive colonization ability. *Applied and Environmental Microbiology* **72**: 3429–3434.

Martínez-Medina A, Van Wees SCM, Pieterse CMJ. **2017**. Airborne signals from *Trichoderma* fungi stimulate iron uptake responses in roots resulting in priming of jasmonic acid-dependent defences in shoots of *Arabidopsis thaliana* and *Solanum lycopersicum*. *Plant, Cell & Environment* **40**: 2691–2705.

Martínez-Viveros O, Jorquera MA, Crowley DE, Gajardo G, Mora ML. **2010**. Mechanisms and practical considerations involved in plant growth promotion by *Rhizobacteria*. *Journal of Soil Science and Plant Nutrition* **10**: 293–319.

Maslov S, Sneppen K. **2017**. Population cycles and species diversity in dynamic Kill-the-Winner model of microbial ecosystems. *Scientific Reports* **7**: 1–8.

Matsuyama BY, Krasteva P V., Baraquet C, Harwood CS, Sondermann H, Navarro MVAS. **2016**. Mechanistic insights into c-di-GMP-dependent control of the biofilm regulator FleQ from *Pseudomonas aeruginosa*. *Proceedings of the National Academy of Sciences of the United States of America* **113**: E209–E218.

McNair K, Bailey BA, Edwards RA. **2012**. PHACTS, a computational approach to classifying the lifestyle of phages. *Bioinformatics* **28**: 614–618.

McNear DH. **2013**. The rhizosphere - roots, soil and everything in between. *Nature Education Knowledge* **4**: 1–15.

Medema MH, Kottmann R, Yilmaz P, Cummings M, Biggins JB, Blin K, de Bruijn I, Chooi YH, Claesen J, Coates RC, *et al.* 2015. Minimum information about a biosynthetic gene cluster. *Nature Chemical Biology* **11**: 625–631.

Meisel JD, Panda O, Mahanti P, Schroeder FC, Kim DH. **2014**. Chemosensation of bacterial secondary metabolites modulates neuroendocrine signaling and behavior of *C. elegans*. *Cell* **159**: 267–280.

Mendes R, Garbeva P, Raaijmakers JM. **2013**. The rhizosphere microbiome: significance of plant beneficial, plant pathogenic, and human pathogenic microorganisms. *FEMS microbiology reviews* **37**: 634–663.

Mendes R, Raaijmakers JM. **2015**. Cross-kingdom similarities in microbiome functions. *The ISME journal* **9**: 1905–1907.

Menouni R, Hutinet G, Petit MA, Ansaldi M. **2015**. Bacterial genome remodeling through bacteriophage recombination. *FEMS Microbiology Letters* **362**: 1–10.

Mercado-Blanco J, van der Drift KM, Olsson PE, Thomas-Oates JE, van Loon LC, Bakker PAHM. **2001**. Analysis of the pmsCEAB gene cluster involved in biosynthesis of salicylic acid and the siderophore pseudomonine in the biocontrol strain *Pseudomonas fluorescens* WCS374. *Journal of Bacteriology* **183**: 1909–1920.

Meziane H, van Der Sluis I, van Loon LC, Höfte M, Bakker PAHM. **2005**. Determinants of *Pseudomonas putida* WCS358 involved in inducing systemic resistance in plants. *Molecular Plant Pathology* **6**: 177–185.

Millet YA, Danna CH, Clay NK, Songnuan W, Simon MD, Werck-Reichhart D, Ausubel FM. **2010**. Innate immune responses activated in *Arabidopsis* roots by microbe-associated molecular patterns. *Plant Cell* **22**: 973–990.

Misselhorn A, Aggarwal P, Ericksen P, Gregory P, Horn-Phathanothai L, Ingram J, Wiebe K. **2012**. A vision for attaining food security. *Current Opinion in Environmental Sustainability* **4**: 7–17.

Mitra S, Mukherjee A, Wiley-Kalil A, Das S, Owen H, Reddy PM, Ané JM, James EK, Gyaneshwar P. **2016**. A rhamnose-deficient lipopolysaccharide mutant of *Rhizobium sp.* IRBG74 is defective in root colonization and beneficial interactions with its flooding-tolerant hosts *Sesbania cannabina* and wetland rice. *Journal of Experimental Botany* **67**: 5869–5884.

Monds RD, O'Toole GA. **2009**. The developmental model of microbial biofilms: ten years of a paradigm up for review. *Trends in Microbiology* **17**: 73–87.

Morris G, Harding S. **2009**. Polysaccharides, Microbial. *Encyclopedia of Microbiology*: 482–494.

Morrissey JP, Dow JM, Mark GL, O'Gara F. **2004**. Are microbes at the root of a solution to world food production? *EMBO Reports* **5**: 922–926.

Moskowitz SM, Foster JM, Emerson J, Burns JL. **2004**. Clinically feasible biofilm susceptibility assay for isolates of *Pseudomonas aeruginosa* from patients with cystic fibrosis. *Journal of Clinical Microbiology* **42**: 1915–1922.

Murata T, Tseng W, Guina T, Miller SI, Nikaido H. **2007**. PhoPQ-mediated regulation produces a more robust permeability barrier in the outer membrane of Salmonella enterica serovar typhimurium. *Journal of Bacteriology* **189**: 7213–7222.

Muriel C, Arrebola E, Redondo-Nieto M, Martínez-Granero F, Jalvo B, Pfeilmeier S, Blanco-Romero E, Baena I, Malone JG, Rivilla R, *et al.* 2018. AmrZ is a major determinant of c-di-GMP levels in *Pseudomonas fluorescens* F113. *Scientific Reports* **8**: 1–10.

Muriel C, Blanco-Romero E, Trampari E, Arrebola E, Durán D, Redondo-Nieto M, Malone JG, Martín M, Rivilla R. **2019**. The diguanylate cyclase AdrA regulates flagellar biosynthesis in *Pseudomonas fluorescens* F113 through SadB. *Scientific Reports* **9**: 1–9.

Murray GL, Attridge SR, Morona R. **2006**. Altering the length of the lipopolysaccharide O antigen has an impact on the interaction of *Salmonella enterica* serovar Typhimurium with macrophages and complement. *Journal of bacteriology* **188**: 2735–2739.

Murtagh F, Legendre P. **2014**. Ward's hierarchical agglomerative clustering method: which algorithms implement ward's criterion? *Journal of Classification* **31**: 274–295.

Muschel LH, Schmoker K. **1966**. Activity of mitomycin C, other antibiotics, and serum against lysogenic bacteria. *Journal of Bacteriology* **92**: 967–971.

Nakao R, Senpuku H, Watanabe H. 2006. *Porphyromonas gingivalis galE* is involved in lipopolysaccharide O-antigen synthesis and biofilm formation. *Infection and Immunity* **74**: 6145–6153.

Nanda AM, Thormann K, Frunzke J. 2015. Impact of spontaneous prophage induction on the fitness of bacterial populations and host-microbe interactions. *Journal of Bacteriology* **197**: 410–419.

Naureen Z, Dautaj A, Anpilogov K, Camilleri G, Dhuli K, Tanzi B, Maltese PE, Cristofoli F, Antoni L De, Beccari T, *et al.* 2020. Bacteriophages presence in nature and their role in the natural selection of bacterial populations. *Acta Biomedica* **91**: 1–13.

Neilands JB. 1966. Naturally occurring non-porphyrin iron compounds. In: Cardin C, Duan X, Gade LH, Sainz LG-H, Lu Y, Macgregor SA, Pariente JP, Schneider S, Stalke D, eds. Structure and Bonding. Structure And Bonding. Springer, Berlin, Heidelberg, 59–108.

Nesper J, Lauriano CM, Klose KE, Kapfhammer D, Kraiß A, Reidl J. 2001. Characterization of Vibrio cholerae O1 El Tor *galU* and *galE* mutants: influence on lipopolysaccharide structure, colonization, and biofilm formation. *Infection and Immunity* **69**: 435–445.

Nev OA, Lindsay RJ, Jepson A, Butt L, Beardmore RE, Gudelj I. 2021. Predicting microbial growth dynamics in response to nutrient availability. *PLoS Computational Biology* **17**: 1–20.

Newman MA, Daniels MJ, Dow JM. 1995. Lipopolysaccharide from *Xanthomonas campestris* induces defense-related gene expression in *Brassica campestris*. *Molecular Plant-Microbe Interactions* **8**: 778–780.

Newman M-A, von Roepenack E, Daniels M, Dow M. 2000. Lipopolysaccharides and plant responses to phytopathogenic bacteria. *Molecular Plant Pathology* **1**: 25–31.

Nguyen DD, Melnik A V., Koyama N, Lu X, Schorn M, Fang J, Aguinaldo K, Lincecum TL, Ghequire MGK, Carrion VJ, *et al.* 2016. Indexing the *Pseudomonas* specialized metabolome enabled the discovery of poaeamide B and the bananamides. *Nature Microbiology* **2**: 1–10.

Noble R. 2019. Create Muller Plots of Evolutionary Dynamics [R package ggmuller version 0.5.4].

Nordgaard M, Blake C, Maróti G, Strube ML, Kovács ÁT. 2021. Experimental evolution of *Bacillus subtilis* on *Arabidopsis thaliana* roots reveals fast adaptation and improved root colonization in the presence of soil microbes. *bioRxiv*: 2021.07.09.451762.

Oberhänsli T, Défago G, Haas D. 1991. Indole-3-acetic acid (IAA) synthesis in the biocontrol strain CHA0 of *Pseudomonas fluorescens*: role of tryptophan side chain oxidase. *Microbiology* **137**: 2273–2279.

Oku S, Komatsu A, Nakashimada Y, Tajima T, Kato J. 2014. Identification of *Pseudomonas fluorescens* chemotaxis sensory proteins for malate, succinate, and fumarate, and their involvement in root colonization. *Microbes and Environments* **29**: 413–419.

Oku S, Komatsu A, Tajima T, Nakashimada Y, Kato J. 2012. Identification of chemotaxis sensory proteins for amino acids in *Pseudomonas fluorescens* Pf0-1 and their involvement in chemotaxis to tomato root exudate and root colonization. *Microbes and Environments* **27**: 462–469.

Oldroyd GED, Murray JD, Poole PS, Downie JA. 2011. The rules of engagement in the legume-rhizobial symbiosis. *Annual Review of Genetics* **45**: 119–144.

Ondov BD, Treangen TJ, Melsted P, Mallonee AB, Bergman NH, Koren S, Phillippy AM. 2016. Mash: fast genome and metagenome distance estimation using MinHash. *Genome Biology* **17**: 1–14.

Ongena M, Jourdan E, Adam A, Paquot M, Brans A, Joris B, Arpigny J-L, Thonart P. 2007. Surfactin and fengycin lipopeptides of *Bacillus subtilis* as elicitors of induced systemic resistance in plants. *Environmental Microbiology* **9**: 1084–1090.

van Opijnen T, Camilli A. 2013. Transposon insertion sequencing: a new tool for systems-level analysis of microorganisms. *Nature Reviews. Microbiology* **11**: 435–442.

Oren Y, Smith MB, Johns NI, Kaplan Zeevi M, Biran D, Ron EZ, Corander J, Wang HH, Alm EJ, Pupko T. **2014**. Transfer of noncoding DNA drives regulatory rewiring in bacteria. *Proceedings of the National Academy of Sciences of the United States of America* **111**: 16112–16117.

Orr HA. **1998**. The population genetics of adaptation: the distribution of factors fixed during adaptive evolution. *Evolution* **52**: 935–949.

Pandey A, Sonti R V. **2010**. Role of the FeoB protein and siderophore in promoting virulence of *Xanthomonas oryzae* pv. *oryzae* on rice. *Journal of Bacteriology* **192**: 3187–3203.

Paradiso R, Orsini M, Censi SB, Borriello G, Galiero G. **2016**. Complete genome sequence of a *Myoviridae* bacteriophage infecting *Salmonella enterica* serovar Typhimurium. *Genome Announcements* **4**: 1–1.

Park Y-S, Dutta S, Ann M, Raaijmakers JM, Park K. **2015**. Promotion of plant growth by *Pseudomonas fluorescens* strain SS101 via novel volatile organic compounds. *Biochemical and Biophysical Research Communications* **461**: 361–365.

Parkins MD, Ceri H, Storey DG. **2001**. *Pseudomonas aeruginosa* GacA, a factor in multihost virulence, is also essential for biofilm formation. *Molecular Microbiology* **40**: 1215–1226.

Parsek MR, Greenberg EP. **2005**. Sociomicrobiology: the connections between quorum sensing and biofilms. *Trends in Microbiology* **13**: 27–33.

Parys K, Colaianni NR, Lee H-S, Hohmann U, Edelbacher N, Trgovcevic A, Blahovska Z, Lee D, Mechtler A, Muhari-Portik Z, *et al.* 2021. Signatures of antagonistic pleiotropy in a bacterial flagellin epitope. *Cell Host & Microbe*.

Patrick M, Korotkov K V., Hol WGJ, Sandkvist M. **2011**. Oligomerization of EpsE coordinates residues from multiple subunits to facilitate ATPase activity. *Journal of Biological Chemistry* **286**: 10378–10386.

Pearson CR, Tindall SN, Herman R, Jenkins HT, Bateman A, Thomas GH, Potts JR, Van der Woude MW. **2020**. Acetylation of surface carbohydrates in bacterial pathogens requires coordinated action of a two-domain membrane-bound acyltransferase. *mBio* **11**: 1–19.

Pearson C, Tindall S, Potts JR, Thomas GH, Woude MW Van Der. **2022**. Diverse functions for acyltransferase-3 proteins in the modification of bacterial cell surfaces. *Microbiology* **168**: 1–16.

Philippot L, Raaijmakers JM, Lemanceau P, Van Der Putten WH. **2013**. Going back to the roots: the microbial ecology of the rhizosphere. *Nature Reviews Microbiology* **11**: 789–799.

Pieterse CMJ, Berendsen RL, de Jonge R, Stringlis IA, Van Dijken AJH, Van Pelt JA, Van Wees SCM, Yu K, Zamioudis C, Bakker PAHM. **2021**. *Pseudomonas simiae* WCS417: star track of a model beneficial rhizobacterium. *Plant and Soil* **461**: 245–263.

Pieterse CMJ, de Jonge R, Berendsen RL. **2016**. The soil-borne supremacy. *Trends in Plant Science* **21**: 171–173.

Pieterse CMJ, Zamioudis C, Berendsen RL, Weller DM, Van Wees SCM, Bakker PAHM. **2014**. Induced systemic resistance by beneficial microbes. *Annual Review of Phytopathology* **52**: 347–375.

Pratama AA, Van Elsas JD. **2017**. A novel inducible prophage from the mycosphere inhabitant *Paraburkholderia terrae* BS437. *Scientific Reports* **7**: 1–14.

Quinlan AR, Hall IM. **2010**. BEDTools: a flexible suite of utilities for comparing genomic features. *Bioinformatics (Oxford, England)* **26**: 841–842.

Raaijmakers JM, Bonsall RF, Weller DM. **1999**. Effect of population density of *Pseudomonas fluorescens* on production of 2,4-Diacetylphloroglucinol in the rhizosphere of wheat. *Phytopathology* **89**: 470–475.

Raaijmakers JM, de Bruijn I, Nybroe O, Ongena M. **2010**. Natural functions of lipopeptides from *Bacillus* and *Pseudomonas*: more than surfactants and antibiotics. *FEMS Microbiology Reviews* **34**: 1037–1062.

Raaijmakers JM, Leeman M, Oorschot van MM., et.al. 1995. Dose-response relationships in biological control of Fusarium wilt of radish by *Pseudomonas* spp.. *Phytopathology* **85**: 1075–1081.

Raaijmakers JM, Paulitz TC, Steinberg C, Alabouvette C, Moënne-Loccoz Y. 2009. The rhizosphere: a playground and battlefield for soilborne pathogens and beneficial microorganisms. *Plant and Soil* **321**: 341–361.

Raetz CRH, Whitfield C. 2002. Lipopolysaccharide endotoxins. *Annual Review of Biochemistry*.

Ramesh R, Joshi AA, Ghanekar MP. 2009. Pseudomonads: major antagonistic endophytic bacteria to suppress bacterial wilt pathogen, *Ralstonia solanacearum* in the eggplant (*Solanum melongena* L.). *World Journal of Microbiology and Biotechnology* **25**: 47–55.

Ramette A, Frapolli M, Saux MF Le, Gruffaz C, Meyer JM, Défago G, Sutra L, Moënne-Loccoz Y. 2011. *Pseudomonas protegens* sp. nov., widespread plant-protecting bacteria producing the biocontrol compounds 2,4-diacetylphloroglucinol and pyoluteorin. *Systematic and Applied Microbiology* **34**: 180–188.

Ramisetty BCM, Sudhakari PA. 2019. Bacterial 'grounded' prophages: hotspots for genetic renovation and innovation. *Frontiers in Genetics* **10**: 1–17.

Ranf S. 2016. Immune sensing of lipopolysaccharide in plants and animals: same but different. *PLoS Pathogens* **12**: 1–7.

Ranf S, Gisch N, Schäffer M, Illig T, Westphal L, Knirel YA, Sánchez-Carballo PM, Zähringer U, Hückelhoven R, Lee J, *et al.* 2015. A lectin S-domain receptor kinase mediates lipopolysaccharide sensing in *Arabidopsis thaliana*. *Nature Immunology* **16**: 426–433.

Rapicavoli JN, Blanco-Ulate B, Muszyński A, Figueroa-Balderas R, Morales-Cruz A, Azadi P, Dobruchowska JM, Castro C, Cantu D, Roper MC. 2018. Lipopolysaccharide O-antigen delays plant innate immune recognition of *Xylella fastidiosa*. *Nature Communications* **9**: 1–12.

Raymond CK, Sims EH, Kas A, Spencer DH, Kutyavin T V., Ivey RG, Zhou Y, Kaul R, Clendenning JB, Olson M V. 2002. Genetic variation at the O-antigen biosynthetic locus in *Pseudomonas aeruginosa*. *Journal of Bacteriology* **184**: 3614–3622.

Reinhold-Hurek B, Bünger W, Burbano CS, Sabale M, Hurek T. 2015. Roots shaping their microbiome: global hotspots for microbial activity. *Annual Review of Phytopathology* **53**: 403–424.

Ristl R, Janesch B, Anzengruber J, Forsthuber A, Blaha J. 2015. Europe PMC funders group description of a putative oligosaccharyl: S-layer protein transferase from the Tyrosine *O*-glycosylation System of *Paenibacillus alvei* CCM 2051^T. **2**: 537–546.

Rodrigues ER, Rocha GA, Ferreira AG, Leão RS, Albano RM, Marques EA. 2016. Draft genome sequences of four *Achromobacter ruhlandii* strains isolated from cystic fibrosis patients. *Memorias do Instituto Oswaldo Cruz* **111**: 777–780.

Rodríguez-Navarro DN, Dardanelli MS, Ruíz-Saínz JE. 2007. Attachment of bacteria to the roots of higher plants. *FEMS Microbiology Letters* **272**: 127–136.

Rodriguez-Valera F, Martin-Cuadrado AB, Rodriguez-Brito B, Pašić L, Thingstad TF, Rohwer F, Mira A. 2009. Explaining microbial population genomics through phage predation. *Nature Reviews Microbiology* **7**: 828–836.

Rohwer F. 2003. Global phage diversity. *Cell* **113**: 141–141.

Rohwer F, Segall AM. 2015. A century of phage lessons. *Nature* **528**: 46–47.

Romling U, Galperin MY, Gomelsky M. 2013. Cyclic di-GMP: the first 25 years of a universal bacterial second messenger. *Microbiology and Molecular Biology Reviews* **77**: 1–52.

Rozen DE, De Visser JAGM, Gerrish PJ. 2002. Fitness effects of fixed beneficial mutations in microbial populations. *Current Biology* **12**: 1040–1045.

Rudrappa T, Biedrzycki ML, Kunjeti SG, Donofrio NM, Czymmek KJ, Paré PW, Bais HP. 2010. The rhizobacterial elicitor acetoin induces systemic resistance in *Arabidopsis thaliana*. *Communicative and Integrative Biology* **3**: 130–138.

Ruffner B, Péchy-Tarr M, Höfte M, Bloemberg G, Grunder J, Keel C, Maurhofer M. 2015. Evolutionary patchwork of an insecticidal toxin shared between plant-associated pseudomonads and the insect pathogens Photorhabdus and Xenorhabdus. *BMC Genomics* **16**: 1–14.

Ruiz JA, Bernar EM, Jung K. 2015. Production of siderophores increases resistance to fusaric acid in *Pseudomonas protegens* Pf-5. *PLOS ONE* **10**: e0117040.

Ryu C, Farag MA, Hu C, Reddy MS, Wei H, Raré PW, Kloepper JW. 2003. Bacterial volatiles promote growth in *Arabidopsis*. *PNAS* **100**: 4927–4932.

Sampedro I, Parales RE, Krell T, Hill JE. 2015. *Pseudomonas* chemotaxis. *FEMS Microbiology Reviews* **39**: 17–46.

Samuel G, Reeves P. 2003. Biosynthesis of O-antigens: genes and pathways involved in nucleotide sugar precursor synthesis and O-antigen assembly. *Carbohydrate Research* **338**: 2503–2519.

Samuel BS, Rowedder H, Braendle C, Félix MA, Ruvkun G. 2016. Caenorhabditis elegans responses to bacteria from its natural habitats. *Proceedings of the National Academy of Sciences of the United States of America* **113**: E3941–E3949.

Sánchez-Contreras M, Martín M, Villacieros M, O'Gara F, Bonilla I, Rivilla R. 2002. Phenotypic selection and phase variation occur during alfalfa root colonization by Pseudomonas fluorescens F113. *Journal of Bacteriology* **184**: 1587–1596.

Sasse J, Martinoia E, Northen T. 2018. Feed your friends: do plant exudates shape the root microbiome? *Trends in Plant Science* **23**: 25–41.

Savary S, Willocquet L, Pethybridge SJ, Esker P, McRoberts N, Nelson A. 2019. The global burden of pathogens and pests on major food crops. *Nature Ecology and Evolution* **3**: 430–439.

Scanlan PD. 2017. Bacteria–bacteriophage coevolution in the human gut: implications for microbial diversity and functionality. *Trends in Microbiology* **25**: 614–623.

Scharf DH, Heinekamp T, Brakhage AA. 2014. Human and plant fungal pathogens: the role of secondary metabolites. *PLOS Pathogens* **10**: e1003859.

Schmidt R, Cordovez V, de Boer W, Raaijmakers J, Garbeva P. 2015. Volatile affairs in microbial interactions. *The ISME journal* **9**: 2329–2335.

Scholz-Schroeder BK, Hutchison ML, Grgurina I, Gross DC. 2001. The contribution of syringopeptin and syringomycin to virulence of *Pseudomonas syringae* pv. *syringae* strain B301D on the basis of *sypA* and *syrB1* biosynthesis mutant analysis. *Molecular plant-microbe interactions: MPMI* **14**: 336–348.

Schwechheimer C, Kuehn MJ. 2015. Outer-membrane vesicles from gram-negative bacteria: biogenesis and functions. *Nature Reviews Microbiology* **13**: 605–619.

Scrucca L, Fop M, Murphy TB, Raftery AE. 2016. Mclust 5: clustering, classification and density estimation using gaussian finite mixture models. *The R journal* **8**: 289–317.

Shafquat A, Sirota-Madi A, Huttenhower C, Franzosa EA, Abu-Ali G, Hsu T, Morgan XC. 2015. Sequencing and beyond: integrating molecular 'omics' for microbial community profiling. *Nature Reviews Microbiology* **13**: 360.

Siegień I, Bogatek R. 2006. Cyanide action in plants - from toxic to regulatory. *Acta Physiologiae Plantarum* **28**: 483–497.

Silipo A, Molinaro A, Sturiale L, Dow JM, Erbs G, Lanzetta R, Newman MA, Parrilli M. 2005. The elicitation of plant innate immunity by lipooligosaccharide of *Xanthomonas campestris*. *Journal of Biological Chemistry* **280**: 33660–33668.

Simm R, Morr M, Kader A, Nimtz M, Römling U. **2004**. GGDEF and EAL domains inversely regulate cyclic di-GMP levels and transition from sessibility to motility. *Molecular Microbiology* **53**: 1123–1134.

Simons M, Permentier HP, de Weger LA, Wijffelman CA, Lugtenberg BJJ. **1997**. Amino acid synthesis is necessary for tomato root colonization by *Pseudomonas fluorescens* strain WCS365. *Molecular Plant-Microbe Interactions* **10**: 102–106.

Simpson BW, Trent MS. **2019**. Pushing the envelope: LPS modifications and their consequences. *Nature Reviews Microbiology* **17**: 403–416.

Slauch JM, Mahan MJ, Michetti P, Neutra MR, Mekalanos JJ. **1995**. Acetylation (O-factor 5) affects the structural and immunological properties of *Salmonella typhimurium* lipopolysaccharide O antigen. *Infection and Immunity* **63**: 437–441.

De Smet J, Hendrix H, Blasdel BG, Danis-Wlodarczyk K, Lavigne R. **2017**. *Pseudomonas* predators: understanding and exploiting phage-host interactions. *Nature Reviews Microbiology* **15**: 517–530.

Smith EE, Buckley DG, Wu Z, Saenphimmachak C, Hoffman LR, D'Argenio DA, Miller SI, Ramsey BW, Speert DP, Moskowitz SM, *et al.* 2006. Genetic adaptation by *Pseudomonas aeruginosa* to the airways of cystic fibrosis patients. *Proceedings of the National Academy of Sciences of the United States of America* **103**: 8487–92.

Smits WK, Kuipers OP, Veening JW. **2006**. Phenotypic variation in bacteria: the role of feedback regulation. *Nature Reviews Microbiology* **4**: 259–271.

Sobrero PM, Muzlera A, Frescura J, Jofré E, Valverde C. **2017**. A matter of hierarchy: activation of orfamide production by the post-transcriptional Gac-Rsm cascade of *Pseudomonas protegens* CHA0 through expression upregulation of the two dedicated transcriptional regulators. *Environmental Microbiology Reports* **9**: 599–611.

Song C. **2015**. Regulation and natural functions of lipopeptide biosynthesis in *Pseudomonas*. *Wageningen University and Research*.

Song C, Kidarsa TA, van de Mortel JE, Loper JE, Raaijmakers JM. **2016**. Living on the edge: emergence of spontaneous *gac* mutations in *Pseudomonas protegens* during swarming motility. *Environmental Microbiology* **18**: 3453–3465.

Stearns FW. **2010**. One hundred years of pleiotropy: a retrospective. *Genetics* **186**: 767–773.

Stefanic P, Kraigher B, Lyons NA, Kolter R, Mandic-Mulec I. **2015**. Kin discrimination between sympatric *Bacillus subtilis* isolates. *Proceedings of the National Academy of Sciences of the United States of America* **112**: 14042–14047.

Strano CP, Bella P, Licciardello G, Fiore A, Lo Piero AR, Fogliano V, Venturi V, Catara V. **2015**. *Pseudomonas corrugata crpCDE* is part of the cyclic lipopeptide corpeptin biosynthetic gene cluster and is involved in bacterial virulence in tomato and in hypersensitive response in *Nicotiana benthamiana*. *Molecular Plant Pathology* **16**: 495–506.

Stringlis IA, Proietti S, Hickman R, Van Verk MC, Zamioudis C, Pieterse CMJ. **2018a**. Root transcriptional dynamics induced by beneficial rhizobacteria and microbial immune elicitors reveal signatures of adaptation to mutualists. *Plant Journal* **93**: 166–180.

Stringlis IA, Yu K, Feussner K, De Jonge R, Van Bentum S, Van Verk MC, Berendsen RL, Bakker PAHM, Feussner I, Pieterse CMJ. **2018b**. MYB72-dependent coumarin exudation shapes root microbiome assembly to promote plant health. *Proceedings of the National Academy of Sciences of the United States of America* **115**: E5213–E5222.

Stringlis IA, Zhang H, Pieterse CMJ, Bolton MD, De Jonge R. **2018c**. Microbial small molecules-weapons of plant subversion. *Natural Product Reports* **35**: 410–433.

Stutz EW, Défago G, Kern H. **1986**. Naturally occurring fluorescent pseudomonads involved in suppression of black root rot of tobacco. *Phytopathology* **76**: 181–185.

Sumby P, Whitney AR, Graviss EA, DeLeo FR, Musser JM. 2006. Genome-wide analysis of group A streptococci reveals a mutation that modulates global phenotype and disease specificity. *PLoS Pathogens* **2**: e5.

Takeuchi K, Noda N, Someya N. 2014. Complete genome sequence of the biocontrol strain *Pseudomonas protegens* Cab57 discovered in Japan reveals strain-specific diversity of this species. *PLoS ONE* **9**: 1–13.

Thingstad TF. 2000. Elements of a theory for the mechanisms controlling abundance, diversity, and biogeochemical role of lytic bacterial viruses in aquatic systems. *Limnology and Oceanography* **45**: 1320–1328.

Tjørve KMC, Tjørve E. 2017. The use of Gompertz models in growth analyses, and new Gompertz-model approach: an addition to the Unified-Richards family. *PLoS ONE* **12**: e0178691-17.

Tracanna V, de Jong A, Medema MH, Kuipers OP. 2017. Mining prokaryotes for antimicrobial compounds: from diversity to function. *FEMS Microbiology Reviews* **41**: 417–429.

Tran H, Ficke A, Asiimwe T, Höfte M, Raaijmakers JM. 2007. Role of the cyclic lipopeptide massetolide A in biological control of *Phytophthora infestans* and in colonization of tomato plants by *Pseudomonas fluorescens*. *The New Phytologist* **175**: 731–742.

Trapet P, Avoscan L, Klinguer A, Pateyron S, Citerne S, Chervin C, Mazurier S, Lemanceau P, Wendehenne D, Besson-Bard A. 2016. The *Pseudomonas fluorescens* siderophore pyoverdine weakens *Arabidopsis thaliana* defense in favour of growth in iron-deficient conditions. *Plant Physiology* **171**: 675–693.

Tsai C-M, Frasch CE. 1982. A sensitive silver stain for detecting lipopolysaccharides in polyacrylamide gels. *Analytical Biochemistry* **119**: 115–119.

Vacheron J, Heiman CM, Keel C. 2021. Live cell dynamics of production, explosive release and killing activity of phage tail-like weapons for *Pseudomonas* kin exclusion. *Communications Biology* **4**: 1–14.

Vacheron J, Kupferschmied P, Resch G, Keel C. 2018. Genome sequence of the *Pseudomonas protegens* phage ΦGP100. *Genome Announcements* **6**: 1–2.

Valentini M, Filloux A. 2016. Biofilms and cyclic di-GMP (c-di-GMP) signaling: lessons from *Pseudomonas aeruginosa* and other bacteria. *Journal of Biological Chemistry* **291**: 12547–12555.

Valverde C, Heeb S, Keel C, Haas D. 2003. RsmY, a small regulatory RNA , is required in concert with RsmZ for GacA-dependent expression of biocontrol traits in *Pseudomonas fluorescens* CHA0. *Molecular Microbiology* **50**: 1361–1379.

Vejan P, Abdullah R, Khadiran T, Ismail S, Nasrulhaq Boyce A. 2016. Role of plant growth promoting rhizobacteria in agricultural sustainability- a review. *Molecules* **21**: 1–17.

Venturi V, Keel C. 2016. Signaling in the rhizosphere. *Trends in Plant Science* **21**: 187–198.

Verbon EH, Trapet PL, Stringlis IA, Kruijs S, Bakker PAHM, Pieterse CMJ. 2017. Iron and Immunity. *Annual Review of Phytopathology* **55**: 355–375.

Visca P, Imperi F, Lamont IL. 2007. Pyoverdine siderophores: from biogenesis to biosignificance. *Trends in Microbiology* **15**: 22–30.

De Vleesschauwer D, Höfte M. 2009. Rhizobacteria-induced systemic resistance. *Advances in Botanical Research* **51**: 223–281.

Vollmer W, Blanot D, De Pedro MA. **2008**. Peptidoglycan structure and architecture. *FEMS Microbiology Reviews* **32**: 149–167.

Vollmer W, Seligman SJ. **2010**. Architecture of peptidoglycan: more data and more models. *Trends in Microbiology* **18**: 59–66.

Waldor MK, Friedman DI. **2005**. Phage regulatory circuits and virulence gene expression. *Current Opinion in Microbiology* **8**: 459–465.

Wang L, Wang Q, Reeves PR. **2010**. The variation of O antigens in gram-negative bacteria. *Sub-Cellular Biochemistry* **53**: 123–152.

De Weert S, Vermeiren H, Mulders IHM, Kuiper I, Hendrickx N, Bloemberg G V., Vanderleyden J, De Mot R, Lugtenberg BJJ. **2002**. Flagella-driven chemotaxis towards exudate components is an important trait for tomato root colonization by *Pseudomonas fluorescens*. *Molecular Plant-Microbe Interactions* **15**: 1173–1180.

Van Wees SCM, Van Pelt JA, Bakker PAHM, Pieterse CMJ. **2013**. Bioassays for assessing jasmonate-dependent defenses triggered by pathogens, herbivorous insects, or beneficial rhizobacteria. In: Goossens A, Pauwels L, eds. Jasmonate Signaling: Methods and Protocols. Totowa, NJ: Humana Press, 35–49.

Van Wees SCM, Pieterse CMJ, Trijssenaar A, Van 't Westende YAM, Hartog F, Van Loon LC. **1997**. Differential induction of systemic resistance in *Arabidopsis* by biocontrol bacteria. *Molecular Plant-Microbe Interactions* **10**: 716–724.

De Weger LA, Bakker PAHM, Schipers B, van Loosdrecht M, Lugtenberg BJJ. **1989a**. *Pseudomonas* spp. with mutational changes in the O-antigenic side chain of their lipopolysaccharide are affected in their ability to colonize potato roots (BJJ Lugtenberg, Ed.). *Signal Molecules in Plants and Plant-Microbe Interactions* **H36**: pp.197-202.

De Weger LA, Van Loosdrecht MC, Klaassen HE, Lugtenberg B. **1989b**. Mutational changes in physiochemical cell surface properties of plant-growth-stimulating *Pseudomonas* spp. do not influence the attachment properties of the cells. *Journal of bacteriology* **171**: 2756–2761.

De Weger LA, van Der Vlugt CIM, Wijfjes AHM, Bakker PA, Schippers B, Lugtenberg B. **1987**. Flagella of a plant-growth-stimulating *Pseudomonas fluorescens* strain are required for colonization of potato roots. *Journal of Bacteriology* **169**: 2769–2773.

Weinbauer MG, Rassoulzadegan F. **2004**. Are viruses driving microbial diversification and diversity? *Environmental Microbiology* **6**: 1–11.

Wen Y, Wu X, Teng Y, Qian C, Zhan Z, Zhao Y, Li O. **2011**. Identification and analysis of the gene cluster involved in biosynthesis of paenibactin, a catecholate siderophore produced by *Paenibacillus elgii* B69. *Environmental Microbiology* **13**: 2726–2737.

Wheatley RM, Poole PS. **2018**. Mechanisms of bacterial attachment to roots. *FEMS Microbiology Reviews* **42**: 448–461.

Whitfield C, Trent MS. **2014**. Biosynthesis and export of bacterial lipopolysaccharides. *Annual Review of Biochemistry* **83**: 99–128.

Winstanley C, O'Brien S, Brockhurst MA. **2016**. *Pseudomonas aeruginosa* evolutionary adaptation and diversification in cystic fibrosis chronic lung infections. *Trends in Microbiology* **24**: 327–337.

Workentine ML, Chang L, Ceri H, Turner RJ. **2009**. The GacS-GacA two-component regulatory system of *Pseudomonas fluorescens*: a bacterial two-hybrid analysis. *FEMS Microbiology Letters* **292**: 50–56.

Xin X-F, Nomura K, Aung K, Velásquez AC, Yao J, Boutrot F, Chang JH, Zipfel C, He SY. **2016**. Bacteria establish an aqueous living space in plants crucial for virulence. *Nature* **539**: 524.

Yang J, Kloepper JW, Ryu C-M. **2009**. Rhizosphere bacteria help plants tolerate abiotic stress. *Trends in Plant Science* **14**: 1–4.

Yi HY, Chowdhury M, Huang YD, Yu XQ. 2014. Insect antimicrobial peptides and their applications. *Applied Microbiology and Biotechnology* **98**: 5807–5822.

York LM, Carminati A, Mooney SJ, Ritz K, Bennett MJ. 2016. The holistic rhizosphere: integrating zones, processes, and semantics in the soil influenced by roots. *Journal of Experimental Botany* **67**: 3629–3643.

Yu K, Liu Y, Tichelaar R, Savant N, Lagendijk E, van Kuijk SJL, Stringlis IA, van Dijken AJH, Pieterse CMJ, Bakker PAHM, *et al.* 2019. Rhizosphere-associated *Pseudomonas* suppress local root immune responses by gluconic acid-mediated lowering of environmental pH. *Current Biology* **29**: 3913-3920.e4.

Yu JM, Wang D, Pierson LS, Pierson EA. 2017. Disruption of MiaA provides insights into the regulation of phenazine biosynthesis under suboptimal growth conditions in *Pseudomonas chlororaphis* 30-84. *Microbiology (Reading, England)* **163**: 94–108.

Zachow C, Jahanshah G, de Bruijn I, Song C, Ianni F, Pataj Z, Gerhardt H, Pianet I, Lämmerhofer M, Berg G, *et al.* 2015. The novel lipopeptide poaeamide of the endophyte *Pseudomonas poae* RE*1-1-14 is involved in pathogen suppression and root colonization. *Molecular Plant-Microbe Interactions* **28**: 800–810.

Zambrano MM, Siegele DA, Almirón M, Tormo A, Kolter R. 1993. Microbial competition: *Escherichia coli* mutants that take over stationary phase cultures. *Science (New York, N.Y.)* **259**: 1757–1760.

Zamioudis C, Hanson J, Pieterse CMJ. 2014. ß-Glucosidase BGLU42 is a MYB72-dependent key regulator of rhizobacteria-induced systemic resistance and modulates iron deficiency responses in *Arabidopsis* roots. *New Phytologist* **204**: 368–379.

Zamioudis C, Korteland J, Van Pelt JA, Van Hamersveld M, Dombrowski N, Bai Y, Hanson J, Van Verk MC, Ling HQ, Schulze-Lefert P, *et al.* 2015. Rhizobacterial volatiles and photosynthesis-related signals coordinate *MYB72* expression in Arabidopsis roots during onset of induced systemic resistance and iron-deficiency responses. *Plant Journal* **84**: 309–322.

Zamioudis C, Mastranesti P, Dhonukshe P, Blilou I, Pieterse CMJ. 2013. Unraveling root developmental programs initiated by beneficial *Pseudomonas* spp. bacteria. *Plant Physiology* **162**: 304–318.

Zamioudis C, Pieterse CMJ. 2012. Modulation of host immunity by beneficial microbes. *Molecular Plant-Microbe Interactions* **25**: 139–150.

Zboralski A, Filion M. 2020. Genetic factors involved in rhizosphere colonization by phytobeneficial *Pseudomonas* spp. *Computational and Structural Biotechnology Journal* **18**: 3539–3554.

Zeidler D, Zähringer U, Gerber I, Dubery I, Hartung T, Bors W, Hutzler P, Durner J. 2004. Innate immunity in *Arabidopsis thaliana*: lipopolysaccharides activate nitric oxide synthase (NOS) and induce defense genes. *Proceedings of the National Academy of Sciences of the United States of America* **101**: 15811–15816.

Zhalnina K, Louie KB, Hao Z, Mansoori N, Rocha da UN, Shi S, Cho H, Karaoz U, Loqué D, Bowen BP, *et al.* 2018. Dynamic root exudate chemistry and microbial substrate preferences drive patterns in rhizosphere microbial community assembly. *Nature Microbiology* **3**: 470–480.

Zhong WL, Wang L, Wu X, Zhang J, Chen XF, Zhang W, Dou X, Yu B. 2016. Development of unlabeled probe based High-Resolution Melting analysis for detection of filaggrin gene mutation c.3321delA. *Journal of Clinical Laboratory Analysis* **30**: 892–896.

Zimmermann L, Stephens A, Nam SZ, Rau D, Kübler J, Lozajic M, Gabler F, Söding J, Lupas AN, Alva V. 2018. A completely reimplemented MPI bioinformatics toolkit with a new HHpred server at its core. *Journal of Molecular Biology* **430**: 2237–2243.

Appendices

Summary
Samenvatting
摘要
Acknowledgements
About the author
Publications

Summary

Plants rely on a variety of microbes for their survival and growth. While most of these microbes are harmless, some can harm our crops, leading to reduced yield and food security risks. In contrast, beneficial bacteria can help plants by improving nutrient uptake and protecting them from pests and diseases. These beneficial bacteria can influence the plant's immune system to establish a mutually beneficial relationship, similar to how friendly bacteria in the human gut help us. Communication is an essential part of plant-bacteria relationships, with small molecules playing a significant role. Both harmful and beneficial bacteria use various methods to communicate with the plants they live on, such as delivering plant immune-suppressive proteins, producing plant hormones, and creating bioactive molecules. Plants also communicate with their associated bacteria by releasing carbon sources and other compounds through their roots.

In **Chapter 1**, we explore the role of small molecules in modulation of beneficial plant-bacteria interactions, as well as assess their potential use as weapons by harmful bacteria. We use comparative genomics to examine the small molecule production potential of diverse pseudomonads, a group of bacteria commonly found in various natural environments, which consist of both helpful and harmful types. Understanding the biosynthesis and activity of these small molecules can aid in the development of sustainable biological agents to boost crop resilience and combat pathogenic bacteria.

In agriculture, some attempts have been made that involve using plant beneficial bacteria as biological agents to promote plant growth and protect them from pests and diseases without using chemical fertilizers and pesticides. For example, when plant growth-promoting pseudomonads, that have been shown to display many benefits for plants under laboratory conditions, are applied in the field, their performance can vary greatly due to factors such as environmental conditions that may favor local microorganisms and the lack of adaptation to the specific crop they are being used on. Researchers have identified some mechanisms that beneficial bacteria use to overcome these challenges, such as the production of compounds that grab iron with high affinity, or by hiding from the host's immune system. In order to improve the use of beneficial bacteria in agriculture, it is important to understand how such organisms adapt to the host plants they are meant to benefit.

To investigate bacterial adaptation towards plant roots, in **Chapter 2**, we conducted experiments to track the genetic and physiological changes of a bacterium called *Pseudomonas protegens* CHA0 while it colonized the root of the laboratory model plant, *Arabidopsis thaliana*. By isolating bacteria from plant roots over time, we were able

to identify the key mechanisms that promote efficient colonization. Even though the bacteria-plant relationship was not mutually beneficial at the start of the experiment, some bacterial isolates that benefit the plant evolved and survived during later stages of the experiment. Among the evolved bacterial isolates, we identified 35 unique mutations, including small polymorphisms, and larger insertions, and deletions, in 28 different genes. Interestingly, we observed mutations in genes that regulate bacterial cell surface decoration, bacterial attachment, and motility repeatedly in multiple replicates, indicating that bacterial adaptation to the plant root can involve multiple strategies. One notable finding was that motility, i.e., the ability of bacteria to move around, increased across multiple independent evolutionary replicated experiments. Overall, these results highlight how experimental evolution can be used to identify key genes and processes involved in bacterial colonization of plant roots.

In addition to bacterial motility, stable colonization of the plant roots is an important factor for bacterial success. From earlier studies, several features have been found that contribute to bacterial plant root colonization including the way the bacterial cell wall is decorated. In **Chapter 3**, we used our evolved bacterial isolates with modifications in genes related to cell wall decoration to further assess its role in bacterial root colonization. Specifically, we investigated how mutations in the *oafA* gene, which encodes a predicted O-antigen acetyltransferase, result in improved root colonization by enhancing root attachment. Mutations in *oafA* affect the functionality of the encoded O-antigen acetyltransferase, likely resulting in modifications of the O-antigen. The O-antigen is a critical component of the cell surface lipopolysaccharide, which is also known as LPS. Our findings indicate that these mutations enhance the fitness of the bacteria specifically in the root environment. This effect was not observed in various other conditions in the absence of plants, suggesting a plant-dependent fitness benefit. Additional experiments revealed that the improved fitness in the root environment of the *oafA* mutants could be linked to accelerated attachment on the root. Moreover, we found that another mutant with a disruption in a gene named *RS09880*, which encodes a predicted glycosyl transferase, also improves bacterial fitness on the root by increasing root attachment. Notably, both genes, *oafA* and *RS09880*, are located in the same gene cluster, called *O-antigenic polysaccharide biosynthesis cluster 3* (*OBC3*) supporting the view that modification of the cell wall decoration represents an important route for bacterial adaptation.

Given the proposed important role in bacterial adaptation, in **Chapter 4**, we investigated whether genetic changes in the *OBC3* gene cluster can also be found among naturally occurring bacteria. Therefore, we studied the genome sequences of all publicly available pseudomonads and evaluated the presence and the variation of *OBC3* genes. Firstly, we identified *OBC3* gene clusters only among strains of the same species, i.e.,

Pseudomonas protegens, and, secondly, we indeed observed a large degree of variation in the *OBC3* genes of these strains. Surprisingly, within this variation we observed highly similar mutations as we observed in the laboratory evolution experiment disrupting the *oafA* gene in the same way in the respective strains. While some strains were sourced from the plant environment, several strains that carried the disruptive mutations in *oafA* were not found in or around plants. Notably, cell wall decoration is not only important for interaction with plant roots, many earlier studies have highlighted its importance in interactions with bacterial viruses (or bacteriophages). Bacteriophages infect bacteria and are commonly found in all the environments where bacteria can be found. As it is known that cell wall decoration also plays a role in bacteriophage susceptibility, we next evaluated the sensitivity of laboratory-evolved bacteria to a bacteriophage and indeed confirmed altered sensitivity in several of our evolved *OBC3* mutants. Altered sensitivity coincided with alterations in cell wall decoration, as revealed by analysis of the global LPS structure and O-antigen patterning. Overall, this study showed that *OBC3* mutations can be found in nature and can occasionally provide bacteria with resistance to certain bacterial viruses, likely via structural modifications of the cell wall decoration.

In **Chapter 5**, I proposed a model, the stepwise adaptation of bacteria in the plant root environment. The model is based on all research presented in this thesis conducted on the bacterial strain *Pseudomonas protegens* CHA0 and its interactions with the plant *Arabidopsis thaliana*. It is explained as follows, in a plant root environment, new for bacteria, bacteria initially colonize the plant and feed on the carbohydrates that the plant produces and exudes. Bacterial attachment and the production of small molecules cause the plant to activate its immune system, resulting in the production of toxic compounds, and reduction of the exudation of carbohydrates. These changes provide selective pressure on the bacteria that leads to the evolution of bacterial mutants that are better suited to this new environment. The mutants include those with modifications on their cell surface decoration which could enhance bacterial resistance to toxins and increase attachment to the plant root surface. Later, succeeding bacterial mutants with reduced random cell movement, for exploration, and enhanced swimming ability are selected. These stepwise accumulated mutations change the bacterial biofilm structure across the bacterial community. This, in turn, not only improves bacterial fitness, it also affects the interactions with other bacteria via quorum-sensing mechanisms. Our research reveals the importance of bacterial phenotypic and genotypic variation in microbial communities and indicates the necessity of using single-cell technologies to track bacterial variation in the future research. Finally, I note that the model proposed in the laboratory experiments could have implications for bacterial evolution in natural environments, as similar mutants have been found in similar strains from natural environments.

Collectively, plant growth-promoting bacteria, such as those within the *Pseudomonas* genus, can be beneficial for sustainable agriculture. However, they may not always perform well due to local environmental factors and their inability to adapt to specific crops. The ability of these bacteria to colonize plant roots is crucial in order for them to exhibit their beneficial effects. Different features of these bacteria, like their ability to move with the help of flagellin and pili, and the attachment to the root surface via structures composed of diverse polysaccharides, contribute to their successful establishment. Their overall ability to form a strong and cohesive biofilm is likely to play an important role. Our research improved our understanding on how bacteria adapt to their environment, which will be important for the practice on improving their effectiveness in field and therewith supporting sustainable agriculture.

Samenvatting

Planten zijn afhankelijk van micro-organismen voor hun overleving en groei. Hoewel de meeste van deze micro-organismen onschadelijk zijn, kunnen sommige ernstige schade toebrengen aan onze gewassen, wat weer leidt tot verminderde opbrengst en voedselveiligheidsrisico's. Daarentegen kunnen nuttige micro-organismen planten helpen door de opname van voedingsstoffen te verbeteren en ze te beschermen tegen ziekten en plagen. Deze gunstige micro-organismen kunnen het immuunsysteem van de plant beïnvloeden om een wederzijds voordelige relatie tot stand te brengen, vergelijkbaar met hoe goedaardige bacteriën in de menselijke darm profiteren van onze voeding en ons helpen met de vertering hiervan. Communicatie is een essentieel onderdeel van plant-micro-organisme relaties, waarbij kleine moleculen een belangrijke rol spelen. Zowel schadelijke als nuttige micro-organismen gebruiken verschillende methoden om te communiceren met de planten waarop ze leven, zoals het afleveren van plantimmuuniteit onderdrukkende eiwitten, het produceren van plantenhormonen en het maken van bioactieve moleculen. Andersom communiceren planten ook met de micro-organismen op hun wortels, onder andere via de exsudatie van suikers en andere verbindingen.

In **Hoofdstuk 1** onderzoeken we de rol van kleine moleculen bij het moduleren van gunstige interacties tussen planten en bacteriën, en beoordelen we hoe ze worden gebruikt als wapens door schadelijke bacteriën. We gebruiken vergelijkende genomica om het productiepotentieel van kleine moleculen te onderzoeken van diverse pseudomonaden, een groep bacteriën die veelvuldig gevonden wordt in natuurlijke omgevingen en die bestaat uit zowel nuttige als schadelijke soorten. Inzicht in de biosynthese en activiteit van deze kleine moleculen kan helpen bij de ontwikkeling van duurzame biologische agentia om de weerbaarheid van gewassen te vergroten en pathogene bacteriën te bestrijden.

In de landbouw zijn er meerdere pogingen gedaan waarbij nuttige bacteriën voor planten worden gebruikt als biologische agentia om plantengroei te bevorderen en ze te beschermen tegen ziekten en plagen zonder gebruik te maken van chemische meststoffen en pesticiden. Wanneer bijvoorbeeld plantengroei-bevorderende pseudomonaden, waarvan is aangetoond dat ze onder laboratoriumomstandigheden veel voordelen voor planten hebben, in het veld worden toegepast, kunnen hun prestaties sterk variëren als gevolg van factoren zoals omgevingsfactoren die de al aanwezige micro-organismen kunnen bevoordelen. Ook het gebrek aan aanpassing aan het specifieke gewas waarop ze worden gebruikt kan in het nadeel werken van deze biologische agentia. Onderzoekers hebben verschillende mechanismen geïdentificeerd die nuttige bacteriën gebruiken om deze uitdagingen te overwinnen, zoals onder andere de productie van

verbindingen die ijzer met hoge affiniteit binden, of door zich te verbergen voor het immuunsysteem van de plant. Om het gebruik van nuttige bacteriën in de landbouw te verbeteren, is het belangrijk om te begrijpen hoe dergelijke micro-organismen zich aanpassen aan de waardplanten welke ze zouden moeten ondersteunen.

Om bacteriële aanpassing aan plantenwortels te onderzoeken, hebben we in **Hoofdstuk 2** experimenten uitgevoerd om de genetische en fysiologische veranderingen van een bacterie genaamd *Pseudomonas protegens* CHA0 te volgen terwijl deze de wortel van de laboratoriummodelplant, *Arabidopsis thaliana*, koloniseerde. Door in de loop van de tijd bacteriën van plantenwortels te isoleren, konden we de belangrijkste mechanismen identificeren die een efficiënte kolonisatie bevorderen. Hoewel de bacterie-plantrelatie aan het begin van het experiment niet wederzijds gunstig was, evolueerden en overleefden sommige bacteriën die de plant ten goede kwamen tijdens latere stadia van het experiment. Onder deze geëvolueerde bacteriën identificeerden we 35 unieke mutaties, waaronder kleine veranderingen van een enkele nucleotide maar ook meerdere grotere inserties en deleties. We vonden deze mutaties verspreid over 28 verschillende genen waaruit al blijkt dat we sommige mutaties in dezelfde genen terugvonden. Interessant is dat we herhaaldelijk mutaties vonden in genen die betrokken zijn bij aanpassingen op het bacteriële celoppervlak, bacteriële aanhechting en bij motiliteit of beweging, wat aangeeft dat bacteriële aanpassing aan de plantenwortel deels voorspelbaar is maar ook meerdere strategieën omvat. Een opmerkelijke bevinding was dat de motiliteit, d.w.z. het vermogen van bacteriën om zich te verplaatsen, toenam bij meerdere onafhankelijke experimenten. Over het algemeen benadrukken deze resultaten hoe experimentele evolutie kan worden gebruikt om sleutelgenen en processen te identificeren die betrokken zijn bij bacteriële kolonisatie van plantenwortels.

Naast bacteriële verplaatsing, is stabiele kolonisatie van de plantenwortels een belangrijke factor voor het succes van bacteriën. Uit eerdere onderzoeken zijn verschillende kenmerken naar voren gekomen die bijdragen aan stabiele kolonisatie van bacteriën op plantenwortels, waaronder de manier waarop het bacteriële celoppervlak is versierd. In **Hoofdstuk 3** hebben we onze geëvolueerde bacteriën met modificaties in genen die verband houden met aanpassingen op dit gebied gebruikt om hun rol bij de kolonisatie van bacteriële wortels verder te onderzoeken. Specifiek hebben we onderzocht hoe mutaties in het *oafA* gen, dat codeert voor een O-antigeen acetyltransferase, leiden tot verbeterde kolonisatie van de wortels door de hechting aan de wortels te verbeteren. Mutaties in *oafA* beïnvloeden de functionaliteit van de acetyltransferase en resulteren waarschijnlijk in modificaties van het O-antigeen. Het O-antigeen is een cruciaal onderdeel van het lipopolysacharide op het celoppervlak, dat ook bekend staat als LPS. Onze bevindingen geven aan dat deze mutaties de fitness van de bacteriën specifiek

in de wortelomgeving verbeteren. Deze verbetering werd namelijk niet waargenomen onder verschillende andere omstandigheden in afwezigheid van planten, wat wijst op een voordeel dat afhankelijk is van één of meerdere plantcomponenten. Aanvullende experimenten hebben aangetoond dat de verbeterde fitheid van de *oafA* mutanten in de wortelomgeving gekoppeld kan worden aan versnelde hechting aan de wortels. Bovendien hebben we ontdekt dat een andere mutant met een verstoring in een gen genaamd *RS09880*, dat codeert voor een voorspelde glycosyltransferase, ook de fitheid van de bacterie op de wortel verbetert door de hechting aan de wortel te vergroten. Opmerkelijk is dat zowel *oafA* als *RS09880* zich bevinden in hetzelfde cluster van genen, genaamd het O-antigeen polysacharide biosynthese cluster 3 (*OBC3*), wat het idee ondersteunt dat modificaties aan componenten op het celoppervlak een belangrijke route is voor bacteriële aanpassing.

Gezien de voorgestelde belangrijke rol van modificaties aan componenten op het celoppervlak bij bacteriële aanpassing, hebben we in **Hoofdstuk 4** onderzocht of genetische veranderingen in het *OBC3* gencluster ook terug te vinden zijn in bacteriën in een natuurlijke omgeving. Om deze reden hebben we de genoomsequenties van alle openbaar beschikbare pseudomonaden bestudeerd en de aanwezigheid en variatie van *OBC3* genen geëvalueerd. Allereerst vonden we dit soort genen alleen bij stammen van dezelfde soort, namelijk de bacterie *Pseudomonas protegens*. Verder zagen we inderdaad een grote mate van variatie in de *OBC3* genen van meerdere stammen binnen deze soort. Verrassend genoeg vonden we zeer vergelijkbare mutaties als welke we hebben gezien in het laboratoriumevolutie-experiment waarbij het *oafA* gen op dezelfde manier verstoord werd in de respectievelijke stammen. Hoewel sommige van deze stammen ook afkomstig waren van een plantenomgeving, waren verschillende andere stammen juist niet gevonden in of rondom planten. Met andere woorden, aanpassingen aan componenten op het celoppervlak zijn waarschijnlijk niet alleen belangrijk voor interactie met plantenwortels maar ook voor interacties met andere omgevingsfactoren. Dit is niet geheel onverwacht, want vele eerdere onderzoeken hebben ook al het belang benadrukt van de bijdrage van deze componenten aan bescherming tegen stressvolle condities en ook voor interacties met bacteriële virussen. Deze virussen, ook wel bacteriofagen genoemd, infecteren bacteriën en worden overal aangetroffen waar bacteriën voorkomen. Gezien onze eigen observaties en deze bekende informatie uit de literatuur hebben we vervolgens onderzocht of de geëvolueerde bacteriën met mogelijke aanpassingen op het celoppervlak uit ons eigen laboratorium experiment mogelijk ook veranderde gevoeligheid tonen ten aanzien van een bacterieel virus. Ook hebben we onderzocht in welke mate de mutaties inderdaad resulteerden in veranderingen op het celoppervlak. Uit beide experimenten kwam naar voren dat de mutaties inderdaad in veel gevallen resulteerden tot waarneembare veranderingen aan de structuur van het LPS, te vinden op het celoppervlak, en dat deze veranderingen

samengaan met verhoogde weerbaarheid tegen het geteste bacteriële virus. Over het algemeen toonde dit onderzoek aan dat mutaties in het *OBC3* gencluster in de natuur kunnen voorkomen en dat bacteriën soms resistentie kunnen bieden tegen bepaalde bacteriële virussen, waarschijnlijk via structurele aanpassingen van de componenten op het celoppervlak.

In **Hoofdstuk 5** heb ik een model voorgesteld, de stapsgewijze aanpassing van bacteriën in de plantenwortelomgeving. Het model is gebaseerd op al het onderzoek dat in dit proefschrift is gepresenteerd, uitgevoerd op de bacteriestam *Pseudomonas protegens* CHA0 en de interacties ervan met de plant *Arabidopsis thaliana*. Het wordt als volgt uitgelegd: in een plantenwortelomgeving, nieuw voor bacteriën, koloniseren bacteriën aanvankelijk de plant en voeden ze zich met de suikers die de plant produceert en uitscheidt. Bacteriële aanhechting en de productie van kleine moleculen zorgen ervoor dat de plant het immuunsysteem activeert, wat resulteert in de productie van antimicrobiële stoffen en een vermindering van de uitscheiding van suikers. Deze veranderingen leggen selectieve druk op de bacteriën die leidt tot de evolutie van bacteriën welke beter geschikt zijn voor deze nieuwe omgeving. De bacteriële veranderingen omvatten modificaties aan componenten op het celoppervlak welke de bacteriële toleranties tegen de antimicrobiële stoffen kunnen verbeteren en de hechting aan het worteloppervlak van de plant kunnen vergroten. Vervolgens worden bacteriën geselecteerd met verminderde willekeurige bewegingen gekoppeld aan verkenning van de omgeving doch verbeterde motiliteit. Deze stapsgewijs opgebouwde mutaties veranderen de structuur van de bacteriële biofilm binnen de bacteriële gemeenschap. Dit verbetert niet alleen de fitheid van individuele bacteriën, maar heeft ook invloed op de interacties met andere bacteriën via mechanismen zoals quorum sensing. Ons onderzoek onthult het belang van bacteriële fenotypische en genotypische variatie in microbiële gemeenschappen en geeft aan dat het gebruik van single-cel technologieën waarschijnlijk noodzakelijk zal zijn om bacteriële adaptie en variatie in toekomstig onderzoek goed te volgen. Ten slotte merk ik nog op dat het voorgestelde model als voorbeeld kan dienen voor de bacteriële evolutie in natuurlijke omgevingen, aangezien vergelijkbare mutaties zijn gevonden in vergelijkbare bacteriën uit natuurlijke omgevingen.

Over het algemeen, kunnen bacteriën die de groei van planten bevorderen, zoals bacteriën binnen het geslacht *Pseudomonas*, gunstig zijn voor duurzame landbouw. Ze presteren echter mogelijk niet altijd goed vanwege lokale omgevingsfactoren en hun onvermogen om zich aan te passen aan specifieke gewassen. Het vermogen van deze bacteriën om plantenwortels te koloniseren is cruciaal om hun gunstige effecten te kunnen uiten. Verschillende kenmerken van deze bacteriën, zoals hun vermogen om zich te verplaatsen met behulp van flagella en pili, en de hechting aan het wor-

teloppervlak via structuren bestaande uit diverse polysachariden, dragen bij aan hun succesvolle vestiging. Hun algemene vermogen om een sterke en coherente biofilm te vormen, speelt waarschijnlijk ook een erg belangrijke rol. Ons onderzoek heeft ons begrip verbeterd van hoe bacteriën zich aanpassen aan hun omgeving, wat belangrijk zal zijn voor het verbeteren van hun effectiviteit in het veld en daarmee het ondersteunen van duurzame landbouw.

摘要

植物依赖各种微生物来维持其生存和生长。尽管这些微生物中的大多数是无害的，但有些会危害我们的庄稼，导致产量减少也增加了食品安全风险。相比之下，有益的细菌可以通过改善养分吸收和保护植物免受害虫和疾病的侵害。这些有益的细菌可以影响植物的免疫系统，建立一种相互有益的关系，这点类似于人体肠道中的益生菌。沟通是植物和细菌之间关系的重要组成部分，各种小分子在他们的交流中起着重要作用。有害和有益的细菌都使用各种方法与它们寄生的植物进行交流，如植物免疫抑制蛋白、植物激素和生物活性分子。植物还通过释放碳源和其他化合物来与它们相关联的细菌进行交互沟通。

在第一章中，我们探讨了不同有机小分子在调节植物-益生菌中的作用，以及评估了病菌利用类似小分子侵染植物的能力。我们使用比较基因组学来评估各种天然环境中常见的假单胞菌（*Pseudomonads*）的分泌这些小分子的潜力，这些假单胞菌包括益生菌和病菌类型。了解这些小分子的生物合成和活性可以有助于开发对环境无害的生物制剂，以增强作物的适应性并抵抗病菌。

在农业领域，人们已经尝试使用植物益生菌作为生物制剂来促进植物生长，并保护它们免受害虫和疾病的侵害，同时取代对环境有害的化学肥料和杀虫剂。例如，在实验室条件下表现出对植物具有多种益处的促生假单胞菌就被用作生物制剂。但是，在田间应用时，由于具体土壤环境条件可能会有利于原生地的微生物，同时引入的假单胞菌缺乏对特定作物的适应性，它们的实际田间表现差强人意。研究人员已经通过进一步研究，了解了益生菌克服这些困难的机制，例如很多益生菌会产生高亲和力的铁结合化合物，或者通过各种方法来躲避植物的免疫系统。为了改善益生菌再农业中使用效果，了解它们如何在进化中适应寄主植物是非常重要的。

在第二章中，为了研究细菌对植物根环境的适应，我们使用一种名为*Pseudomonas protegens* CHA0的细菌在实验模式植物拟南芥的根际进行定殖，同时取样和观察细菌的遗传和生理变化。通过不同时间段从植物根表面分离的细菌菌株，我们能够了解促进细菌在植物上有效定殖的关键机制。尽管在实验开始时，这种细菌-植物关系并不是互惠的，但在实验的后期，一些有益于植物的细菌菌株得以进化和存活。在进化后的细菌菌株中，我们分析确定了35个独特的突变，涉及28个不同的细菌基因，包括小的多态性和更大的分子插入、删除和突变片段。有趣的是，在多个重复实验中，调节细菌细胞表面装饰、细菌根系附着能力和细菌运动的基因都出现了突变，这表明细菌对植物根的适应可能涉及多种策略。一个值得注意的发现是，在多个独立的进化重复实验中，细菌运动性，即细菌移动的能力，随时间进化增加了。这些实验结果也说明了利用进化学实验来确定细菌定殖植物根的关键基因和过程的可行性。

除了细菌的运动能力，稳定的植物根际定殖是细菌存活的重要因素。在早期研究，研究者就已经发现细菌细胞壁装饰是一个有助于细菌植物根际定殖的特征。在第三章

中，我们使用进化的细菌菌株来进一步评估细胞壁装饰在细菌根际定殖中的作用。具体来说，我们研究了*oafA*基因中的突变如何通过增强细菌在植物根上附着来改善根际定殖能力。*oafA*基因的突变会影响编码O-抗原乙酰转移酶的功能，可能会导致O-抗原的修饰。O-抗原是细胞表面脂多糖的关键组成部分。我们的研究结果表明，这些突变特别提高了细菌在根环境中的适应性，同时此适应性并没有在无植物的其他条件下观察到，这表明此适应性是植物环境相关的适应性。后续的实验进一步阐述了*oafA*突变体在根环境中改善适应性与加速根附着之间的关联。此外，我们发现另一种被命名为*RS09880*的突变体也是通过增加根附着来提高了细菌在根环境中的适应性。值得注意的是，*oafA*和*RS09880*两个基因都位于同一基因簇中，称为O-抗原多糖合成簇3（*OBC3*），这支持了细胞壁装饰的修改是改善细菌适应性重要途径的观点。

鉴于细胞壁修饰在细菌适应性的重要角色，在第四章中我们研究了*OBC3*基因簇的遗传变化是否也存在于自然界的细菌中。因此，我们研究了所有公开可用的假单胞菌基因组序列，并评估了*OBC3*基因的存在和变异。首先，我们发现OBC3基因簇仅存在于同一物种（即*Pseudomonas protegens*）的菌株中，并且我们确实观察到这些菌株的*OBC3*基因存在大量变异。令人惊讶的是，在这种变异中，我们观察到与我们在实验进化中观察到的高度相似的突变，以相同的方式破坏了相应菌株的*oafA*基因。而且，这些菌株有的来自植物环境，而有的则存活于非植物环境。值得注意的是，细胞壁装饰不仅对植物根系的相互作用很重要，许多早期的研究也强调了它在与细菌病毒（或噬菌体）的相互作用中的重要性。噬菌体普遍存在于细菌可以存在的所有环境中。因此我们随后评估了实验进化的细菌对噬菌体的敏感性，并确实确认了我们进化的*OBC3*突变体中有部分对噬菌体的耐受性发生了改变。通过分析突变体的LPS结构和O-抗原电泳成像得出，这种对噬菌体耐受性的改变是与细胞壁装饰的结构改变相关联的。总体而言，这项研究表明自然界中存在细菌*OBC3*突变体，并且这种突变可以为增加细菌对某些细菌病毒的抵抗力，这中增强也是通过细胞壁装饰的结构修饰实现的。

在第五章中，我提出了一种模型——细菌在植物根系环境中的逐步适应。该模型基于本论文所进行的所有关于假单胞菌*Pseudomonas protegens* CHA0及其与拟南芥的相互作用的研究。模型的解释如下，在植物根系环境中，细菌最初定殖在植物上，并以植物产生和分泌的碳水化合物为食。细菌附着和小分子物质的产生激活了植物免疫系统，植物开始产生细菌毒素并减少碳水化合物的分泌。这些变化对细菌施加了选择压力，导致细菌突变体被筛选出来以适应这一新环境的特征。这些新出现的突变体包括那些细胞壁结构修饰的细菌，这使得它们增强了附着在植物根表面上的能力，同时也学增强了它们对毒素的抗性。之后，在此基础上，新的突变体出现了，它们具有减弱了自身随机运动的能力和同时增强了定向移动的能力。这些逐步积累的突变改变了细菌群落中的细菌生物膜结构。这反过来不仅改善了细菌的适应性，还通过群体感应机制影响了与其他细菌的相互作用。我们的研究也揭示了微生物群落中细菌表型和基因型变异的重要性，并建议今后的研究需要使用单细胞技术来跟踪特定生长位点的细菌变异。最后，我指出，实验中提出的模型可能对自然环境中的细菌进化具有阐述意义，因为我们在自然环境中发现了类似于实验室产生的突变体。

总体而言，促进植物生长的假单胞菌属细菌对农业的可持续发展非常有益。然而，由于当地环境因素和它们无法适应特定作物，它们的田间表现不佳。这些细菌在植物根部的定殖能力是生产应用的关键。改变细菌的不同生物学特征都有助于它们的成功定殖，例如改变鞭毛和纤毛的移动能力，以及修饰多种多样的表面多糖组成结构来增加其与根的附着能力。同时这些改变导致的细菌群落在生物膜上的改变，也可能起着重要作用。本研究提高了我们对细菌适应环境机制的理解，这将对改善它们在田间施用效果以农业可持续发展的实践至关重要。

Acknowledgements

'The best way out is always through.'

In my dissertation, I would like to express my appreciation for the people who have supported me during my PhD journey, which has been a significant and meaningful part of my life. While I hope I have not left out anyone's name, I am aware that nothing has been, is, or will be perfect, as I have learned during this journey.

I am deeply grateful to my promoter, **Corné**, who has been instrumental in guiding me throughout my research. From the moment you responded to my email about the possibility of starting my PhD track in PMI, everything has been different. Your guidance has been unwavering, even though you are always incredibly busy. You are an exceptional professor and a great person, and I am grateful to have had you as my promoter.

To my co-promoter, **Ronnie**, I cannot express my gratitude enough. You have been a witness of my whole PhD life. You have undoubtedly noticed how much I have developed from the first year to now, with your support, of course. Thank you for all of your efforts in guiding me through my PhD and teaching me critical and skeptical thinking as a scientist. Please continue on correcting my English & Dutch in pronunciation, writing, and spelling, while I'm around. As the ancient Chinese philosopher Confucius said, 'Finding a loyal friend is a challenge, and finding a virtuous tutor who is willing to instruct you is equally arduous (得友难，遇良师亦难)'. Full-heartedly, I express my gratitude to you.

I would like to extend my gratitude to **Guido** for motivating me to switch my research topic during one of my half-year report discussions. This change has helped me avoid wasting more time on the previous topic and move into the current research. Additionally, your own marathon experience and suggestions have been instrumental in supporting my marathon running. **Saskia**, thank you for your dedication to the younger generation. I appreciate your time and effort, and it has been great working with you on the PhD program. I hope to hear your laughter in our corridor again soon. **Roeland**, I remember the fun time we had at the football match in the Olympos, and I am delighted to have been part of that group, even if only for the drinking part. I have noticed that you have been increasingly diligent in your academic pursuits, sacrificing your leisure and social activities for your working. I wish you all the best in your endeavors.

I would like to extend my thanks to the remarkable individuals who have provided me with their support during my research journey. I would like to thank **Peter** for his invaluable input to my research, especially his experience and knowledge on the plant-microbe topics. I wish you a happy retirement. **Erqin**, I could not have completed my PhD research without you. I appreciate your efforts and thoughts on this topic, and I have benefited from your incredible research on evolutionary experiments. Although we argued a lot on many topics, I am pleased to see your professionalism in research still going strong. **Ke**, I look up to you as a big brother in the lab. You provided me with invaluable assistance when I first arrived, guiding me through the lab. I am amazed at how much you read and know on PMI research topics and have never doubted that you will be a great scientist. **Giannis**, I cannot believe that I have known you for over seven years, and you are one of the few people who have stayed in the group since I started. You are always helpful when I encountered some problems on the research topics. You are very welcoming to all international PhDs & Postdocs in the group, and I believe we should have all kissed your ring when we arrived. Your exceptional scientific abilities and cutting-edge ideas have convinced me that research is your true calling. All the best to all of you.

I was fortunate to have the opportunity to supervise several students throughout my PhD journey. I would like to thank **Odile**, **Dennis**, **Jason**, **Hannah**, **Meltem**, **Amber**, **Daan**, **Charlie**, and **Arianne**. Not everyone's work is showcased in this thesis, but I won't forget your contributions and efforts. I want to express my gratitude to each of you for entrusting me with the guidance of your projects. I was happy to have you around and work together in the lab.

Without the invaluable assistance of the remarkable support staff, my PhD journey would have been significantly more challenging and less pleasurable. **Hans**, your beautiful pictures have enhanced my research and (will be) defense ceremony. You're the backbone of our group, and I appreciate all the effort you've put in. **Anja**, our conversations about sports and your stunning hiking route in the Netherlands will always be memorable to me. I'll never forget the cake you and Sanne baked to celebrate my first Marathon in Paris. **Joyce**, thank you for your patience and help in my early years of the PhD program, especially with DNA kits. I must admit that I'm most impressed by your baking skills, and I look forward to more delicious cakes! **Miek**, you went above and beyond by preparing Sinterklaas gifts for group members and offering free mental health consultations to many PhDs. I wish you all the best and hope to see you more often. **Jolanda**, I appreciate your strict attitude towards lab management and your contributions to keep the lab in order. And **Marrit**, even though we never talked about research, I'm delighted that we became friends. I wish to extend my heartfelt gratitude to **Susan Urbanus** from EPS graduate school, who not only guided me with

my career path but also supported me in making a crucial decision. Thank you very much.

I would like to take this opportunity to express my gratitude to my dear colleagues in Ronnie's team. **Juan**, I can still remember the day when I gave you a lab tour after your interview in the group. You are a very affable and knowledgeable person. I'm grateful to have you around. **Sanne**, your first PowerPoint presentation surprised me, and I was even more impressed when I learned that you had switched your major during MSc. I admire your resilience, and I hope you will always remember that you are stronger than you think. As for **Gijs**, I regret to say that you joined during the lockdown, which did not allow us much time to get to know each other in the beginning. However, I have since learned that you are a more reserved person than I had initially thought, even though you are an electric guitar player in a band. I wish all three of you the best of luck in completing your PhDs smoothly and successfully.

To my esteemed paranymphs **Eline** and **Tijmen**, I would like to express my gratitude. **Eline**, my dear friend, colleague and paranymph, meeting you was one of the highlights of my PhD journey. Your positive attitude and self-discipline have been an inspiration to me and I still benefit from them to this day. Our friendship has grown stronger over the years, and I am glad that we still keep in touch. Words cannot express how grateful I am for your support. I wish you, **Joep**, and your son **Sam** all the best. **Tijmen**, it's amazing that you are still in Utrecht. :p Our trip to Eeeeengland was unforgettable. Even before that trip, I admired your relaxed presentation style, which reminded me that science can also be enjoyable. We have faced similar challenges in our PhD journeys, which has helped us to understand each other better. I hope you continue to thrive and I look forward to seeing you around.

If life is meant to be filled with happiness, then you are the embodiment of happiness. My PhD journey would have been miserable without all of you around. **Pauline**, your presence is greatly missed by everyone in the group, and your name is still mentioned even after you left. I'm grateful to have met you and to have kept in touch with you over the years. Your lively spirit and cheerful countenance will always be remembered by me. I wish you all the best and hope to see you again soon. **Merel**, my first PhD meeting with you in Barcelona was a memorable experience, and since then we've gone on many trips together, including France and Oman. You often express your grievances, but I find it amusing and enjoyable to listen to, at least from my perspective. I'm happy to see that you're enjoying a fulfilling career and that your smile has returned. **Gilles**, I'm grateful to have been a part of your and Nikita's wedding in Oman. Since then, we've gotten to know each other better, and your decision to switch careers and become a lawyer still amazes me. I appreciate your parents'

kindness and hospitality towards me. Please pass along my greetings to them. **Sietske**, you're an excellent listener. It's hard to believe that we'll both be completing our PhDs in the same year, considering you started two years after me. You're doing an amazing job with your PhD! The trip we took together a few years back is an unforgettable memory, and I'm truly grateful for your companionship during that time and at every day. **Alberto**, I have seen you joined and left the group, and then came back again. From that, I truly admire your dedication to your research. Despite your occasional complaints and self-doubt, you are doing an excellent job. Please remember that. **Pim**, I am grateful for your trust in me to be your paranymph. It is an honor I will never forget. **Melissa,** I had a great time with you and I encourage you to continue pursuing your passion for singing. I am confident that more people will appreciate your talent, just like I do. **Yang**, you are doing great as always. I wish you all the best in your new project and your academic career. **Marciel**, it is wonderful to see you back in the group, and I wish you a success in your new position. I would also like to express my gratitude to some former members, **Manon** and **Joël**, also current members, **Run**, **Shuhua**, **Dmitry**, **Sebastian**, **Robin**, **Niels**, **Jelle**, **Tessa**, **Dharani**, **Melanie**, **Max**, and **Inigo**, for all the helpful conversations we had and the support you gave me. Finally, I would like to thank **Changfeng**, **Hangyu**, **Jie**, **Xintong**, **Xing**, and **Jiayu** for the enjoyable time we had together at PMI.

There were more people I met during this journey. **Sarah**, when I think about you, your cheerful smile always come first. Thank you for supporting me when I was struggling with writing stress. I wish you all the best in your research. **Sjon**, it's great to have met you through Sarah, and we've become closer while fighting for the Alliance in Azeroth. I hope we can continue to do so, even though we're getting busier in real life. Aside from that, I wish you both a wonderful life in Freiburg - it's an incredible place to live, with breathtaking natural views. Thank you for hosting me there last summer, I will never forget it. **Zeguang**, it was wonderful to meet you, and I won't forget the delicious food you cooked. I hope to meet you again soon and hear from more stories about you in the near few years. Also, thanks to **Sara** and **Elaine** for the fun time we shared in Greece, and other memories we shared in Utrecht. Thanks to **Zhang** for the chitchat during coffee break, and **Linge** for suggesting and promoting me joining the university council. **Nathalie**, **Zhilei**, and **Jie**, thank you for inviting me to join fun events in the Ecology & Biodiversity group, and we became friends from that time. Through you, I also meet nice person like **Julian** and **Jay**. **Tom**, We have been acquainted for many years, and we have begun to exchange stories about games and cuisine. I wish you all the best on your journey through your PhD, and let's continue to explore and enjoy various leisure activities together. **Sophie**, I first met you in PMI and got introduced by Eline, and it's remarkable how we connected again and again from different social circles. It's heartening to see that you have found

a career path that you are passionate about, and you are excelling in it. Wishing you all the best!

I would like to express my gratitude to the friends I met during my time in Wageningen (*it's a magical place*). **Ningjing**, **Wei**, and **Peiyu**, I am thankful for all the wonderful memories we created together. Despite our different research interests, we developed a strong bond after arriving in the Netherlands. It is amazing how we managed to become friends despite our differences. I am grateful that we still keep in touch and that we continue to share our thoughts and feelings with each other. Your friendship and support mean a lot to me, and I appreciate it. I would also like to thank **Ioannis** and **Tryntsje**, both of you have been great friends and provided me with support during my difficult times in Wageningen. I am glad that we have remained friends over the years. Furthermore, I would like to extend my appreciation to **Ningyi**. I left Wageningen around the time you arrived, and I have been amazed by your successful research career. Your confidence and determination are admirable, and I believe you will achieve all that you desire. In addition, I would like to thank **Haikun**, **Shenglai**, and **Huayi** for the unforgettable moments we shared, and for your support during my PhD. Your care and kindness are deeply appreciated. I would like to express my gratitude to **Yang Yu**, **Junqi**, and **Fang** for being like big brothers and sister to me and providing me with support during that challenging period in Wageningen. Thank you so much.

I would like to express my gratitude to some old friends. **Liang**, we shared a student dormitory during our BSc studies in China and later did our PhDs in neighboring countries, the Netherlands and Belgium. Among all valuable moments we shared, I cherish the memories of playing on the slide like 7-year-old kids in the park next to you house in Belgium. Even though we don't talk as often now after you started your professorship in Beijing, whenever we do, it feels like we still understand each other very well. I wish you all the best in your career and good wishes to your family members, especially your new born daughter. **Xiaomin**, we met during our BSc studies at NWAFU and started our PhDs in Europe in the same year. It's always great to have old friends with whom you can catch up every now and then. I wish you all the best in your work and research. As I reflect on my academic journey, I would like to express my gratitude to my BSc and MSc supervisor, Prof. **Xiaohui Hu**, for introducing me to the world of research and for providing me with invaluable support throughout my PhD journey, both academically and emotionally.

Last but not least, I express my gratitude to my **mother**, who has always been supportive of me, regardless of the circumstances, and who even tries to pamper me,

whether I like it or not. To my **father**, although I may not always realize it, I know that you have been supportive of me in ways that may not be immediately apparent.

I'm here. This is it.

'I took the one less traveled by, And that has made all the difference.' – Robert Frost

癸卯年三月廿三于荷兰
May 12, 2023 Utrecht

About the author

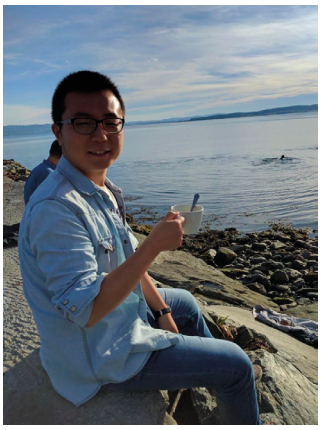

Hao Zhang（张浩）was born on the 4th of November 1988 in Lingbao, P. R. China. He obtained his BSc degree in Protected Agriculture Science and Engineering from Northwest Agriculture & Forestry University (NWAFU) in Yangling, P. R. China in 2011. During his undergraduate studies, he developed a strong interest in plant research and subsequently enrolled in the same university's MSc program, focusing on plant physiology and molecular biology. During his master's program, he conducted research on the physiological and biochemical changes in tomatoes grown in saline-alkaline stress soil, a prevalent issue in greenhouses for local farmers. In June 2014, Hao completed his MSc degree in Protected Horticulture Engineering, and his thesis was recognized as an outstanding thesis in the College of Horticulture. Inspired by his passion for science, he applied for and was awarded a scholarship from the China Scholarship Council to pursue a PhD outside of China, in the Netherlands. He began his PhD studies at Wageningen University & Research in 2014. Despite his initial focus on developing a mathematical model of plant photosynthesis with multiple soil nutrient parameters, he eventually realized that this research area did not align with his interests. Consequently, he did not continue in this particular project. Since April 2016, Hao has been pursuing his current position as a PhD candidate in the Plant-Microbe Interactions group at Utrecht University, where his doctoral research centers on characterizing adaptive mutations in *Pseudomonas* that enable bacterial plant adaptation in the rhizosphere. Alongside his research, Hao has been actively involved in PhD events and councils, including serving as a PhD council member of the Experimental Plant Sciences National Graduate School and the organizing board for the European Plant Science Retreat in 2018. Hao is committed to supporting other PhD candidates in their academic journeys and plans to continue his supportive work at Utrecht University as a program coordinator and a University Council member after completing his PhD.

Publications

- Stringlis IA, **Zhang H**, Pieterse CMJ, Bolton MD, De Jonge R. 2018. Microbial small molecules-weapons of plant subversion. *Natural Product Reports* 35: 410–433.

- Li E*, **Zhang H***, Jiang H, Pieterse CMJ, Jousset A, Bakker PAHM, De Jonge R. 2021. Experimental-evolution-driven identification of Arabidopsis rhizosphere competence genes in *Pseudomonas protegens*. *mBio* 12: e0092721.

- Sanchez-Gil JJ, Poppeliers SWM, Vacheron J, **Zhang H**, Odijk B, Keel C, De Jonge R. 2023. Identification of the conserved iol gene cluster involved in rhizosphere competence in *Pseudomonas*. *Current Biology:* (*TBA*).

- Bakker PAHM, Berendsen RL, Van Pelt JA, Vismans G, Yu K, Li E, Van Bentum S, Poppeliers SWM, Sanchez-Gil JJ, **Zhang H**, *et al.* 2020. The soil-borne identity and microbiome-assisted agriculture: looking back to the future. *Molecular Plant* 13: 1394–1401.

- van der Horst S, van Butselaar T, **Zhang H**, Vismans G, Steenbergen M, Courbier S, Neilen M, Küpers JJ. 2019. Bringing together Europe's young plant scientists. *New Phytologist* 222: 29–32.